PhD in

CHEMICAL SCIENCES

CYCLE XXXVIII

COORDINATOR Prof. ANNA MARIA PAPINI

Biochar Synthesis, Characterization, and Application in Constructed Wetlands Systems for Removing Organic Matter, Nutrients, Pathogens, and Pharmaceutical Pollutants

Academic Discipline CHIM/01

Doctoral Candidate

Dr. Sofiane El Barkaoui

_____

Supervisor

Prof. Massimo Del Bubba

_____

Co-Supervisor

Prof. Carla Bazzicalupi

_____

Coordinator

Prof. Anna Maria Papini

_____

Academic Years 2022/2025

Table of Contents

Abstract

Growing pressures on water resources and inadequate wastewater treatment infrastructure in many regions call for low-cost, efficient, and sustainable solutions capable of addressing both conventional and emerging contaminants. This thesis investigates the valorisation through pyrolysis processes of local agro-industrial residues, mainly argan press cakes (white and black), olive pomace, and lignocellulosic materials, into biochar for decentralized wastewater treatment systems. Furthermore, sewage sludge together with sawdust has been used as feedstock for biochar production via a co-pyrolysis process. The research combined feedstock characterization, pyrolysis optimization, and performance evaluation in filtration and constructed wetland systems, with a focus on both classical pollution parameters and pharmaceutical contaminants. Detailed physicochemical and thermal analyses showed that the selected agro-industrial residues contained high carbon percentages (52–61%) and exhibited good energy potential, making them suitable feedstocks for pyrolysis. Biochar yields ranged from 8% to 34% depending on feedstock and pyrolysis temperature, with fixed carbon increasing and volatile matter decreasing as temperature rose. At 800 °C, olive pomace biochar achieved the highest specific surface area (22 m^2/g) and methylene blue adsorption capacity (432 mg/g), confirming the strong effect of pyrolysis conditions on sorption properties. In the second phase, biochar was incorporated at different proportions (0%, 10%, 25%, and 50%) into filtration systems and pilot-scale vertical flow constructed wetlands (VF-CWs) treating domestic wastewater. Results demonstrated a significant enhancement of treatment performance compared to unamended systems. The 10% biochar dose provided the best balance between efficiency and hydraulic performance, achieving up to 92% removal of total suspended solids (TSS), 83% of chemical oxygen demand (COD), 87% of organic nitrogen, and 44% of total phosphorus, with faecal indicator contamination removal reaching 3–4 log units. Hydraulic conductivity was maintained, indicating good substrate stability. In the third phase, the removal of contaminants of emerging concern was investigated. Biochar-amended VF-CWs exhibited high removal efficiencies for several pharmaceutical compounds, including clarithromycin, erythromycin, and ketoprofen (up to 99–100%), while others, such as carbamazepine and fluoxetine showed low to moderate removal (≤35%). These findings reflect both the sorption properties of biochar and the differential biodegradability of pharmaceuticals. Biochar effectively improved micropollutant retention without compromising system operation, confirming its suitability as an integrated, low-cost substrate. Overall, this work demonstrates the technical feasibility and environmental relevance of converting local biomass residues into high-performance biochar for sustainable wastewater treatment. It provides robust experimental evidence that biochar can substantially enhance the efficiency of decentralized systems, contributing to improved water quality, waste valorisation, and climate co-benefits through carbon sequestration. These results support the development of scalable, resource-efficient sanitation solutions for rural and peri-urban communities facing both biomass accumulation and water pollution challenges. Particularly interesting results were obtained in vertical systems by replacing conventional substrates (sand and gravel) with biochar obtained from the co-pyrolysis of sewage sludge and sawdust, and subsequently chemically and thermally activated (surface area approximately 400 m^2/g). In this study, which lasted approximately eight months, the biochar systems showed removal rates almost double those of conventional systems, achieving a mean removal of about 70% over the whole period and thus highlighting very promising aspects of their practical application.

Keywords: Biochar, Agro-industrial residues, Sewage sludge, Constructed wetlands, Filtration systems, Wastewater treatment, Pharmaceutical contaminants, Circular economy, Biomass valorization.

General Introduction

Rapid population growth and urbanisation have greatly contributed to increased waste generation and water pollution, exacerbating freshwater scarcity and intensifying the demand for clean water. Parallelly, the expansion of industrial and agricultural activities has led to significant wastewater production, often containing a complex mix of contaminants such as heavy metals, inorganic and organic pollutants, pathogenic microorganisms, and emerging substances (Saravanan et al. 2021). These pollutants are discharged into the public sewer and reach municipal wastewater treatment plants, which are not designed to remove them effectively. As a consequence, the occurrence of pollutants, particularly contaminants of emerging concern (CECs), including personal care products, industrial chemicals, pesticides, and pharmaceutical compounds (PhCs), in environmental waters (i.e., surface and ground waters) has raised significant concerns regarding the safety and sustainability of water resources (Gadipelly et al. 2014).

Constructed wetlands (CWs) are a sustainable solution and a nature-based green technology for wastewater treatment (Younas et al. 2022). In these systems, plants and especially substrate play critical roles in pollutant removal (Addo-Bankas et al. 2021; Ohore et al. 2022). The former enhances biological activity by releasing oxygen through its roots, absorbing nutrients, and influencing the system's hydraulic conductivity (Srivastava et al. 2008; Guittonny-Philippe et al. 2015; Kataki et al. 2021; Karungamye 2022). Moreover, the substrate facilitates mechanical, physical, and biological processes of contaminant removal, supporting biofilm adhesion, promoting plant growth, and enabling chemical transformations (Deng et al. 2021). Many materials have been tested in order to improve the efficiency of CWs' substrate, such as gravel and sand (Fu et al. 2020; Zhang et al. 2021), pozzolan (El Ghadraoui et al. 2020), zeolite (Du et al. 2020), and charcoal (Hamada et al. 2021), showing moderate effectiveness in treating common pollutants, such as suspended solids, nutrients, and biodegradable organic matter (Huong et al. 2020; Zhuang et al. 2022). However, their efficiency drops considerably when addressing a range of ecotoxic substances, including detergents, heavy metals, plasticisers, disinfectants, pesticides, and pharmaceutical residues, which remain largely unremoved in CWs' effluents (Kőnig-Péter et al. 2014; Gosset et al. 2020). This limitation raises significant concerns regarding the safety and quality of reclaimed water resources.

Recently, there has been growing interest in using biochar (BC) as an effective filter system substrate, thanks to its high specific surface area, well-developed porosity, and abundant surface functional groups, which enhance adsorption and contaminant removal (Zhang et al. 2022; Shahraki and Mao 2022). These include its sustainability, cost-effectiveness, low environmental impact, and the ability to produce water suitable for irrigation (Stefanakis 2019). This aligns closely with key sustainable development goals, particularly water accessibility and waste reduction. A promising integrated strategy involves converting agricultural residues and sewage sludge into biochar and using it in wastewater treatment, creating a circular model that simultaneously supports waste valorisation, resource conservation, and environmental protection. The use of biochar for wastewater treatment is even more advantageous when this material is obtained from the thermal conversion of sewage sludge, as a high level of circularity is provided to the wastewater treatment sector in accordance with the European Directive 2024/3019 (European Parliament and the Council, 2024). Moreover, this process allows to inhibit the intrinsic chemical and biological risks related to the management and disposal of sewage sludge (Bakari et al., 2024).

Many authors highlighted the high capacity of BC in eliminating most pollutants, including inorganic and organic contaminants, and heavy metals from wastewater, compared to conventional materials (e.g., soil, sand, and gravel) (Cha et al. 2016; Deng et al. 2019; Ayadi et al. 2024). For instance, Ayadi et al. (2024) investigated the influence of filling media on the performance of CWs by comparing systems with BC and gravel. The BC-based CW demonstrated superior treatment efficiency, achieving enhancements of 22% and 35% in chemical oxygen demand (COD) and ammonia removal, respectively. Additionally, greater reductions were observed in UV–Vis absorbance, with decreases of 32–34% at 254 nm and 28% at 420 nm, compared to the gravel-based system. Similarly, Chen et al. (2024) compared the efficiency of gravel-based and BC-based CWs, pointing out a higher performance of the latter in removing various water quality parameters, particularly total phosphorus (TP), whose removal increased from 56% to 90%. Tang et al. (2016) demonstrated that plant-derived BC incorporated into a CW significantly enhanced the removal efficiency of four pesticides from wastewater (>99%) compared to the control CW (64–99%). Furthermore, BC was tested for the removal of benzofluoranthene (BbFA), a representative PAH in CWs, demonstrating a removal efficiency exceeding 99%, likely due to enhanced PAH biodegradation (Guo et al. 2020). Abedi and Mojiri (2019) found that adding BC to CWs enhanced the removal efficiency of heavy metals such as Mn and Pb to 99%, compared to 58% and 52% in gravel-based CWs. This improvement is

attributed to BC's capacity to retain metals by enhancing abiotic removal pathways. However, there is a deficiency of appropriate literature studies on the use of BC in CWs, particularly for removing PhCs. Ofiera et al. (2025) examined the impact of incorporating BC (from undefined biomass) into CWs, finding that BC-enhanced CWs effectively reduced all target PhCs to below quantification limits. In contrast, conventional CWs showed inconsistent removal, with maximum efficiencies of 86% for metoprolol, 62% for clarithromycin (CLA), and 48% for diclofenac (DIC). While candesartan, carbamazepine (CBZ), and hydrochlorothiazide were not removed (Ofiera et al. 2025). Yuan et al. (2020) demonstrated that integrating BC derived from fruit stones into zeolite-based CWs significantly enhanced the removal efficiency of antibiotics, achieving removal rates of approximately 88% for CIP and 56% for sulfamethazine. Chand et al. (2022) evaluated the performance of vertical flow constructed wetlands (VF-CWs) incorporating BC derived from cow dung pats for the removal of pharmaceutical contaminants, including amoxicillin (AMX), caffeine (CF), and ibuprofen (IBU). The BC-amended VF-CW demonstrated significantly enhanced removal efficiencies, achieving 75.5% for AMX, 87.5% for CF, and 79.9% for IBU, compared to 53.82%, 69.8%, and 63.98%, respectively, in VF-CWs utilizing conventional filter media. Similarly, Ajibade et al. (2023) highlighted that adding bamboo-derived BC to CWs markedly improved the elimination of sulfamethoxazole (SMZ), with a removal efficiency of 65% compared to 28% in sand-filled CWs. Moreover, Ilyas and Hosney (2024) assessed the role of softwood-bagasse BC-added CWs in addressing some PhCs, including SMZ, irbesartan, erythromycin (ERY), DIC, and CBZ, showing a high performance exceeding 91% compared to conventional CWs filled with gravel (72%, 50%, 84%, 22%, and 36%, respectively). On the other hand, Venditti et al. (2022) reported that VF-CWs amended with plant-derived BC exhibited lower performance than sand-based VF-CWs, which achieved average removal efficiencies exceeding 91% and 94% for a range of PhCs, respectively. However, the exact mechanisms underlying the removal of PhCs by CW substrates remain unclear.

Despite ongoing research, the optimal properties of BC for effective wastewater treatment remain unclear, especially concerning its feedstock source and preparation conditions. In addition, the literature still lacks clear guidance on the appropriate type, concentration, placement of BC within CW substrates, the suitable organic loading rate to be applied, and their efficiency towards pollutants and its mechanism, especially pharmaceutical compounds. Based on the aforementioned considerations, the primary objective of this work was to optimize the performance of BC-based CWs in treating various pollutants, particularly the PhCs.

Therefore, we attempted throughout this work to:

- Determine the most effective position of the BC substrate within CWs based on findings from our comprehensive review.

- Compare the physicochemical and structural properties of argan residues as feedstocks for BC production.

- Assess the effect of biomass composition and the pyrolysis conditions on the BC properties and its adsorption capacity towards methylene blue (MB) as an organic molecule model.

- Investigate the impact of increasing the percentage of BC-based substrate on the treatment performance of the filter.

- Examine the influence of substrate type on the filtration performance.

- Explore the effect of increasing the Organic Load Rate (OLR) on the treatment efficiency of CWs.

- Study the impact of vegetation on the treatment efficiency of CWs.

- Evaluate the impact of adding BC into CWs on the removal efficiency of PhCs.

This work is divided into 4 chapters, as follows:

Chapter I aims to review the preparation conditions and feedstocks used for BC integrated into CWs, along with the resulting properties relevant to wastewater treatment. It also highlights BC-based CW design configurations, factors influencing treatment efficiency, mechanisms driving contaminant removal, and the advantages and limitations of using BC as a CW substrate.

Chapter II compares the physicochemical and structural properties of four types of local residue obtained from the production of Moroccan argan and olive oils: black argan press cake (BAC), white argan press cake (WAC), pellet argan cake (PAC), and de-oiled olive mill waste (DOW), with a view to their potential use in the production of biochar. Furthermore, it aims to optimise BC preparation and investigate the impact of pyrolysis temperature (600, 700, and 800 °C) and biomass type on the physicochemical, structural, and morphological properties of the resulting BCs. It also aims to evaluate their adsorption capacity towards methylene blue (MB) as a model organic pollutant, and to determine the optimal BC for use in large-scale filters for treating organic

pollutants in wastewater.

Chapter III aims to evaluate the impact of adding BC into column filtration systems (CFS) and CWs in removing conventional and pathogen pollutants from wastewater, and to determine the optimum percentage (0%, 10%, 25%, and 50%) and type of BC (olive pomace, orange wood waste, filao, and cypress), as well as the optimum OLR (20–70 g COD/m².d) for an efficient treatment.

Chapter IV investigates the performance of vertical flow VF-CWs amended with BC from olive pomace and sludge in removing PhCs. Furthermore, the occurrence, distribution, and removal efficiency of 36-39 PhCs in influent wastewater and particulate matter (PM) are assessed.

Chapter I –

A Critical Review on Using Biochar as Constructed Wetland Substrate: Characteristics, Feedstock, Design, and Pollutants Removal Mechanisms

This work was published as a review paper:

El Barkaoui, S., Mandi, L., Aziz, F., Del Bubba, M., & Ouazzani, N. (2023). A critical review on using biochar as constructed wetland substrate: Characteristics, feedstock, design and pollutants removal mechanisms. Ecological Engineering, 190, 106927.
https://doi.org/10.1016/j.ecoleng.2023.106927.

Abstract

Constructed wetlands (CWs) are constructed systems that simulate natural wetlands and can be used to treat wastewater from several sources of pollution through physical, chemical, and biological depuration processes. This work aims to critically review the updated literature on CWs integrating biochar in the substrate. In detail, the study focuses on the characteristics of biochar that are generally integrated into this treatment ecotechnology and the processes used to prepare the materials, including conditions of thermal conversion and the kind of feedstock used (e.g., agricultural, food, and wood wastes, sewage sludge, and argal marine feedstock). Based on the literature review, it is found that the feedstock must be rich in carbon and low in mineral matter to produce good quality biochar, i.e., large pore volume and high specific surface area, thus allowing for effective removal of pollutants from wastewater. The biochar quality is affected by the conditions involved in preparing biochars (e.g., pyrolysis temperature, heating rate, and carbonization time). The properties of biochar used for wastewater treatment, the effect of its implementation as CW substrate, and its treatment efficiency have also been described. Several factors alter the removal efficiency of pollutants in CWs, such as substrate chemical and physical properties, hydraulic retention time, oxygenation, and redox conditions in the reed bed. In addition, the mode by which biochar is implemented in the filter and the choice of macrophyte are crucial for regulating the efficiency of the treatment system. *Phragmites australis* was the most used plant in the previous studies because of its large advantages. Different configurations of CWs integrating biochar into the wetland as a filling medium were reported and compared. In vertical flow CWs (VF-CWs), which are the system mostly investigated, several studies have shown that the optimal position for the biochar substrate is the intermediate one between two layers of inert materials, to avoid clogging of the filtration system or biochar flotation.

Keywords: Natural-based solutions; Sorbent materials; Wastewater treatment; Biomass thermal conversion; Configuration of constructed wetlands; Emerging contaminants.

1. Introduction

Constructed wetlands (CWs) are a kind of green technology that can be considered a sustainable, nature-based solution for wastewater treatment (Younas et al., 2022). In such systems, the plant and the substrate play an important role in the removal of pollutants (Addo-Bankas et al., 2021; Ohore et al., 2022). The substrate is an essential component of CWs since it can mediate and promote the implementation of mechanical, physical, and biological mechanisms for reducing pollutant concentrations in CW effluents, allowing for the direct removal of contaminants, making available reactive agents for transforming pollutants, promoting plant growth, and ensuring biofilm adhesion (Deng et al., 2021). Furthermore, plants uptake nutrients, directly increase biological activity in the substrate by supplying oxygen through their roots, and play an important role in the hydraulic conductivity within the filter. Hence, choosing the most appropriate plant species is important for obtaining the best performance (Srivastava et al., 2008; Guittonny-philippe et al., 2015; Kataki et al., 2021;

Karungamye, 2022).

The CWs have been widely tested for urban wastewater treatment, while the purification of sewage from industrial or mixed urban-industrial origin has been investigated to a lesser extent (Stefanakis, 2018; Kataki et al., 2021). CWs demonstrated high efficiency in removing conventional pollutants such as suspended solids, nutrients, and biodegradable organic matter (Huong et al., 2020; Zhuang et al., 2022). However, in most cases, CWs have shown a lower efficiency against various ecotoxic pollutants, such as detergents, heavy metals, plasticizers, disinfectants, pesticides, and pharmaceutical residues, which remain largely unremoved in CWs' effluents (Gosset et al., 2020). To improve CWs' efficiency, various materials, other than those conventionally used in CWs (i.e., gravel and sand) (Zhang et al., 2021; Fu et al., 2020), have been tested as substrates, namely pozzolan (El Ghadraoui et al., 2020), charcoal (Hamada et al., 2021), zeolite (Du et al., 2020), and biochar (Vymazal et al., 2021). Among them, biochar has recently gained increasing interest (Rozari et al., 2016) as a stable, porous, carbon-rich and originating from inexpensive material obtained by thermochemical conversion of waste biomass through various thermochemical processes such as hydrothermal carbonization (HTC), hydrothermal liquefaction (HTL), gasification, and pyrolysis (Deng et al., 2021). Slow pyrolysis (i.e., thermal conversion in the absence of oxygen and with contact time from minutes to hours) is commonly used as it is cheaper than other processes and/or gives rise to a higher yield of the solid fraction(i.e., biochar) with low syngas and bio-oil production (Enaime et al., 2020; Wang et al., 2020a). Various renewable and locally available waste biomaterials, such as compost, agricultural by-products, sludge, manure, and shellfish, have been used to produce biochar (Zhuang et al., 2022). In addition, biochar may also be produced from wetland plant straws and then reintroduced into wastewater treatment environments, thereby facilitating wetland plant management and sustainable exploitation of wastewater treatment systems (Wang et al., 2020a; Deng et al., 2021). Introducing biochar as a substrate in CWs can significantly increase the system's efficiency since it may have a high sorption capacity for organic and inorganic pollutants (Srivastava et al., 2008; Wang and Wang, 2019). However, the sorption capacity of biochar depends on the kind of feedstock used and its preparation conditions (Tan et al., 2015). The location of the biochar substrate in the filter can also affect the efficiency of the treatment system. Recently, several existing studies have investigated the effect of biochar used in CWs. Nevertheless, each study focused on one of the aforementioned aspects separately, while no review exists to date that critically evaluates all parameters

involved in the treatment and how they might interact to improve the treatment efficacy of CWs (Wu and Wu, 2019; Wang et al., 2020a; Ambaye et al., 2021; Cui et al., 2022; Zhuang et al., 2022). Nevertheless, no synthetic review exists until now discussing the optimal position of substrate biochar in the CW. We tried to collect all these aspects to enrich our synthetic review. In addition, very few reviews have described the emergent pollutants removal capacities of constructed wetlands integrating biochar.

According to a literature overview performed using the search engines SciFinder, Elsevier ScienceDirect, and Google Scholar, this paper critically reviewed data and information on (i) the characteristics and properties of biochars used in constructed wetlands (e.g. the conditions of thermal conversion and the type of feedstock used for the preparation of biochars, as well as the specific surface area (SSA) and environmental compatibility of the material), (ii) the methods of integrating the biochar within the CWs, and (iii) the results obtained in terms of removal of macro-parameters, as well as conventional and emerging micropollutants.

2. Biochar incorporated into CWs

2.1. Biochar feedstock

Biochar can be made from a wide variety of feedstocks (Gabhane et al., 2020; Berslin et al., 2022; Garcia et al., 2022; Zhuang et al., 2022). The composition of the feedstock and its availability are essential factors in the production of efficient and cost-effective biochar. Therefore, proper classification and characterization of feedstocks are required for their successful application.

Biochar feedstock used in the literature comes from various materials that can be classified into sewage sludge, agricultural waste and wood, food waste, and marine feedstock (**Table I-1**)

Table I-1: Feedstocks used for the production of biochars intended to be used in CWs, preparation conditions, and characteristics of the material obtained.

Feedstock	Pyrolysis temperature	Surface characteristics (SA, PV, PS) and pH	Composition	Reference
Bamboo	500 ◦C	SA(335 m^2/g)	C (68%)	(Zhang et al., 2021)
Bamboo	tubular furnace 500 °C - 10 °C/min - 2 h	SA(116.24 m^2/g)	C (74.56%); H (1.12%); O (6.28%); N (1.06%)	(Xin et al., 2021)
Bamboo	600 °C	SA (2.5 × 108 m^2/m^3)	C (59.44%); H (2.06%); O (15.89%); N (0.40%); P (0.34%)	(Jia et al., 2020)
Bamboo chips Bamboo	500 °C - 2h - N_2 700 °C - 10 °C/min - 6 h	PS(10 µm) SA(228.26 m^2/g); PV(0.086 cm^3/g)pH(9.5)	C (56.4%); O (6.3%) -	(Feng et al., 2021a) (Ajibade et al., 2020)
Arundo donax	600 °C- 1h	SA(281.15 m^2/g)	C (63.18%); H (1.80%); N (1.13%)	(Li et al., 2018b)
Arundo donax	Muffle furnace 500 ◦C - 10 ◦C.min^{-1} - 1h - N_2	SA(1272.67 m^2/g) ; PV(1.021 cm^3/g)	C(79.9 %) ;N(2.27 %) ; O(17.84 %)	(Shen et al., 2020)
Agricultural waste	500 ◦ C	SA(809 m^2/g); PV(0.22 cm^3/g)	-	(Abedi and Mojiri, 2019)
Lodgepole Pine Wood	1000 °C	SA(152 m^2/g); PS(1 - 40 µm) pH(9.66)	-	(Huggins et al., 2016)
Oak woody (*Quercus Sp*)	600˚C - 10h -10˚C/min	PS(1 - 10 µm)	O (8%); C (90%); P (0.54%); K (0.38%); S (0.1%); Ca (0.38%)	(Gupta et al., 2016)
Wood	600 °C - 10 °C/min - 10h	SA(147 m^2/g); PV(0.176 cm^3/g); PS(5.3 nm) pH(9.8)	C (90%); H (1.5%); O (8.3%); N (0.5%); S (0.3%)	(Kizito et al., 2017)
Wood dust	700 °C	SA(488.60 m^2/g); PV(0.286 cm^3/g)	C (81.50%); H (1.87%); O (15.63%); N (0.07%)	(Lun, L. Chen, 2018)
Cattail (Typha latifolia)	600 °C - 2h - 10 ◦C/min	SA(6.14 m^2/g); PV(0.02 cm^3/g)pH(8.9)	-	(Zheng et al., 2022)
Tree branches	550 °C - 2h - N_2	SA(32.09 m^2/g); PV(2.31 mm^3g^{-1})	-	(Ji et al., 2020)
Softwoods	700 °C – (gasification)	SA(485 m^2/g) pH(7.8)	C (89.2%); H (1.6%); O (1.9%); N (1%); S (0.04%); P (4.3%)	(Kaetzl et al., 2018)
Corn on the cob	600 °C - 10 °C/min - 10h	SA(123 m^2/g); PV(0.098 cm^3/g); PS(6.2 nm) pH(8.9)	C (69%); H (3.4%); O (17.6%); N (6.1%); S (4.4%)	(Kizito et al., 2017)
Corn cob	600 °C -2h	SA(263.0 m^2/g)	-	(Gotore et al., 2022)

Feedstock	Pyrolysis temperature	Surface characteristics (SA, PV, PS) and pH	Composition	Reference
Giant reed straw	500 °C - 2h	SA(345.92 m^2/g); PV(0.2467 cm^3/g); PS(1.95 nm)	-	(Deng et al., 2019)
Corn straw	450 °C, 2 h - 10 °C min^{-1} - N_2	SA(232.715 m^2/g); PV(0.098 cm^3/g); PS(1.286 nm)	C (77.30%) H (2.35%) N (0.87%) O (11.26%) S (0.02%) P (1.43%) Cl (l0.38%)	(Wang et al., 2022)
Nut shells	450 ◦C - 2h	SA(14.76 m^2/g)-pH(8.1)	C (68.6%); K (5.1%); Ca (4.0%)	(Chang et al., 2022)
Sludge	600 °C - 2h - 10 ◦C/min	SA(13.13 m2/g); PV(0.12 cm3/g); PS(18.71 nm) pH(7.9)	-	(Zheng et al., 2022)
Walnut shells	450 ◦C - 2h- N_2	SA(14.76m^2/g)	C (68.6%); K (5.1%); Ca (4.0%)	(Chang et al., 2022)

SA: Surface area; PV: Pore volume; PS: Particle size.

Agricultural waste and wood-derived biochar have been recently employed for the application in CWs. Bamboo is widely used as a raw material for biochar production, due to its abundance and high carbon content (>50%), which gives a good quality of biochar (Zhou et al., 2017; Jia et al., 2020; Gao et al., 2018; Zhang et al., 2021; Xin et al., 2021). Furthermore, plants such as *Arundo donax* and cattail (*Typha latifolia*) can absorb phosphorus and nitrogen from wastewater through their roots and transport them to the shoot, which may then be harvested and converted into biochar that can be reused as functional substrates in CWs, thus achieving a virtuous circular approach in this field (Guo et al., 2020; Li et al., 2018). Other vegetal materials have been transformed into biochar and used for wastewater treatment, such as cut residues of *Alnus* (Kasak et al., 2018), *Acacia auriculiformis* (Nguyen et al., 2020), Gliricidia (Yasaratne, 2017), coconut shell (You et al., 2019), and various agricultural waste (Abedi and Mojiri, 2019), because of their wide availability and high productivity. However, terrestrial macroplants have so far been the primary source of biochar used in CWs(Aghoghovwia et al., 2020; Du et al., 2020). The biochar performance derived from sewage sludge or marine life (e.g., macroalgae) may differ from terrestrial plants (Zhuang et al., 2022). In addition, Deng et al. (2021) stated that the biochars used in the CW treatment systems are generally made from *Arundo donax* straw, corn/straw cobs, bamboo, shells, tree branches, and wooden containers (Deng et al., 2021). Finally, the feedstock must be rich in carbon and low in mineral matter to produce good-quality biochar.

2.2. Biochar production conditions

Pyrolysis is commonly performed to prepare biochar used in CWs because of its advantages, generally consisting of higher yields of biochar and lower content of bio-oil and syngas (Enaime et al., 2020; Abdelhafez et al., 2021; Pereira and Astruc, 2021; Zhuang et al., 2022)..The temperature range between 400 and 600 °C was the most commonly adopted to prepare the biochar used in the filters (**Table I-1**) (Abedi and Mojiri, 2019; Chand et al., 2021; Zheng et al., 2022). The time and the temperature of pyrolysis are determining factors of the biochar characteristics (e.g., density, carbon content, pH, porosity) (Gong et al., 2019; Xiao et al., 2020) and, consequently, the performance of wastewater treatment (Alsewaileh et al., 2019; Hsu et al., 2019). Even though the kind of feedstock used for biochar preparation affects the characteristics of the material, it has been demonstrated that the increase in temperature generally produces higher percentages of ash, which is regulated by the EN 12915-1 standard

(European Committee for Standardisation (CEN), 2009) in materials intended for water filtration, since a high ash content in filtering media is expected to reduce adsorption activity (Castiglioni et al., 2022). Also, the presence of polycyclic aromatic hydrocarbons (PAHs), themselves regulated by the EN 12915-1, depends on the conversion temperature adopted, which plays a main role in PAH formation up to about 500 ◦C, but also in their degradation beyond this value (Castiglioni et al., 2022). The conversion temperature is also crucial in determining the SSA of the biochar and its microporosity/mesoporosity distribution, being the highest SSA values obtained at the highest temperatures, due to the increase of both pore size classes (Del Bubba et al., 2020). This result is also related to the progressive loss of the functional groups present in the material as the temperature increases (Del Bubba et al., 2020). However, the yield of fabricated biochar decreases with the rise of pyrolysis temperature (Apolin and Conceptualization, 2020).

Based on the above considerations, the adsorption performance of biochars obtained under different experimental conditions (e.g., different feedstock, conversion temperature, and contact time) will be better or worse depending on the contaminant to be removed. Accordingly, researchers used materials produced at very different temperatures to achieve the removal of their target contaminants. For example, the pyrolysis temperature of the sludge-based biochar at 400°C showed optimal ammonia adsorption, while pyrolysis temperatures at 350 °C or 550 °C were not favorable for the biochar's adsorption capability (Tang et al., 2018), i.e., without any clear consistent effect of pyrolysis temperature on biochar adsorption performance towards ammonia (Tang et al., 2018). However, Ajibade et al. (2020) and Huggins et al. (2016) prepared the biochar at high pyrolysis temperatures (700 and 1000 °C), resulting in a high surface area and pore volume of the produced biochar, which may serve as a niche for microbes for the effective treatment of pollutants (Ajibade et al., 2020).

2.3. Biochar characteristics for wastewater treatment

The physicochemical properties of biochar, such as pore distribution and size, surface functional groups, alkalinity, SSA, etc., which strongly depend on the feedstock and thermal conversion conditions, are responsible for pollutant adsorption capacity and biofilm adhesion (Wang et al., 2019; Tan et al., 2015). As a result, biochar's ability to remove inorganic and organic contaminants is determined by its characteristics as well as the characteristics of the molecules to be eliminated, such as the size, charge, and chemical moieties. As mentioned

above, the preparation of biochar at low temperatures results in a higher abundance of oxygen-containing functional groups, which are favourable for the adsorption of polar compounds. This biochar may also exhibit higher mechanical strength, making it preferable for use in CWs. In contrast, biochar produced at high temperatures has a larger porosity and SSA, a higher aromaticity, a higher carbon content, and overall a higher hydrophobic character (Del Bubba et al., 2020; Castiglioni et al., 2021). The net surface charge of the biochar (commonly evaluated by the pH of the point of zero charge and/or Boehm's titration), which mainly depends on the surface functional groups of the material and is often related to its ash content, is a further crucial parameters to explain the adsorption behaviours of biochars, particularly towards ionized or ionisable compounds (Castiglioni et al., 2022). Accordingly, best-performing biochars can be obtained at lower or higher temperatures, depending on the target molecule to be removed. For example, phenol adsorption was higher for biochars produced at 900 °C than for those prepared at a lower temperature (600 °C), probably due to the relative increase in SSA at the higher pyrolysis temperature(Mohammed et al., 2018). Similarly, Xu and Lu. (2019) reported an increasing removal efficiency of biochar towards bisphenol from aqueous solutions with increasing preparation temperature. However, Del Bubba et al., (2020), studying the removal of 16 alkylphenols and alkylphenol ethoxylates from real wastewater, with biochar produced at 450, 650, and 850°C, observed higher absolute absorption maxima for materials produced at the two highest temperatures, depending on the investigated molecule.

The biochar can be modified chemically, physically, or biologically to increase its properties and achieve greater adsorption and catalysis capacities for the target pollutants (Xu and Lu, 2019). In addition, the pH of the solution played a key role in controlling the deprotonation and hydrophobicity of the compounds, which is in agreement with the correlation analysis of the maximum sorption capacity. The pH of biochar produced to be used as a substrate in CWs was generally alkaline and varied between 7.9 and 9.8 (**Table I-1**) (Enaime et al., 2020; Kizito et al., 2017; Zheng et al., 2022).

The carbon content can give an early indication of biochar quality. Generally carbon (C) was the main compositional element of biochar, varying approximately from 50% to 90%, followed by oxygen (O) and nitrogen (N) and other elements that were present at much lower percentages (**Table I-1**) (Gupta et al., 2016; Kizito et al., 2017). In Kizito's study, element C was found at 69% in biochar derived from corn cobs and 90% in wood, confirming that biochar characteristics are feedstock dependent (Kizito et al., 2017). The biochar generally had a high

surface area of several hundred m^2/g (Abedi and Mojiri, 2019; Deng et al., 2019); for example, in Abedi's study, the BET surface area of biochar was around 809 m^2/g (Abedi and Mojiri, 2019). However, other investigations have found it as low as a few tens of m^2/g (Ji et al., 2020; Zheng et al., 2022). For example, the study by Zheng, who works on two feedstocks, the cattail (*Typha latifolia*) and sludge, shows that the two feedstocks give low specific surfaces of 6.14 and 13.13 m^2/g, respectively (Zheng et al., 2022). With increasing pyrolysis temperature, the porosity, surface area, and carbon content of biochar increased. However, bio-assimilation decreased. The percentage of carbon in biochar grew from 57.8% to 63.2% as the pyrolysis temperature increased from 300 to 500 °C. On the other hand, the surface area increased by more than one magnitude from 10.0 m^2/g to 281 m^2/g (Li et al., 2018a). This shows that the porosity is extremely sensitive to temperature variation compared to the percentage of carbon. These properties will probably influence their function in CWs. According to Liao et al. (2022), the biochar must have a large pore volume and surface area to adsorb pollutants and provide adhesion of microorganisms (Liao et al., 2022). In most cases, the biochar used in CWs has a higher specific surface area (>200 m^2/g) to provide a higher number of adsorption sites (Shen et al., 2020; Zhang et al., 2021; Gotore et al., 2022).

3. Configurations of biochar-based CWs and their removal efficiency

The performance of a CW depends on the type of CW, temperature, vegetation, water flow regime (hydraulic regime), dissolved oxygen (DO), substrate nature, redox potential (Eh), and applied hydraulic load (Parde et al., 2021; Malyan et al., 2021). **Table I-2** shows the order, dose, dimension of substrates, different plants used in CW, and the removal efficiency of pollutants of each configuration.

Table I-2: Characteristics of CWs integrated with biochar.

Implementation mode of the substrate (by order)	Plant species and density	Wastewater	CW size	Aeration	Feeding	HLR	HRT	Experiment duration	Removal efficiency	Reference
- Sand (0.5-2 mm) h=50 mm - Biochar (2.95%) + gravel: h=300 mm - Gravel (10–20 mm) h=50 mm	Acorus calamus L. 4 rhizomes	Tail water	VF-CW h=450 mm d=160 mm	No	-	0.055 $m^3 \cdot (m^2 \cdot d)^{-1}$	3 days	2 months	COD (76%), TP (52%), TN (82%), NH_4^+ (84%), $N0_3^-$ (89%)	(Wang et al., 2022)
- Zeolite (d=2-4 mm) h=30 cm - Biochar (d=3-5 mm) h=30 cm - Cobblestone (d=20-30 mm) h=5 cm	Phragmites australis	Synthetic wastewater	VF-CW h=75 cm d=14 cm V= 2 L	No	-	260 $L \cdot m^{-2} \cdot d^{-1}$	12 h	4 months	NH_4^+ (95.49%), $N0_3^-$ (83.24%), TN (83%)	(Zhong et al., 2021)
- Clay ceramite (d= 2-5 mm) h=7 cm - Biochar (d= 2-5 mm) h=14 cm - Clay ceramite (d= 2-5 mm) h=7 cm	Lythrum salicaria	Domestic wastewater	HF-CW l= 30 cm w= 15 cm h= 30 cm	Yes	Manually 4 L	-	24h	6 months	COD (75.5%), TP (76.2%), TN (59.2%), NH_4^+ (62.5%)	(Ji et al., 2020)
- Gravel (d=7-8 mm) h =3 cm - Biochar (d= 6-8 mm) h=10 cm - Gravel (d= 7-8 mm) h =3 cm	Plants hydroponics	Synthetic wastewater	VF-CW d = 12 cm	-	-	-	-	6 months	COD (99.84 %), NH_4^+ (92.00 %), TP (88.63 %)	(Liao et al., 2022)
- Gravel (d=1-3 cm) - Biochar (d=1-2 cm) h=3-6-9 cm - Gravel (d=1-3 cm)	Acorus calamus 30 rhizomes$\cdot m^{-2}$	Synthetic Wastewater	VF-CW h=35 cm d=33 cm	-	Manually 10 L	0.05 $m^3.m^{-2}.d^{-1}$	48 h	6 months	COD (89.88%), TN (86.36%), NH_4^+ (63.51%)	(Deng et al., 2019)
- Pebbles (d= 90 mm) h=5 cm - Biochar (d= 10 cm) - Gravel (d= 15 mm) h=17 cm - Gravel (d= 10 mm) h=5 cm	Canna sp	Synthetic wastewater	HF-CW 1m x 0.3m x 0.3m	Yes	32 L	-	72 h	-	COD (91.3%), TN (58.3%), NH_3^- (58.3%), NO_3^- (92%), TP (79.5%), PO_4^{3-} (67.7%)	(Gupta et al., 2016)
- Pebbles (d=5-7mm) h=5 cm - Coke (d=3-5 mm) h=74 cm - Fe-modified biochar (50 mm×10 mm×5 mm) - Pebbles (d=5-7mm) h=5 cm	Canna	River water	VF-CW h=100 cm d=30 cm	-	-	-	-	5 months	Abamectin (99%), COD (98%), NH_4^+ (65%), TP (80%)	(Sha et al., 2020)
- Sandy soil h=10 cm	Colocasia	Domestic	VF-CW	Yes	-	-	-	6 months	COD (73%), DBO_5	(Nguyen et

Implementation mode of the substrate (by order)	Plant species and density	Wastewater	CW size	Aeration	Feeding	HLR	HRT	Experiment duration	Removal efficiency	Reference
- Sand (d= 2 mm) h=20 cm - Biochar (d=1-3 cm) h=40 cm - Gravel (d=2-3 cm) h=10 cm	esculenta 64 seedlings/m^2	wastewater	h=1.0 m d=0.5 m						(79%), NH_4^+ (91%), TSS (71%), Total coliforms (70%)	al., 2020)
- Sand (d < 2 mm) h= 15 cm - Gravel + Biochar (v/v=1:1): (d=1-2 cm) h=15 cm - Gravel + Biochar (v/v=1:1): (d=2-4 cm) h=25 cm - Gravel (d=5-7 cm) h=10 cm	Iris pseudacorus 6 rhizomes	Swine wastewater	VF-CW h=65 cm d=20 cm	Yes	-	33.74 $g.m^{-3}.d^{-1}$	72 h	2 months	COD (77.18 %), NH_4^+ (96.54 %), TN (40.12 %), ARGs (99.3%)	(Feng et al., 2021a)
- Sand (d= 1-2 mm) h=150cm - Biochar + fine gravel (v/v=3:1): (d= 10-20 mm) h=150 mm - Gravel (d= 20-40 mm) h=250 mm - Gravel (d= 50-70 mm) h=100 mm	Oenanthe Javanica 12 rhizomes	Domestic wastewater	VF-CW h=65 cm d=20 cm	Yes	5.5 L	-	72 h	3 months	COD (91.80%), NH_4^+ (50.05%), TN (49.90%)	(Zhou et al., 2018)
- Gravel (d= 5-8 mm) h= 0.1 m - Biochar (sludge) + gravel (v/v=1:4) h= 0.2 m - Gravel (d= 5-8 mm) h= 0.1 m	Typha latifolia	Synthetic wastewater	VF-CW h= 0.5 m d= 0.2 m	No	-	-	72 h	60 batches	COD (90.99%), NO_3^- (99.50%), NH_4^+ (99.59%), TN (90.94%), TP (51.59%)	(Zheng et al., 2022)
- Gravel (d= 5-8 mm) h= 0.1 m - Biochar (cattail) + gravel (v/v=1:4) h= 0.2 m - Gravel (d= 5-8 mm) h= 0.1 m	Typha latifolia	Synthetic wastewater	VF-CW h= 0.5 m d= 0.2 m	No	-	-	72 h	60 batches	COD (77.4%), NO_3^- (84.7%), NH_4^+ (96.1%), TN (80.7%), TP (43.95%)	(Zheng et al., 2022)
- Gravel (d=2-6 mm) h=0.05 m - Biochar (v/v=1%) + sand (d=2-10 mm) h=0.2 m - Gravel (d=2-6 mm) h=0.05 m - Gravel (d=2-10 mm) h=0.05 m	Iris pseudacorus 5 rhizomes	Synthetic wastewater	VF-CW h=0.45 m d=0.15 m	No	-	-	72 h	4 months	COD (89.1%), TN (90.2%), NH_4^+ (81%)	(Ajibade et al., 2020)
- Soil h=10 cm - Quartz sand h=5 cm - Zeolite d=8–10 mm + biochar d=2–4 mm (v/v=1:1) h=30 cm - Cobblestones (d=7–10 cm) h=10 cm	Phragmites communis 6 plants	Synthetic wastewater	VF-CW l=50 cm w=40 cm d=60 cm	Yes	30 L	0.050 $m^3.m^{-2}.d^{-1}$	72 h	4 months	TN (62.98%), NH_4^+ (93.93%), NO_3^- (93.28%), COD (86.64%), CIP (88.05%), SMZ	(Yuan et al., 2020)

Implementation mode of the substrate (by order)	Plant species and density	Wastewater	CW size	Aeration	Feeding	HLR	HRT	Experiment duration	Removal efficiency	Reference
									(56.57%)	
- Sand (d = 2-4 mm) h = 2 cm - Biochar (2%) + Sand (98%): (d=5-10 mm) h= 15 cm - Sand (d = 2-4 mm) h = 3 cm	Phragmites australis	Synthetic stormwater	VF-CW h = 25 cm d = 11 cm	-	-	10-40 cm/h	5 days	3 months	TSS (71.1%), TOC (29.3%), NH_4^+ (13.5%), TN (11.7%), TP (8%), *E.coli* (87.1%)	(Chen, 2018)
- Sand - Biochar + gravel: v/v = 50%. - Gravel	Iris pseudacorus 6 rhizomes	Synthetic wastewater	VF-CW h = 50 cm d = 10 cm	Yes	-	-	72 h	5 months	COD (93.21 %), NH_4^+ (98.30 %), TN (72.22 %),TP (53.32%)	(Li et al., 2019)
- Gravel (d=8-10 mm) h=0.1 m - Biochar + gravel (v/v=4:1) h=0.2 m - Gravel (d=8-10 mm) h=0.1 m	Typha latifolia	Synthetic wastewater	VF-CW l= 0.3 m w= 0.3 m h = 0.5 m	-	-	-	5 days	60 batches	NH_4^+ (66.3%), TN (65.4%), COD (90%)	(Guo et al., 2020)
- Biochar (d=2-3 cm) h=25 cm - Zeolite (d=2-3 cm) h=25 cm - Gravel (d=2-3 cm) h=25 cm	Phragmites australis	Synthetic Wastewater	VF-CW h=80 cm d=40 cm	Yes	-	-	57.4 h	3 months	COD (99.9%), NH_3^- (99.9%), Phenols (99.9%), Pb (99.9%), Mn (99.9%)	(Abedi and Mojiri, 2019)
- Biochar (20%) + sand (80%) h=20 cm - Gravel h=5 cm	O. javanica 12 rhizomes	Synthetic wastewater	VF-CW h = 50 cm d = 25 cm	No	-	0.13 m^3m^{-2} $batch^{-1}$	7 days	8 months	COD (78.71%), NO_3^- (92.72%), TN (93.26%), NH_4^+ (94.26%)	(Li et al., 2018a)
- Biochar + sand: (d=0.5-1 mm) h=15cm - Gravel (d=4-6 mm) h=10cm - Gravel (d=8-12 mm) h=10cm - Rocks (d=20-21 mm) h=5cm	Colocasia esculenta 10 rhizomes	Domestic wastewater	VF-CW h=37cm d=33.5cm	Yes	-	-	10 days	40 days	COD (96.8%), NO_3^- (57.85%), TN (68.02%), NH_4^+ (88.16%), PO_4^{3-} (75.26%), SO_4^{2-} (80.50)	(Chand et al., 2021)
- Biochar (corn cobs) (d= 2-10 mm) h= 0.6 m - Gravel (d=50 mm) h=0.1 m	-	Industrial wastewater	VF-CW h = 0.9 m d = 0.2 m	No	-	-	-	5 months	COD (59%), BOD_5 (75%), TN (37%), NH_4^+ (76%), PO_4^{3-} (71%)	(Kizito et al., 2017)
- Biochar (wood) (d= 2-10 mm) h= 0.6	-	Industrial	VF-CW	No	-	-	-	5 months	COD (72%), BOD_5	(Kizito et al.,

Implementation mode of the substrate (by order)	Plant species and density	Wastewater	CW size	Aeration	Feeding	HLR	HRT	Experiment duration	Removal efficiency	Reference
m - Gravel (d=50 mm) h=0.1 m		wastewater	h = 0.9 m d = 0.2 m						(83%), TN (47%), NH_4^+ (83%), PO_4^{3-} (85%)	2017)
- Biochar (d=2–4 mm) h=120 mm	Salicaria seedling	Synthetic wastewater	VF-CW d=110 mm h=150 mm	Yes	550 mL	-	24 h	> 3 months	Hg (>94%), COD (>88%), NH_4^+ (92.1), TP (74.7%)	(Chang et al., 2022)
Mixture of Quartz rock d=2 - 4 mm (v/v=25 %), Bioceramic d=3 - 6 mm (v/v=25 %), and biochar d=1 - 7 mm (v/v= 50%) h=200 mm	Cyperus alternifolius	Synthetic wastewater	HF-CW l=670 mm h=310 mm w=300 mm	No	30 L	-	25 h	-	NO_3^- (67.16%), TP (74.25%), TN (64.31%), NO_2^- (51.6%), PO_4^{3-} (96.73%)	(Gao et al., 2018)
Mixture of quartz sand + soil (v/v=1:1) and Fe-modified biochar (v/v:10%)	Iris hexagonus 13 plants/m^2	Tailwater	VF-CW l= 100 cm w= 60 cm d= 75 cm	-	-	-	96 h	-	NO_3^- (95.30 %), TN (86.68 %), NH_4^+ (86.33 %), NO_2^- (79.35 %), COD (63.36 %)	(Jia et al., 2020b)
Mixture of biochar (v/v=10%) (d<20mm) and LECA (d=2-4 mm)	Typha latifolia 10 plants/mesocosm	Municipal wastewater	HF-CW l=1.5 m w=0.6 m d=0.6 m	-	-	60 L/d	48 h	4 months	TN (20.0 %), TP (22.5 %)	(Kasak et al., 2018)
- Gravel (d=2-6 mm) h=0.05 m - Biochar (v/v=1%) + sand (d=2-10 mm) h=0.2 m - Gravel (d=2-6 mm) h=0.05 m - Gravel (d=2-10 mm) h=0.05 m	Iris pseudacorus 5 rhizomes	Synthetic wastewater	VF-CW h=0.45 m d=0.15 m	No	-	-	72 h	4 months	COD (75.9%), TN (69.2%), NH_4^+ (70.8%), NO_3^- (74.7%), SMZ (65.3%)	(Ajibade et al., 2021)
- Biochar + sand (d=0.25–1 mm) h=6 cm - Gravel (d=4-6 mm) h=10 cm - Gravel (d= 8-12 mm) h=10 cm - Boulders (d= 20-21 mm) h=5 cm	Colocasia	Synthetic wastewater	VF-CW d=33.5 cm h=37 cm V=30 L	No	-	-	-	-	COD (88.8%), NH_4^+ (83.1%), and NO_3^- (64.9%), AMX (75.51%), FC (87.53%), IBU (79.93%)	(Chand et al., 2022)
Sand h=15 cm Biochar h= 20 cm	G. maxima	Synthetic wastewater	VF-CW d=15 cm	No	-	2 L/ 4d	-	3 months	PPCPs (99.99 %)	(Kang et al., 2019)

Implementation mode of the substrate (by order)	Plant species and density	Wastewater	CW size	Aeration	Feeding	HLR	HRT	Experiment duration	Removal efficiency	Reference
Gravel h=15 cm			h=55 cm							
Stones (d= 5-10mm) h=0.05 m Biochar (d= 5-10mm) h=0.76 m Stones (d= 5-10mm) h=0.05 m	Phragmites	Municipal wastewater	VF-CW h=0.91 d=0.15 m	No	-	-	-	-	NH_4^+ (89.8%), NO_2^- (38.5%), TN (82.5%), TP (91%), BOD_5 (95%), COD (96.2%), TSS (99.7%)	(Saeed et al., 2020)
Gravel (d=2 cm) Biochar v/v=30% (d=2 cm) Gravel (d=2 cm)	Cyperus alternifolius L	Synthetic wastewater	VF-CW h=35 cm S=0.1 m^2	Yes	-	-	24 h	-	COD (93.4%), TN (94.9%), NH_4^+ (99.4%)	(Liang et al., 2020)
Fe-modified biochar v/v=1/3 (d=1–2 mm) + gravel (diameter of 2–4 mm) h=50 cm	Acorus calamus	Synthetic wastewater	VF-CW h=60 cm d=25 cm	-	-	-	3 days	-	NH_4^+ (44.8%), NO_3^- (51.8%)	(Kang et al., 2023)
Cu-Biochar (40%) + sand (60%): h= 50 cm	Iris pseudacorus 6 plants/unit	Synthetic wastewater	VF-CW h= 75 cm d=25 cm	No	-	-	3 days	2 months	COD (75.33%), NO_3^- (91.11%), Phenanthrene (94.09%)	(Shen et al., 2020)
Two cells: the first one with gravel and the second with biochar	Melaleuca quinquenervia	Domestic wastewater	HF-CW 1.2 m × 0.76 m × 0.4 m	No	-	0.023 m/day	5.1 days	7 months	PO_4^{3-} (97%)	(Bolton et al., 2019)
Gravel (v/v=80% ; d=1–2 cm) + soil (v/v=10%) + biochar (v/v=10% ; d=0.1–0.5 mm)	Hydrocotyle verticillata + Iris germanica 100 clumps/m^2	Tail wastewater	HF-CW S= 900 m^2	No	-	-	1 day	3 months	TN (62.62%), TP (52.99%), NO_3^- (73.28%), NH_3^- (53.11%), PO_4^{3-} (67.58%)	(Gao et al., 2019)
Zeolite (d=20 cm) Biochar (d=10 cm) Gravel (d=20 cm)	Canna indica 16 plant/m^2	Synthetic wastewater	HF-CW 110 cm ×40 cm ×60 cm	No	-	-	-	11 months	NH_4^+ (89.1%), TN (88.1%), TP (75.9%)	(Wu et al., 2022)

HRL: Hydraulic loading rate, HRT: Hydraulic retention time

3.1. Integration mode of biochar in CWs

3.1.1. Biochar in vertical flow CW

When used as a substrate in VF-CWs, biochar can potentially promote contaminant removal. As illustrated in **Figure I-1A**, most CWs are implemented by positioning the biochar between two layers of inert material (**Table I-2**), thereby avoiding the clogging of the filtration system (Ji et al., 2020; Liang et al., 2020; Liao et al., 2022). In this interlayer, the biochar is used alone or mixed with other materials, namely sand, gravel, etc. (**Table I-2**) (Ajibade et al., 2020; Liao et al., 2022; Zhong et al., 2021; Zhou et al., 2018).

Several authors have used the biochar substrate alone as an interlayer of the filter system in order to increase the removal rate of different pollutants. For example, in the study of Nguyen et al. (2020), the biochar substrate is used under two sand and sandy soil layers. This distribution increases the removal efficiencies of total coliforms up to 70% (Nguyen et al., 2020). Moreover, using biochar substrate under a coarse stone substrate allows the removal of total phosphorus up to 91% and organic matter such as BOD_5 and TSS up to 95% and 99.7%, respectively, from municipal wastewater (Saeed et al., 2020). Another study placed the biochar substrate under a coarse pebble layer to improve nitrate removal performance up to 92% and orthophosphate up to 67.7% (Gupta et al., 2016). However, using gravel substrate over biochar increases the removal performance up to 94.9% for TN, 99.4% for $NH_4^{+,}$ and 99.84% for COD (Liang et al., 2020; Liao et al., 2022). On the other hand, the modification of biochar with iron shows high removal performance of pollutants such as Abamectin (99%), COD (98%), NH_4^+ (65%), and TP (80%) (Sha et al., 2020).

Biochar can be mixed with gravel (Feng et al., 2021a), sand (Ajibade et al., 2020), or zeolite (Yuan et al., 2020) to form a single substrate to filter various micropollutants from wastewater. Zheng et al. (2022) found that mixing biochar with gravel at a volume ratio of 1:4 resulted in high removal efficiency of COD (90.99%), NO_3^- (99.50%), TN (90.94%), NH_4^+ (99.59%), and TP (51.59%). On the other hand, mixing biochar with sand with a low volume ratio of biochar (2%) gave low removal rates (TOC (29.3%); NH_4^+ (13.5%); TN (11.7%); TP (8%)) except for *E.coli*, TSS and coliforms, which show high removal efficiency, coming up to 87.1% and 71.1% for *E.coli* and TSS, respectively (Chen, 2018). Similarly, Ajibade et al. (2020) also mixed biochar with sand. Still, this time gave a high performance compared to the study of Lun and

Chen. (2018), where the removal efficiency of some pollutants reached 89.1 % for COD, 90.2% for TN, and 81% for NH_4^+ (Ajibade et al., 2020). The ratio of biochar can explain the difference between these two studies, which is higher in the second one. Yuan et al. (2020) reported that mixing biochar with zeolite can improve the removal percentage up to 63% for TN, 94% for NH_4^+, 93% for NO_3^-, and 87% for COD. This result may be justified by the fact that the biochar inhibited the formation of quinolone resistance genes and enhanced the COD removal efficiency by increasing the abundance of bound microorganisms (Yuan et al., 2020). In most studies, biochar substrates mixed with gravel showed higher removal efficiency of various pollutants compared to biochar substrates mixed with sand (**Table I-2**).

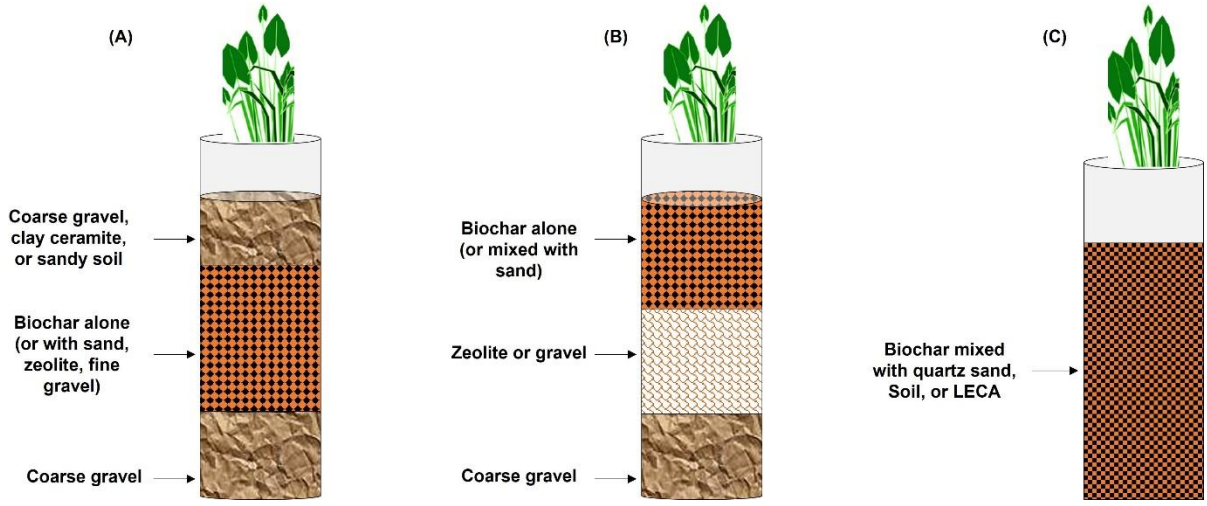

Figure I-1: Position of biochar substrate (A): as an interlayer of VF-CW, (B): on top of the VF-CW, (C): filling the whole VF-CW.

Biochar can also be placed at the top (**Figure I-1B** and **Table I-2**) of the filtration system with a large grain size (2-30 mm) in order to avoid the clogging phenomenon (Abedi and Mojiri, 2019; Kizito et al., 2017). In Abedi and Mojiri. (2019), the top biochar layer played an important role in decreasing the content of various pollutants such as COD, NH_4^+, phenols, Pb, and Mn. This study showed the best removal performance compared to the literature, since the removal efficiency was quantitative for COD, NH_4^+, phenols, Pb, and Mn (Abedi and Mojiri, 2019). This result can be explained because biochar is mainly attributed to the greater adsorption capacity and microbial culture in the porous medium of biochar (Kizito et al., 2017). Furthermore, the use of biochar at the upper filter level revealed that adding biochar in VF-CWs improves the oxidative removal of NH^{4+}-N, SO_4^{2-}, and PO_4^{3-} and contributes to the uptake of other plants (Chand et al., 2021). Another study conducted by Chand et al. (2021) used

biochar on top of a system with small grain size (d = 0.5-1 mm), but to avoid clogging, they mixed the biochar with sand, which allowed them to increase the treatment efficiency and thus removed up to 97% for COD, 58% for NO_3^-, 68% for TN, 88% for NH_4^+, 75.26% for PO_4^{3-} and 80% for SO_4^{2-} (Chand et al., 2021).

Sometimes the whole filter is filled from top to bottom with biochar (**Figure I-1C** and **Table I-2**) mixed at a low rate (10%) with another material (quartz sand, soil, LECA), to avoid the clogging of the system. For example, Jia et al. (2020) mixed 10% biochar with quartz sand and soil to fill the entire filter and obtained an increase of the removal efficiency of pollutants (NO_3^- (95.30%); TN (86.68%); NH_4^+ (86.33%); NO_2^- (79.35%); COD (63.36%)) (Jia et al., 2020).

3.1.2. Biochar substrate in the horizontal flow CW

The use of biochar in horizontal flow CWs (HF-CWs) is still limited, and a limited number of articles were found (Gao et al., 2018; Bolton et al., 2019; Gao et al., 2019; Jia and Yang, 2021; Wu et al., 2022). For example, Bolton et al., (2019) implemented two small pilot-scale HF-CWs planted with *Melaleuca quinquenervia* trees, each one consisting of two cells separated by a polyethylene baffle. The first wetland contained two cells in series filled with gravel (control wetlands), while in the other wetland, the first cell was filled with gravel to trap sediments, thus avoiding blockages in the downstream cell, the latter filled with an enriched biochar cell (biochar wetlands). This study showed that the removal efficiencies of PO_4^{3-}-P in the biochar wetland were up to 97%, probably due to the higher number of adsorption sites in the substrate. In contrast, the control achieved only an average PO_4^{3-}-P removal of 91%, indicating a rapid saturation of the gravel. Another study conducted by Gupta et al., (2016) revealed that HF-CWs with biochar were more efficient in reducing various pollutants (organic and inorganic) as compared to the wetland with gravels alone. Hence, the removal efficiencies achieved around 58% of TN, 79% of TP, 92% of NO_3-N, 58% of NH_3-N, 68% of PO_4^{3-}-P, and 91 % of COD. The high removal of NH_4^+-N obtained in HF-CWs is probably related to the enhanced microbial nitrification when adding biochar (Gupta et al., 2016). The improved NO_3-N removal efficiency is attributed to higher denitrification, due to the anoxic conditions in HF-CWs. These results indicate clearly that integrating biochar in HF-CW can be primarily used for a secondary treatment of municipal and domestic wastewaters, leading to nutrient removal. In general, the use of biochar in HF-CWs can be a cost-effective and sustainable wastewater treatment option with a smaller energy footprint (Wu et al., 2022; Gupta et al., 2016).

3.2. Effect of substrate nature, biochar dose, and granulometry on CWs efficiency

The fundamental element of the CW system is the substrate or media, which is essential for removing contaminants from wastewater. It serves as a platform for biofilm development, macrophyte root growth, and a reaction site for pollutants' immobilization and supporting matrix (Wu et al., 2015). Therefore, the choice of bed materials is highly important in a CW. Inexpensive and locally available materials can be used depending on the size of the media, its hydraulic conductivity, texture, porosity, and other factors (Wu et al., 2015). Gravel, biochar, zeolite, composite materials, and activated carbon have been used as CW substrates (Kataki et al., 2021). Substrates such as sawdust, light expanded clay aggregate (LECA), zero-valent iron, and gravel can effectively remove phosphorus, organic matter, arsenates, and sulfates (Parde et al., 2021).

Biochar-based CWs show promising wastewater treatment efficiency (Enaime et al., 2020). However, granular biochar is more suitable for applications than powdered biochar. This can be explained by its good pore size distribution, low abrasion index, durability, high bulk density, and ability to regenerate (Louarrat, 2019). In addition, this type of biochar has sufficient mechanical strength and is suitable for ensuring the stability and hydraulic permeability of the matrix (Deng et al., 2021). In addition, particle size has a significant effect on pollutant adsorption. Nitrate-nitrogen content, ammonia nitrogen content, and denitrification intensity of the wetland substrate decreased by 51%, 47%, and 35%, respectively, after the introduction of biochar with a particle size ranging from 1-2 mm in CW (Zhou et al., 2018), when compared to biochar with a particle size lower than 1 mm. Biochar with a 1-3 cm diameter is widely used as a substrate in CWs to avoid clogging (**Table I-2**) (Nguyen et al., 2020). Other factors influence the adsorption of pollutants, such as increasing the contact time, pH, temperature, and concentration of NH_3. But adsorption is decreasing with increasing size of biochar particles (Kizito et al., 2015). According to these results, we can state that the biochar granulometry has a significant effect on the efficiency of the treatment of the pollutants.

On the other hand, the biochar dose in CW substrate strongly influences the removal performance of various pollutants. However, a study conducted by Deng et al. (2019) was built based on different volumes of biochar in common gravel (0%, 10%, 20%, and 30%) to test the effect of increasing biochar substrate depth on the characteristics of metabolites and microbes. This experiment found that increasing the biochar dose in the gravel medium enhanced the

contaminant removal efficiency in CWs. Hence, Illumina MiSeq sequencing reported that the microbial community showed some obvious variations. The relative abundances of *Candidatus competibacter, Thauera, Dechloromonas, Chlorobium, Thiobacillus,* and *Desulfobulbus* were significantly improved with the biochar dose. On the other hand, the content of total Extra Polymeric Substances (EPS) decreased with increasing biochar percentage.

Furthermore, the increase in biochar dose in CWs substrate reflects an improvement in the biodegradation of EPS and the richness of microbial communities, which promotes the removal of organic and nitrogenous substances (Deng et al., 2019). Similarly, Liang et al. (2020) used 4 CW microcosms with different volume ratios of biochar (0%, 10%, 20%, and 30%) to analyze the improvement of pollutant removal performance. The results showed that the increase in biochar dose increased the average removal efficiencies of total nitrogen (TN) and ammonium (NH_4^+-N). At the same time, nitrous oxide (N_2O) emissions were reduced. The increase in biochar dose can explain this change in the diversity and similarity of the microbial community. In addition, the relative abundance of functional microorganisms such as Nitrospira, Nitrosomonas, Pseudomonas, and Thauera increased due to the increase in biochar content, which favored nitrogen cycling and reduced N_2O emissions.

3.3. Effect of macrophytes used and their role in CWs implemented with biochar

Plants are essential in removing pollutants, as they generally play an indirect role in the wastewater treatment performance in CWs (Fu et al., 2022). The choice of appropriate plant species is crucial for the best performance (Guittonny-Philippe et al., 2015; Srivastava et al., 2008; Kulshreshtha et al., 2022). Hence, the right choice was based on several parameters; the species that are preferred are characterized by high ecological adaptability, adaptation to local climatic and nutritional conditions, high biomass productivity, resistance to pests and diseases; having good coverage with high prospects of successful establishment, tolerance to pollutants and hypertrophic waterlogging conditions, low tendency to dominate or forming monocultures, a high capacity for pollutant removal, easy propagation, and rapid establishment (Nuamah et al., 2020; Kataki et al., 2021). According to literature the *Phragmites australis* was the most used plant in the studies (**Table I-2**), due to its effect on the efficiency of CW, resistance to pests and diseases, tolerance to pollutants and hypertrophic waterlogging conditions, high capacity for pollutant removal, easy propagation and adaptation to local climatic and nutritional conditions (Zhong et al., 2021; Yuan et al., 2020; Chen, 2018). However, a comparative study

done by Qadiri et al., (2021) has demonstrated that the CWs transplanted with *Phragmites* have more capacity in removing TN, COD, TP, and TSS than *Sagittaria latifolia* and *Iris kashmiriana*, due to their well-developed roots in the substrates, which gives a better remediation effect. Furthermore, the presence of a biochar substrate in the CW promotes plant growth, microbial metabolism, and substrate characteristics in many aspects (Qadiri et al., 2021). Another key parameter in selecting CW species is the higher water use efficiency index (Stefanakis, 2020). Several studies have shown that plants with fibrous root systems provide a greater surface area for biofilm enhancement, sedimentation, and particulate matter trapping. They show higher photosynthesis and radial oxygen loss levels and are more effective in removing contaminants than plants with thick roots (Lai et al., 2012; Borne et al., 2013; Kataki et al., 2021). In addition, previous studies have shown that plant density affects CWs' performance at 5 to 50 plants/m^2. A low density (16 m^2) CW planting may result in lower nitrogen removal than a CW with a high plant density (32 m^2) (reduced by almost half) (Hernández et al., 2017). Another factor to consider is the age of the plant, as oxygen release and contaminant uptake are lower in older plants due to the presence of older lignified roots (Valipour and Ahn, 2015).

3.4. Effectiveness of biochar in removing various pollutants

Biochar is a solid material with high porosity, a high surface area, and diverse surface functional groups and properties, making it an attractive option for wastewater treatment. Biochar has been proposed as an effective substrate for capturing wastewater supplements that may be connected to soil alteration. The adsorption properties and high porosity allow pollutants to accumulate on its surfaces, resulting in supplement-rich biochar and a clean effluent (Peiris et al., 2017; Yaashikaa et al., 2020). Biochar adsorbents have been used to remove various contaminants (**Table I-2**) such as antibiotics (Ahmed et al., 2017), pesticides (Mandal et al., 2021), pharmaceuticals (Masrura et al., 2021; Solanki and Boyer, 2017), and personal care products from aquatic environments (Keerthanan et al., 2020). The use of biochar for wastewater treatment is becoming more viable due to the low cost of the raw material and the ease of the manufacturing process, as well as the various improved physicochemical characteristics of biochar, which have been successfully used in a diverse range of applications for the contaminated wastewater remediation, including toxic heavy metals adsorption (the following techniques have been used: chemisorption, physical sorption, ion exchange, and precipitation) and dyes from aqueous solutions, as immobilization support for microorganisms, as a support

for catalysts, and as an adsorbent for inhibiting substances during anaerobic digestion, thanks to its unique and very versatile characteristics. Overall, it is clear that biochar has multiple potential economic and environmental benefits, and its effectiveness in removing various contaminants on a laboratory scale has been widely reported (Ahmad et al., 2021; Enaime et al., 2020; Chen et al., 2022).

Biochar added to CW substrate can considerably enhance the wastewater purification effect (Kizito et al., 2017), as biochar can remove more nutrients and reduce greenhouse gas (GHG) emissions than other substrates, e.g., ceramite, while promoting more diverse bacterial communities and greater abundances of available taxa (Ji et al., 2020). The average N_2O and CO_2 fluxes were significantly lower, while CH_4 fluxes were greater in the biochar-added and non-biochar CWs (Guo et al., 2020). Biochar combined with sand, zeolite, and other artificial CW substrates can enhance microbial activity and compensate for the lack of carbon sources (Wang et al., 2020b). Abedi and Mojiri. (2019) reported that CW containing three substrate layers, namely biochar, gravel, and zeolite layers, showed high performance in wastewater treatment compared to the other CWs containing gravel as a substrate; the first CW can remove pollutants from wastewater better than the second one. At an optimum retention time (57.4 h) and pH (6.3), this biochar-integrated CW can remove up to 99.9% of COD (1000 mg/L), ammonia (1000 mg/L), phenols (50 mg/L), Pb (50 mg/L), and Mn (50 mg/L). In addition, the emission of nitrous oxide was lower in gravel CW than in the integrating biochar CW (Abedi and Mojiri, 2019). These results can explain that the introduction of biochar considerably improved the abundance of biological bacteria in CW, consequently increasing the efficiency of removing various contaminants in wastewater (Li et al., 2018a). This agrees with the results of Liang's study (**Table I-2**), which explains the increase in nitrogen removal efficiency and the decrease in N_2O emissions resulting from the increase in biochar addition ratio. This shows that biochar addition changed the diversity and similarity of the microbial community (Liang et al., 2020).

In general, the removal efficiency of pollutants was increased due to biochar adsorption (Meng et al., 2019). In addition, the total amount of extracellular polymeric substance (EPS) decreased significantly with the addition of biochar, which is explained by the change in the functional groups of EPS, including amide, carbonyl, and hydroxyl groups of proteins. Furthermore, biochar has the potential to convert metabolized high molecular weight compounds into low molecular weight compounds (Deng et al., 2019).

The biochar can be used at various stages of the wastewater treatment process to increase treatment capacity and recover value-added by-products. The adsorption, buffering, and immobilization mechanisms of microbial cells may influence the use of biochar in the wastewater treatment system. For example, properly modified biochar could effectively adsorb nutrients such as phosphorus and nitrogen from treated effluent, allowing it to be used for soil rehabilitation as a nutrient-enriched material. In addition, biochar could help develop activated sludge's treatment and settling capacity by adsorbing inhibitors and hazardous chemicals or providing a surface for microbial immobilization when used in the treatment process. The introduction of biochar to the biological system can also help increase the soil amendment capabilities of biosolids, extend the value chain, and provide other economic benefits as interest in its use in soil applications increases (Mumme et al., 2014). The following sections discuss biochar's role in removing various contaminants from wastewater.

3.4.1. Removal of organic pollutants

Numerous studies have been conducted in recent years to test the effectiveness of biochar in removing various organic substances from water, such as antibiotics, drugs, agrochemicals, polycyclic aromatic hydrocarbons (PAHs), cationic aromatic dyes, and volatile organic compounds (VOCs) (**Table I-2**) (Adeel et al., 2016; Mondal et al., 2016).

3.4.1.1. Removal of conventional pollutants

Organic pollutants are another important type of pollutant in the aquatic environment. Biochar has shown a high removal efficiency towards this kind of pollutant. Based on the literature, the biochar prepared at a higher pyrolysis temperature will improve non-polar organic compounds' removal efficiencies due to higher microporosity and surface area (Mohamed et al., 2016; Mohanty et al., 2013). On the other hand, the biochar prepared at a temperature below 500 °C comprises a higher amount of hydrogen and oxygen-containing functional groups, so it is more likely to have a high affinity for polar organic molecules (Suliman et al., 2016). For example, biochar derived from rice husk and pyrolyzed soybeans at 600-700 °C facilitates the removal of trichloromethylene (VOC) and non-polar carbofuran (pesticide) from contaminated water (Suliman et al., 2016). In addition, at T >700 °C, red gum wood chips and chicken litter-derived biochar efficiently removed pyrimethanil and diesopropylatrazine (fungicide/pesticide), whereas the same biochar at T <500 °C proved ineffective (Chen and Chen, 2009; Yu et al.,

2010). And for the removal of polar insecticides and herbicides such as norflurazon, 1-naphthol, and fluridone was performed using biochar produced at <300 °C, as a result of the pollutant's interaction with the biochar's functional groups (Li et al., 2016; Sun et al., 2011). On the other hand, the biochar with more O and H functional groups (<400 °C) showed higher sorption of aromatic cationic dyes such as methyl-blue and methyl-violet. Still, the process strongly depended on pH (Adeel et al., 2016; Teixid et al., 2011). In addition, the polar antibiotic sulfamethazine exhibits pH-dependent interactions when sorbed to softwood/hardwood-derived biochars (pyrolyzed at 300-700 °C) (Mohan et al., 2014). Therefore, it can be considered an important parameter for biochar interactions and polar organic contaminant removal.

Generally, organic matter from wastewater may be removed by filtration, adsorption, hydrolysis, chemical reduction or oxidation by microbial degradation, etc. (Vymazal and Tereza, 2015). The degradation by the microbiota attached to the substrates is responsible for the elimination of organic matter in aqueous solutions (Faulwetter et al., 2009). Conventional organic compounds such as chemical oxygen demand (COD) and biological oxygen demand (BOD_5) can be removed effectively due to the coupling role of anaerobic and aerobic degradation in CW systems (Saeed and Sun, 2017; Zhao et al., 2020). Thus, the integration of biochar into CWs plays an important role in COD removal, even though organic matter can be leached from biochar (Zhou et al., 2019). However, Several studies have shown that biochar amendment promotes COD removal in CWs (Deng et al., 2019; Guo et al., 2020). This result can be explained by the good adsorption capacity of biochar toward organic molecules and provides a heterogeneous surface with very high porosity for oxygen filling and habitation by various organic degradation microbes. Moreover, biochar can promote plant growth, releasing additional oxygen into CW substrates for aerobic COD decomposition. A recent finding by some researchers show that the introduction of biochar into CWs can reduce the quantity of microbial extracellular polymeric substances (EPS) accumulated in the wastewater matrix and induce their metabolization of heavy molecular weight EPS metabolites into lower molecular weight compounds because biochar increases the metabolic and abundance activities of heterotrophic bacteria, thus reflecting organic decomposition, which is conducive to mitigating the clogging of wastewater treatment substrate.

3.4.1.2. Emerging pollutants

Emerging hazardous organic pollutants that can be contained in stormwater, livestock wastes, agricultural waters, and industrial wastewaters, etc., such as dyes, pesticides, herbicides, endocrine disruptors (e.g., phthalic acid esters, polycyclic aromatic hydrocarbons, and bisphenol A), and antibiotics (**Table I-2**), pose serious long-term threats to ecosystems and public health, even at minute concentrations (Vymazal and Tereza, 2015). Hydrophobic effects, electrostatic attraction, conjugation of aromatic donors and cationic acceptors, pore filling, and hydrogen bonding are all processes that biochar can use to adsorb these contaminants (Xiang et al., 2020; Zhang et al., 2019). Most importantly, biochar possesses catalytic and redox-reactive activities, allowing it to accept/donate electrons or promote generate ROS and electrical conduction, thus accelerating the abiotic decomposition of adsorbed organic pollutants (Devi and Saroha, 2015; Zhang et al., 2019). In addition, biochar substrates may stimulate the reproduction and development of microbes involved in decomposing organic pollutants. However, this augmentation role of biochar has only been studied profoundly so far (Yan et al., 2017; You et al., 2020). The mechanisms involved depend mainly on biochar properties, operating conditions, and contaminants. Due to the exceptional ability of biochar to adsorb bisphenol A, Lu and Chen. (2018) found that integrating biochar into CWs improved the elimination of bisphenol A from stormwater and increased the life of CW systems. According to the same authors, the biochar prepared at 700 °C performed significantly better than biochar prepared at 300 and 500 °C. In addition, the biochar substrate supported the increase of functional microbes and served as an excellent biofilm carrier to indirectly enhance the decomposition of bisphenol A. Improved plant growth in CWs also facilitates the removal of organic pollutants (Chen, 2018). Tang et al. (2016) used plant-derived biochar that was planted in a *Cyperus alternifolius* CW and then modified with $Fe(NO_3)_3$ solution to achieve higher removal efficiencies (>99%) and a constant rate for four pesticides in wastewater than the non-biochar control (64 - 99%) (Tang et al., 2016). The cause is that biochar adsorbs the pesticides and promotes their microbial decomposition. The use of biochar derived from fruit pits in zeolite-based CWs significantly increased antibiotic removal rates (sulfamethazine and ciprofloxacin) while also decreasing the production of sulfonamide and quinolone resistance genes, which was attributed to the biochar's ability to facilitate antibiotic biodegradation and adsorption (Yuan et al., 2020). Biochar is a good attachment medium for microbes that degrade organic matter. For example, Mahmood et al. (2015) used corn-derived biochar manufactured

at 400 °C as a biofilm support for *Pseudomonas putida* cells to adsorb and reduce dyes and Cr (VI) in a continuous flow bioreactor for the efficient treatment of tannery wastewater containing azo dyes, aniline, and Cr (VI).

Other organic compounds, such as pharmaceuticals and pesticides, are considered emerging contaminants because of their effects on human health and have been detected in municipal wastewater treatment plants (Firouzsalari et al., 2019**;** Shi et al., 2021). Wastewater from the pharmaceutical industry contains pharmaceutical intermediates used in production (Karunanayake et al., 2017), antibiotics, and active ingredients such as hormones (Rashid et al., 2021). However, pesticides are found in industrial wastewater through pesticide production (Pinto et al., 2018), washing of commercial containers used to store or transport pesticides (Zapata et al., 2010), and agri-food industries (Lopes et al., 2020). The biochar as an adsorbent promotes the degradation of antibiotics and antibiotic resistance genes (ARGs) from wastewater, and dissolved organic carbon release in CWs indicated that water and alkaline media portray the optimum conditions for sulfamethoxazole (SMZ)and ARGs removal, this shows the feasibility of using biochar for regulated SMZ removal and ARG accumulation (Ajibade et al., 2021). However, the study of Feng et al., (2021) showed the relation between ARGs removal and dissolved organic matter (DOM). They noted that the photosensitized DOM is responsible for producing reactive intermediates to remove ARGs. Hence, incorporating biochar under forced aeration into CWs could remove ARGs up to 99.3% and DOM 72% effectively from swine wastewater. Abas et al., (2022) confirmed that the integration of biochar substrate has an effect in improving Chlorantraniliprole (CAP) removal to up to 99%. The biochar also enhances the treatment efficiency of the pharmaceuticals and personal care products (PPCPs) from wastewater. The presence of the colonization of arbuscular mycorrhizal fungi (AMF) in CWs enhanced the best removal performance for PPCPs in biochar-added systems (more than 99.99%). These results can be attributed to the higher adsorption capacity of PPCPs of biochar, due to its large surface area and porous structures of biochar substrate, which could also promote the development and growth of microbes and the adsorption of PPCPs, thus enhancing its biodegradation (Hu et al., 2022; Hu et al., 2022).

Polycyclic aromatic hydrocarbons (PAHs) are hydrophobic organic compounds with at least two aromatic rings (Kang et al., 2019; Gaurav et al., 2021). They include compounds such as phenanthrene, naphthalene, anthracene, pyrene, fluorine, and benzofluoranthene (Jain et al., 2020; Kong et al., 2021). Several studies have used biochar as an adsorbent substrate to remove

this pollutant, because biochar may provide a reproduction habitat for microbes and enhance the microbial community to improve denitrification and PAHs removal performance (Cao et al., 2021). Furthermore, the biochar was also tested to remove benzofluoranthene (BbFA), a typical PAH in CWs, and has shown higher BbFA with its removal efficiency exceeding 99%, which could be attributed to enhanced PAH biodegradation (Guo et al., 2020). In the same way, Kang et al., (2023) studied the removal efficiency of representative PAH and BbFA, using biochar modified by iron as a supplement to the CW substrate, reaching to increase the performance of BbFA removal by 20.4 %, because the biochar may increase dissolved organic carbon content, particularly low-aromaticity, which contributed to PAH degradation by microorganisms. In addition, the presence of functional groups on the biochar surface may improve the electron interactions between microorganisms and PAHs.

3.4.2. Removal of inorganic pollutants

Inorganic contaminants in wastewater include compounds such as nitrite (NO_2^-), ammonium (NH_4^+), nitrate (NO_3^-), hydrogen sulfide (H_2S), phosphorus (PO_4^{3-}) and heavy metals (Cu, Cr, Cd, Pb, Fe, Hg, Zn and As ions) (**Table I-2**) that cause a dangerous risk to human health and the environment (Cao et al., 2009). Generally, biochar produced at low pyrolysis temperature (about 500°C) is used to remove inorganic contaminants. The nature of biochar sorption is influenced by the morphological structure and chemical composition (Abdelhafez and Li, 2016).

3.4.2.1. Nitrogen removal

Multiple pathways are used to remove nitrogen from wastewater in CW, substrate adsorption, ammonia volatilization, plant uptake, and microbial processes (Saeed and Sun, 2017). Classical microbial nitrification, followed by denitrification, and finally converting N to N_2O or N_2, is considered the most common mechanism (Jia et al., 2020b; Vymazal, 2011). However, the insufficient ability of sand and gravel to adsorb nitrogen and provide habitable microsites for denitrifying microorganisms remains a major challenge in conventional CW systems filled with gravel, ceramite, or sand (Kizito et al., 2017; Yang et al., 2018), although ceramite gives better results than gravel or sand, which are widely used (Vohla et al., 2011). In addition, low dissolved oxygen (DO) due to inadequate reoxygenation may limit nitrification in flooded streams, and/or denitrification can be limited by electron donors deficient for nitrate reduction

(Lu et al., 2020; Vymazal, 2011). Therefore, several solutions are being investigated to improve nitrogen removal from wastewater, including introducing substrates with high nitrogen removal capacity (Jia et al., 2020b; Shen et al., 2018).

Cation exchange can keep cations in biochars with a high surface charge density. Consequently, the internal porosity, high biochar surface, and presence of polar and non-polar sites on the biochar surface promote nitrifier growth and nutrient adsorption, and simpler and easier atmospheric aeration and oxygen replenishment at the bottom of the CW matrix. As well as, the addition of the biochar substrate can increase the rate of nitrification, resulting in a great improvement in total nitrogen (TN) and NH_4^+ removal in CW (Kizito et al., 2017; Rozari et al., 2018; Zhou et al., 2019). However, the leaching of dissolved organic matter (DOM) can be done with the help of biochar, which is mainly based on humic acid, which allows it to temporarily trap the influent DOM in the pores as a carbon source to stimulate denitrification after desorption (Li et al., 2018a; Zhou et al., 2019). Denitrifier proliferation may also be enhanced, resulting in nitrate denitrification for low C/N effluents (Zhou et al., 2019). On the other hand, biochar acts as a chemically redox-active material with electroactive functional groups on its surface (e.g., phenols and quinones), which promotes the biochemical transfer of the material into wastewater (Yuan et al., 2018; Zhang et al., 2019). According to Wu et al. (2018), biochar derived from cattail stalks prepared at 300°C can increase the electron conversion efficiency between the metabolism of carbon and nitrate reduction by modulating the electron shuttle mechanism and increasing the activities of denitrifying enzymes, which can increase the rate of denitrification in wastewater, in contrast, biochar made at 800 °C inhibits these mechanisms. As a result, many studies have reported that biochar addition to domestic, swine, anaerobic, and secondary wastewater effluents improved nitrogen removal efficiency (by more than 20% on average). Removal efficiency increased proportionally with biochar dosage, although the performance improvement depended on biochar loading and preparation conditions, wastewater properties, and wastewater operating conditions. Biochar substrates in settling ponds showed better nitrogen removal than conventional gravel or sand and some functional fillers, such as zeolite and ceramite (Ji et al., 2020; Yuan et al., 2020).

3.4.2.2. Phosphorus removal

Phosphorus compounds (P) in wastewater may be eliminated by a variety of processes, including substrate precipitation, adsorption, plant uptake, and microbial uptake into

wastewater, with substrate retention generally being the most widely used process (Kumar and Dutta, 2019; Saeed and Sun, 2017). Elements such as Fe, Ca, Mg, and Al in CW fillers can bind phosphorus stably; therefore, materials rich in these elements (Fe, Ca, Al, Mg) are preferable as CW substrates enable phosphorus removal efficiently and also increase the lifetime of CW systems. Conventional CW substrates consisting of sand or gravel can only effectively remove total phosphorus (TP) from wastewater for a short time (Chang et al., 2016; Shi et al., 2017). In some studies, biochar-based filters (CWs) were found to have higher phosphorus removal efficiencies than control systems filled with zeolite or gravel. Still, the improved impact for Phosphorus compounds removal was much lower than for N removal. The biochar substrates could trap more phosphorus from wastewater than gravel, especially from wastewater with a high phosphorus concentration (e.g., anaerobic digestion effluent) (Kizito et al., 2017). In addition, the incorporation of biochar into CWs can enhance plant growth and the proliferation of phosphorus-compound-accumulating microorganisms, thereby improving biotic phosphorus removal pathways (Ji et al., 2020; Shi et al., 2017). However, this ameliorative effect cannot be easily maintained. The chemical properties of biochar and wastewater, especially the biochar's surface charge, are important factors in removing anionic phosphates (Wichern et al., 2018). However, other studies have shown that adding biochar to gravel-filled CW did not improve phosphorus removal (Zhou et al., 2019). Mixed biochar and sand substrates are even less efficient than sand alone in phosphorus removal (Rozari et al., 2016). These results can be explained because biochar has a negative surface charge and a low affinity for phosphate. Other negatively charged molecules in the wastewater (organic matter) can compete with phosphate for exchange sites in biochar (Rozari et al., 2016). Biochar substrates made from /Fe/Al/Ca-rich feedstocks, such as crab shells, can improve P's recovery/removal capacity from wastewater (Dai et al., 2017). Biochar can be modified with metal salts (iron, magnesium, and aluminum compounds) to make metallic biochar before filling (Wang., 2019; Zheng et al., 2019), or combined with other fillers with high Phosphorus compounds adsorption efficiency (crab shells) to prepare biochar (Shi et al., 2017; Yang et al., 2018). There is still a need for further research and relevant applications in phosphorus removal using biochar substrates.

3.4.2.3. Metals removal

Heavy metals are generally non-biodegradable and are found in large quantities in rainwater, mining effluents, and industrial wastes. Biochar with a unique pore structure, a high percentage of organic carbon, and many functional groups has a high chance of interacting with heavy

metals in several ways (Oliveira et al., 2017). Heavy metals are absorbed by biochar mainly through complexation and ion exchange between heavy metal ions and functional groups of biochar (e.g., COOH, OH, R-OH) (Hsu et al., 2009; Lu et al., 2011). Additionally, the coordination of metal ions with π-electrons (C = C) of biochar (Yu et al., 2010) and the formation of metal precipitates with inorganic constituents (Ippolito et al., 2012; Lu et al., 2011) could play a role in the P removal by biochar. Adsorption through the biochar matrix is affected by its chemical properties, which are affected by feedstock type, pyrolysis temperature, application rate, pH, and other factors. For example, copper (Cu^{2}+) had a high affinity for OH- and COOH- groups in hardwood and crop biochars, which varied with pH and feedstock type (Lima et al., 2010). Similarly, biochars derived from soybean straw, guayule shrub, hermaphrodite sida, and wheat straw effectively removed Ni^{2+}, Cu^{2+}, Zn^{2+}, and Cd^{2+} (Lu et al., 2017). The higher biochar efficiency was attributed to the high O and C contents, polarity index, and high O/C molar ratio, which were regulated mainly by pH (Bogusz et al., 2015; Peng et al., 2016). In addition, the removal of mercury (Hg^{2+}) was effectively performed using alkaline biochar prepared from both manure and various agricultural residues (corn stover, soybean straw, cocoa husks, switchgrass, and corn stover). Due to its high sulfur content (SH and sulfate groups), biochar produced from cocoa hulls and animal manure was particularly effective in removing Hg^{2+}, precipitating up to 90% of the Hg^{2+} as $HgCl_2$ or $Hg(OH)_2$, mainly by co-precipitation with the anions (O, S, Cl) in the biochar (Baltrenaite, 2015; Mohamed et al., 2016). Similarly, the biochar dosage affected the removal of heavy metals such as Cd^{2+}, Zn^{2+}, Pb^{2+}, and Cu^{2+}. Thus, the removal efficiency was higher with rising biochar loading in the aqueous system, due to the increase in surface area and pH (Laird et al., 2010; Xu et al., 2013).

Dissolved heavy metals in wastewater, such as hydroxides and sulfides, can be removed mainly by precipitation, adsorption from the abiotic substrate, and microbial reduction of sulfates for hydroxides and sulfides precipitation (Kosolapov et al., 2004). Adding biochar can help gravel ponds improve metal holding capacity by increasing abiotic pathways. Under ideal conditions, a study was conducted in a gravel-filled pond to remove just 58% Mn and 51.6% Pb from synthetic industrial wastewater. In comparison, adding biochar and zeolite increased the removal efficiency of both metals up to 99.9%. These results can be explained because both metals have high adsorption capacities toward biochar and zeolite (Abedi and Mojiri, 2019). In addition, the inorganic components of the biochar impart an alkaline nature to the biochar, allowing it to raise the pH value of acidic mine wastewater and subsequently reduce the metal

ions solubility by inducing the formation of metal hydroxide precipitates (Gwenzi et al., 2017). Biochar substrates can be modified before amendment with heteroatoms and oxidizing agents, acids, or anionic moieties (e.g., HSO_3, OH, S_2, etc.) to enhance the metal retention capacity of CWs (Wang et al., 2019).

3.4.2.4. Pathogen removal

The removal of pathogens from wastewater is essential for protecting human health. Removal was accomplished by filtration, predation, adsorption, oxidation, and inactivation by exposure to several regulatory standards for pathogens in wastewater effluent for reuse (Wu et al., 2016). The high porosity of biochar, high specific surface area, numerous pores with a wide range of sizes, hydrophobicity, and organic leaching may make biochar more suitable for removing microbial contaminants than gravel or sand. However, there has been relatively little research on removing pathogens from wastewater using biochar-enhanced CWs. According to Mohanty et al. (2014) and Lau et al. (2017), the introduction of biochar into sand-based biofilters significantly increased the presence of *Escherichia coli* in stormwater. In addition, it decreased the remobilization of sequestered nuisance bacteria during intermittent influx and highlighted the high potential of using biochar substrate in CWs for wastewater disinfection. Furthermore, biochar with volatile content and polarity had a higher removal efficiency for *E. coli* (Mohanty et al., 2014). This improvement effect may be explained by the fact that biochar can produce antimicrobials that significantly adsorb viruses and bacteria, mainly using hydrophobic interactions, and reduce the driving forces that detach pathogens.

On the other hand, another recent study by Kaetzl et al. (2019) found that CWs filled with rice husk-derived biochar can remove bacteriophages and fecal indicator bacteria (FIB) from pretreated municipal wastewater as well as or as much as CWs filled with sand or original rice husk (Kaetzl et al., 2019). The ability of biochar to remove pathogens varies with preparation conditions and feedstock (Mohanty et al., 2014). Modifying biochar with H_2SO_4 increases the surface area of biochar prepared from wood, reflecting a significant improvement in *E. coli* elimination in bioretention systems and reducing remobilization during drainage and intermittent flow (Lau et al., 2017). Even though biochar-based filters show high FIB removal efficiency comparable to sand-based filters (Wichern et al., 2018), biochar remains an attractive feedstock in CW systems for pathogen removal due to its economic production and performance, using locally available biological waste, and can be reused as a soil amendment.

4. Mechanisms and factors influencing the pollutants adsorption on biochar

The heterogeneity of the biochar surface allows a variety of sorption processes to occur. The chemical characteristics of the adsorbent surface and the nature of the contaminants determine the adsorption mechanism (Rosales et al., 2017). The three main adsorption mechanisms, according to Pignatello (Pignatello., 2011), are the precipitation mechanism, in which the adsorbent forms layers on the adsorbent surface, and the physical mechanism, in which the adsorbate (e.g., pollutants) is deposited on the adsorbent surface (e.g., biochar), and the pore-filling mechanism, in which the adsorbate (e.g., pollutants) condenses in the adsorbent pores (e.g., biochar). The adsorption process of organic pollutants is generally carried out by electrostatic attraction, complex adsorption, electron-acceptor-donor interaction, pore filling, hydrophobic interactions, and hydrogen bonding (**Figure I-2**) (Pignatello., 2011). For example, the sorption of organic contaminants by the biochar surface via the pore filling process is influenced by the total volume of the mesopores and micropores; so that the penetration of the pollutant into the internal structure of the biochar is all the more favored when its ionic radius is small, which reflects an increase in the biochar adsorption efficiency (Ahmad et al., 2014; Rosales et al., 2017). Soluble pollutants may attach to the alkaline surface of the hydrophobic biochar using their hydrophobic functional group or be precipitated. Due to the dissociation of oxygen-containing functional groups on the biochar surface, the biochar is generally negatively charged, causing an electrostatic attraction between the positively charged molecules and biochar (Ahmad et al., 2014; Qambrani et al., 2017).

The biochar produced at high temperatures lost its functional group-containing hydrogen and oxygen, making it more aromatic and less polar and, consequently, less suitable for removing polar organic pollutants. However, the electrostatic repulsion between the biochar and the negatively charged anionic organic molecules could favor the production of hydrogen bonds, leading to adsorption. On the other hand, if there is no hydrogen interaction, non-polar pollutants are more likely to penetrate hydrophobic areas (Ahmad et al., 2014). On the other hand, many mechanisms can be involved in removing inorganic pollutants, such as heavy metals, such as ion exchange and complexation, surface precipitation under alkaline circumstances, and anionic and cationic electrostatic attraction (**Figure I-2**). Similarly, Lu et al. (2011) examined the relative contributions of different Pb adsorption mechanisms on sludge-derived biochar. They arrived at the following mechanisms: (i) co-precipitation and complexation with mineral oxides and organic matter in the biochar, (ii) electrostatic

complexation due to the exchange of the metal with cations (sodium and potassium) present in the biochar, (iii) surface precipitation as lead silicate- phosphate ($5PbO.P_2O_5.SiO_2$), and (iv) surface complexation with free carboxyl and mineral oxides in the biochar.

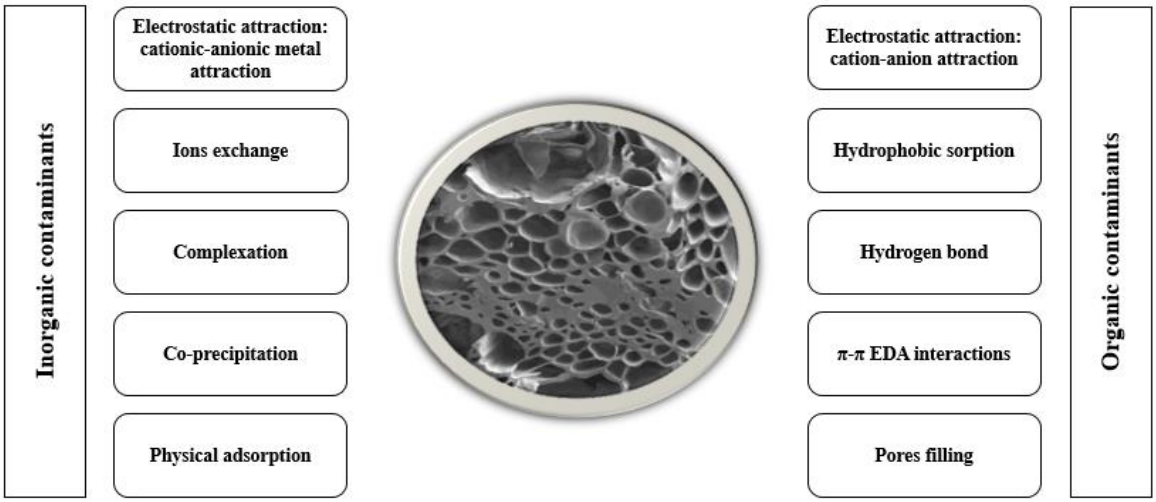

Figure I-2: Mechanisms for biochar's elimination of organic and inorganic contaminants.

The variation in these removal mechanisms and the physicochemical properties of biochar greatly implicates its suitability and efficacy for the remediation of the targeted pollutants. Several factors, such as biochar characteristics, dosage of biochar, solution pH, and temperature of the medium, greatly influence the biochar's overall adsorption capacity by modifying the removal mechanisms involved in the remediation of specific pollutants in aqueous systems (Abbas et al., 2018; Ambaye et al., 2021).

4.1. Characteristics of biochar

The volume of micropores in an adsorbent controls its ability to absorb an adsorbate (Lowell, 2004; Zabaniotou et al., 2008). Pores of different sizes are found in adsorbent materials and classified into macropores, micropores, and mesopores based on the width of the opening (Mosher, 2011). The experimental conditions strongly influence the distribution and size of the pores during the preparation of the biochar, and especially the pyrolysis temperature has the greatest influence (Zhou et al., 2010). The micropores are the most abundant in the biochar structure and would be responsible for their high adsorption capacity and surface area. Zabaniotou et al. (2008) reported that biochar prepared at a high pyrolysis temperature contains a very high volume of micropores that varies between 50%-78% of the total pores. The sorption

rate of the biochar is controlled by the size of the adsorbate, such that larger particles can cause blockage or exclusion of sorption sites. In comparison, smaller particles increase the van der Waals force of penetration of the adsorbate into the adsorbent and decrease the mass transfer limitation (Daifullah and Girgis, 1998). It also depends on the surface functional groups' levels and types (Qambrani et al., 2017). The carbonization process, the feedstock's chemical composition, and the carbonization temperature all influence the distribution of surface functional groups (Ahmad et al., 2012). Gascó et al. (2018) compared the properties of hydrochar and biochar produced from pig manure using HTC and pyrolysis.

The results showed that when the pyrolysis temperature is high, the broad peak around 3400 cm^{-1}, corresponds to the -OH stretching vibration in the hydroxyl and carboxyl groups and becomes less visible for biochars compared to the feedstock. Due to the decarboxylation and dehydration reactions during the HTC process, the HTC hydrochars revealed broadband at 3400 cm-1 with less intensity than the feedstock. Several scientists agreed that a high aromatic structure characterizes biochar prepared at a high temperature of around 600 °C. On the other hand, hydrochar prepared using the HTC method at a temperature between 200 and 240 °C for 2 h favors biochar with more aliphatic structures. According to Qambrani et al. (2017), the functional groups (-CH_2, O-H, C=O, C=C, and -CH_3) of biochar have changed due to the pyrolytic conditions, which promote the hydrophobic interactions of biochar. The hydrophobic character of biochar is determined by the amount of oxygen and nitrogen-containing functional groups; the lower the nitrogen and oxygen-containing functional groups in the biochar, the higher hydrophobic the biochar (Moreno-castilla, 2004). Hence, the presence of oxygen-containing functional groups on the hydrophilic biochar surface facilitates water to penetrate through hydrogen bonds, resulting in competition between the adsorbate and water on the available sites of the biochar surface. Hydrophobic biochars are expected to contribute to insoluble adsorbate adsorption, while hydrophilic biochars are considered less effective due to water sorption. Adsorbates that are less soluble or insoluble are most likely to be absorbed into the biochar pores in aqueous solutions (Li et al., 2002).

4.2. Dosage of the adsorbent

The adsorbent dosage significantly impacts the sorbent-sorbate balance of an adsorption system. Hence, using a high adsorbent dosage increases the removal efficiency of inorganic and organic contaminants due to the availability of a larger number of sorption sites (Chen, 2013;

Chen et al., 2011). On the other hand, the application of a dosage rate that is too high leads to a reduction of the adsorption capacity of the biochar and consequently, an overlapping of the adsorption layers will be produced, which protects the accessible active sites on the sorbent surface (Kizito et al., 2015; Linville et al., 2017). Therefore, the adsorbent dosing must be well optimized to achieve high elimination capacity and make the process cost-effective.

4.3. pH of the solution

The pH of the solution is a crucial factor that controls the adsorption process by influencing the ionization degree and charge of the adsorbate, the adsorbent surface charge and the speciation (Kılıc et al., 2013). The competition between protons and cationic pollutants decreases as the pH of the solution is above the point of zero charges, and a negative charge appears on the adsorbent surface as a result of the deprotonation of carboxylic groups and phenolic groups on the surface. Basic functional groups, such as amines, are protonated and positively charged at low pH, improving anions' adsorption (Kumar et al., 2011). This means that deprotonation of the functional groups and the pH of the medium influence the biochar adsorption behavior. Kizito et al. (2015) and Hu et al. (2019) studied the effect of pH on the adsorption capacity of biochar towards ammonium (NH_4^+). They showed that the adsorption capacity of NH_4^+ increased with the initial solution pH between 4 and 8 and then decreased when the pH was above 9.

4.4. Temperature of the medium

The medium temperature at which the biochar is applied impacts its adsorption capacity. Most studies showed that adsorption efficiency increased with temperature, confirming that the adsorption process is endothermic. The study by Enaime et al. (2017) indicated that the indigo carmine sorption on potassium hydroxide (KOH) activated biochar rises with temperature due to the endothermic nature of the sorption process. The increase in temperature leads to an increase in the mobility of the dye molecule and the possibility of an increase in the adsorbent porosity. This can be explained by the swelling effect of the adsorbent's internal structure when the temperature increases, allowing more dye to penetrate further. Another study, Kizito et al. (2015) found that increasing the temperature from 300 °C to 450 °C is beneficial for maximum removal efficiency.

5. Advantages and limitations of biochar as a CW substrate

The use of biochar as a substrate in CWs solves the problem of environmental pollution (**Table I-3**). Due to the low-cost availability of the raw materials and the high commercial potential of biochar. The preparation of biochar has developed rapidly in recent years (Lili et al., 2017). Due to its adsorption capacity and porous structure, biochar is commonly used as a slow-release fertilizer filler (Xu and Lu, 2019). However, biochar is rarely used in water treatment due to its high cost, high ash content, and difficulty in ash removal (Kasak et al., 2018). Theoretically, biochar may considerably enhance the purification of wastewater (Deng et al., 2019), as an additional carbon source for CWs (Kasak et al., 2018), and its surface allows the adsorption of various pollutants.

Furthermore, biochar may improve the activity of the microorganisms in CWs (Tang et al., 2017). Therefore, biochar could improve the degradation of high molecular weight compounds in low molecular weight compounds in CW (Deng et al., 2019). The biochar's main objective is to increase the adsorption efficiency of the substrate and provide a carbon source to enhance the denitrification efficiency. However, the application of the CW substrate is easy to generate a blockage due to the low structural strength of the biochar and the ease of generating a powder (Saeed et al., 2019).

Table I-3: Limitations and advantages of biochar as a CW substrate.

Advantages	**Reference**	**Disadvantages**	**Reference**
- Sustainable and abundant resources, cheap and more oxygen groups present in biochar, improve pollutant adsorption.	(Houben et al., 2013)	- Elimination of pollutants' efficiency is undetermined and heavy metals retain in soil.	(Houben et al., 2013)
- Effective medium for capturing pollutants from wastewater, which can connect to the soil and result in an alteration -Reduce greenhouse gas emissions	(Yaashikaa et al., 2020)	- High cost, high ash content, and difficulty in ash removal	(Kasak et al., 2018)
- Improve the activity of microorganisms in CWs	(Tang et al., 2017)	- Easy to generate a blockage, and the ease of generating a powder	(Saeed et al., 2019)
- Provide reactive sites for microbes	(Li et al., 2019)		
- Adsorb NO_3-N, NH_4^+ and PO_4^{3-} - Remove suspended solids, BOD_5, metals, and coliforms	(Gao et al., 2018)	Substance release (e.g., N, P, salt, alkaline)	(Zhuang et al., 2022)

Conclusion and perspectives

The present review highlighted the constructed wetlands (CWs), a natural system that is largely investigated for different kinds of wastewater (urban, industrial, mixture) treatment through physical (porosity of substrate), chemical (adsorption, precipitation, and biological processes (biodegradation, nitrification denitrification), under vertical or horizontal flow regime. The constructed wetland has proven good performance for the elimination of organic matter (99 %), nutrients, especially phosphates (88 %), and nitrogen (96 %). However, constructed wetlands are still very limited in removing recalcitrant or emergent pollutants such as heavy metals, pesticides, drugs, PAHs, volatile organic compounds (VOCs), etc. According to previous literature, the removal capacity of CW depends on the type of macrophytic plant and the substrate of the bed. According to the analyzed references, different plants can be used in CW. Nevertheless, *Phragmites australis* and *Arundo donax* have been the most widely used, resistant to high organic loads, capable of oxygenating the substrate, and enhancing the hydraulic conductivity of the filter. The substrate also plays an important role in constructed wetland depuration efficiency, which could reach NH_4^+-N (40.23%), NO_3^--N (48.94 %), TN (52%), and COD (35%) when sand or gravel substrate is used. Any improvement of the CW efficiency must be performed via the integration of a good substrate in the filter. Among several materials generally tested as substrate for CW such as zeolite, pozzolan, charcoal, and biochar is gaining big interest recently, due to its promising characteristics as an optimal adsorbent having the ability to remove not only conventional pollutants but owing to good removal performances for even emergent ones that are very toxic and recalcitrant. Furthermore, biochar could introduce carbon into the substrate and greatly impact the biodegradation of pollutants by providing an ideal environment for the functional groups of microorganisms. The removal percentage could reach COD (99 %), TP (88 %), NH_4^+ (96 %), Abamectin (99 %), TSS (71 %), total coliforms (70 %), TN (40 %), and ARGs (99 %).

These interesting characteristics of the biochar are obviously dependent on the processes used to prepare the material, and the conditions of the preparation, including conditions of thermal conversion and the kind of feedstock used. Based on the literature review, it was found that the optimum pyrolysis temperature must be around 400 and 600 °C, with the possibility of having an oriented prepared biochar depending on the targeted pollutants, based on the temperature. Furthermore, feedstock must have some specific characteristics to give a good quality of the biochar that depends on the feedstock's richness in carbon and low quantity of mineral matter.

The large pore volume and high specific surface area, reaching 200 m^2/g, thus allowing for the effective removal of pollutants and pathogens from wastewater. The biochar quality is affected by the conditions involved in preparing biochars (e.g., pyrolysis temperature, heating rate, and carbonization time).

Several factors alter the removal efficiency of pollutants in CWs, such as substrate chemical and physical properties, hydraulic retention time, oxygenation conditions, and redox conditions. In addition, a configuration where the biochar is implemented as an interlayer between two inert layers (sand, gravel, zeolite) has been reported as an optimal design for CW integrating biochar to avoid clogging of the filtration system or biochar flotation.

Overall, the use of biochar in horizontal flow CW is still limited, and a few papers have discussed this aspect. Similarly, there is only limited information on the removal of emerging organics and pathogens from wastewaters by biochar CWs, which means the involved mechanisms and potential capability of biochar CWs in the removal of these pollutants should be further explored and elucidated. Moreover, it is undeniable that biochar offers various economic and environmental benefits and advantages, and its effectiveness in removing various contaminants at the laboratory scale has been widely reported. However, more in situ experiments should be conducted to test the effectiveness of biochar using real effluents and to examine the actual effect of biochar on the environment before its large-scale application. Furthermore, the biochar stability after many use cycles and its regeneration should be further studied.

References

Abas, K., Brisson, J., Amyot, M., Brodeur, J., Storck, V., Montiel-León, J.M., Duy, S.V., Sauvé, S., Kõiv-Vainik, M., 2022. Effects of plants and biochar on the performance of treatment wetlands for removal of the pesticide chlorantraniliprole from agricultural runoff. Ecol. Eng. 175. https://doi.org/10.1016/j.ecoleng.2021.106477

Abbas, Z., Ali, S., Rizwan, M., Zaheer, I.E., Malik, A., Riaz, M.A., Shahid, M.R., Rehman, M.Z. ur, Al-Wabel, M.I., 2018. A critical review of mechanisms involved in the adsorption of organic and inorganic contaminants through biochar. Arab. J. Geosci. 11. https://doi.org/10.1007/s12517-018-3790-1

Abdelhafez, A.A., Li, J., 2016. Removal of Pb (II) from aqueous solution by using biochars derived from sugar cane bagasse and orange peel. J. Taiwan Inst. Chem. Eng. 000, 1–9. https://doi.org/10.1016/j.jtice.2016.01.005

Abdelhafez, A.A., Zhang, X., Zhou, L., Cai, M., Cui, N., Chen, G., Zou, G., Abbas, M.H.H., Kenawy, M.H.M., Ahmad, M., Alharthi, S.S., Hamed, M.H., 2021. Eco-friendly production of biochar via conventional pyrolysis: Application of biochar and liquefied smoke for plant productivity and seed germination. Environ. Technol. Innov. 22, 101540. https://doi.org/10.1016/j.eti.2021.101540

Abedi, T., Mojiri, A., 2019. Constructed wetland modified by biochar/zeolite addition for enhanced wastewater treatment. Environ. Technol. Innov. 16, 100472. https://doi.org/10.1016/j.eti.2019.100472Addo-Bankas, O., Zhao, Y., Vymazal, J., Yuan, Y., Fu, J., Wei, T., 2021. Green walls: A form of constructed wetland in green buildings. Ecol. Eng. 169, 106321. https://doi.org/10.1016/j.ecoleng.2021.106321

Addo-Bankas, O., Zhao, Y., Vymazal, J., Yuan, Y., Fu, J., Wei, T., 2021. Green walls: A form of constructed wetland in green buildings. Ecol. Eng. 169, 106321. https://doi.org/10.1016/j.ecoleng.2021.106321

Adeel, M., Song, X., Wang, Y., Francis, D., Yang, Y., 2016. Environmental impact of estrogens on human , animal and plant life : A critical review. Environ. Int. https://doi.org/10.1016/j.envint.2016.12.010

Aghoghovwia, M.P., Hardie, A.G., Rozanov, A.B., 2020. Characterisation , adsorption and desorption of ammonium and nitrate of biochar derived from different feedstocks. Environ. Technol. 0, 1–38. https://doi.org/10.1080/09593330.2020.1804466

Ahmad, J., Patuzzi, F., Rashid, U., Shahabz, M., Ngamcharussrivichai, C., Baratieri, M., 2021. Exploring untapped effect of process conditions on biochar characteristics and applications. Environ. Technol. Innov. 21, 101310. https://doi.org/10.1016/j.eti.2020.101310

Ahmad, M., Lee, S.S., Dou, X., Mohan, D., Sung, J.K., Yang, J.E., Ok, Y.S., 2012. Effects of pyrolysis temperature on soybean stover- and peanut shell-derived biochar properties and TCE adsorption in water. Bioresour. Technol. 118, 536–544. https://doi.org/10.1016/j.biortech.2012.05.042

Ahmad, M., Rajapaksha, A.U., Lim, J.E., Zhang, M., Bolan, N., Mohan, D., Vithanage, M., Lee, S.S., Ok, Y.S., 2014. Biochar as a sorbent for contaminant management in soil and water: A review. Chemosphere 99, 19–33. https://doi.org/10.1016/j.

Ahmed, M.B., Zhou, J.L., Ngo, H.H., Guo, W., Johir, M.A.H., Belhaj, D., 2017. Competitive sorption affinity of sulfonamides and chloramphenicol antibiotics toward functionalized biochar for water and wastewater treatment. Bioresour. Technol. 238, 306–312. https://doi.org/10.1016/j.biortech.2017.04.042

Ajibade, F., Ying-ke, F., Muhammad, H., Sharif, A., 2020. Total nitrogen removal in biochar amended non-aerated vertical flow constructed wetlands for secondary wastewater effluent with low C / N ratio : Microbial community structure and dissolved organic carbon. Bioresour. Technol. 124430. https://doi.org/10.1016/j.biortech.2020.124430

Ajibade, F.O., Yin, W., Guadie, A., Ajibade, F., Liu, Y., Kumwimba, M.N., Liu, W., 2021. Impact of biochar amended on antibiotic removal and resistant genes accumulation in constructed wetlands for low C/N wastewater treatment: Performance and mechanism. https://dx.doi.org/10.2139/ssrn.4289781.

Ajibade, F.O., Yin, W., Guadie, A., Ajibade, T.F., Liu, Y., Kumwimba, M.N., Liu, W., Han, J.-L., Wang, H.-C., Wang, A.-J., 2023. Impact of biochar amendment on antibiotic removal and ARGs accumulation in constructed wetlands for low C/N wastewater treatment. Chem. Eng. J. 459, 141541. https://doi.org/10.1016/j.cej.2023.141541

Alsewaileh, A.S., Usman, A.R., Al-wabel, M.I., 2019. Effects of pyrolysis temperature on nitrate-nitrogen (NO 3 − -N) and bromate (BrO 3 −) adsorption onto date palm biochar. J. Environ. Manage. 237, 289–296. https://doi.org/10.1016/j.jenvman.2019.02.045

Ambaye, T.G., Vaccari, M., van Hullebusch, E.D., Amrane, A., Rtimi, S., 2021. Mechanisms and adsorption capacities of biochar for the removal of organic and inorganic pollutants from industrial wastewater. Int. J. Environ. Sci. Technol. 18, 3273–3294. https://doi.org/10.1007/s13762-020-03060-w

Athapattu, B.C.L., Thalgaspitiya, T. W. L. R., Yasaratne, U. L. S., Vithanage, M., 2017. Biochar-based constructed wetlands to treat reverse osmosis rejected concentrates in chronic kidney disease endemic areas in Sri Lanka. Environ. Geochem. Health. https://doi.org/10.1007/s10653-017-9931-8

Apolin, P., Conceptualization, V., 2020. Production of high-performance biochar using a simple and low-cost method: optimization of pyrolysis parameters and evaluation for water treatment. J. Pre-proof. https://doi.org/10.1016/j.jaap.2020.104823

Ayadi, M., Passaseo, D., Bonaccorso, G., Fichera, M., Renai, L., Venturini, L., Colzi, I., Fibbi, D., Del Bubba, M., 2024. Biochar from co-pyrolysis of biological sludge and sawdust in comparison with the conventional filling media of vertical-flow constructed wetlands for the treatment of domestic-textile wastewater. Water Sci. Technol. 89, 1252–1263. https://doi.org/10.2166/wst.2024.056

Bachmann Pinto, H., Miguel de Souza, B., Dezotti, M., 2018. Treatment of a pesticide industry wastewater mixture in a moving bed biofilm reactor followed by conventional and membrane processes for water reuse. J. Clean. Prod. 201, 1061–1070. https://doi.org/10.1016/j.jclepro.2018.08.113

Bakari, Z., Fichera, M., El Ghadraoui, A., Renai, L., Giurlani, W., Santianni, D., Fibbi, D., Bruzzoniti, M.C. and Del Bubba, M. 2024. Biochar from co-pyrolysis of biological sludge and woody waste followed by chemical and thermal activation: end-of-waste procedure for sludge management and biochar sorption efficiency for anionic and cationic dyes. Environmental Science and Pollution Research 31(24), 35249-35265.

Baltrenaite, J.K.E., 2015. Biochar as adsorbent for removal of heavy metal ions [Cadmium (II), Copper (II), Lead (II), Zinc (II)] from aqueous phase. Int. J. Environ. Sci. Technol. https://doi.org/10.1007/s13762-015-0873-3

Berslin, D., Reshmi, A., Sivaprakash, B., Rajamohan, N., Kumar, P.S., 2022. Remediation of emerging metal pollutants using environment friendly biochar- Review on applications and mechanism. Chemosphere 290, 133384. https://doi.org/10.1016/j.chemosphere.2021.133384

Bogusz, A., Oleszczuk, P., Dobrowolski, R., 2015. Application of laboratory prepared and commercially available biochars to adsorption of cadmium , copper and zinc ions from water. Bioresour. Technol. 196, 540–549.

https://doi.org/10.1016/j.biortech.2015.08.006
Bolton, L., Joseph, S., Greenway, M., Donne, S., Munroe, P., Marjo, C.E., 2019. Phosphorus adsorption onto an enriched biochar substrate in constructed wetlands treating wastewater. Ecol. Eng. X 1, 100005. https://doi.org/10.1016/j.ecoena.2019.100005
Borne, K.E., Fassman, E.A., Tanner, C.C., 2013. Floating treatment wetland retrofit to improve stormwater pond performance for suspended solids , copper and zinc. Ecol. Eng. 54, 173–182. https://doi.org/10.1016/j.ecoleng.2013.01.031
Cao, Q., Li, Y., Kang, Y., Guo, Z., 2021. Enhanced Benzofluoranthrene Removal in Surface Flow Constructed Wetlands with the Addition of Carbon. ACS Omega 6, 2865–2872. https://doi.org/10.1021/acsomega.0c05202
Cao. X, Ma. L, Gao. B, Harris. W., 2009. Dairy-Manure Derived Biochar Effectively Sorbs Lead and Atrazine. J. Environ. Sci. Technol, vol. 43,p. 3285–3291, 2009, doi.org/10.1021/es803092k.
Castiglioni, M., Rivoira, L., Ingrando, I., Del Bubba, M., Bruzzoniti, M.C., 2021. Characterization techniques as supporting tools for the interpretation of biochar adsorption efficiency in water treatment: A critical review. Molecules 26. https://doi.org/10.3390/molecules26165063
Castiglioni, M., Rivoira, L., Ingrando, I., Meucci, L., Binetti, R., Fungi, M., El-Ghadraoui, A., Bakari, Z., Del Bubba, M., Bruzzoniti, M.C., 2022. Biochars intended for water filtration: A comparative study with activated carbons of their physicochemical properties and removal efficiency towards neutral and anionic organic pollutants. Chemosphere 288, 132538. https://doi.org/10.1016/j.chemosphere.2021.132538
Cha, J.S., Park, S.H., Jung, S.-C., Ryu, C., Jeon, J.-K., Shin, M.-C., Park, Y.-K., 2016. Production and utilization of biochar: A review. J. Ind. Eng. Chem. 40, 1–15. https://doi.org/10.1016/j.jiec.2016.06.002
Chand, N., Suthar, S., Kumar, K., Kumar, V., 2021. Enhanced removal of nutrients and coliforms from domestic wastewater in cattle dung biochar-packed Colocasia esculenta -based vertical subsurface flow constructed wetland. Journal of Water Process Engineering. Journal of Water Process Engineering. 41. 101994. https://doi.org/10.1016/j.jwpe.2021.101994.
Chand, N., Suthar, S., Kumar, K., Singh, V., 2022. Removal of pharmaceuticals by vertical flow constructed wetland with different configurations: Effect of inlet load and biochar addition in the substrate. Chemosphere 307, 135975. https://doi.org/10.1016/j.chemosphere.2022.135975
Chang, J., Lu, Y., Chen, J., Wang, X., Luo, T., Liu, H., 2016. Simultaneous removals of nitrate and sulfate and the adverse effects of gravel-based biofilters with flower straws added as exogenous carbon source. Ecol. Eng. 95, 189–197. https://doi.org/10.1016/j.ecoleng.2016.06.032
Chang, J., Peng, D., Deng, S., Chen, J., Duan, C., 2022. Efficient treatment of mercury (II) -containing wastewater in aerated constructed wetland microcosms packed with biochar. Chemosphere 290, 133302. https://doi.org/10.1016/j.chemosphere.2021.133302
Chen, Y., Chen, Z., Dong, Y., Wu, H., 2024. Enhanced treatment performance and reduction of antibiotic resistance genes of biochar-aeration vertical flow constructed wetland for treating real domestic wastewater. Process Saf. Environ. Prot. 189, 11–20. https://doi.org/10.1016/j.psep.2024.06.041
Chen, B., Chen, Z., 2009. Sorption of naphthalene and 1-naphthol by biochars of orange peels with different pyrolytic temperatures. Chemosphere 76, 127–133. https://doi.org/10.1016/j.chemosphere.2009.02.004
Chen, X., Chen, G., Chen, L., Chen, Y., Lehmann, J., Mcbride, M.B., Hay, A.G., 2011. Adsorption of copper and zinc by biochars produced from pyrolysis of hardwood and corn straw in aqueous solution. Bioresour. Technol. 102, 8877–8884. https://doi.org/10.1016/j.biortech.2011.06.078
Chen, Y., Wu, Q., Tang, Y., Liu, Z., Ye, L., Chen, R., Yuan, S., 2022. Application of biochar as an innovative soil ameliorant in bioretention system for stormwater treatment: A review of performance and its influencing factors. Water Sci. Technol. 86, 1232–1252. https://doi.org/10.2166/wst.2022.245
Comite Europeen de Normalisation (CEN), 2009. Produits chimiques utilisés pour le traitement de l'eau destinée à la consommation humaine - Charbon actif en grains - Partie 1: Charbon actif en grains vierge.
Cui, X., Wang, J., Wang, X., Khan, M.B., Lu, M., Khan, K.Y., Song, Y., He, Z., Yang, X., Yan, B., Chen, G., 2022. Biochar from constructed wetland biomass waste: A review of its potential and challenges. Chemosphere 287, 132259. https://doi.org/10.1016/j.chemosphere.2021.132259
Dai, L., Tan, F., Li, H., Zhu, N., He, M., Zhu, Q., Hu, G., Wang, L., Zhao, J., 2017. Calcium-rich biochar from the pyrolysis of crab shell for phosphorus removal. J. Environ. Manage. 198, 70–74. https://doi.org/10.1016/j.jenvman.2017.04.057
Daifullah, A.A.M., Girgis, B.S., 1998. REMOVAL OF SOME SUBSTITUTED PHENOLS BY ACTIVATED CARBON OBTAINED FROM AGRICULTURAL. Water Research. 32. 4. 1169-1177. https://doi.org/10.1016/S0043-1354(97)00310-2.
Deng, C., Huang, L., Liang, Y., Xiang, H., Jiang, J., Wang, Q., 2019. Response of microbes to biochar strengthen nitrogen removal in subsurface flow constructed wetlands : Microbial community structure and metabolite characteristics. Sci. Total Environ. 694, 133687. https://doi.org/10.1016/j.scitotenv.2019.133687
Deng, S., Chen, J., Chang, J., 2021. Application of biochar as an innovative substrate in constructed

wetlands/biofilters for wastewater treatment: Performance and ecological benefits. J. Clean. Prod. 293, 126156. https://doi.org/10.1016/j.jclepro.2021.126156
Devi, P., Saroha, A.K., 2015. Simultaneous adsorption and dechlorination of pentachlorophenol from effluent by Ni-ZVI magnetic biochar composites synthesized from paper mill sludge. Chem. Eng. J. https://doi.org/10.1016/j.cej.2015.02.087
Du, L., Zhao, Y., Wang, C., Zhang, H., Chen, Q., Zhang, X., Zhang, L., Wu, J., Wu, Z., Zhou, Q., 2020. Removal performance of antibiotics and antibiotic resistance genes in swine wastewater by integrated vertical- fl ow constructed wetlands with zeolite substrate. Science of the Total Environment. 721, 1–10. https://doi.org/10.1016/j.scitotenv.2020.137765
El Ghadraoui, A., Ouazzani, N., Ahmali, A., El Mansour, T.E.H., Aziz, F., Hejjaj, A., Del Bubba, M., Mandi, L., 2020. Treatment of olive mill and municipal wastewater mixture by pilot scale vertical flow constructed wetland. Desalin. Water Treat. 198, 126–139. https://doi.org/10.5004/dwt.2020.26009
Enaime, G., Baçaoui, A., Yaacoubi, A., Lübken, M., 2020b. Biochar for wastewater treatment-conversion technologies and applications. Appl. Sci. 10. https://doi.org/10.3390/app10103492
Enaime, G., Ennaciri, K., Ounas, A., Baçaoui, A., Seffen, M., Selmi, T., Yaacoubi, A., 2017. Preparation and characterization of activated carbons from olive wastes by physical and chemical activation : Application to Indigo carmine adsorption 8, 4125–4137.
Faulwetter, J.L., Gagnon, V., Sundberg, C., Chazarenc, F., Burr, M.D., Brisson, J., Camper, A.K., Stein, O.R., 2009. Microbial processes influencing performance of treatment wetlands : A review 35, 987–1004. https://doi.org/10.1016/j.ecoleng.2008.12.030
Feng, L., He, S., Wei, L., Zhang, J., Wu, H., 2021a. Impacts of aeration and biochar on physiological characteristics of plants and microbial communities and metabolites in constructed wetland microcosms for treating swine wastewater. Environ. Res. 200, 111415. https://doi.org/10.1016/j.envres.2021.111415
Feng, L., Wu, H., Zhang, J., Brix, H., 2021b. Simultaneous elimination of antibiotics resistance genes and dissolved organic matter in treatment wetlands: Characteristics and associated relationship. Chem. Eng. J. 415, 128966. https://doi.org/10.1016/j.cej.2021.128966
Firouzsalari, N.Z., Shakerkhatibi, M., Pourakbar, M., Yadeghari, A., Safari, G.H., Sarbakhsh, P., 2019. Pyrethroid pesticide residues in a municipal wastewater treatment plant: Occurrence, removal efficiency, and risk assessment using a modified index. J. Water Process Eng. 29. https://doi.org/10.1016/j.jwpe.2019.100793
Fu, G., Wu, J., Han, J., Zhao, L., Chan, G., Leong, K., 2020. Effects of substrate type on denitrification efficiency and microbial community structure in constructed wetlands. Bioresour. Technol. 307. https://doi.org/10.1016/j.biortech.2020.123222
Fu, J., Zhao, Y., Yao, Q., Addo-Bankas, O., Ji, B., Yuan, Y., Wei, T., Esteve-Núñez, A., 2022. A review on antibiotics removal: Leveraging the combination of grey and green techniques. Sci. Total Environ. 838. https://doi.org/10.1016/j.scitotenv.2022.156427
Gabhane, J.W., Bhange, V.P., Patil, P.D., Bankar, S.T., Kumar, S., 2020. Recent trends in biochar production methods and its application as a soil health conditioner: a review. SN Appl. Sci. 2, 1–21. https://doi.org/10.1007/s42452-020-3121-5
Gadipelly, C., Pérez-González, A., Yadav, G.D., Ortiz, I., Ibáñez, R., Rathod, V.K., Marathe, K. V., 2014. Pharmaceutical Industry Wastewater: Review of the Technologies for Water Treatment and Reuse. Ind. Eng. Chem. Res. 53, 11571–11592. https://doi.org/10.1021/ie501210j
Gao, Y., Yan, C., Wei, R., Zhang, W., Shen, J., Wang, M., Gao, B., Yang, Y., Yang, L., 2019. Photovoltaic electrolysis improves nitrogen and phosphorus removals of biochar-amended constructed wetlands. Ecol. Eng. 138, 71–78. https://doi.org/10.1016/j.ecoleng.2019.07.004
Gao, Y., Zhang, W., Gao, B., Jia, W., Miao, A., Xiao, L., Yang, L., 2018. Highly efficient removal of nitrogen and phosphorus in an electrolysis-integrated horizontal subsurface-flow constructed wetland amended with biochar. Water Res. https://doi.org/10.1016/j.watres.2018.04.007
Garcia, B., Alves, O., Rijo, B., Lourinho, G., Nobre, C., 2022. Biochar: Production, Applications, and Market Prospects in Portugal. Environ. 9, 1–21. https://doi.org/10.3390/environments9080095
Gascó, G., Paz-Ferreiro, J., Álvarez, M.L., Saa, A., Méndez, A., 2018. Biochars and hydrochars prepared by pyrolysis and hydrothermal carbonisation of pig manure. Waste Manag. 79, 395–403. https://doi.org/10.1016/j.wasman.2018.08.015
Gaurav, G.K., Mehmood, T., Kumar, M., Cheng, L., Sathishkumar, K., Kumar, A., Yadav, D., 2021. Review on polycyclic aromatic hydrocarbons (PAHs) migration from wastewater. J. Contam. Hydrol. 236, 103715. https://doi.org/10.1016/j.jconhyd.2020.103715
Gong, H., Tan, Z., Zhang, L., Huang, Q., 2019. Preparation of biochar with high absorbability and its nutrient adsorption – desorption behaviour. Sci. Total Environ. 694, 133728. https://doi.org/10.1016/j.scitotenv.2019.133728
Gosset, A., Polomé, P., Perrodin, Y., Lyon, U. De, Claude, U., Lyon, B., Lehna, U.M.R., Lyon, U. De, Lyon, U., Gate, U.M.R., 2020. Ecotoxicological risk assessment of micropollutants from treated urban wastewater

effluents for watercourses at a territorial scale : Application and comparison of two approaches. Int. J. Hyg. Environ. Health 224, 113437. https://doi.org/10.1016/j.ijheh.2019.113437
Gotore, O., Rameshprabu, R., Itayama, T., 2022. Adsorption performances of corn cob-derived biochar in saturated and semi-saturated vertical-flow constructed wetlands for nutrient removal under erratic oxygen supply. Environ. Chem. Ecotoxicol. 4, 155–163. https://doi.org/10.1016/j.enceco.2022.05.001
Guittonny-philippe, A., Monnier, Y., Malleret, L., Coulomb, B., Combroux, I., Baumberger, T., Viglione, J., Laffont-schwob, I., 2015. Selection of wild macrophytes for use in constructed wetlands for phytoremediation of contaminant mixtures. Journal of Environmental Management. 147, 108–123. https://doi.org/10.1016/j.jenvman.2014.09.009
Guo, F., Zhang, J., Yang, X., He, Q., Ao, L., Chen, Y., 2020. Impact of biochar on greenhouse gas emissions from constructed wetlands under various influent chemical oxygen demand to nitrogen ratios. Bioresour. Technol. 303, 122908. https://doi.org/10.1016/j.biortech.2020.122908
Guo, Z., Kang, Y., Hu, Z., Liang, S., Xie, H., Ngo, H.H., Zhang, J., 2020. Removal pathways of benzofluoranthene in a constructed wetland amended with metallic ions embedded carbon. Bioresour. Technol. 311, 123481. https://doi.org/10.1016/j.biortech.2020.123481
Gupta, P., Ann, T., Lee, S., 2016. Use of biochar to enhance constructed wetland performance in wastewater reclamation. Environ. Eng. Res. 21, 36–44. https://doi.org/10.4491/eer.2015.067.
Gwenzi, W., Chaukura, N., Noubactep, C., Mukome, F.N.D., 2017. Biochar-based water treatment systems as a potential low-cost and sustainable technology for clean water provision. J. Environ. Manage. 197, 732–749. https://doi.org/10.1016/j.jenvman.2017.03.087
Hamada, M.S., Ibaid, Z.Z., Shatat, M., 2021. Performance of citrus charcoal and olivepomace charcoal as natural substrates in the treatment of municipal wastewater by vertical flow subsurface constructed wetlands. Bioresour. Technol. Reports 15, 100801. https://doi.org/10.1016/j.biteb.2021.100801
Hernández, M.E., Galindo-zetina, M., Hernández-hernández, J.C., 2017. wetlands with ornamental plants under subtropical conditions. Ecol. Eng. 1–8. https://doi.org/10.1016/j.ecoleng.2017.06.001
Houben, D., Evrard, L., Sonnet, P., 2013. Mobility, bioavailability and pH-dependent leaching of cadmium, zinc and lead in a contaminated soil amended with biochar. Chemosphere 92, 1450–1457. https://doi.org/10.1016/j.chemosphere.2013.03.055
Hsu, D., Lu, C., Pang, T., Wang, Y., Wang, G., 2019. Adsorption of Ammonium Nitrogen from Aqueous Solution on Chemically Activated Biochar Prepared from Sorghum Distillers Grain. Appl. Sci. 9(23). 5249. https://doi.org/10.3390/app9235249.
Hsu, N., Wang, S., Liao, Y., Huang, S., Tzou, Y., Huang, Y., 2009. Removal of hexavalent chromium from acidic aqueous solutions using rice straw-derived carbon. Journal of Hazardous Materials. 171, 1066–1070. https://doi.org/10.1016/j.jhazmat.2009.06.112
Hu, B., Hu, S., Vymazal, J., Chen, Z., 2022. Application of arbuscular mycorrhizal fungi for pharmaceuticals and personal care productions removal in constructed wetlands with different substrate. J. Clean. Prod. 339. https://doi.org/10.1016/j.jclepro.2022.130760
Hu, X., Zhang, X., Ngo, H.H., Guo, W., Wen, H., Li, C., Zhang, Y., Ma, C., 2019. Comparison study on the ammonium adsorption of the biochars derived from different kinds of fruit peel. Journal Pre. Sci. Total Environ. 135544. https://doi.org/10.1016/j.scitotenv.2019.135544
Hu, Y., Xiao, R., Kuang, B., Hu, Yanping, Wang, Y., Bai, J., Wang, C., Zhang, L., Wei, Z., Zhang, K., Jorquera, M.A., Acuña, J.J., Pan, W., 2022. Application of Modified Biochar in the Treatment of Pesticide Wastewater by Constructed Wetland. Water. 14(23). 3889. https://doi.org/10.3390/w14233889.
Huggins, T.M., Haeger, A., Biffinger, J.C., Ren, Z.J., 2016. Granular biochar compared with activated carbon for wastewater treatment and resource recovery. Water Res. 94, 225–232. https://doi.org/10.1016/j.watres.2016.02.059
Huong, M., Costa, D.T., van Hoi, B., 2020. Enhanced removal of nutrients and heavy metals from domestic-industrial wastewater in an academic campus of Hanoi using modified hybrid constructed wetlands. Water Sci. Technol. 82, 1995–2006. https://doi.org/10.2166/wst.2020.468
Ilyas, H., Hosney, H., 2024. Biochar - Integrated Constructed Wetlands for Organic Micropollutants Removal Biochar - Integrated Constructed Wetlands for Organic Micropollutants Removal.
Ippolito, J.A., Strawn, D.G., Scheckel, K.G., Novak, J.M., M. Ahmedna, Niandou, M.A.S., 2012. Macroscopic and Molecular Investigations of Copper Sorption by a Steam-Activated Biochar. Journal of Environmental Quality. 41. 4. 1150-1156. https://doi.org/10.2134/jeq2011.0113
Jain, M., Majumder, A., Ghosal, P.S., Gupta, A.K., 2020. A review on treatment of petroleum refinery and petrochemical plant wastewater: A special emphasis on constructed wetlands. J. Environ. Manage. 272, 111057. https://doi.org/10.1016/j.jenvman.2020.111057
Ji, B., Chen, J., Mei, J., Chang, J., Li, X., Jia, W., Qu, Y., 2020. Roles of biochar media and oxygen supply strategies in treatment performance , greenhouse gas emissions , and bacterial community features of subsurface- fl ow constructed wetlands. Bioresour. Technol. 302, 122890.

https://doi.org/10.1016/j.biortech.2020.122890
Jia, W., Sun, X., Gao, Y., Yang, Y., Yang, L., 2020a. Fe-modified biochar enhances microbial nitrogen removal capability of constructed wetland. Sci. Total Environ. 740, 139534. https://doi.org/10.1016/j.scitotenv.2020.139534Jia, W., Yang, L., 2021. Community composition and spatial distribution of n-removing microorganisms optimized by fe-modified biochar in a constructed wetland. Int. J. Environ. Res. Public Health 18, 1–20. https://doi.org/10.3390/ijerph18062938
Kaetzl, K., Lübken, M., Gehring, T., Wichern, M., 2018. Efficient Low-Cost Anaerobic Treatment of Wastewater Using Biochar and Woodchip Filters. Water. 10, 818. https://doi.org/10.3390/w10070818
Kaetzl, K., Lübken, M., Uzun, G., Gehring, T., Nettmann, E., Stenchly, K., Wichern, M., 2019. On-farm wastewater treatment using biochar from local agroresidues reduces pathogens from irrigation water for safer food production in developing countries. Sci. Total Environ. 682, 601–610. https://doi.org/10.1016/j.scitotenv.2019.05.142
Kang, Y., Ma, H., Jing, Z., Zhu, C., Li, Y., Wu, H., Dai, P., Guo, Z., Zhang, J., 2023. Enhanced benzofluoranthrene removal in constructed wetlands with iron- modified biochar: Mediated by dissolved organic matter and microbial response. J. Hazard. Mater. 443, 130322. https://doi.org/10.1016/j.jhazmat.2022.130322
Kang, Y., Xie, H., Li, B., Zhang, J., Hao Ngo, H., Guo, W., Guo, Z., Kong, Q., Liang, S., Liu, J., Cheng, T., Zhang, L., 2019. Performance of constructed wetlands and associated mechanisms of PAHs removal with mussels. Chem. Eng. J. 357, 280–287. https://doi.org/10.1016/j.cej.2018.09.152
Karunanayake, A.G., Todd, O.A., Crowley, M.L., Ricchetti, L.B., Pittman, C.U., Anderson, R., Mlsna, T.E., 2017. Rapid removal of salicylic acid, 4-nitroaniline, benzoic acid and phthalic acid from wastewater using magnetized fast pyrolysis biochar from waste Douglas fir. Chem. Eng. J. 319, 75–88. https://doi.org/10.1016/j.cej.2017.02.116
Karungamye, P.N., 2022. Potential of Canna indica in Constructed Wetlands for Wastewater Treatment: A Review. Conservation 2, 499–513. https://doi.org/10.3390/conservation2030034
Kasak, K., Truu, J., Ostonen, I., Sarjas, J., Oopkaup, K., Paiste, P., Kõiv-vainik, M., Mander, Ü., Truu, M., 2018. Biochar enhances plant growth and nutrient removal in horizontal subsurface flow constructed wetlands. Sci. Total Environ. 639, 67–74. https://doi.org/10.1016/j.scitotenv.2018.05.146
Kataki, S., Chatterjee, S., Vairale, M.G., Dwivedi, S.K., Gupta, D.K., 2021. Constructed wetland, an eco-technology for wastewater treatment : A review on types of wastewater treated and components of the technology (macrophyte, biolfilm and substrate). J. Environ. Manage. 283, 111986. https://doi.org/10.1016/j.jenvman.2021.111986
Keerthanan, S., Bhatnagar, A., Mahatantila, K., Jayasinghe, C., Ok, Y.S., Vithanage, M., 2020. Engineered tea-waste biochar for the removal of caffeine, a model compound in pharmaceuticals and personal care products (PPCPs), from aqueous media. Environ. Technol. Innov. 19, 100847. https://doi.org/10.1016/j.eti.2020.100847
Kılıc. M, Kırbıyık. C, Cepeliogullar. Ö, Pütün. A.E., 2013. Adsorption of heavy metal ions from aqueous solutions by bio-char , a by-product of pyrolysis. Applied Surface Science. 283, 856–862. https://doi.org/10.1016/j.apsusc.2013.07.033
Kizito, S., Lv, T., Wu, S., Ajmal, Z., Luo, H., Dong, R., 2017. Treatment of anaerobic digested effluent in biochar-packed vertical flow constructed wetland columns : Role of media and tidal operation. Sci. Total Environ. 592, 197–205. https://doi.org/10.1016/j.scitotenv.2017.03.125
Kizito, S., Wu, S., Kirui, W.K., Lei, M., Lu, Q., Bah, H., Dong, R., 2015. Evaluation of slow pyrolyzed wood and rice husks biochar for adsorption of ammonium nitrogen from piggery manure anaerobic digestate slurry. Sci. Total Environ. 505, 102–112. https://doi.org/10.1016/j.scitotenv.2014.09.096
Kong, J., Dai, Y., Han, M., He, H., Hu, J., Zhang, J., Shi, J., Xian, Q., Yang, S., Sun, C., 2021. Nitrated and parent PAHs in the surface water of Lake Taihu, China: Occurrence, distribution, source, and human health risk assessment. J. Environ. Sci. (China) 102, 159–169. https://doi.org/10.1016/j.jes.2020.09.025
Kőnig-Péter, A., Kocsis, B., Kilár, F., Pernyeszi, T., 2014. Bioadsorption characteristics of Pseudomonas aeruginosa PAOI. J. Serbian Chem. Soc. 79, 495–508. https://doi.org/10.2298/JSC130314070K
Kosolapov, B.D.B., Kuschk, P., Vainshtein, M.B., Vatsourina, A. V, Wieûner, A., Kästner, M., Müller, R.A., 2004. Review Microbial Processes of Heavy Metal Removal from Carbon-Deficient Effluents in Constructed Wetlands. Engineering in Life Sciences. 4. 5. 403–411. https://doi.org/10.1002/elsc.200420048
Kulshreshtha, N.M., Verma, V., Soti, A., Brighu, U., Gupta, A.B., 2022. Exploring the contribution of plant species in the performance of constructed wetlands for domestic wastewater treatment. Bioresour. Technol. Reports 18, 101038. https://doi.org/10.1016/j.biteb.2022.101038
Kumar, S., Dutta, V., 2019. Constructed wetland microcosms as sustainable technology for domestic wastewater treatment : an overview. Environmental Science and Pollution Research. 26, 11662–11673 https://doi.org/10.1007/s11356-019-04816-9.
Kumar, S., Loganathan, V.A., Gupta, R.B., Barnett, M.O., 2011. An Assessment of U (VI) removal from groundwater using biochar produced from hydrothermal carbonization. J. Environ. Manage. 92, 2504–

2512. https://doi.org/10.1016/j.jenvman.2011.05.013
Lai, W., Zhang, Y., Chen, Z., 2012. Radial oxygen loss, photosynthesis, and nutrient removal of 35 wetland plants. Ecol. Eng. 39, 24–30. https://doi.org/10.1016/j.ecoleng.2011.11.010
Laird, D., Fleming, P., Wang, B., Horton, R., Karlen, D., 2010. Geoderma Biochar impact on nutrient leaching from a Midwestern agricultural soil. Geoderma 158. 436–442. https://doi.org/10.1016/j.geoderma.2010.05.012
Lau, A.Y.T., Tsang, D.C.W., Graham, N.J.D., Sik, Y., Yang, X., 2017. Surface-modified biochar in a bioretention system for Escherichia coli removal from stormwater. Chemosphere 169, 89–98. https://doi.org/10.1016/j.chemosphere.2016.11.048
Li, G., Zhu, W., Zhang, C., Zhang, S., Liu, L., Zhu, L., Zhao, W., 2016. Effect of a magnetic field on the adsorptive removal of methylene blue onto wheat straw biochar. Bioresour. Technol. 206, 16–22. https://doi.org/10.1016/j.biortech.2015.12.087
Li, J., Fan, J., Liu, D., Hu, Z., Zhang, J., 2018a. Enhanced nitrogen removal in biochar-added surface flow constructed wetlands : dealing with seasonal variation in the north China. Environmental Science and Pollution Research. 26. 3675 –3684. https://doi.org/10.1007/s11356-018-3895-9.
Li, J., Fan, J., Zhang, J., Hu, Z., Liang, S., 2018b. Preparation and evaluation of wetland plant-based biochar for nitrogen removal enhancement in surface flow constructed wetlands. Environ. Sci. Pollut. Res. 25, 13929–13937. https://doi.org/10.1007/s11356-018-1597-y
Li, J., Hu, Z., Li, Fazhan, Fan, J., Zhang, J., Li, Fengmin, Hu, H., 2019. Effect of oxygen supply strategy on nitrogen removal of biochar-based vertical subsurface flow constructed wetland : Intermittent aeration and tidal flow. Chemosphere 223, 366–374. https://doi.org/10.1016/j.chemosphere.2019.02.082
Li, L., Quinlivan, P.A., Knappe, D.R.U., 2002. Effects of activated carbon surface chemistry and pore structure on the adsorption of organic contaminants from aqueous solution. Carbon. 40. 2085-2100. https://doi.org/10.1016/S0008-6223(02)00069-6.
Liang, Y., Wang, Q., Huang, L., Liu, M., Wang, N., Chen, Y., 2020. Insight into the mechanisms of biochar addition on pollutant removal enhancement and nitrous oxide emission reduction in subsurface flow constructed wetlands: Microbial community structure, functional genes and enzyme activity. Bioresour. Technol. 307, 123249. https://doi.org/10.1016/j.biortech.2020.123249
Liao, Y., Jiang, L., Cao, X., Zheng, H., Feng, L., Mao, Y., 2022. Efficient removal mechanism and microbial characteristics of tidal flow constructed wetland based on in-situ biochar regeneration (BR-TFCW) for rural gray water. Chem. Eng. J. 431, 134185. https://doi.org/10.1016/j.cej.2021.134185
Lili, H., Lixin, Z., Zonglu, Y., Haibo, M., 2017. 霍丽丽，赵立欣 ※， **姚宗路**，**孟海波**，丛宏斌.
Lima, I.M., Boateng, A., Klasson, K.T., 2010. Physicochemical and adsorptive properties of fast-pyrolysis bio-chars and their steam-activated counterparts.J. Chemical Technology and Biotechnology. 85. 11. 1515–1521. https://doi.org/10.1002/jctb.2461
Linville, J.L., Shen, Y., Leon, P.A.I., Schoene, R.P., Urgun-demirtas, M., 2017. In-situ biogas upgrading during anaerobic digestion of food waste amended with walnut shell biochar at bench scale. Waste Management and Research: The Journal for a Sustainable Circular Economy. 35. 6. https://doi.org/10.1177/0734242X17704716
Lopes, T.S. de A., Heßler, R., Bohner, C., Athayde Junior, G.B., de Sena, R.F., 2020. Pesticides removal from industrial wastewater by a membrane bioreactor and post-treatment with either activated carbon, reverse osmosis or ozonation. J. Environ. Chem. Eng. 8. https://doi.org/10.1016/j.jece.2020.104538
Louarrat, M., 2019. Elaboration Du Charbon Actif a Partir Des Noyaux D'Olive Et Application Pour L'Extraction De L'or Par Cyanuration, Thèse de Doctorat.
Lowell, S., 2004. Micropore Analysis. https://doi.org/10.1007/978-1-4020-2303-3_9
Lu, H., Zhang, W., Yang, Y., Huang, X., Wang, S., Qiu, R., 2011. Relative distribution of Pb 2D sorption mechanisms by sludge-derived biochar. Water Res. 46, 854–862. https://doi.org/10.1016/j.watres.2011.11.058
Lu, J., Guo, Z., Kang, Y., Fan, J., Zhang, J., 2020. Recent advances in the enhanced nitrogen removal by oxygen-increasing technology in constructed wetlands. Ecotoxicol. Environ. Saf. 205, 111330. https://doi.org/10.1016/j.ecoenv.2020.111330
Lu, K., Yang, X., Gielen, G., Bolan, N., Sik, Y., Khan, N., Xu, S., Yuan, G., Chen, X., Zhang, X., Liu, D., Song, Z., Liu, X., Wang, H., 2017. Effect of bamboo and rice straw biochars on the mobility and redistribution of heavy metals (Cd , Cu , Pb, and Zn) in contaminated soil. J. Environ. Manage. 186, 285–292. https://doi.org/10.1016/j.jenvman.2016.05.068
Lun, L. Chen, B., 2018. Enhanced bisphenol A removal from stormwater in biochar-amended biofilters: Combined with batch sorption and fixed-bed column studies. Environ. Pollut. https://doi.org/10.1016/j.envpol.2018.09.097
Mahmood, S., Khalid, A., Mahmood, T., Arshad, M., 2015. Biotreatment of simulated tannery wastewater

containing Reactive Black 5, aniline and CrVI using a biochar-packed bioreactor. RSC Adv. 5, 106272–106279. https://doi.org/10.1039/C5RA16809K
Maleki Shahraki, Z., Mao, X., 2022. Biochar application in biofiltration systems to remove nutrients, pathogens, and pharmaceutical and personal care products from wastewater. J. Environ. Qual. 51, 129–151. https://doi.org/10.1002/jeq2.20331
Malyan, S.K., Yadav, S., Sonkar, V., Goyal, V.C., Singh, O., Singh, R.S., 2021. Mechanistic understanding of the pollutant removal and transformation processes in the constructed wetland system. Water Environ. Res. https://doi.org/10.1002/wer.1599
Mandal, A., Kumar, A., Singh, N., 2021. Sorption mechanisms of pesticides removal from effluent matrix using biochar: Conclusions from molecular modelling studies validated by single-, binary and ternary solute experiments. J. Environ. Manage. 295, 113104. https://doi.org/10.1016/j.jenvman.2021.113104
Masrura, S.U., Dissanayake, P., Sun, Y., Ok, Y.S., Tsang, D.C.W., Khan, E., 2021. Sustainable use of biochar for resource recovery and pharmaceutical removal from human urine: A critical review. Crit. Rev. Environ. Sci. Technol. 51, 3016–3048. https://doi.org/10.1080/10643389.2020.1818497
Meng, F., Feng, L., Yin, H., Chen, K., Hu, G., Yang, G., 2019. Assessment of nutrient removal and microbial population dynamics in a non-aerated vertical ba ffl ed fl ow constructed wetland for contaminated water treatment with composite biochar addition. J. Environ. Manage. 246, 355–361. https://doi.org/10.1016/j.jenvman.2019.06.011
Mohamed, B.A., Ellis, N., Soo, C., Bi, X., Emam, A.E., 2016. Engineered biochar from microwave-assisted catalytic pyrolysis of switchgrass for increasing water-holding capacity and fertility of sandy soil. Sci. Total Environ. 566–567, 387–397. https://doi.org/10.1016/j.scitotenv.2016.04.169
Mohammed, N.A.S., Abu-zurayk, R.A., Hamadneh, I., Al-dujaili, A.H., 2018. Phenol adsorption on biochar prepared from the pine fruit shells : Equilibrium , kinetic and thermodynamics studies. J. Environ. Manage. 226, 377–385. https://doi.org/10.1016/j.jenvman.2018.08.033
Mohan, D., Sarswat, A., Sik, Y., Pittman, C.U., 2014. Organic and inorganic contaminants removal from water with biochar , a renewable , low cost and sustainable adsorbent – A critical review. Bioresour. Technol. 1–12. https://doi.org/10.1016/j.biortech.2014.01.120
Mohanty, P., Nanda, S., Pant, K.K., Naik, S., Kozinski, J.A., Dalai, A.K., 2013. Evaluation of the physiochemical development of biochars obtained from pyrolysis of wheat straw , timothy grass and pinewood : Effects of heating rate. J. Anal. Appl. Pyrolysis 104, 485–493. https://doi.org/10.1016/j.jaap.2013.05.022
Mohanty, S.K., Cantrell, K.B., Nelson, K.L., Boehm, A.B., 2014. Efficacy of biochar to remove Escherichia coli from stormwater under steady and intermittent flow. Water Res. https://doi.org/10.1016/j.watres.2014.05.026
Mondal, S., Bobde, K., Aikat, K., Halder, G., 2016. Biosorptive uptake of ibuprofen by steam activated biochar derived from mung bean husk : Equilibrium, kinetics, thermodynamics, modeling and eco-toxicological studies. J. Environ. Manage. 182, 581–594. https://doi.org/10.1016/j.jenvman.2016.08.018
Moreno-castilla, C., 2004. Adsorption of organic molecules from aqueous solutions on carbon materials. Carbon. 42, 83–94. https://doi.org/10.1016/j.carbon.2003.09.022
Mosher, K., 2011. THE IMPACT OF PORE SIZE ON METHANE AND CO2 ADSORPTION IN CARBON.
Mumme, J., Srocke, F., Heeg, K., Werner, M., 2014. Use of biochars in anaerobic digestion. Bioresour. Technol. 164, 189–197. https://doi.org/10.1016/j.biortech.2014.05.008
Nguyen, X.C., Tran, T.C.P., Hoang, V.H., Nguyen, T.P., Woong, S., Duc, Dinh, Guo, W., Kumar, A., Duc, Duong, Bach, Q., 2020. Combined biochar vertical flow and free-water surface constructed wetland system for dormitory sewage treatment and reuse. Sci. Total Environ. 713, 136404. https://doi.org/10.1016/j.scitotenv.2019.136404
Nuamah, L.A., Li, Y., Pu, Y., Nwankwegu, A.S., Haikuo, Z., Norgbey, E., Banahene, P., Bofah-Buoh, R., 2020. Constructed wetlands, status, progress, and challenges. The need for critical operational reassessment for a cleaner productive ecosystem. J. Clean. Prod. 269, 122340. https://doi.org/10.1016/j.jclepro.2020.122340
Ofiera, L.M., Wintgens, T., Kazner, C., 2025. Comparative analysis of conventional and modified constructed wetlands for the removal of trace organic compounds from municipal wastewater effluent. Sci. Total Environ. 987, 179796. https://doi.org/10.1016/j.scitotenv.2025.179796
Ohore, O.E., Qin, Z., Sanganyado, E., Wang, Y., Jiao, X., Liu, W., Wang, Z., 2022. Ecological impact of antibiotics on bioremediation performance of constructed wetlands: Microbial and plant dynamics, and potential antibiotic resistance genes hotspots. J. Hazard. Mater. 424, 127495. https://doi.org/10.1016/j.jhazmat.2021.127495
Oliveira, F.R., Patel, A.K., Jaisi, D.P., Adhikari, S., Lu, H., Khanal, K., 2017. Environmental application of biochar : Current status and perspectives. Bioresour. Technol. https://doi.org/10.1016/j.biortech.2017.08.122
Parde, D., Patwa, A., Shukla, A., Vijay, R., Killedar, D, J., Kumar, R., 2021. A review of constructed wetland on type, treatment and. Environ. Technol. Innov. 21, 101261. https://doi.org/10.1016/j.eti.2020.101261

Peiris, C., Gunatilake, S.R., Mlsna, T.E., Mohan, D., Vithanage, M., 2017. Biochar-based removal of antibiotic sulfonamides and tetracyclines in aquatic environments: A critical review. Bioresour. Technol. 246, 150–159. https://doi.org/10.1016/j.biortech.2017.07.150

Peng, A., Carol, L., David, J.P., Richard, W.B., Landis, C., 2016. Mechanisms of Mercury Removal by Biochars Produced from Different. J. Hazard. Mater. https://doi.org/10.1016/j.jhazmat.2016.01.007

Pereira, R., Astruc, D., 2021. Biochar as a support for nanocatalysts and other reagents : Recent advances and applications, Coordination Chemistry Reviews. Elsevier B.V. https://doi.org/10.1016/j.ccr.2020.213585

Pignatello, J. J., 2011. Interactions of anthropogenic organic chemicals with natural organic matter and black carbon in environmental particles. https://doi.org/10.1002/9780470944479.ch1.

Qadiri, R.Z.Z., Gani, K.M., Zaid, A., Aalam, T., Kazmi, A.A., Khalil, N., 2021. Comparative evaluation of the macrophytes in the constructed wetlands for the treatment of combined wastewater (greywater and septic tank effluent) in a sub-tropical region. Environ. Challenges 5, 100265. https://doi.org/10.1016/j.envc.2021.100265

Qambrani, N.A., Rahman, M.M., Won, S., Shim, S., Ra, C., 2017. Biochar properties and eco-friendly applications for climate change mitigation, waste management, and wastewater treatment: A review. Renew. Sustain. Energy Rev. 79, 255–273. https://doi.org/10.1016/j.rser.2017.05.057

Rashid, T., Sher, F., Hazafa, A., Hashmi, R.Q., Zafar, A., Rasheed, T., Hussain, S., 2021. Design and feasibility study of novel paraboloid graphite-based microbial fuel cell for bioelectrogenesis and pharmaceutical wastewater treatment. J. Environ. Chem. Eng. 9, 104502. https://doi.org/10.1016/j.jece.2020.104502

Rosales, E., Meijide, J., Pazos, M., Sanromán, M.A., 2017. Challenges and recent advances in biochar as low-cost biosorbent : from. Bioresour. Technol. https://doi.org/10.1016/j.biortech.2017.06.084

Rozari, P. De, Greenway, M., Hanandeh, A. El, 2018. Nitrogen removal from sewage and septage in constructed wetland mesocosms using sand media amended with biochar. Ecol. Eng. 111, 1–10. https://doi.org/10.1016/j.ecoleng.2017.11.002

Rozari, P. De, Greenway, M., Hanandeh, A. El, 2016. Phosphorus removal from secondary sewage and septage using sand media amended with biochar in constructed wetland mesocosms. Sci. Total Environ. 569–570, 123–133. https://doi.org/10.1016/j.scitotenv.2016.06.096

Saeed, T., Miah, J., Khan, T., Ove, A., 2019. Pollutant removal employing tidal flow constructed wetlands : media and feeding strategies. Chem. Eng. J. 122874. https://doi.org/10.1016/j.cej.2019.122874

Saeed, T., Miah, M.J., Khan, T., Ove, A., 2020. Pollutant removal employing tidal flow constructed wetlands: Media and feeding strategies. Chem. Eng. J. 382, 122874. https://doi.org/10.1016/j.cej.2019.122874

Saeed, T., Sun, G., 2017. A comprehensive review on nutrients and organics removal from different wastewaters employing subsurface flow constructed wetlands. Critical Reviews in Environmental Science and Technology. 203-288. 47. https://doi.org/10.1080/10643389.2017.1318615.

Saravanan, A., Senthil Kumar, P., Jeevanantham, S., Karishma, S., Tajsabreen, B., Yaashikaa, P.R., Reshma, B., 2021. Effective water/wastewater treatment methodologies for toxic pollutants removal: Processes and applications towards sustainable development. Chemosphere 280, 130595. https://doi.org/10.1016/j.chemosphere.2021.130595

Sha, N., Wang, G., Li, Y., Bai, S., 2020. RSC Advances Removal of abamectin and conventional pollutants in vertical flow constructed wetlands with Fe-modified biochar. Royal Society of Chemistry. 44171–44182. https://doi.org/10.1039/d0ra08265a

Shen, X., Zhang, J., Xie, H., Hu, Z., Liang, S., Ngo, H.H., Guo, W., Chen, X., Fan, J., Zhao, C., 2020. Intensive removal of PAHs in constructed wetland filled with copper biochar. Ecotoxicol. Environ. Saf. 205, 111028. https://doi.org/10.1016/j.ecoenv.2020.111028

Shen, Y., Zhuang, L., Zhang, J., Fan, J., Yang, T., Sun, S., 2018. A study of ferric-carbon micro-electrolysis process to enhance nitrogen and phosphorus removal efficiency in subsurface flow constructed wetlands. Chem. Eng. J. https://doi.org/10.1016/j.cej.2018.11.152

Shi, X., Fan, J., Zhang, J., Shen, Y., 2017. Enhanced phosphorus removal in intermittently aerated constructed wetlands filled with various construction wastes. Environmental Science and Pollution Research. 24. 22524–22534. https://doi.org/10.1007/s11356-017-9870-z

Shi, Y., Shen, G., Geng, J., Fu, Y., Li, S., Wu, G., Wang, L., Xu, K., Ren, H., 2021. Predictive models for the degradation of 4 pharmaceutically active compounds in municipal wastewater effluents by the UV/H2O2 process. Chemosphere 263, 1–10. https://doi.org/10.1016/j.chemosphere.2020.127944

Solanki, A., Boyer, T.H., 2017. Pharmaceutical removal in synthetic human urine using biochar. Environ. Sci. Water Res. Technol. 3, 553–565. https://doi.org/10.1039/c6ew00224b

Srivastava, J., Gupta, Æ.A., Chandra, Æ.H., 2008. Managing water quality with aquatic macrophytes. Reviews in Environmental Science and Bio/Technology. 7. 255–266. https://doi.org/10.1007/s11157-008-9135-x

Stefanakis, A.I., 2020. Constructed Wetlands for Sustainable Wastewater Treatment in Hot and Arid Climates : Opportunities, Challenges and Case Studies in the Middle East. water. 12(6), 1665; https://doi.org/10.3390/w12061665.

Stefanakis, A.I., 2019. The Role of Constructed Wetlands as Green Infrastructure for Sustainable Urban Water Management. Sustainability 11, 6981. https://doi.org/10.3390/su11246981
Stefanakis, A.I., 2018. Introduction to Constructed Wetland Technology. Constr. Wetl. Ind. Wastewater Treat. 1–21. https://doi.org/10.1002/9781119268376.ch0
Sudarsan, J.S., Srihari, V., 2019. Evaluation of adsorption capacity of biochar mixed substrate to treat tannery wastewater by constructed wetland, 020176. https://doi.org/10.1063/1.5112361
Suliman, W., Harsh, J.B., Abu-lail, N.I., Fortuna, A., Dallmeyer, I., Garcia-perez, M., 2016. Biomass and Bioenergy Influence of feedstock source and pyrolysis temperature on biochar bulk and surface properties. Biomass and Bioenergy 84, 37–48. https://doi.org/10.1016/j.biombioe.2015.11.010
Sun, K., Ro, K., Guo, M., Novak, J., Mashayekhi, H., Xing, B., 2011. Sorption of bisphenol A, 17α-ethinyl estradiol and phenanthrene on thermally and hydrothermally produced biochars. Bioresour. Technol. 102, 5757–5763. https://doi.org/10.1016/j.biortech.2011.03.038
Tan, X., Liu, Y., Zeng, G., Wang, X., Hu, X., Gu, Y., 2015. Application of biochar for the removal of pollutants from aqueous solutions. Chemosphere. https://doi.org/10.1016/j.chemosphere.2014.12.058
Tang, X., Yang, Y., Huang, W., Mcbride, M.B., Guo, J., Tao, R., Dai, Y., 2017. Transformation of Chlorpyrifos in Integrated Recirculating Constructed Wetlands (IRCWs) as Revealed by Compound-Specific Stable Isotope (CSIA) and Microbial Community Structure Analysis. Bioresour. Technol. https://doi.org/10.1016/j.biortech.2017.02.077
Tang, X., Yang, Y., Tao, R., Chen, P., Dai, Y., Jin, C., Feng, X., 2016. Fate of mixed pesticides in an integrated recirculating constructed wetland (IRCW). Sci. Total Environ. https://doi.org/10.1016/j.scitotenv.2016.07.079
Tang, Y., Alam, S., Konhauser, K.O., Alessi, D.S., Xu, S., Tian, W., Liu, Y., 2018. Influence of pyrolysis temperature on production of digested sludge biochar and its application for ammonium removal from municipal wastewater. J. Clean. Prod. https://doi.org/10.1016/j.jclepro.2018.10.268
Teixid, M., Pignatello, J.J., Beltr, L., 2011. Speciation of the Ionizable Antibiotic Sulfamethazine on Black Carbon (Biochar). Environ. Sci. Technol. 45. 23. 10020–10027. https://doi.org/10.1021/es202487h.
Tsai, W.T., Chen, H.R., 2013. Adsorption kinetics of herbicide paraquat in aqueous solution onto a low-cost adsorbent, swine-manure-derived biochar. International Journal of Environmental Science and Technology. 10. 1349–1356. https://doi.org/10.1007/s13762-012-0174-z
Valipour, A., Ahn, Y., 2015. Constructed wetlands as sustainable ecotechnologies in decentralization practices : a review. Environ. Sci. Pollut. Res. https://doi.org/10.1007/s11356-015-5713-y
Venditti, S., Brunhoferova, H., Hansen, J., 2022. Behaviour of 27 selected emerging contaminants in vertical flow constructed wetlands as post-treatment for municipal wastewater. Sci. Total Environ. 819, 153234. https://doi.org/10.1016/j.scitotenv.2022.153234
Vohla, C., Kõiv, M., Bavor, H.J., Chazarenc, F., Mander, Ü., 2011. Filter materials for phosphorus removal from wastewater in treatment wetlands — A review. Ecol. Eng. 37, 70–89. https://doi.org/10.1016/j.ecoleng.2009.08.003
Vymazal, J., 2011. Plants used in constructed wetlands with horizontal subsurface flow : a review. Hydrobiologia. 674. 133–156. https://doi.org/10.1007/s10750-011-0738-9
Vymazal, J., Tereza, B., 2015. The use of constructed wetlands for removal of pesticides from agricultural runoff and drainage : A review. Sustainability. 75, 11–20. https://doi.org/10.1016/j.envint.2014.10.026
Vymazal, J., Zhao, Y., Mander, Ü., 2021. Recent research challenges in constructed wetlands for wastewater treatment: A review. Ecol. Eng. 169, 106318. https://doi.org/10.1016/j.ecoleng.2021.106318c
Wang, H., Teng, H., Wang, X., Xu, J., Sheng, L., 2022. Physicochemical modification of corn straw biochar to improve performance and its application of constructed wetland substrate to treat city tailwater. J. Environ. Manage. 310, 114758. https://doi.org/10.1016/j.jenvman.2022.114758
Wang, H., Xu, J., Sheng, L., 2020a. Preparation of straw biochar and application of constructed wetland in China: A review. J. Clean. Prod. 273, 123131. https://doi.org/10.1016/j.jclepro.2020.123131
Wang, H., Xu, J., Sheng, L., 2020b. Purification mechanism of sewage from constructed wetlands with zeolite substrates: A review. J. Clean. Prod. https://doi.org/10.1016/j.jclepro.2020.120760
Wang, J., Wang, S., 2019. Preparation, modification and environmental application of biochar: A review. J. Clean. Prod. 227, 1002–1022. https://doi.org/10.1016/j.jclepro.2019.04.282
Wang, Q., Cao, Z., Hu, Y., Kong, Q., Xu, F., Du, Y., and C.Z., 2019. Season effects on subsurface constructed wetlands performance: Role of radial oxygen loss of Phragmites australis. CLEAN – Soil, Air, Water. 47. 8. https://doi.org/10.1002/clen.201800428
Wichern, M., Buerkert, A., Werner, S., Korbinian, K., Steiner, C., Marschner, B., 2018. Agronomic benefits of biochar as a soil amendment after its use as a wastewater filtration medium. Environmental Pollution. 233. 561-568. https://doi.org/10.1016/j.envpol.2017.10.048
Wu, J., Zheng, J., Ma, K., Jiang, C., Zhu, L., Xu, X., 2022. Tertiary treatment of municipal wastewater by a novel flow constructed wetland integrated with biochar and zero-valent iron. J. Water Process Eng. 47.

https://doi.org/10.1016/j.jwpe.2022.102777
Wu, S., Carvalho, P.N., Müller, J.A., Remony, V., Dong, R., 2016. Sanitation in constructed wetlands : A review on the removal of human pathogens and fecal indicators. Sci. Total Environ. 541, 8–22. https://doi.org/10.1016/j.scitotenv.2015.09.047
Wu, S., Wallace, S., Brix, H., Kuschk, P., Kirui, W.K., Masi, F., Dong, R., 2015. Treatment of industrial effluents in constructed wetlands: Challenges, operational strategies and overall performance. Environ. Pollut. 201, 107–120. https://doi.org/10.1016/j.envpol.2015.03.006
Wu, S., Wu, H., 2019. Incorporating Biochar into Wastewater Eco-treatment Systems: Popularity, Reality, and Complexity. Environ. Sci. Technol. 53, 3345–3346. https://doi.org/10.1021/acs.est.9b01101
Wu, Z., Xu, F., Yan, C., Su, X., Guo, F., Xu, Q., Peng, G., He, Q., Chen, Y., 2018. Highly efficient nitrate removal in a heterotrophic denitrification system amended with redox-active biochar : a molecular and electrochemical mechanism Key Laboratory of the Three Gorges Reservoir Region's Eco-Environment, Ministry School of Environment. Bioresour. Technol. https://doi.org/10.1016/j.biortech.2018.12.058
Xiang, W., Zhang, X., Chen, J., Zou, W., He, F., Hu, X., Tsang, D.C.W., Sik, Y., Gao, B., 2020. Biochar technology in wastewater treatment : A critical review. Chemosphere 252, 126539. https://doi.org/10.1016/j.chemosphere.2020.126539
Xiao, H., Jie, B.A.I., Kuiran, L.I., Yangguo, Z., Weijun, T., 2020. Preparation of Clay / Biochar Composite Adsorption Particle and Performance for Ammonia Nitrogen Removal from Aqueous Solution. Journal of Ocean University of China. 19, 729–739. https://doi.org/10.1007/s11802-020-4150-9.
Xin, X., Liu, S., Qin, J., Ye, Z., Liu, W., Fang, S., Yang, J., 2021. Performances of simultaneous enhanced removal of nitrogen and phosphorus via biological aerated filter with biochar as fillers under low dissolved oxygen for digested swine wastewater treatment. Bioprocess Biosyst. Eng. 44, 1741–1753. https://doi.org/10.1007/s00449-021-02557-z
Xu, C., Lu, Z., 2019. Treatment of Domestic Wastewater in Biochar-packed Tidal Flow Constructed Wetland. Sci. Environ. 28, 1443–1449. https://doi.org/10.16258/j.cnki.1674-5906.2019.07.018
Xu, X., Cao, X., Zhao, L., 2013. Comparison of rice husk- and dairy manure-derived biochars for simultaneously removing heavy metals from aqueous solutions : Role of mineral components in biochars. Chemosphere 92, 955–961. https://doi.org/10.1016/j.chemosphere.2013.03.009
Yaashikaa, P.R., Kumar, P.S., Varjani, S., Saravanan, A., 2020. A critical review on the biochar production techniques, characterization, stability and applications for circular bioeconomy. Biotechnol. Reports 28, e00570. https://doi.org/10.1016/j.btre.2020.e00570
Yan, Y., Ma, M., Liu, X., Ma, W., Li, M., Yan, L., 2017. Effect of biochar on anaerobic degradation of pentabromodiphenyl ether (BDE-99) by archaea during natural groundwater recharge with treated municipal wastewater. Int. Biodeterior. Biodegradation 1–9. https://doi.org/10.1016/j.ibiod.2017.04.019
Yang, Y., Zhao, Y., Liu, R., Morgan, D., 2018. Technology Global development of various emerged substrates utilized in constructed wetlands. Bioresour. Technol. 261, 441–452. https://doi.org/10.1016/j.biortech.2018.03.085

You, X., Jiang, H., Zhao, M., Suo, F., Zhang, C., Zheng, H., Sun, K., Zhang, G., Li, F., Li, Y., n.d. Biochar reduced Chinese chive (Allium tuberosum) uptake and dissipation of thiamethoxam in an agricultural soil. J. Hazard. Mater. 121749. https://doi.org/10.1016/j.jhazmat.2019.121749
Younas, F., Niazi, N.K., Bibi, I., Afzal, M., Hussain, K., Shahid, M., Aslam, Z., Bashir, S., Hussain, M.M., Bundschuh, J., 2022. Constructed wetlands as a sustainable technology for wastewater treatment with emphasis on chromium-rich tannery wastewater. J. Hazard. Mater. 422, 126926. https://doi.org/10.1016/j.jhazmat.2021.126926
Yu, X., Pan, L., Ying, G., Kookana, R.S., 2010. Enhanced and irreversible sorption of pesticide pyrimethanil by soil amended with biochars. J. Environ. Sci. 22, 615–620. https://doi.org/10.1016/S1001-0742(09)60153-4
Yuan, H., Ding, L., Zama, E.F., Liu, P., Hozzein, W.N., Zhu, Y., 2018. Characterization of Natural and Affected Environments Biochar modulates methanogenesis through electron syntrophy of microorganisms with ethanol as a substrate. Environ. Sci. Technol. 52. 21. 12198–12207. https://doi.org/10.1021/acs.est.8b04121
Yuan, Y., Yang, B., Wang, H., Lai, X., Li, F., Salam, M.M.A., Pan, F., Zhao, Y., 2020. The simultaneous antibiotics and nitrogen removal in vertical flow constructed wetlands: Effects of substrates and responses of microbial functions. Bioresour. Technol. 310. https://doi.org/10.1016/j.biortech.2020.123419
Zabaniotou, A., Stavropoulos, G., Skoulou, V., 2008. Activated carbon from olive kernels in a two-stage process : Industrial improvement. Bioresource Technology. 99, 320–326. https://doi.org/10.1016/j.biortech.2006.12.020
Zapata, A., Oller, I., Sirtori, C., Rodríguez, A., Sánchez-Pérez, J.A., López, A., Mezcua, M., Malato, S., 2010. Decontamination of industrial wastewater containing pesticides by combining large-scale homogeneous solar photocatalysis and biological treatment. Chem. Eng. J. 160, 447–456.

https://doi.org/10.1016/j.cej.2010.03.042
Zhang, M., Shen, J., Zhong, Y., Ding, T., Dissanayake, P.D., Yang, Y., Tsang, Y.F., Ok, Y.S., 2022. Sorption of pharmaceuticals and personal care products (PPCPs) from water and wastewater by carbonaceous materials: A review. Crit. Rev. Environ. Sci. Technol. 52, 727–766. https://doi.org/10.1080/10643389.2020.1835436
Zhang, Y., Li, Mengqi, Dong, L., Han, C., Li, Ming, Wu, H., 2021. Effects of biochar dosage on treatment performance, enzyme activity and microbial community in aerated constructed wetlands for treating low C/N domestic sewage. Environ. Technol. Innov. 24, 101919. https://doi.org/10.1016/j.eti.2021.101919
Zhang, C., Zeng, G., Huang, D., Lai, C., Chen, M., Cheng, M., Tang, W., Tang, L., Dong, H., Huang, B., Tan, X., Wang, R., 2019. Biochar for environmental management : Mitigating greenhouse gas emissions, contaminant treatment, and potential negative impacts. Chem. Eng. J. 373, 902–922. https://doi.org/10.1016/j.cej.2019.05.139
Zhang, Q., Yang, Y., Chen, F., Zhang, L., Ruan, J., Wu, S., Zhu, R., 2021. Effects of hydraulic loading rate and substrate on ammonium removal in tidal flow constructed wetlands treating black and odorous water bodies. Bioresour. Technol. 321, 124468. https://doi.org/10.1016/j.biortech.2020.124468
Zhao, Y., Ji, B., Liu, R., Ren, B., Wei, T., 2020. Constructed treatment wetland : Glance of development and future perspectives. Water Cycle 1, 104–112. https://doi.org/10.1016/j.watcyc.2020.07.002
Zheng, F., Fang, J., Guo, F., Yang, X., Liu, T., 2022. Biochar-based constructed wetland for secondary effluent treatment : Waste resource utilization. Chem. Eng. J. 432, 134377. https://doi.org/10.1016/j.cej.2021.134377
Zheng, Y., Wang, B., Wester, A.E., Chen, J., He, F., Chen, H., Gao, B., 2019. Reclaiming Phosphorus from Secondary Treated Municipal Wastewater with Engineered Biochar State Key Laboratory of Environmental Geochemistry, Institute of Geochemistry, Chinese. Chem. Eng. J. https://doi.org/10.1016/j.cej.2019.01.036
Zhong, L., Yang, S., Ding, J., Wang, G., Chen, C., Xie, G., Xu, W., Yuan, F., Ren, N., 2021. Enhanced nitrogen removal in an electrochemically coupled biochar-amended constructed wetland microcosms : The interactive effects of biochar and electrochemistry. Sci. Total Environ. 789, 147761. https://doi.org/10.1016/j.scitotenv.2021.147761
Zhou, X., Liang, C., Jia, L., Feng, L., Wang, R., Wu, H., 2017. An innovative biochar-amended substrate vertical flow constructed wetland for low C/N wastewater treatment: Impact of influent strengths. Bioresour. Technol. https://doi.org/10.1016/j.biortech.2017.09.044
Zhou, X., Wang, R., Liu, H., Wu, S., Wu, H., 2019. Nitrogen removal responses to biochar addition in intermittent-aerated subsurface flow constructed wetland microcosms : Enhancing role and mechanism. Ecol. Eng. 128, 57–65. https://doi.org/10.1016/j.ecoleng.2018.12.028
Zhou, X., Wu, S., Wang, R., Wu, H., 2018. Nitrogen removal in response to the varying C / N ratios in subsurface flow constructed wetland microcosms with biochar addition. Environ. Sci. Pollut. Res. https://doi.org/doi.org/10.1007/s11356-018-3871-4
Zhou, Z., Shi, D., Qiu, Y., Sheng, G.D., 2010. Sorptive domains of pine chars as probed by benzene and nitrobenzene. Environ. Pollut. 158, 201–206. https://doi.org/10.1016/j.envpol.2009.07.020
Zhuang, L.L., Li, M., Li, Y., Zhang, L., Xu, X., Wu, H., Liang, S., Su, C., Zhang, J., 2022. The performance and mechanism of biochar-enhanced constructed wetland for wastewater treatment. J. Water Process Eng. 45, 102522. https://doi.org/10.1016/j.jwpe.2021.102522

Chapter II – Preparation and Characterization of Different Biochars: A Comparative Study

II-I. Physicochemical and Thermal Characterization of Argan Residues for Biochar Production: Potential Future Prospects

This work was published as a research paper:

El Barkaoui, S., Ouazzani, N., Mandi, L., Zafeiropoulos, J., Isari, E.A., Del Bubba, M., Kalavrouziotis, I.K. 2025. Physicochemical and thermal characterization of argan residues for biofuel and biochar production: potential future prospects. Biomass Conv. Bioref. 15, 17309–17319 (2025). https://doi.org/10.1007/s13399-024-06442-z

Abstract

The recovery of biomass waste by conversion to biochar or biofuel is an efficient and environmentally friendly method of biomass valorisation. This paper compares for the first time the physicochemical, structural, thermal, and energetic properties of three types of argan residues: black argan press cake (BAC), white argan press cake (WAC), and pellet argan cake (PAC) for their potential use as biofuel or biochar. The study showed that the three residues have a high content of carbon (52% - 61%), volatile matter (86% - 91%), and calorific value (higher and lower heating value 24 – 27 MJ/kg and 23 – 25 MJ/kg, respectively), and a low content of ash (3.3% - 4.2%) and moisture (1.5% - 3.3%), confirming their suitability as efficient sources for the production of fuel and biochar. The calorific value and combustion rate of argan residues were higher compared to other residues reported in the literature, thus underlining the potential utility of these biomasses as biofuels. In addition, the thermal analysis showed that the three biomasses exhibit a reactive behaviour during the pyrolysis processes, which ends at about 450°C, suggesting their possibility of converting into biochar at relatively low temperatures. Overall, the results obtained suggest WAC as the best compromise in terms of energetic properties and attributes prone to generate a valuable sorption material to be used in wastewater treatment. Thus, WAC could be a credible alternative to conventional fuels and offer new perspectives for its use as an optimal bioresource for biochar and biofuel production.

Keywords: Argan oil residues, Characterization, Feedstock, Biofuel, Biochar, Application

1. Introduction

The Argania spinosa plant is an ancient tree endemic to the South Atlantic area of Morocco and is renowned worldwide for its miraculous argan oil, which has several cosmetic and therapeutic properties (Babty et al., 2021). Surviving since the Tertiary era, argan (also known as ironwood) is an oil tree that is very resistant to heat and perfectly adapted to poor and dry soils. It serves as a source of food for livestock and as firewood. The annual argan oil production is 2500 – 4000 tons, and 1.15 – 1.31 kg of residues, usually retaining a low economic value, are obtained to produce 1 kg of argan oil (Bahani et al., 2024). These residues consist of the nutshell (about 80% of the fruit by weight), which is usually reused as wood fuel (El Kourdi et al., 2024), and the so-called “argan cake”, which is partially valued in various fields such as cosmetics (e.g., shampoo), pharmaceuticals (e.g., anti-scabies), and agri-food (e.g., animal feed) (Bourhim et al., 2021; Charrouf et al., 2007; El Kourdi et al., 2024). However, notwithstanding these reuse strategies, argan cakes still represent a waste and are becoming an acute problem due to the growing market of argan oil in Morocco (Lybbert et al., 2010). An alternative strategy for reusing argan cakes lies in their pyrolytic conversion, which allows to obtain biochar and biofuels (i.e., bio-oil and syngas). In fact, these wastes are rich in lignocellulosic material (Zeghlouli et al., 2023), suggesting their potential to be reused as a renewable product and energy source (i.e., biochar or biofuel). This field is attracting considerable attention because of its potential to address the environmental and

socio-economic challenges associated with fossil fuel use and energy insecurity in the future.

Argan oil production generates three different kinds of argan cake residues: 1) black argan press cake (BAC), which is the residue from food oil extraction, 2) white argan press cake (WAC), derived from the extraction of cosmetic oil (Charrouf and Guillaume, 1999), and 3) pellet argan cake (PAC), the final residue from the argan oil production by pressing machine (Folayan and Anawe, 2019). The traditional method of extracting oil from the BAC and WAC involves manually crushing argan almonds with a rotating stone until an oily mass is obtained. Water is then added, and the mass is kneaded manually for a proper time to produce a cake, which is then manually pressed to separate the oily emulsion from the cake (Charrouf and Guillaume, 1999).

Only a few studies have so far focused on the characterization of argan cakes. Rahib et al., (2020) studied the physicochemical properties and thermal characteristics of argan cakes in order to evaluate their energy value. More in detail, argan cakes were characterized as such and after the extraction of the oil residue with n-hexane, pointing out that the two matrices have high heating values (HHV, 22.4 and 19.3 $MJ.kg^{-1}$, respectively), being comparable with those of lignite and anthracite coals. Similar results in terms of energy power were obtained by El Kourdi et al., (2024), who determined an HHV of about 20 $MJ\ kg^{-1}$. On the contrary, the two papers report very different percentages of fixed carbon (FC), a parameter strongly correlated with the calorific value of the material (ÖzyuğUran and Yaman, 2017). In addition, the ash content (AC) of the argan cakes analysed in the two studies was about twice as high in one case as in the other (El Kourdi et al., 2024; Rahib et al., 2020), thus influencing the energy power of the argan residues and their pyrolysis products (El Kourdi et al., 2024). These differences are probably attributable to the different origins of the argan cakes, especially considering the different argan oil extraction methods mentioned above and related argan cakes obtained (i.e., BAC, WAC, and PAC).

Based on the above considerations, it is therefore important to characterise argan cakes from the different argan oil production methods and to determine their energy value. In fact, there are currently no characterisation studies of argan cakes that distinguish and/or give information on the production method by which they were obtained. Accordingly, in this study batches of BAC, WAC, and PAC, representative of the three argan oil production methods, were provided by the company AFOUS (Essaouira, Morocco) and characterised for pH, proximate (i.e., moisture content (MC), volatile matter (VM), AC, and FC) and elemental (CHNS-O) analyses, X-ray fluorescence (XRF) analysis, burning rate (BR), higher and lower heating value (HHV and LHV, respectively), thermo-analytical methods (thermogravimetric analysis (TGA) and derivative

thermogravimetry (DTG)), X-ray diffraction (XRD), Fourier transform infrared spectroscopy (FTIR), and scanning electron microscopy/energy dispersive X-ray spectroscopy (SEM-EDX) to determine their potential for reuse in the production of biochar and biofuel.

2. Materials and methods

2.1. Fruit sampling and argan cake preparation

The fruits of Argania spinosa were collected at full maturity (generally in July) from different regions of Morocco: Essaouira, Agadir, Ait Baha Tafraout, and Taroudant (Atlantic coast of Morocco). The cake samples analysed here were produced in the AFOUS Argan company (**Figure II-1**). Argan oil extraction can be carried out following different procedures. The procedures performed to obtain the argan oil cakes analysed in this study, in use at the AFOUS company, are described below. Fruits harvested at the right degree of ripeness are peeled, and the kernel of the fruit is separated from the pulp. The kernels are then crushed, and the almonds contained within are dried. Roasted and unroasted almonds are used for obtaining food and cosmetic argan oils, respectively. For both products, the roasted/unroasted almonds are crushed using a manual rotating mill and then kneaded with warm water, thus obtaining a brown-coloured paste. Finally, the paste is manually pressed to separate the oily emulsion from the cake, providing a compact dark brown cake (BAC) or a compact light-brown cake (WAC) in the case of roasted and unroasted almonds, respectively (Charrouf and Guillaume, 1999; El Monfalouti, 2013). In the case of cosmetic applications, in addition to the manual process, mechanical pressing is used (PAC), which does not require the addition of water to the milled almonds, thus ensuring a faster extraction process and higher argan oil extraction yields (Folayan and Anawe, 2019).

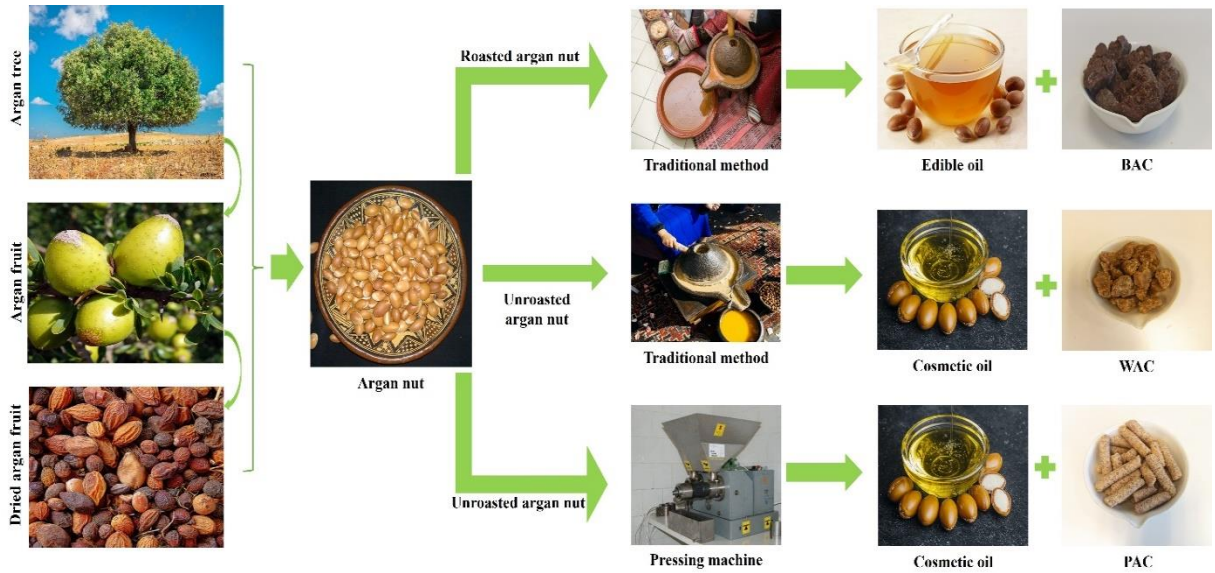

Figure II-1: Schematic illustration of traditional and mechanical argan oil production processes and obtaining corresponding PAC, WAC, and BAC residues.

2.2. Feedstock characterization

The contents of M, VM, and AC were determined according to AFNOR XP CEN/TS 14774–3, ASTM Standard D5142, and ASTM D1762-84 methods, respectively. FC is a measure of the amount of non-volatile carbon in the sample and is calculated from other parameters measured in a proximate analysis according to the equation: FC=100-(VM%+M%+AC%) (Bakari et al., 2024; Kuhe et al., 2021; Rabichi et al., 2024).

Elemental analysis (CHNS-O) of biomasses was performed using an elemental analyzer model EURO EA (EUROVECTOR, Pavia, Italy). This technique provides the content of carbon, hydrogen, nitrogen, and sulfur in a sample by their complete and instantaneous oxidation via combustion with oxygen at an approximate temperature of 1020 °C. The combustion products (CO_2, H_2O, NO_2, and SO_2) are transported by a gas carrier to a chromatographic column where they are separated and finally determined by a thermal conductivity detector (Bini et al., 2024; Oubannin et al., 2022). The oxygen percentage (O%) was determined by the following equation: O%=100-C%-N%-H%-ash% (Bakari et al., 2024).

The composition of inorganic elements was determined by using the Bruker (Billerica, MA, USA) S2 PUMA X-ray fluorescence spectrometer. Approximately 1.0 g of the sample was placed in a Spectra Membrane Ultra-Polyester Thin-Film with a diameter of 4 cm and a thickness of 1.5 µm.

The XRF analysis was performed under an air atmosphere, and the data were analysed by Spectra Elements software (AXS-34).

HHV was measured (3 replicates) by combusting the samples in an adiabatic oxygen bomb calorimeter (IKA C-200). Utilizing this value, along with the percentage content of hydrogen, LHV was calculated according to Equation (1) (Rabichi et al., 2024). BR represents the rate of mass loss per unit time during combustion. To assess the burning rate of biomasses, the sample was positioned on a steel wire mesh grid supported by three points to facilitate unrestricted air flow. Subsequently, the entire setup was situated on a digital mass balance. The sample ignited from the top, and data on mass loss were recorded at 10-second intervals (Kuhe et al., 2021), and were calculated by the equation (2).

$$\mathrm{LHV}\left(\mathrm{MJ{\cdot}Kg^{-1}}\right) = \mathrm{HHV} - 2.447 \cdot \left(\frac{\mathrm{H}\,(\%)}{100}\right) \cdot 9.011 \qquad (1)$$

$$\mathrm{BR}\left(\mathrm{g{\cdot}s^{-1}}\right) = \frac{\text{total mass lost}}{\text{total time}} \qquad (2)$$

The TG-DTG analysis was performed by using a Perkin Elmer (Waltham, MA, USA) TGA thermogravimetric analyzer under a nitrogen atmosphere in a temperature range from 50 °C to 950 °C and with a heating rate of 10 °C·min^{-1}.

FT-IR analysis was performed using a Perkin Elmer (FTIR spectrometer, model FT-IR 100), thus, the spectra were recorded on KBr pellets in the range of 400-4000 cm^{-1}, with a resolution of 4 cm^{-1} for each determination.

The crystal phases of the biomass samples were analysed by XRD. The patterns were registered in the 2Θ range from 5 to 80 using a Bruker D8 Advance diffractometer, equipped with a Ni-filtered CuKa (1.5418 Å) radiation source (0.1 ° step, 1.00 s step time).

SEM-EDX is a method capable of generating high-resolution images of the sample surface and collecting element spectra in selected points of the material. In this study, the images and the spectra were carried out using a TESCAN (Brno, Czech Republic) SEM, model VEGA3.

2.3. Statistical analysis

Statistical analyses were performed using Minitab (State College, PA, USA) version 17.1.0, which

included analysis of variance (ANOVA). Significance levels were reported as insignificant or significant, according to a 5% probability level. The Fisher and Games-Howell tests were used depending on the results of the homogeneity tests for variance.

3. Results and discussion

3.1. Physicochemical properties

Table II-1 shows the results of pH, proximate analysis, elemental analysis, and inorganic percentage elemental composition as measured by XRF. BAC and WAC had very similar pH values (mean value of 5.37 and 5.39, respectively), while for PAC, a significantly lower acidity was observed, probably due to its mechanical production method, which is capable of extracting more argan oil compared to manual pressing. The acidic nature of BAC and WAC is consistent with a higher residual oil content in the cake resulting from the manual extraction procedure, which imparts higher acidity due to the free fatty acids contained in the argan oil (Gharby and Charrouf, 2022; Oubannin et al., 2022). The acidic nature of the raw materials, and in particular of BAC and WAC, could contribute to the obtaining of a biochar with less pronounced basic characteristics than that commonly obtained from plant wastes. A biochar characterized by a pH of point of zero charge close to neutrality can be advantageous both for agricultural applications (Bini et al., 2024) and for use as an adsorbent, as it does not show markedly different behaviours in the removal of charged species (Ayadi et al., 2024).

All samples showed M content <4%, i.e., well below the threshold percentage of 10%, above which it is considered necessary to dry the biomass before its use as feedstock in pyrolysis/gasification processes (Gharby and Charrouf, 2022; Gómez et al., 2016). Overall, the argan cakes are interesting from the energy production viewpoint, since they have lower M than other residual biomass considered valuable for their energy content, such as cardoon, riparian residues, olive pruning, almond shells, and grapevine pruning (Déniel et al., 2016; Rago et al., 2018). In more detail, the three cakes showed statistically different moistures, with PAC exhibiting the lowest value, in agreement with the mechanical procedure used for argan oil production, which does not require the addition of water.

PAC, BAC, and WAC showed VM content of about 86%, 89%, and 91%, respectively. These values, although similar, were statistically different, suggesting slightly different behaviour in syngas yield during pyrolysis or gasification. In fact, volatile compounds are potential syngas

precursors in pyrolytic thermal conversion (Muigai et al., 2021), and higher VM values commonly provide higher syngas yields (Gao et al., 2023), thus representing an interesting feature for feedstock responsiveness and ignition performance (Muigai et al., 2021). It is also worth mentioning that, according to the available literature, VM values of argan cakes are much higher than those determined in other parts of argan fruits, such as argan nut shell (67-73%) and pulp (59-67%) (El Kourdi et al., 2024; Rahib et al., 2020), as well as in other biomasses such as olive residues (60.2%), almond shell (69%), oil palm trunk (80%), oil palm fronds (79%), oil palm shell (73%), oil palm roots (68%), oil palm decanter cake (72%), empty fruit bunches (79%), oil palm fibre (75%), and oil palm sewage sludge (52%) (Shrivastava et al., 2021; Vassilev et al., 2010).

In addition, BAC, WAC, and PAC showed moderate AC (3.8%, 3.3%, and 4.2%, respectively), which are comparable to other waste biomasses deriving from argan fruits (Rahib et al., 2020). Even though the three cakes exhibited similar AC, their mean percentage contents were statistically different, with the highest value found in PAC samples, in agreement with the mechanical production method, which gave rise to a more deoiled and less wet argan cake. The quite low AC found in the three kinds of argan cakes indicates the suitability of these biomasses for their thermal conversion via pyrolysis or gasification (Ulusal et al., 2021), minimizing the risk of slagging and fouling, which can be very problematic in thermal conversion processes (Rago et al., 2018). It should also be noted that a low-ash biomass is better suited for energy recovery since it results in an increased yield of bio-oil (Déniel et al., 2016). In addition, a feedstock with low AC can result in a biochar that meets the European limit for materials intended to be used for water treatment (15%) even with yields as low as 30%, which are quite commonly obtained during slow pyrolysis processes (Castiglioni et al., 2022).

In pyrolysis processes, FC content represents the portion of biomass that cannot be converted into gases or vapours, resulting in the production of biochar. Therefore, in order to achieve a substantial biochar yield during pyrolysis, it is advisable to use biomass with a high FC content (Shrivastava et al., 2021). FC of argan cakes was in the order PAC > BAC > WAC, with the three values statistically different from each other, thus pointing out the better characteristics of PAC also for this parameter.

Table II-1: Values of pH, proximate (M, VM, AC, FC) and elemental (C, H, N, S, O) analyses, and energy potential (BR, HHV, LHV) of black argan press cake (BAC), white argan press cake (WAC), and pellet argan cake (PAC).

	BAC	**WAC**	**PAC**
pH	5.4 ± 0.7^{a}	5.4 ± 0.3^{a}	6.9 ± 0.8^{b}
Proximate analysis			
Moisture (%)	3.3 ± 0.1^{a}	2.60 ± 0.09^{b}	1.50 ± 0.06^{c}
Volatile matter (%)	88.8 ± 0.1^{a}	90.8 ± 0.3^{b}	85.9 ± 0.2^{c}
Ash content (%)	3.82 ± 0.03^{a}	3.29 ± 0.04^{b}	4.19 ± 0.01^{c}
Fixed carbon (%)	4.03 ± 0.06^{a}	3.26 ± 0.08^{b}	8.4 ± 0.2^{c}
Elemental analysis			
Carbon (%)	55 ± 1^{a}	61.3 ± 0.2^{b}	52 ± 3^{a}
Hydrogen (%)	7.72 ± 0.05^{a}	8.7 ± 0.5^{a}	7 ± 1^{a}
Nitrogen (%)	5.3 ± 0.7^{a}	5.3 ± 0.3^{a}	6.0 ± 0.4^{a}
Sulfur (%)	0.28 ± 0.05^{a}	0.28 ± 0.02^{a}	0.32 ± 0.02^{a}
Oxygen (%)	28 ± 3^{a}	21 ± 1^{b}	30 ± 3^{a}
Energy potential			
Burning rate (g/s)	0.27 ± 0.01^{a}	0.35 ± 0.03^{b}	0.29 ± 0.01^{a}
Higher heating value (MJ/kg)	25.50 ± 0.07^{a}	26.97 ± 0.09^{b}	24.40 ± 0.06^{c}
Lower heating value (MJ/kg)	23.80 ± 0.07^{a}	25.04 ± 0.09^{b}	22.78 ± 0.06^{c}

Elemental analysis pointed out significantly different contents in carbon and oxygen among the three cakes, while the difference observed for the other elements resulted statistically insignificant. In particular, WAC was the residue that showed the highest and lowest values for carbon (61%) and oxygen (21%), respectively. Overall, the three biomasses contained high percentages of carbon (52-61%), which were comparable to values found in agricultural waste, woody biomass, and forest residues (50-54%) (Castiglioni et al., 2022; Cavalaglio et al., 2020; Ghesti et al., 2022). The predominance of carbon and oxygen in the cakes was also highlighted by SEM-EDX analysis (**Figure II-2**), which is in accordance with the large amounts of lignin and cellulose reported elsewhere as the main components of these residues (Ifguis et al., 2022).

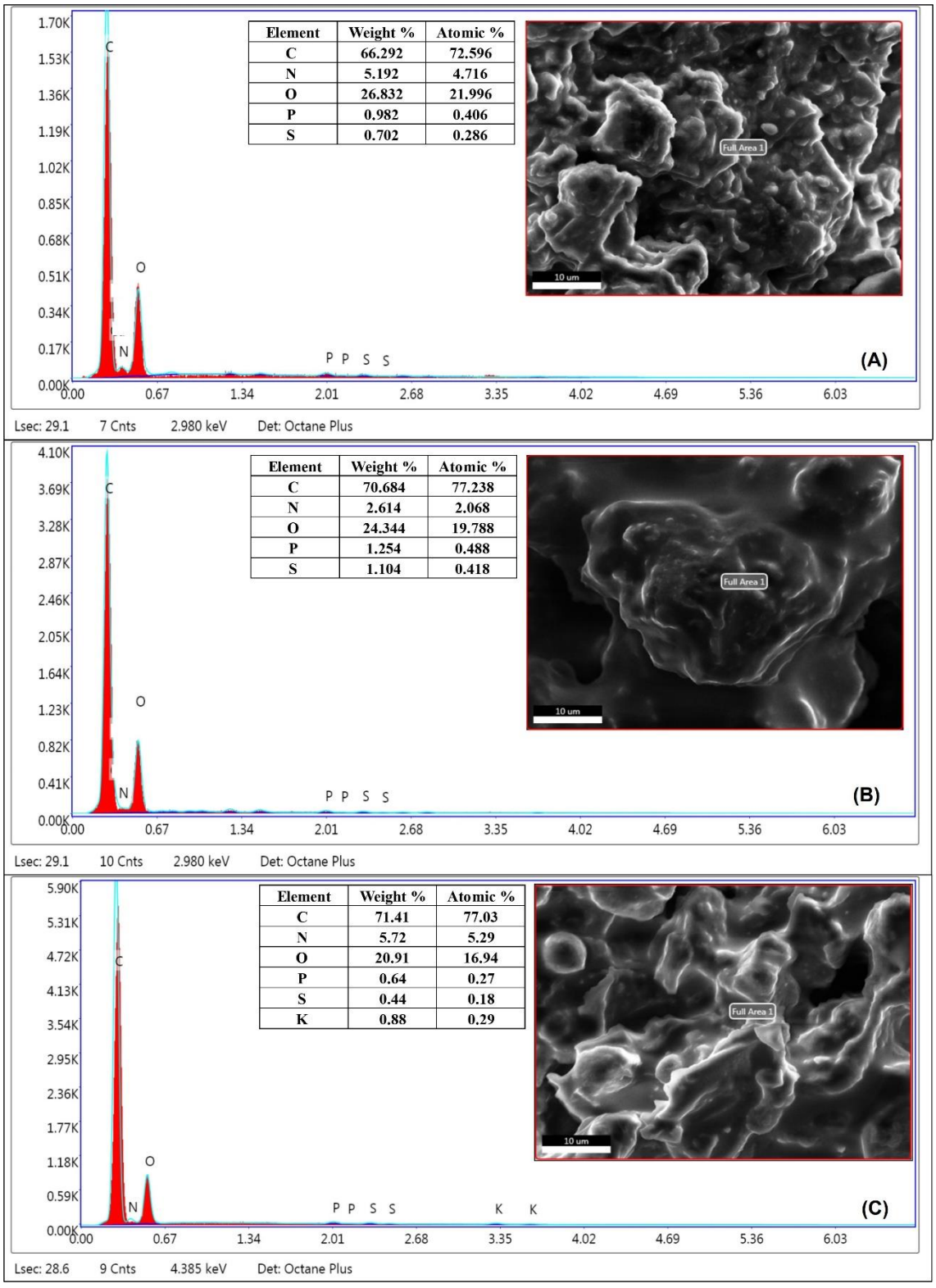

Figure II-2: SEM-EDX mapping of (A) BAC, (B) WAC, and (C) PAC.

Elemental analysis provides interesting information about the conversion of biomass into biofuels and biochar (Yang et al., 2015a). For example, a large carbon content gives an early indication of the high quality of biochar that can be produced from this feedstock (El Barkaoui et al., 2023),

while the high carbon and hydrogen percentages are an index of good biochar yields (Saeed et al., 2019). Moreover, the low nitrogen and sulphur contents translate into reduced potential for the release of nitrogen and sulphur oxides (NOx and SO_2) during direct combustion of the biomass, resulting in a lower environmental impact (Rabichi et al., 2024).

XRF analysis (**Figure II-3**) provided very similar spectra for the three argan cakes, thus pointing out almost the same composition in terms of inorganic fraction, which was mainly constituted by K and Ca, while other elements such as S, Cl, and P, and especially some metals (i.e., Mn, Fe, Cu, and Zn) gave rise to much lower signals.

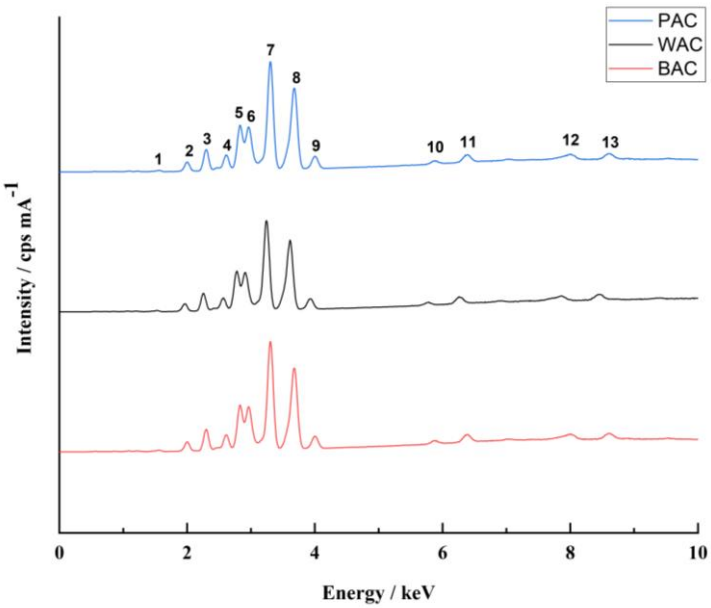

Figure II-3: X-ray fluorescence spectrum of PAC, WAC, and BAC. Peaks 1, 5, and 6 were present as background signals in the absence of samples. The other peaks were attributed to the following elements: 2 (P), 3 (S), 4 (Cl), 7 (K), 8 and 9 (Ca), 10 (Mn), 11 (Fe), 12 (Cu), 13 (Zn).

3.2. Biomass energy potential and thermal degradation

To assess the viability and conduct a technical evaluation of biomass energy, it is essential to ascertain the HHV and LHV of biomass fuels, cause when purchasing biomass fuels, payment should be based on energy content ($/MJ) (Rabichi et al., 2024). HHV and LHW are obviously influenced by the composition of the biomass, a high C and H content being favorable to their increase and a high O content having the opposite effect (Saidur et al., 2011). The calorific values (HHV and LHV) of the three residue types are shown in **Table II-1**. WAC showed the highest HHV (27.0 ± 0.09 MJ/kg), followed by BAC (25.5 ± 0.07 MJ/kg) and PAC (24.4 ± 0.06 MJ/kg),

with the three values found to be statistically different. The energy content of the three types of cake should be considered high when compared to HHV data reported for many plant wastes, such as cardoon, grapevine pruning, avocado tone, olive pruning, peanut shells, pine pellets, almond shells, and turkey oak (14 - 20 MJ/kg) (Déniel et al., 2016; El Barkaoui et al., 2023; Ghesti et al., 2022; Yang et al., 2015b), indicating the argan cakes as an interesting biofuel. As expected on the basis of equation 1, LHV followed the same trend of HHV, with values of 25.0 ± 0.09, 23.8 ± 0.07, and 22.8 ± 0.06 MJ/kg for WAC, BAC, and PAC, respectively. Interestingly, these values were higher than those reported in the literature for other biomasses, which were less than 20 MJ/kg (El Kourdi et al., 2024; Ezealigo et al., 2023; Rabichi et al., 2024).

Similar to the results for HHV and LHV, WAC also showed higher values for BR (0.35 g/s), compared with PAC (0.29 g/s) and BAC (0.27 g/s). Comparison with the literature showed higher values for BR than for other biomasses; for example, Kuhe et al., (2021) reported that the BR of the millet husk ranged between 0.09 g/s and 0.18 g/s, depending on particle size, binder concentration, and compaction pressure.

TGA and DTG are useful for understanding the thermal behaviour of raw materials under heating in an inert environment and for selecting the optimal pyrolysis temperature of biochar (García-Ibañez et al., 2006). Studying the thermal decomposition of biomass, particularly complex materials such as lignocellulosic substances (e.g., BAC, WAC, PAC, and plant biomass in general), which have multiple components and degrade through complicated processes, may indicate their suitability for producing biofuel or biochar. TGA and DTG curves of the studied biomasses are shown in **Figures II-4A and II-4B**, respectively. TGA and DTG curves showed that the three argan cakes were degraded in three steps, consistently with literature findings reported for other biomasses (Gómez et al., 2016; Suliman et al., 2016). The three steps of decomposition included (1) dehydration/drying (80 – 100 °C), which is characterized by a slight mass loss, due to the release of the inherently bound light volatile portion and moisture; (2) devolatilization (150 – 450 °C), which is mainly associated to the pyrolysis of holocellulose, characterized by a greater weight loss. The relatively high temperatures in this step led to the degradation of holocellulose and the transformation of high molecular-weight compounds in smaller molecular-weight pyrolysis products; (3) lignin depolymerization, occurring above 450 °C, resulted in a gradually decreasing weight loss rate until their stabilization at about 25%, 27%, and 32% of the original weight, for WAC, BAC, and PAC, respectively (**Figure II-4A**) (Khiari et al., 2021). The significant volatile release starts at about 150 °C and reaches its peak at around

450 °C, where WAC and BAC showed high and very similar total mass losses (75% and 73%, respectively), while for PAC, the weight loss was lower (68%) (**Figure II-4A**). This result may be due to the PAC preparation conditions, which exploit the mechanical pressing method, leading to a more compact structure.

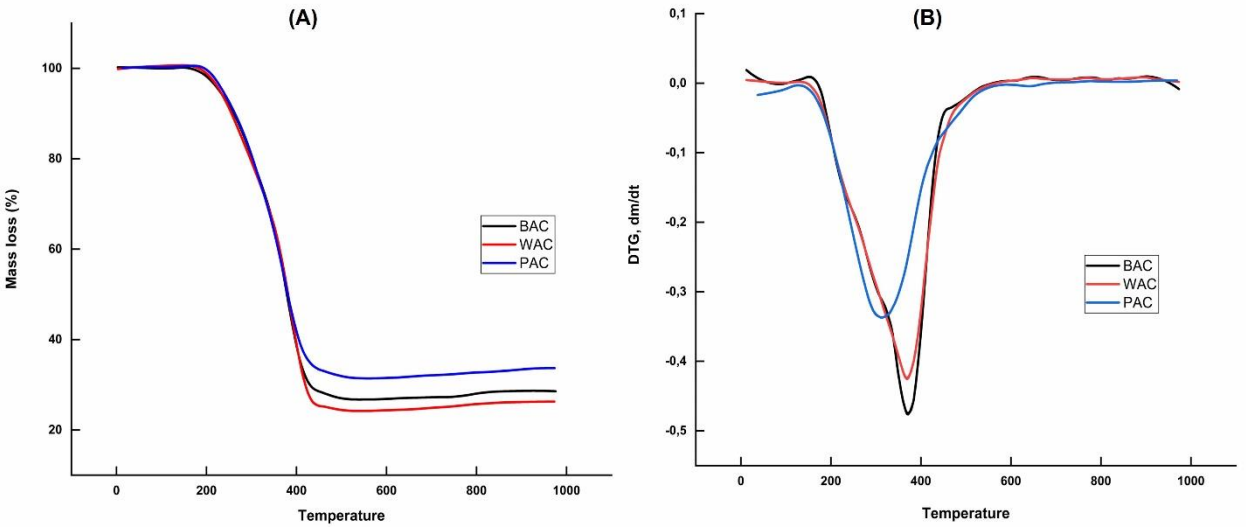

Figure II-4: Thermogravimetric analysis (A) and derivative thermogravimetry (B) curves of PAC, BAC, and WAC.

3.3. Structural and morphological characterisation

The structural and morphological characterisation of the argan cakes under investigation was performed by FTIR (**Figure II-5**), XRD (**Figure II-6**), and SEM (**Figure II-2**) analyses.

The FTIR spectra of the three argan cakes were found to be very similar, in agreement with the same type of raw material from which they are derived. The three spectra, in fact, showed strong bands attributable to the stretching vibrations of the hydroxyl groups (O-H) of the alcohols/phenols, strong bands associated with the stretching of the (C-O) stretching vibration of the ethers or alcohols, and carbonyl groups (C=O) (Mokhati et al., 2021). In detail, the most intense band found in the higher energy region, at about 3444 cm^{-1}, is due to a large amount of OH groups in the carbohydrates and secondary phenolic metabolites, as well as in the adsorbed water (El-Nabarawy et al., 1997). The band at 2923 cm^{-1} corresponds to (C-H) vibrations in aliphatic stretching, indicating the presence of cellulose, hemicellulose, and lignin (Sahoo et al., 2022). The band appearing at 1650 cm^{-1} could be attributed to the aromatic bonds (C=C) (Bouchelta et al., 2008). The presence of a peak at 1390-1400 cm^{-1} could be assigned to (C-O) vibrations in carboxylate groups (Ji et al., 2007). The peak detected at 1087 cm^{-1} may be related

to the stretching of C–O due to the presence of lignin and polysaccharides (Mokhati et al., 2022; Sahoo et al., 2022). The lower energy band located at about 600-620 cm^{-1} was associated with the C–H out of plane twisting due to the presence of sugars like β-D fructose, galactan, and arabinan (Ji et al., 2007; Sahoo et al., 2022). Similar identifications for FTIR spectra are reported in the literature (Sahoo et al., 2021; Ulusal et al., 2021; Uzoagba et al., 2024). The FTIR results suggest that there are suitable functional groups (carboxylates and/or alcohols and/or phenols) in all biomasses that could be preserved during biochar production at low pyrolysis temperatures, thus enabling a long-term heavy metal removal strategy from contaminated waters (Saeed et al., 2019).

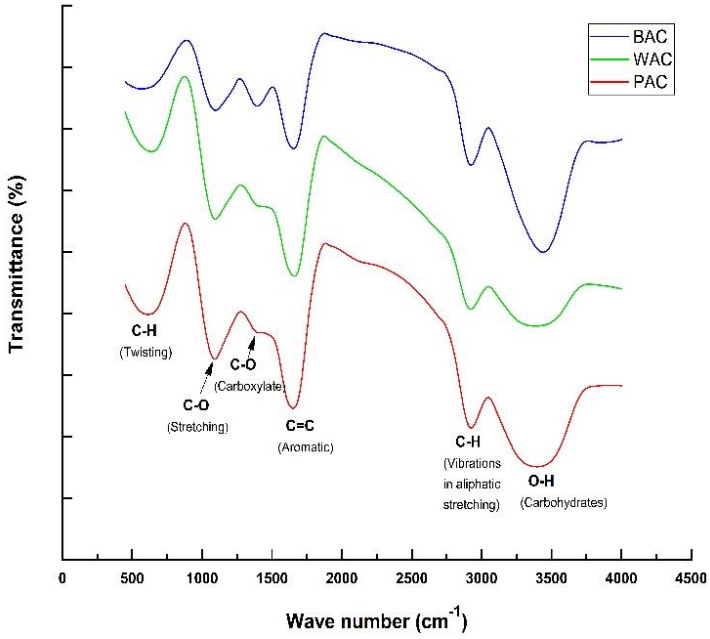

Figure II-5: FT-IR Spectra of PAC, BAC, and WAC.

Mineralogical characterisation of the studied raw materials was performed by XRD analysis (**Figure II-6**). The XRD patterns showed similar profiles for BAC, WAC, and PAC, with a difference in intensity depending on the cellulose content in the biomass material. The XRD diffractograms are characterised by the presence of a broad and intense peak at $2\theta = 19.66°$ and a small peak at 38.24°, which indicates the presence of amorphous hemicellulose and cellulose. The broad peak is typical of the disordered regions within the cellulose fibre and the amorphous nature of the lignin and hemicellulose (Uzoagba et al., 2024). However, WAC exhibited higher degrees of crystallinity (73%), followed by BAC (72%) and PAC (65%), which may be due to the presence of higher crystallised cellulose in the atrium (Saeed et al., 2019). Moreover, cellulose crystallinity has a significant effect on the thermal degradation behaviour, while the thermal degradation temperature decreases due to lower crystallinity (Sahoo et al., 2022). Confirming the TGA results

(**Figure II-4A**) for the three biomasses, which illustrates the higher total mass loss WAC (75%), followed by BAC (73%); however, PAC showed the lowest weight loss (68%). Some literature has pointed out that biomass crystallinity is based on waxy substances. It has also been considered that crystalline cellulose produces less gas and char than amorphous cellulose, which contributes less to levoglucosan during pyrolysis (Sahoo et al., 2022).

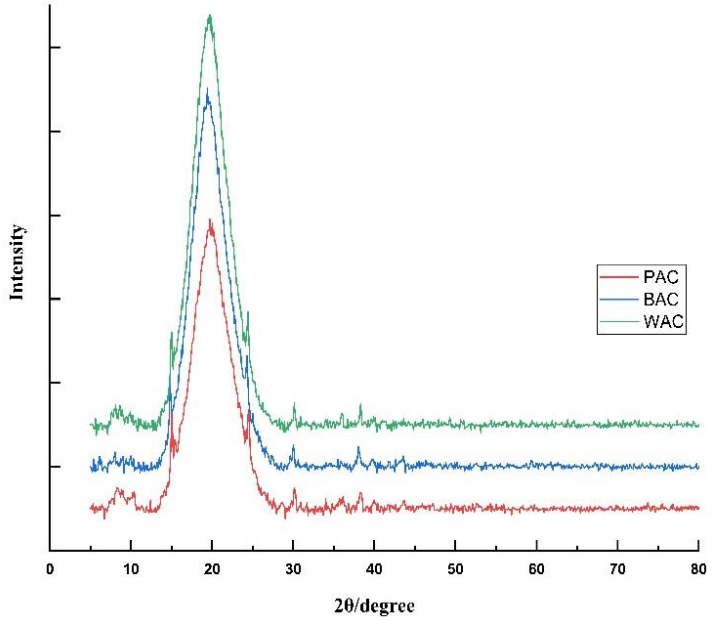

Figure II-6: XRD diffractogram of PAC, BAC, and WAC.

SEM is an essential technique for examining the micro-scale and nano-scale behaviours of biomasses. **Figure II-2** shows representative SEM images of BAC, PAC, and WAC. The latter exhibits a predominance of large particles with heterogeneous geometry, with uniform sizes and smooth outer surfaces. Conversely, BAC and PAC exhibit an irregular shape and porous structure, resulting in a much lower apparent density (Hakeem et al., 2015), which could enable the production of biochar with a porous surface.

Conclusion

This study compares, for the first time, the characteristics of three different types of argan residues (i.e., BAC, WAC, and PAC) as potential sources of energy and bio-based materials, providing crucial information on their usability as biofuels or biochars. The results indicate that the three types of biomass, and in particular WAC, possess excellent characteristics for their direct use as fuel and/or for the production of biochar and biofuel. In fact, these residues showed a high content of carbon, volatile matter, and calorific value, and a low content of ash and moisture, confirming

their suitability as efficient sources for the production of fuel and biochar. The calorific value and combustion rate of argan residues, higher than other residues, underline the potential utility of these biomasses as biofuels. Furthermore, previous studies indicated that biofuels produce less carbon monoxide, particulate matter, and volatile organic compounds than traditional fuels, thus suggesting their significant role in cleaner energy production in the next future. However, challenges remain in using biofuels, such as the increased nitrogen oxide emissions compared to the first-generation hydrocarbon biofuels. However, blending biofuels with first generation fuels can address these issues and contribute to obtain a cleaner energy (Khan et al., 2021).

Thermal analysis showed that the three biomasses exhibit a reactive behaviour during the pyrolysis processes, which ends around 450°C, without further changes up to temperatures of about 1000°C, suggesting the possibility of converting argan cakes into biochar at relatively low temperatures, obtaining a very robust material that at the same time maintains a surface functionalization suitable for the adsorption of organic and/or inorganic micropollutants. SEM images also supported this possible application. In fact, argan cakes resulted inhomogeneous raw materials characterized by high roughness and are probably prone to form porous structures during the pyrolysis process, functional to the use of biochar as an adsorbent in wastewater treatment.

References

Ayadi, M., Passaseo, D., Bonaccorso, G., Fichera, M., Renai, L., Venturini, L., Colzi, I., Fibbi, D., Del Bubba, M., 2024. Biochar from co-pyrolysis of biological sludge and sawdust in comparison with the conventional filling media of vertical-flow constructed wetlands for the treatment of domestic-textile wastewater. Water Sci. Technol. 89, 1252–1263. https://doi.org/10.2166/wst.2024.056

Babty, F., Hachim, A., Mourabit, M., Mordane, S., Bettachy, A., Assyry, A. El, Derouiche, A., 2021. Study of the swelling of a composite based on argan nut, urea-formaldehyde and water as a non-polluting solvent. Rev. des Compos. des Mater. Av. 31, 297–300. https://doi.org/10.18280/rcma.310505

Bahani, N., El Kourdi, S., Abderafi, S., 2024. Argan Cake Oil Transesterification Kinetics and an Optimized Choice of a High-Performance Catalyst for Biodiesel Production. Waste and Biomass Valorization 15, 2591–2610. https://doi.org/10.1007/s12649-023-02315-0

Bakari, Z., Fichera, M., El Ghadraoui, A., Renai, L., Giurlani, W., Santianni, D., Fibbi, D., Bruzzoniti, M.C., Del Bubba, M., 2024. Biochar from co-pyrolysis of biological sludge and woody waste followed by chemical and thermal activation: end-of-waste procedure for sludge management and biochar sorption efficiency for anionic and cationic dyes. Environ. Sci. Pollut. Res. 31, 35249–35265. https://doi.org/10.1007/s11356-024-33577-3

Bini, L., Renai, L., Fichera, M., Petrucci, W.A., Lenzi, A., Biricolti, S., Giordani, E., Rivoira, L., Bruzzoniti, M.C., Piesik, D., Del Bubba, M., 2024. Assessing the Impact of Sustainable Biochar-Enriched Substrates on Safety and Quality of Tomato (Solanum lycopersicum L.) as Relevant Model Crop. ACS Agric. Sci. Technol. 4, 681–689. https://doi.org/10.1021/acsagscitech.3c00589

Bouchelta, C., Medjram, M.S., Bertrand, O., Bellat, J.P., 2008. Preparation and characterization of activated carbon from date stones by physical activation with steam. J. Anal. Appl. Pyrolysis 82, 70–77. https://doi.org/10.1016/j.jaap.2007.12.009

Bourhim, T., Villareal, M.O., Gadhi, C., Isoda, H., 2021. Elucidation of Melanogenesis-Associated Signaling Pathways Regulated by Argan Press Cake in B16 Melanoma Cells. Nutrients 13, 2697. https://doi.org/10.3390/nu13082697

Castiglioni, M., Rivoira, L., Ingrando, I., Meucci, L., Binetti, R., Fungi, M., El-Ghadraoui, A., Bakari, Z., Del

Bubba, M., Bruzzoniti, M.C., 2022. Biochars intended for water filtration: A comparative study with activated carbons of their physicochemical properties and removal efficiency towards neutral and anionic organic pollutants. Chemosphere 288, 132538. https://doi.org/10.1016/j.chemosphere.2021.132538
Cavalaglio, G., Cotana, F., Nicolini, A., Coccia, V., Petrozzi, A., Formica, A., Bertini, A., 2020. Characterization of Various Biomass Feedstock Suitable for Small-Scale Energy Plants as Preliminary Activity of Biocheaper Project. Sustainability 12, 6678. https://doi.org/10.3390/su12166678
Charrouf, Z., Guillaume, D., 1999. Ethnoeconomical, ethnomedical, and phytochemical study of Argania spinosa (L.) Skeels. J. Ethnopharmacol. 67, 7–14. https://doi.org/10.1016/S0378-8741(98)00228-1
Charrouf, Z., Hilali, M., Jauregui, O., Soufiaoui, M., Guillaume, D., 2007. Separation and characterization of phenolic compounds in argan fruit pulp using liquid chromatography–negative electrospray ionization tandem mass spectroscopy. Food Chem. 100, 1398–1401. https://doi.org/10.1016/j.foodchem.2005.11.031
Déniel, M., Haarlemmer, G., Roubaud, A., Weiss-Hortala, E., Fages, J., 2016. Optimisation of bio-oil production by hydrothermal liquefaction of agro-industrial residues: Blackcurrant pomace (Ribes nigrum L.) as an example. Biomass and Bioenergy 95, 273–285. https://doi.org/10.1016/j.biombioe.2016.10.012
El-Nabarawy, T., Petro, N.S., Abdel-Aziz, S., 1997. Adsorption Characteristics of Coal-based Activated Carbons. II. Adsorption of Water Vapour, Pyridine and Benzene. Adsorpt. Sci. Technol. 15, 47–57. https://doi.org/10.1177/026361749701500105
El Barkaoui, S., Mandi, L., Aziz, F., Del Bubba, M., Ouazzani, N., 2023. A critical review on using biochar as constructed wetland substrate: Characteristics, feedstock, design and pollutants removal mechanisms. Ecol. Eng. 190, 106927. https://doi.org/10.1016/j.ecoleng.2023.106927
El Kourdi, S., Chaabane, A., Abderafi, S., Abbassi, M.A., 2024. Valorizing argan residues into biofuels and chemicals through slow pyrolysis. Results Eng. 21, 101659. https://doi.org/10.1016/j.rineng.2023.101659
El Monfalouti, H., 2013. Contribution a La Determination Des Proprietes Photo- Protectrices Et Anti-Oxydantes Des Derives De L'Arganier: Etudes Chimiques Et Physiologiques. Sci. York.
Ezealigo, U.S., Ezealigo, B.N., Plaza, M.G., Dim, E.N., Kemausuor, F., Achenie, L.E.K., Onwualu, A.P., 2023. Preliminary characterisation and valorisation of Ficus benjamina fruits for biofuel application. Biomass Convers. Biorefinery 13, 12643–12654. https://doi.org/10.1007/s13399-021-02230-1
Folayan, A.J., Anawe, P.A.L., 2019. Synthesis and characterization of Argania spinosa (Argan oil) biodiesel by sodium hydroxide catalyzed transesterification reaction as alternative for petro-diesel in direct injection, compression ignition engines. Heliyon 5, e02427. https://doi.org/10.1016/j.heliyon.2019.e02427
Gao, Y., Wang, M., Raheem, A., Wang, F., Wei, J., Xu, D., Song, X., Bao, W., Huang, A., Zhang, S., Zhang, H., 2023. Syngas Production from Biomass Gasification: Influences of Feedstock Properties, Reactor Type, and Reaction Parameters. ACS Omega 8, 31620–31631. https://doi.org/10.1021/acsomega.3c03050
García-Ibañez, P., Sánchez, M., Cabanillas, A., 2006. Thermogravimetric analysis of olive-oil residue in air atmosphere. Fuel Process. Technol. 87, 103–107. https://doi.org/10.1016/j.fuproc.2005.08.005
Gharby, S., Charrouf, Z., 2022. Argan Oil: Chemical Composition, Extraction Process, and Quality Control. Front. Nutr. 8, 1–10. https://doi.org/10.3389/fnut.2021.804587
Ghesti, G.F., Silveira, E.A., Guimarães, M.G., Evaristo, R.B.W., Costa, M., 2022. Towards a sustainable waste-to-energy pathway to pequi biomass residues: Biochar, syngas, and biodiesel analysis. Waste Manag. 143, 144–156. https://doi.org/10.1016/j.wasman.2022.02.022
Gómez, N., Rosas, J.G., Cara, J., Martínez, O., Alburquerque, J.A., Sánchez, M.E., 2016. Slow pyrolysis of relevant biomasses in the Mediterranean basin. Part 1. Effect of temperature on process performance on a pilot scale. J. Clean. Prod. 120, 181–190. https://doi.org/10.1016/j.jclepro.2014.10.082
Hakeem, K.R., Jawaid, M., Alothman, O.Y., 2015. Agricultural Biomass Based Potential Materials. Agric. Biomass Based Potential Mater. 1–505. https://doi.org/10.1007/978-3-319-13847-3
Ifguis, O., Bouhdadi, R., Ziat, Y., George, B., Mbarki, M., 2022. Characterization and Analysis of Argania spinosa Shells from Souss-Massa Area: Application in the Adsorption of Methylene Blue in Aqueous Solution. J. Nanomater. 2022, 1–14. https://doi.org/10.1155/2022/6403838
Ji, Y., Li, T., Zhu, L., Wang, X., Lin, Q., 2007. Preparation of activated carbons by microwave heating KOH activation. Appl. Surf. Sci. 254, 506–512. https://doi.org/10.1016/j.apsusc.2007.06.034
Khan, M.A.H., Bonifacio, S., Clowes, J., Foulds, A., Holland, R., Matthews, J.C., Percival, C.J., Shallcross, D.E., 2021. Investigation of Biofuel as a Potential Renewable Energy Source. Atmosphere (Basel). 12, 1289. https://doi.org/10.3390/atmos12101289
Khiari, B., Ibn Ferjani, A., Azzaz, A.A., Jellali, S., Limousy, L., Jeguirim, M., 2021. Thermal conversion of flax shives through slow pyrolysis process: in-depth biochar characterization and future potential use. Biomass Convers. Biorefinery 11, 325–337. https://doi.org/10.1007/s13399-020-00641-0
Kuhe, A., Terhemba, A.V., Iortyer, H., 2021. Biomass valorization for energy applications: A preliminary study on millet husk. Heliyon 7, e07802. https://doi.org/10.1016/j.heliyon.2021.e07802
Lybbert, T.J., Magnan, N., Aboudrare, A., 2010. Household and local forest impacts of Morocco's argan oil bonanza. Environ. Dev. Econ. 15, 439–464. https://doi.org/10.1017/S1355770X10000136

Mokhati, A., Benturki, O., Benturki, A., Fennouh, R., Kecira, Z., Bernardo, M., Matos, I., Lapa, N., Ventura, M., Soares, O.S.G.P., Do Rego, A.M.B., Fonseca, I., 2022. Conversion of Argan Nutshells into Novel Porous Carbons in the Scope of Circular Economy: Adsorption Performance of Emerging Contaminants. Appl. Sci. 12, 7607. https://doi.org/10.3390/app12157607

Mokhati, A., Benturki, O., Bernardo, M., Kecira, Z., Matos, I., Lapa, N., Ventura, M., Soares, O.S.G.P., do Rego, A.M.B., Fonseca, I.M., 2021. Nanoporous carbons prepared from argan nutshells as potential removal agents of diclofenac and paroxetine. J. Mol. Liq. 326, 115368. https://doi.org/10.1016/j.molliq.2021.115368

Muigai, H.H., Bordoloi, U., Hussain, R., Ravi, K., Moholkar, V.S., Kalita, P., 2021. A comparative study on synthesis and characterization of biochars derived from lignocellulosic biomass for their candidacy in agronomy and energy applications. Int. J. Energy Res. 45, 4765–4781. https://doi.org/10.1002/er.6092

Oubannin, S., Bijla, L., Gagour, J., Hajir, J., Aabd, N.A., Sakar, E.H., Salama, M.A., Gharby, S., 2022. A comparative evaluation of proximate composition, elemental profiling and oil physicochemical properties of black cumin (Nigella sativa L.) seeds and argan (Argania spinosa L. Skeels) kernels. Chem. Data Collect. 41, 100920. https://doi.org/10.1016/j.cdc.2022.100920

ÖzyuğUran, A., Yaman, S., 2017. Prediction of Calorific Value of Biomass from Proximate Analysis. Energy Procedia 107, 130–136. https://doi.org/10.1016/j.egypro.2016.12.149

Rabichi, I., Yaacoubi, F.E., Ennaciri, K., Sekkouri, C., Bacaoui, A., Yaacoubi, A., 2024. Transforming olive-processed waste and almond shells into high-quality Biofuels: a comprehensive development and evaluation approach. Energy Sources, Part A Recover. Util. Environ. Eff. 46, 8671–8685. https://doi.org/10.1080/15567036.2024.2374747

Rago, Y.P., Surroop, D., Mohee, R., 2018. Assessing the potential of biofuel (biochar) production from food wastes through thermal treatment. Bioresour. Technol. 248, 258–264. https://doi.org/10.1016/j.biortech.2017.06.108

Rahib, Y., Sarh, B., Bostyn, S., Bonnamy, S., Boushaki, T., Chaoufi, J., 2020. Non-isothermal kinetic analysis of the combustion of argan shell biomass. Mater. Today Proc. 24, 11–16. https://doi.org/10.1016/j.matpr.2019.07.437

Saeed, A.A.H., Harun, N.Y., Nasef, M.M., 2019. Physicochemical Characterization of Different Agricultural Residues in 2, 10–22.

Sahoo, A., Kumar, S., Mohanty, K., 2022. A comprehensive characterization of non-edible lignocellulosic biomass to elucidate their biofuel production potential. Biomass Convers. Biorefinery 12, 5087–5103. https://doi.org/10.1007/s13399-020-00924-6

Sahoo, S.S., Vijay, V.K., Chandra, R., Kumar, H., 2021. Production and characterization of biochar produced from slow pyrolysis of pigeon pea stalk and bamboo. Clean. Eng. Technol. 3, 100101. https://doi.org/10.1016/j.clet.2021.100101

Saidur, R., Abdelaziz, E.A., Demirbas, A., Hossain, M.S., Mekhilef, S., 2011. A review on biomass as a fuel for boilers. Renew. Sustain. Energy Rev. 15, 2262–2289. https://doi.org/10.1016/j.rser.2011.02.015

Shrivastava, P., Khongphakdi, P., Palamanit, A., Kumar, A., Tekasakul, P., 2021. Investigation of physicochemical properties of oil palm biomass for evaluating potential of biofuels production via pyrolysis processes. Biomass Convers. Biorefinery 11, 1987–2001. https://doi.org/10.1007/s13399-019-00596-x

Suliman, W., Harsh, J.B., Abu-Lail, N.I., Fortuna, A.-M., Dallmeyer, I., Garcia-Perez, M., 2016. Influence of feedstock source and pyrolysis temperature on biochar bulk and surface properties. Biomass and Bioenergy 84, 37–48. https://doi.org/10.1016/j.biombioe.2015.11.010

Ulusal, A., Apaydın Varol, E., Bruckman, V.J., Uzun, B.B., 2021. Opportunity for sustainable biomass valorization to produce biochar for improving soil characteristics. Biomass Convers. Biorefinery 11, 1041–1051. https://doi.org/10.1007/s13399-020-00923-7

Uzoagba, C.E.J., Okoroigwe, E., Kadivar, M., Anye, V.C., Bello, A., Ezealigo, U., Odette Ngasoh, F., Pereira, H., Azikiwe Onwualu, P., 2024. Characterization of Wood, Leaves, Barks, and pod wastes from Prosopis africana biomass for biofuel production. Waste Manag. Bull. 2, 172–182. https://doi.org/10.1016/j.wmb.2024.07.007

Vassilev, S. V., Baxter, D., Andersen, L.K., Vassileva, C.G., 2010. An overview of the chemical composition of biomass. Fuel 89, 913–933. https://doi.org/10.1016/j.fuel.2009.10.022

Yang, L., Lu, M., Carl, S., Mayer, J.A., Cushman, J.C., Tian, E., Lin, H., 2015a. Biomass characterization of Agave and Opuntia as potential biofuel feedstocks. Biomass and Bioenergy 76, 43–53. https://doi.org/10.1016/j.biombioe.2015.03.004

Yang, L., Lu, M., Carl, S., Mayer, J.A., Cushman, J.C., Tian, E., Lin, H., 2015b. Biomass characterization of Agave and Opuntia as potential biofuel feedstocks. Biomass and Bioenergy 76, 43–53. https://doi.org/10.1016/j.biombioe.2015.03.004

Zeghlouli, J., Schiavone, N., Askanian, H., Guendouz, A., El Modafar, C., Michaud, P., Delattre, C., 2023. Thermal, Morphological and Mechanical Properties of a BioPE Matrix Composite: Case of Shell, Pulp,

and Argan Cake as Biofillers. Materials (Basel). 16, 2241. https://doi.org/10.3390/ma16062241

II-II. Valorization of olive and argan wastes into optimized biochar for efficient methylene blue adsorption.

This work was published as a research paper:

El Barkaoui, S., Mandi, L., Rabichi, I., Del Bubba, M., Isari, E.A., Kalavrouziotis, I.K., & Ouazzani, N. (2025). Valorization of olive and argan wastes into optimized biochar for efficient methylene blue adsorption. Environ. Process. 12, 57. https://doi.org/10.1007/s40710-025-00801-2.

Abstract

The objective of this study was to optimize the production of biochar (BC) from agricultural waste by evaluating the impact of biomass type and pyrolysis conditions on the physicochemical properties and adsorption performance in wastewater treatment. Four feedstocks, de-oiled olive mill waste (DOW), pellet argan cake (PAC), white argan press cake (WAC), and black argan press cake (BAC), were pyrolyzed at 600, 700, and 800 °C for a period of two hours with a heating rate of 2 °C/min. The resulting biochars were characterized using proximate and elemental analyses, FT-IR, XRD, SEM-EDX, and BET surface area measurements. Adsorption capacity was evaluated through methylene blue (MB) batch tests. Increasing the pyrolysis temperature increased the carbon content, fixed carbon, and thermal stability but decreased the yield, moisture content, and volatile matter. Structural analyses confirmed significant changes in crystallinity, porosity, and functional groups. MB adsorption increased with temperature. DOW-derived biochar consistently outperformed argan-derived biochar. The DOW sample produced at 800 °C exhibited the highest yield (31–33%), surface area (22 m^2/g), thermal stability (0.66–0.68), and adsorption capacity (432 mg/g). Statistical modelling validated the experimental outcomes ($R^2 > 0.96$). Overall, both the type of feedstock and the pyrolysis temperature strongly influenced the properties of the biochar. DOW-derived biochar produced at 800 °C was the optimal material, offering high adsorption efficiency and robust physicochemical quality. It represents a promising, low-cost adsorbent for wastewater treatment applications.

Keywords: Biochar optimization; Olive mill waste; Argan press cake; Pyrolysis conditions; Methylene blue adsorption; Wastewater treatment

1. Introduction

Climate change is a global challenge that exacerbates water insecurity by amplifying pollution, scarcity, and stress to ecosystems (Dabare et al., 2025; Šarović and Klaić, 2023; Stamou et al., 2024). One of the most pressing concerns is the growing contamination of aquatic environments by organic and emerging pollutants, such as dyes, pharmaceuticals, and phenolic compounds. These chemicals are carried by wastewater, which threatens the quality of both surface and groundwater resources (Bracamontes-Ruelas et al., 2022; Gadipelly et al., 2014). Conventional treatment plants often fail to efficiently remove such contaminants, and traditional filters (e.g., sand, soil, and gravel) are also ineffective, highlighting the need for alternative materials and treatment approaches (El Barkaoui et al., 2025a).

Biochar (BC) has emerged as a promising adsorbent due to its high surface area, porosity, and functional groups that facilitate pollutant retention (El Barkaoui et al., 2023; El Barkaoui et al., 2025b; Nautiyal et al., 2017). Recent reviews confirm its potential for dye and micropollutant removal but also highlight significant variability in performance depending on feedstock and pyrolysis parameters (Hamieh et al., 2024; Haris et al., 2024; Nawaz et al., 2023). Higher

pyrolysis temperatures (>500 °C) generally enhance carbon content, aromatization, and porosity, thereby improving adsorption of hydrophobic organic molecules and cationic dyes, though often at the expense of yield (Nawaz & Razzak, 2025; Chafi et al., 2025; Mahdi et al., 2017). Systematic optimization is therefore essential, yet many studies still rely on single-point experiments without robust design approaches, limiting comparability across studies (Hamieh et al., 2024; Haris et al., 2024).

With regard to feedstocks, olive mill wastes have been extensively studied in Europe and the Mediterranean basin, showing high potential for dye removal. For instance, Chafi et al. (2025) achieved almost complete methylene blue (MB) removal using olive pomace BC at low pyrolysis temperatures, while Hamieh et al. (2024) reported the high performance of chemically activated olive mill waste BC at around 500 °C. However, results are inconsistent across studies, reflecting the sensitivity of adsorption efficiency to pyrolysis and activation strategies. In contrast, argan industry residues, though abundant in Morocco, remain poorly explored. Recent work has focused on characterising argan residues for energy and BC production (El Barkaoui et al., 2025c) or developing composite materials, such as argan nutshell BC-alginate beads (Bahsaine et al., 2024). Nevertheless, a systematic evaluation of adsorption performance across different argan press cakes (white, black, and pellet) and under varying pyrolysis conditions is lacking.

In addition to these feedstock-specific gaps, there are ongoing methodological shortcomings. Recent international reviews highlight that methylene blue is widely used as a model pollutant (Zhu et al. 2018), but inconsistencies in experimental protocols and data reporting hinder cross-comparison (Bollinger et al., 2025; Haris et al., 2024). Furthermore, there is a lack of studies that adopt factorial or multi-objective optimisation approaches. These approaches would be beneficial as they would simultaneously consider yield, surface area, and adsorption performance. These are critical metrics for scaling up BC production and assessing its feasibility for real wastewater treatment (Hamieh et al., 2024).

Based on these considerations, the present study addresses three major research gaps: (1) the lack of a systematic comparison of multiple, locally abundant agro-residues (olive mill waste and different types of argan press cake) under identical, controlled pyrolysis conditions; (2) the scarcity of pyrolysis studies at high temperatures (600–800 °C) using low heating rates, which have a significant impact on aromatisation, porosity and functional groups; and (3) the limited

application of experimental design methodologies to optimise yield, surface area and adsorption capacity simultaneously.

The aim of this work is therefore to valorise de-oiled olive mill waste (DOW), pellet argan cake (PAC), white argan press cake (WAC), and black argan press cake (BAC) for BC production, to optimise pyrolysis conditions for maximum MB removal, and to identify the most effective BC candidate for wastewater treatment applications.

2. Methodology

2.1. Preparation of BCs

The collection of raw materials is the first step in the production of BC. The four types of biomass (DOW, BAC, PAC, and WAC) were crushed and ground to a size of between 1 and 5 mm. They were then washed with distilled water for purification and oven-dried at 105 °C for 24 hours to remove moisture. The biomasses were then placed in a Nabertherm GmbH (Lilienthal/Bremen, Germany) muffle furnace, which was equipped with a digital temperature controller properly adjusted for heating under N_2-saturated conditions. Slow pyrolysis was performed at temperatures of 600, 700, and 800 °C. The samples were held at each temperature for two hours, with a heating rate of 2 °C min^{-1}. After production, the biochar was filtered by dissolving it in distilled water to remove impurities. It was then dried in an oven at 105 °C for 24 hours to eliminate moisture (**Figure II-7**).

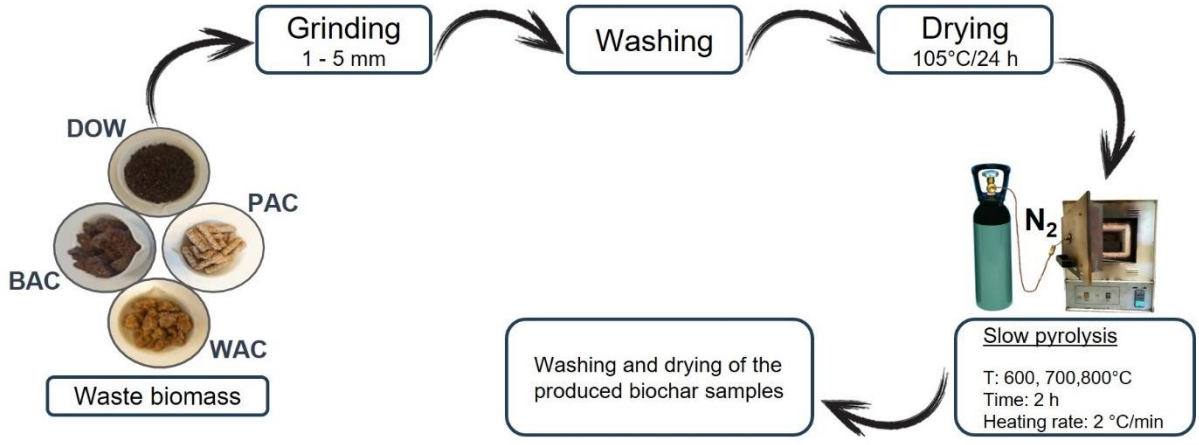

Figure II-7: Process of biochars preparation from de-oiled olive mill waste (DOW), pellet argan cake (PAC), white argan press cake (WAC), and black argan press cake (BAC).

2.2. Characterization of BCs

The environmental compatibility of the produced BCs was assessed following European regulation EN 12915-1 (European Committee for Standardization, 2009). Several analyses were performed, such as elemental (CHNS-O) and proximate analysis, including volatile matter (VM), ash content (AC), fixed carbon (FC), moisture (M), and thermal stability (TS). Additionally, the thermal, structural, and morphology analyses were carried out using Fourier transform infrared spectroscopy (FT-IR), thermogravimetric analysis, X-ray fluorescence (XRF), X-ray diffraction (XRD), scanning electron microscopy/energy dispersive X-ray spectroscopy (SEM-EDX), and Brunauer–Emmett–Teller (BET) specific surface area (SSA) measurements. The detailed methodology is provided in *Supplementary Material 1 (SM1)*.

2.3. Adsorption tests from aqueous solutions

The adsorption experiments were carried out in 150 mL opaque flasks, each containing 10 mg of adsorbent (BC) and 100 mL of MB (300 mg L^{-1}) solution. The flasks were thoroughly mixed and then placed in a reciprocating shaker (Edmund Bühler GmbH) for 4 h (Yaacoubi et al., 2024). The absorbent was separated from the solution by filtering the mixture through cellulose nitrate filter paper with a 0.45 μm pore size. The residual MB concentration was determined using an Anthelie UV–Visible spectrophotometer (Secomam) at 660 nm, referencing an external calibration curve. Each sample was analyzed in triplicate, and the average values were recorded. The adsorption capacity (Q_{ad}) was determined using the following equations (Baçaoui et al., 2001).

$$Q_{ad} = \frac{(C_i - C_f)}{W} * V$$

Where: C_i is the initial concentration of MB (mg/g), C_f is the MB concentration after 4 h of mixing (mg/g), V is the volume of solution (L), and W represents the weight of adsorbent (dry) (g).

3. Results and discussion

3.1. Physicochemical properties of the feedstocks

Figure II-8 illustrates the TGA-DTG thermal analysis of DOW, PAC, BAC, and WAC, indicating a rapid pyrolysis progression between 200 and 500 °C. Pyrolysis-induced mass loss initiates at around 200 °C due to hemicellulose decomposition, preceded by moisture evaporation at 90-100 °C. The peak values in the DTG appeared at 304 °C, 313 °C, 371 °C, and 369 °C for DOW, PAC, BAC, and WAC, respectively, corresponding to the active decomposition of cellulose (Wang et al., 2017). At 500 °C, the remaining solids (BC) are approximately 40% for DOW, 32% for PAC, 27% for BAC, and 25% for WAC of the original weight. Beyond this temperature, pyrolysis continues slowly under a stable weight loss rate. Overall, the TGA results offer a comprehensive weight loss profile across a temperature range for fine powder samples. While the decomposition of large particle size involves different chemical and physical mechanisms, which alter the yield and properties of the desired materials (Yu et al., 2019).

The data of the proximate and elemental analysis of the four types of biomasses are shown in **Table II-2**. The four biomasses studied had a low moisture content (<4%), which is an additional helpful feature for pyrolysis (Déniel et al., 2016; Rago et al., 2018; Muigai et al., 2021). Furthermore, the biomasses had high VM content (>70%); thus, they were potential precursors for pyrolysis (Muigai et al., 2021) and small percentages of AC (<6%). DOW had higher FC content than PAC, BAC, and WAC (20%, 8%, 4%, and 3%, respectively), which is in accordance with some feedstocks (lantana stem, rice straw, maize straw, sugarcane trash, and pine needles) reported in the literature (Chauhan et al., 2024). TS shows a similar trend to FC content (0.22, 0.09, 0.04, 0.03 for DOW, PAC, BAC, and WAC, respectively). For the elemental analysis data, the results show high carbon content (>48%), as well as oxygen content (>21%), and low nitrogen content (<6%). Overall, the studied samples contained carbon percentages comparable to other biomasses, such as woody biomass, forest residues, and agricultural waste (50% - 54%) (Ahmed et al., 2020; Castiglioni et al., 2022; Ghesti et al., 2022).

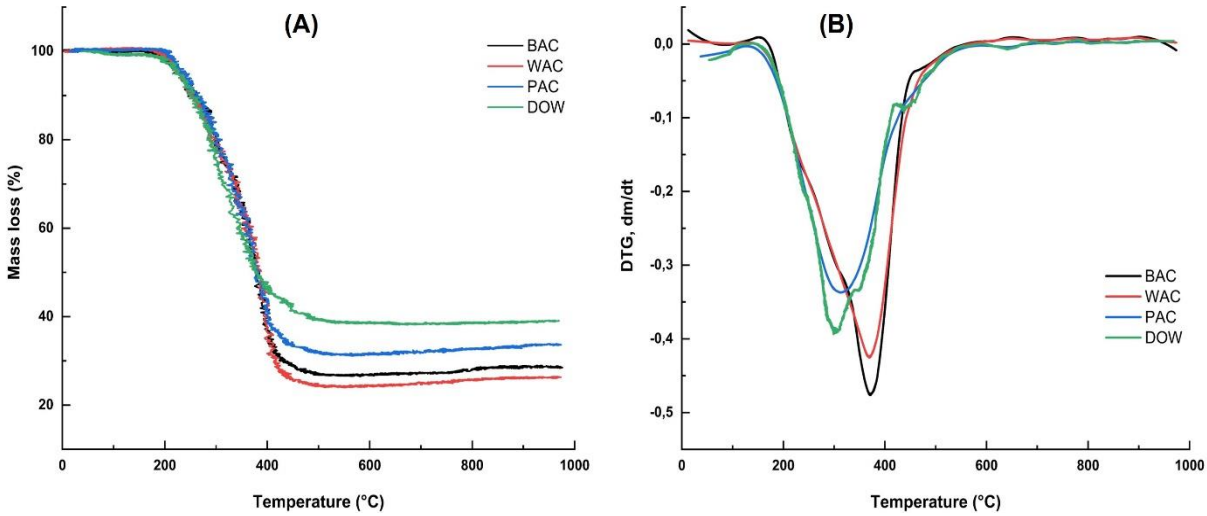

Figure II-8: Thermogravimetric analysis (A) and derivative thermogravimetry (B) curves of de-oiled olive mill waste (DOW), black argan press cake (BAC), pellet argan cake (PAC), and white argan press cake (WAC).

Table II-2: Effect of pyrolysis temperature on the proximate (M: moisture, VM: volatile matter, AC: ash content, FC: fixed carbon, TS: thermal stability) and elemental (C, H, N, S, O) analyses, and pH values of biochar samples.

Sample	Proximate analysis					Element analysis (dry-weighted mass percentages)					pH
	M (%)	VM (%)	AC (%)	FC (%)	TS	C (%)	H (%)	N (%)	S (%)	O (%)	
BAC	3.3 ± 0.1	88.8 ± 0.1	3.82 ± 0.03	4.03 ± 0.06	0.043 ± 0.001	55 ± 1	7.72 ± 0.05	5.3 ± 0.7	0.28 ± 0.05	28 ± 3	5.4 ± 0.7
BBAC600	1.9 0 ± 0.01	39.6 ± 0.8	7.3 ± 0.6	51.2 ± 0.2	0.560 ± 0.004	71 ± 1	1.73 ± 0.03	8.3 ± 1	0.17 ± 0	11.5 ± 0.9	10.27 ± 0.05
BBAC700	1.10 ± 0.01	36 ± 1	7.80 ± 0.09	55.40 ± 0.07	0.610 ± 0.007	72 ± 2	1.01 ± 0.09	7.78 ± 0.07	0.18 ± 0.01	11 ± 2	10.5 ± 0.1
BBAC800	0.60 ± 0.02	33 ± 1	8.5 ± 0.3	57.7 ± 0.1	0.630 ±0.007	73.1 ± 0.8	0.76 ± 0.01	7.5 ± 0.5	0.18 ± 0.01	10 ± 1	10.5 ± 0.4
WAC	2.60 ± 0.09	90.8 ± 0.3	3.29 ± 0.04	3.26 ± 0.08	0.035 ± 0.001	61.3 ± 0.2	8.7 ± 0.5	5.3 ± 0.3	0.28 ± 0.02	21 ± 1	5.4 ± 0.3
BWAC600	1.70 ± 0.01	41 ± 1	8 ± 2	49.1 ± 0.4	0.550 ± 0.006	70 ± 2	1.6 ± 0	7.8 ± 0.9	0.21 ± 0.01	11 ± 1	10.44 ± 0.08
BWAC700	1 ± 0	37 ± 2	8.7 ± 0.5	53.40 ± 0.06	0.59 ± 0.01	67.74 ± 0.9	0.99 ± 0.06	7 ± 1	0	15.4 ± 0.5	10.4 ± 0.2
BWAC800	0.80 ± 0.01	34.1 ± 0.9	8.6 ± 0.6	56.50 ± 0.03	0.620 ± 0.006	70.4 ± 0.4	0.78 ± 0.01	7.2 ± 0.2	0.23 ± 0	12.7 ± 0.8	10.5 ± 0.5
PAC	1.50 ± 0.06	85.9 ± 0.2	4.19 ± 0.01	8.4 ± 0.2	0.089 ± 0.002	52 ± 3	7 ± 1	6.0 ± 0.4	0.32 ± 0.02	30 ± 3	6.9 ± 0.8
BPAC600	1.3 ± 0	38.3 ± 0.9	9 ± 1	51.30 ± 0.05	0.570 ± 0.006	60 ± 1	1.64 ± 0.02	8.0 ± 0.1	2.61 ± 0.01	18.6 ± 2	10.1 ± 0.1
BPAC700	0.80 ± 0.01	37.7 ± 0.7	8.9 ± 0.8	52.60 ± 0.08	0.580 ± 0.005	65.7 ± 0.6	1.24 ± 0.3	8.1 ± 0.3	1.24 ± 0.02	14.8 ± 0.4	10.25 ± 0.09
BPAC800	0.3 ± 0	35 ± 1	10 ± 3	55.2 ± 0.1	0.610 ± 0.006	66.7 ± 0.8	0.98 ±0.01	7.9 ± 0.3	0	14.7 ± 0.7	10.5 ± 0.3
DOW	2.5 ± 0.2	71.6 ± 0.1	5.80 ± 0.04	20.1 ± 0.1	0.22 ± 0.02	48 ± 2	5.8 ± 0.3	2.4 ± 0.5	3.50 ± 0.5	34 ± 4	5.9 ± 0.6
BDOW600	1.5 ± 0.03	28.2 ± 0.8	13.4 ± 0.3	56.97 ± 0.08	0.670 ± 0.006	72 ± 3	3.16 ± 0.07	2.2 ± 0.2	0	8.8 ± 2	10.42 ± 0.06
BDOW700	1.2 ± 0.05	26 ± 1	20.6 ± 0.4	51.9 ± 0.3	0.660 ± 0.009	64.9 ± 0.6	2.1 ± 0.1	1.4 ± 0.6	0	11.0 ± 0.6	10.37 ± 0.08
BDOW800	0.9 ± 0.01	26 ± 1	16 ± 1	56.6 ± 0.1	0.680 ± 0.008	78 ± 1	2.43 ± 0.5	2.1 ± 0.5	0	1.2 ± 1	10.98 0.04

3.2. Optimization of biochar production

Experimental Design Expert 13.0 was employed throughout the process, serving two primary objectives: first, to determine the optimal conditions using the fewest possible experiments, and second, to identify the most significant factors and understand the interactions and influence relationships among them (Yazid et al., 2025). For this carbonization analysis, two factors were selected: carbonization temperature (A) and biomass type (B). The design matrix and experimental results for BC yield, SAA, and MB adsorption efficiency are summarized in **Table SM1-1**, and their iso-response curves are shown in **Figure II-9**. The BC yield ranges from 8.3% to 33.5%, with lower yields observed at higher carbonization temperatures. At the three pyrolysis temperatures of 600, 700, and 800 °C, DOW always produced the highest BC yield (31.1% - 33.5%), followed by PAC (22.3% - 22.4%), and BAC (15.7% - 19.9%), while WAC produced the lowest BC yield (8.3% - 12.7%). Recent studies have reported comparable BC yields. For example, Lustosa Filho et al. (2024) obtained yields of 33–39% from olive mill by-products (olive pomace and stones) when pyrolysing at temperatures above 500 °C. Similarly, El Kourdi et al. (2024) produced biochar from argan residues (nut shells, pulp, and press cakes) using slow pyrolysis at 550 °C with residence times of 50–105 minutes and heating rates of 5–10 °C per minute, achieving average yields of 21–23%. The higher BC yields obtained from DOW could be mainly due to its higher FC contents of biomass. Thus, the variations in the composition of biomasses affect their BC yields. In addition, BC yields are highly affected by the particle size of its feedstock, which may limit heat transfer efficiency (El Kourdi et al., 2024). These results align with the TGA analysis of the four biomasses, indicating higher decomposition in WAC, followed by BAC, PAC, and DOW (**Figure II-8A**), consistent with the identical pyrolysis parameters used in both experiments. It should also be noted that the parameter control in the TGA analysis is more accurate than in the pyrolysis experiment (El Kourdi et al., 2024). Furthermore, increasing the carbonization temperature leads to greater decomposition of cellulose and hemicellulose (Rabichi et al., 2024b), resulting in a reduction of the BC mass yield with R^2 above 0.99 for BCs produced from argan cakes (WAC, BAC, and PAC), while 96% for BDOW (**Figure SM1-1**). The adsorption efficiency of MB on BCs varies significantly, ranging from 40 mg/g to 432 mg/g. This variation is closely linked to the specific surface area, ranging from 7 m²/g to 22 m²/g. Similar findings were reported by Rabichi et al., (2024b), who optimized BC production from olive waste using Response Surface Methodology. By applying multicriteria optimization using a desirability

function and Doehlert design, they identified the optimal pyrolysis conditions as 585 °C, a residence time of 90 min, and a heating rate of 15 °C/min. Under these conditions, the resulting BC achieved a yield of 27.7%, a BET surface area of 6.29 m^2/g, and an adsorption capacity of 274 mg/g for MB.

Increasing the pyrolysis temperature from 600 °C to 800 °C enhanced SSA, reaching a maximum of 22 m^2/g for BDOW800. These results were attributed to the removal of VM by dehydration, melting, softening, and carbonization, resulting in a high surface area and pore structure of the BC (Muigai et al., 2021). The analysis of the effects highlights the substantial influence of the two factors—carbonization temperature and biomass type on both the adsorption process and BC synthesis. The high adsorption capacity of the various BC samples can be attributed to their specific surface area (SSA), surface functional groups (such as hydroxyl and carboxyl groups), and π-π interactions between the BC surface and MB molecules. Other factors include electrostatic attraction, hydrogen bonding, and pore-filling effects (**Figure II-10**) (Regti et al., 2017; Ren et al., 2025). The negatively charged surface functional groups on BC, such as –OH and –COOH, attract cationic MB molecules through electrostatic forces. Meanwhile, BC's aromatic structures facilitate π–π interactions with MB's aromatic rings (Wang et al., 2023). Hydrogen bonding between the dye's polar groups and the BC surface's oxygen-containing groups also contributes to the adsorption process. Furthermore, BC's highly porous structure allows dye molecules to be physically trapped within its pores, thereby enhancing removal efficiency (Kataya et al., 2025). The relative contribution of these mechanisms depends on the BC precursor, the pyrolysis temperature, and the surface chemistry. Studies have demonstrated that physical adsorption (physisorption) occurs most frequently, with monolayer coverage dominating when Langmuir isotherms are observed (Wang et al., 2023). Overall, MB adsorption onto BC is a hybrid process combining surface-controlled interactions and structural porosity to effectively remove dyes from aqueous solutions.

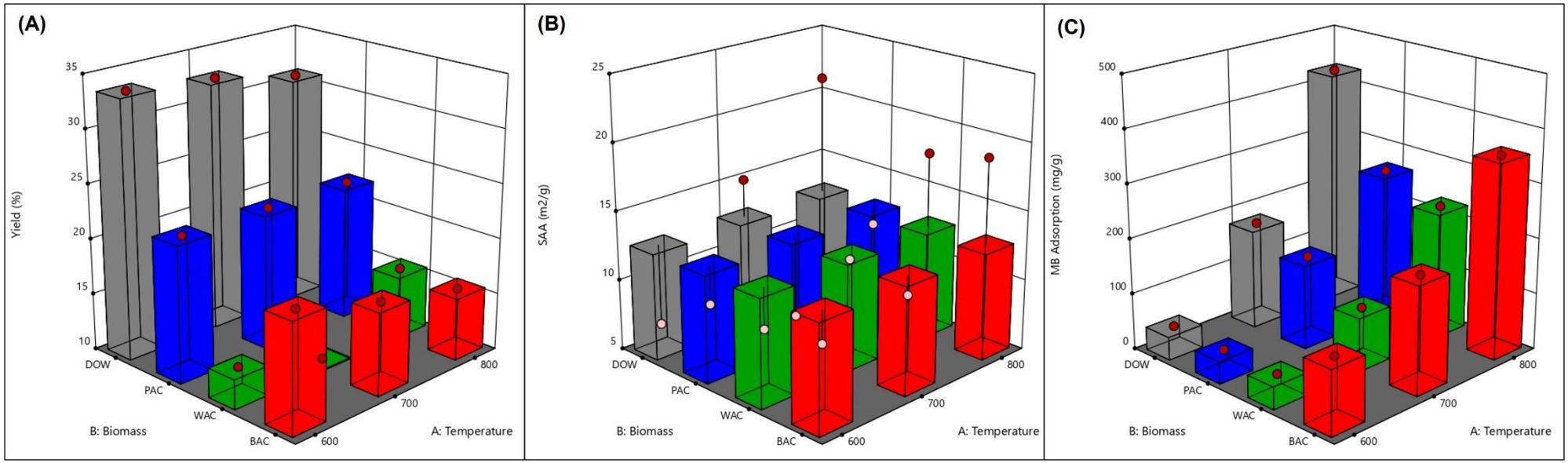

Figure II-9: Variation of the yield % (A), surface specific area (SSA) m2/g (B), and the Methylene blue (MB) adsorption mg/g (C) of biochars (iso-response curves), as a function of biomass type and carbonization temperature.

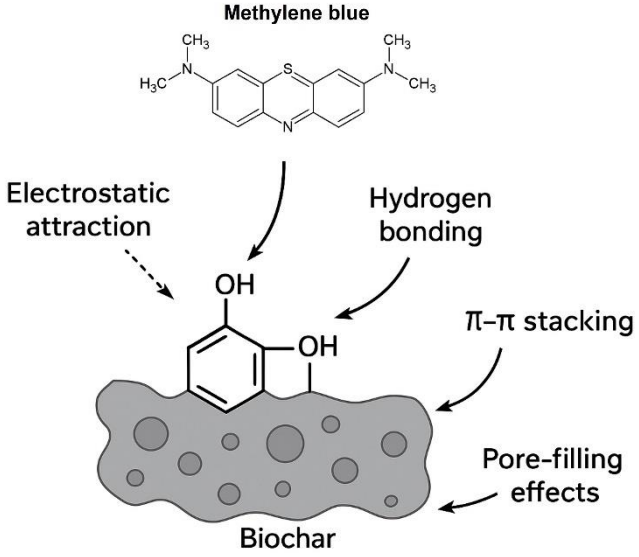

Figure II-10: Schematic representation of the adsorption pathways of MB on the biochar.

The scatterplots in **Figure II-11A** and **II-11C** show that the experimental data points are closely aligned along the diagonal line, indicating a strong correlation and satisfactory agreement between the predicted and actual values for both BC yield and MB adsorption. This alignment validates the accuracy and reliability of the applied model in predicting the experimental outcomes, further supporting its suitability for optimizing the BC synthesis process. The consistency between the predicted and observed results reinforces the robustness of the factorial design approach and the statistical tools used for analysis. Despite this limitation, the strong agreement for BC yield and MB adsorption demonstrates the model's effectiveness in optimizing other critical parameters of BC synthesis (Annadurai et al., 2002).

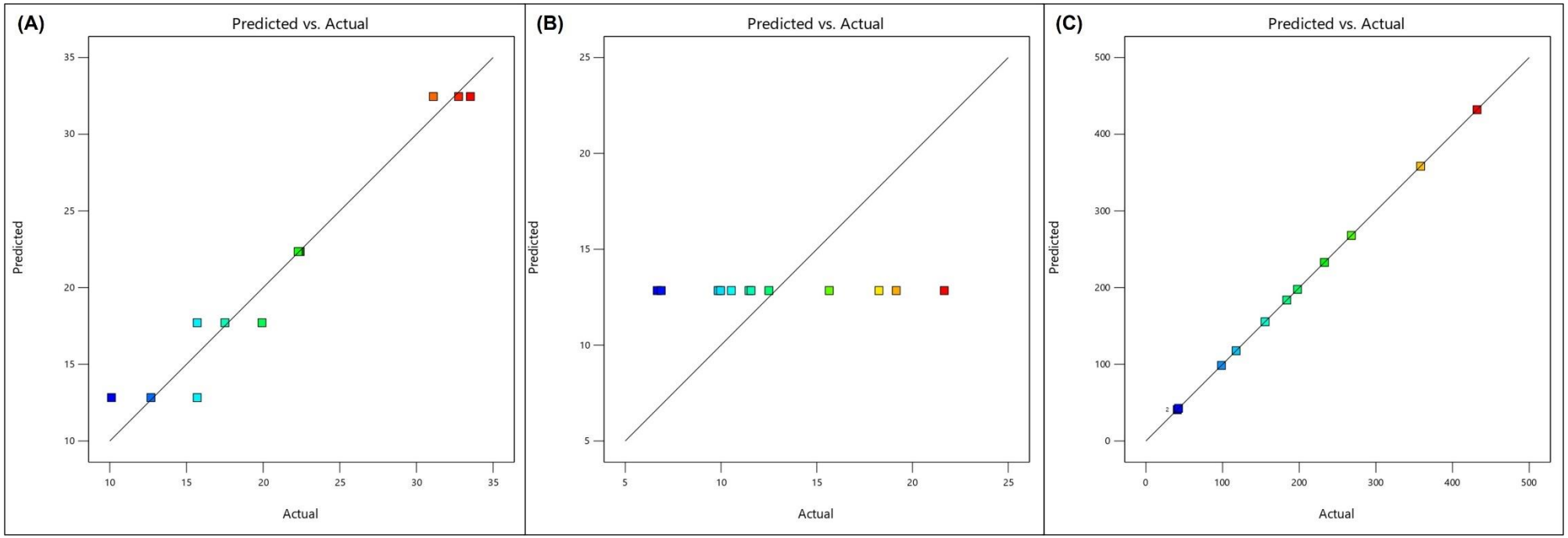

Figure II-11: Actual versus predicted data of the responses Y1: Yield (A), Y2: SAA (B), and Y3: methylene blue adsorption capacity (C).

The process desirability function was employed to identify the optimal operating conditions and ensure the responses met the desired criteria. The desirability values range from 0 to 1, with values closer to 1 indicating greater optimization reliability. The results demonstrated a desirability score of 0.908, reflecting highly reliable optimization for the maximum removal of MB, as well as for achieving the highest yield (Grich et al., 2024). Furthermore, the optimal conditions for maximizing yield, specific surface area, and methylene blue adsorption involve using DOW biomass at a pyrolysis temperature of 800°C.

3.3. Characteristics of biochars

3.3.1. Physicochemical characteristics

Table II-2 illustrates the physicochemical characteristics, including proximate and elemental analyses, as well as the pH of the produced BCs. The VM content of the studied BCs decreased in line with increasing pyrolysis temperature from 40%, 41%, 38%, and 28% at 600 °C to 33%, 34%, 35%, and 26% at 800 °C for BAC, WAC, PAC, and DOW, respectively, indicating progressive loss of more volatile components with charring. Inversely, FC content in BCs derived from argan cake residues increased with pyrolysis temperature, exhibiting an inverse correlation with VM. This increase in FC is attributed to the progressive release of VM during pyrolysis (Crombie et al., 2013). Moreover, the FC content of the BC samples was mostly above 50%, depending on the pyrolysis temperature, indicating that BC consists mainly of carbon. Increasing the temperature of pyrolysis from 600 °C to 800 °C leads to an increase in the FC content of the produced BCs from 51% to 58% for BAC, 49% to 57% for WAC, and 51% to 55% for PAC. The produced BCs have a relatively low AC (approximately 7.3% – 20.6%), reflecting their high quality (Tran et al., 2016). At the three pyrolysis temperatures 600, 700, and 800 °C, BAC showed the lowest AC (7.3%, 7.8%, and 8.5%), while DOW-derived BC showed the highest (13.4%, 16.0%, and 20.6%); the latter may result in high mineral concentration and destructive volatilization of lignocellulosic matter (Zhang et al., 2015). These results were consistent with previous reports indicating that the FC content increased and the VM decreased as the pyrolysis temperature raised (Crombie et al., 2013; Tran et al., 2016; Zhang et al., 2017).

Generally, these results generally align with those reported by Hadey et al. (2022), who produced BCs from peanut shells and sugarcane bagasse at 400–500 °C, yielding 15–40% FC,

<10% AC, and 45–69% VM. Similar characteristics were also observed by Nawaz et al. (2024) for *Spirulina platensis*-derived BC pyrolyzed at 550 °C (4 h, 10 °C/min), which showed 2.6% moisture, 37.3% VM, 8.7% AC, and 51.4% FC. Likewise, Chaudhuri et al. (2025) obtained similar values of moisture (3.4%), VM (18.6%), AC (12.3%), and FC (65.7%) for a bamboo-derived BC produced at a temperature range of 400–550 ◦C and a heating rate of 10 ◦C/min. Furthermore, the studied BCs had high TS ratios (0.55–0.68) compared to their raw materials (0.03–0.22), demonstrating that higher pyrolysis temperatures enhance organic matter stability. The high stability of BCs is due to the formation of heat-resistant carbon, resulting from dehydrogenation and aromatization at high temperatures (Muigai et al., 2021). The results mentioned above are in agreement with many researchers who studied the TS of BCs derived from de-inking paper sludge (Méndez et al., 2014), oak acorn shells, jift, and deseeded carob pods (Albalasmeh et al., 2020), and sugar cane bagasse (Chauhan et al., 2024). The elemental analysis data highlighted high carbon content of the produced BCs (71–73% from BAC, 68–70% from WAC, 60–67% from PAC, and 65–78% from DOW) compared to their biomasses (55%, 61%, 52%, and 48% for BAC, WAC, PAC, and DOW, respectively), which increased with the pyrolysis temperature. However, the oxygen and hydrogen contents of the BC samples showed lower values at the three pyrolysis temperatures of 600, 700, and 800 °C compared to their raw materials (**Table II-2**), which may be attributed to the release of hydroxyl functional groups and the evaporation of VM. Elevated pyrolysis temperatures (>600 °C) triggered dehydration, thermal degradation reactions, decarboxylation, and aromatization, resulting in an increased concentration of carbon in the produced BC (Muigai et al., 2021). The carbon contents obtained in this study were higher compared with some recent studies (D'Eusanio et al., 2024; Kasambala et al., 2025; Kundu et al., 2024; Panizio et al., 2024; Wang et al., 2024). For example, D'Eusanio et al. (2024) investigated BCs from diverse feedstocks (e.g., Grape seeds, defatted grape seeds, wood stems, and whole grape seeds), pyrolysed at 300 °C for 3 and 24 h, resulting in a content of carbon ranging from 51% to 69%, hydrogen from 3.1% to 6%, and oxygen from 19% to 39%. After the pyrolysis process, the pH values of biomass samples tended to increase from 5.4 - 6.9 to above 10 for the BC samples. This alkalinity may result from alkali salt release during the pyrolysis of biomass and carbonate ($CaCO_3$) formation (Zhang et al., 2015). Similar phenomena were observed by Khater et al. (2024) and Birhanu et al. (2025).

The physicochemical characteristics of BCs play a crucial role in determining their adsorption

efficiency towards MB. Low moisture and volatile matter content combined with high fixed carbon levels and thermal stability indicate a well-carbonised structure with a stable porous matrix that enhances MB uptake (Mahdi et al., 2017; Vafakish et al., 2025). High carbon content contributes to the development of an extensive aromatic surface favourable for π–π interactions with MB molecules (Ji et al., 2025). The presence of oxygen- and nitrogen-containing functional groups, as determined by elemental composition analysis, provides active sites for electrostatic attraction and hydrogen bonding (Mortada et al., 2024). Additionally, an alkaline pH increases the negative charge on the surface of the BC, promoting the adsorption of the cationic MB dye via electrostatic interactions (Zhu et al., 2018). Together, these factors enhance the BC's affinity for MB synergistically, making it an effective adsorbent.

3.3.2. Morphological and structural characterisation

This section presents the characterization data obtained through SEM/EDX, XRF, XRD, and FT-IR analyses. These techniques were employed to investigate the morphological, chemical composition, crystalline structure, and functional group features of the studied biomasses and BCs, providing a comprehensive understanding of the materials' properties and their relevance to the intended application.

Morphological characterisation of the studied biomass and BC samples was performed by SEM/EDX analysis (**Figures II-12 and SM2**). SEM analysis revealed that pyrolysis conditions have a significant impact on the surface morphology of BCs, resulting in the development of well-defined pores, particularly in samples produced at 800 °C (**Figure II-12**). These pore structures and surface morphologies can directly affect the accessible surface area and diffusion pathways for MB molecules (Charmas et al., 2023). The BCs derived from argan cakes exhibited heterogeneous surface morphologies characterized by porous structures and irregular network formations with varying sizes and shapes, distinct from the original biomass. Whereas the SEM images exhibited that the BC samples from DOW have well-developed pores and homogenous structures on the BC surfaces, allowing dye to be absorbed into these BC samples (Enaime et al., 2017). This porosity may result from the release of VM during the pyrolysis process. Overall, the rising temperature leads to the release of the VM contained in the feedstock in the form of H_2O, CH_4, CO, and CO_2, forming pores on the façade (Yang et al., 2018). In addition, volatiles trapped within the biomass inflated the BC surface due to the expansion and thermal degradation of the holocellulose, resulting in the porous nature of the

BC samples (Enaime et al., 2017). The EDX analysis determined the elemental composition of different biomass and BC samples (**Figure SM1-2**). Carbon is the predominant element in all samples, followed by oxygen. The findings are consistent with the literature (Tan et al., 2018; Saeed et al., 2020).

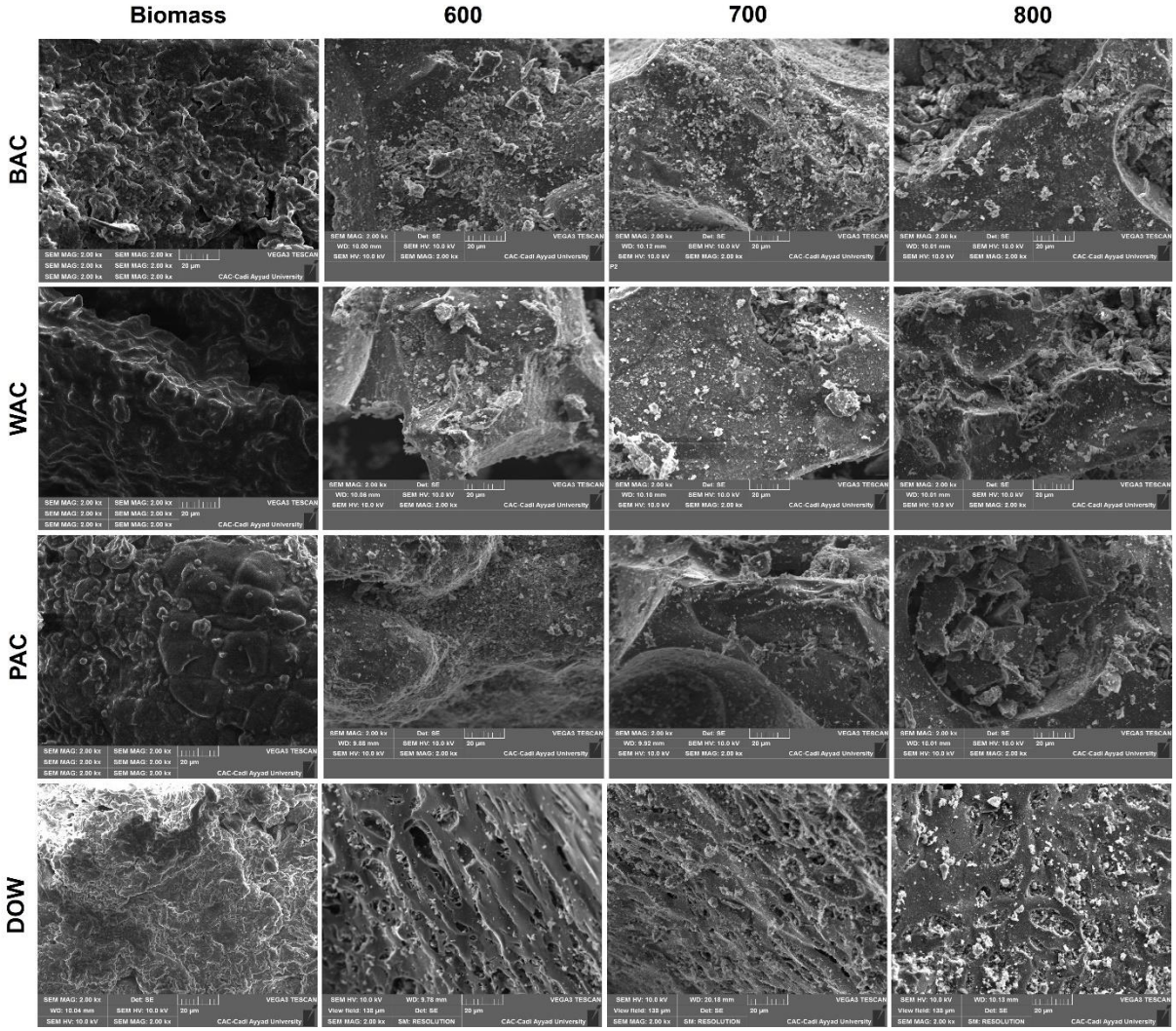

Figure II-12: Scanning electron microscopy micrographs of the produced biochars derived from DOW: de-oiled olive mill waste, BAC: black argan press cake, PAC: pellet argan cake, and WAC: white argan press cake at 600,700, and 800 °C, respectively.

Figure II-13 shows the XRF spectra of the BC and biomass samples. The XRF analysis illustrates similar spectra for each BC type to its raw material, indicating almost the same inorganic composition, with a difference in intensity. This composition was mainly composed of K and Ca for the three BC samples derived from argan cakes and their biomass, while other elements such as S, Cl, P, and especially some metals (e.g., Mn, Fe, Cu, and Zn) gave much

lower signals. Similarly, DOW, BDOW600, BDOW700, and BDOW800 have a similar composition with a high percentage of Fe, which may be considered one of the main constituents. These metal elements may behave as catalysts due to their ability to change the state of oxidation and therefore adsorb other compounds more embedded on their surfaces (Hossain et al., 2020). Furthermore, Chaves Fernandes et al., (2020) pointed out that the increased ash content obtained at elevated pyrolytic temperatures was attributed to the enhanced minerals' stability, such as Ca, P, and K, in the pyrolysed material after the progressive loss of VM during the pyrolysis process.

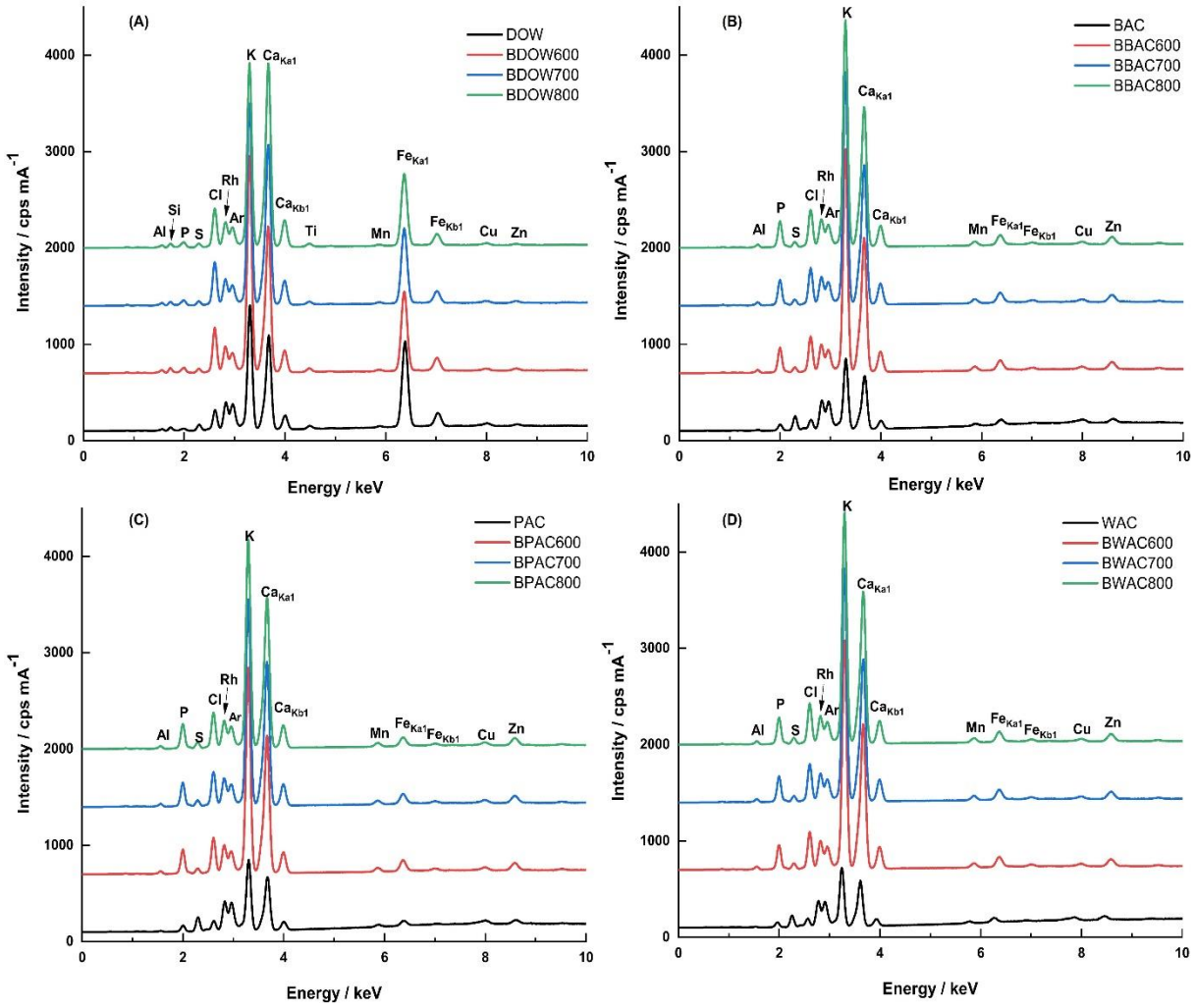

Figure II-13: X-ray fluorescence spectrum of the produced biochars derived from DOW: de-oiled olive mill waste (A), BAC: black argan press cake (B), PAC: pellet argan cake (C), and WAC: white argan press cake (D) at 600,700, and 800 °C, respectively.

Figure II-14 presents the mineralogical characterisation of the BC samples and their source materials, as determined by XRD analysis. Firstly, the XRD patterns of the four types of

biomasses displayed similar profiles, with variations in peak intensity depending on their cellulose content. The XRD diffractograms of the biomass samples revealed a prominent, broad, and intense peak at $2\theta = 19.66°$, which is characteristic of the disordered regions within the cellulose fibre, as well as the amorphous structure of the hemicellulose and lignin (El Barkaoui et al., 2025c). A second small peaks at 30° and 38° were detected, indicating the presence of amorphous hemicellulose and cellulose (Uzoagba et al., 2024), which is partially composed of sheets of randomly oriented aromatic carbon (Suganuma et al., 2008). Conversely, the XRD diffractograms of the produced BCs exhibit similar profiles, completely different from their raw materials, essentially composed of five crystalline phases: calcite, hydroxyapatite, kalsilite, quartz, and sylvite. These results are comparable to the XRD reference libraries (Muigai et al., 2021; Bakari et al., 2024). Furthermore, the XRD spectra of all BC samples show that the narrow peaks slightly decrease as the temperature increases from 600 °C to 800 °C, indicating that the degree of crystallinity decreases with the increase of pyrolysis temperature and formation of carbon-rich amorphous BC.

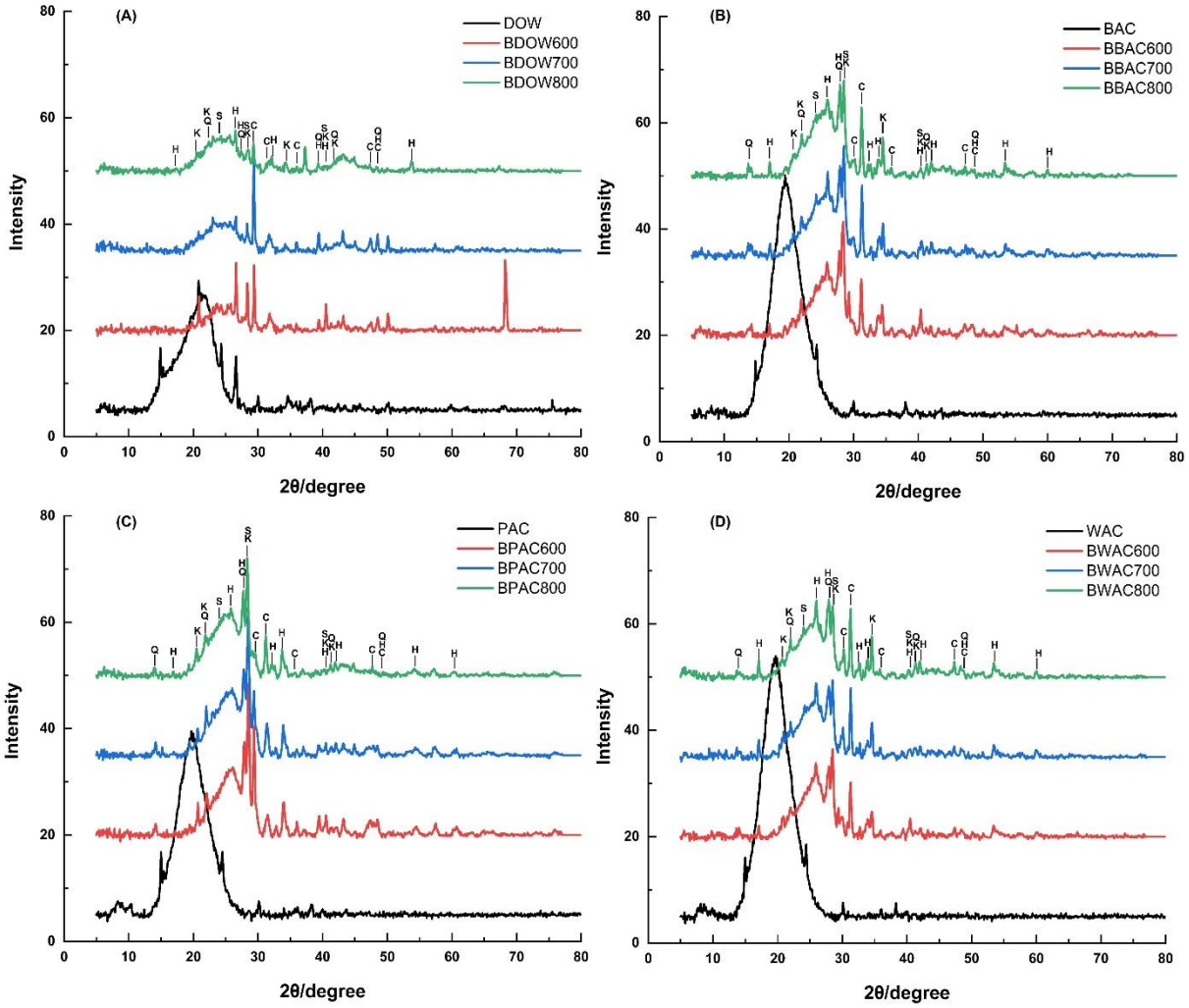

Figure II-14: X-ray diffraction diffractogram of the produced biochars derived from DOW: de-oiled olive mill waste (A), BAC: black argan press cake (B), PAC: pellet argan cake (C), and WAC: white argan press cake (D) at 600,700, and 800 °C, respectively. The phases are labeled C: calcite, H: hydroxyapatite, K: kalsilite, Q: quartz, and S: sylvite.

Determining the functional groups in BC samples was essential, as these groups influence the sorption properties of the BC samples, and hence play a crucial role in forming linkages between the adsorbent and the adsorbed substance (Ifguis et al., 2022). **Figure II-15** shows the FT-IR spectra of the studied BCs and their biomasses, while **Table SM1-2** shows their band assignment. A comparative analysis of the FTIR spectra of the four biomass types showed the presence of the same bands. After pyrolysis, the BC samples' spectra revealed significant structural changes in particular functional groups initially present in the biomass after pyrolysis, indicating that the carbon structure of BCs was more dependent on the temperature of pyrolysis than on the raw material. Increasing the pyrolysis temperature from 600 °C to 800 °C resulted

in a decrease in the intensities of some peaks, such as OH and C=O stretching vibrations (3000-3700 cm^{-1} and 1745 cm^{-1}, respectively), due to decarboxylation and dehydration during the pyrolysis process (Zhang et al., 2017). The transmittance of the bands at 2856 cm^{-1} and 2923 cm^{-1} corresponding to CH_3 stretching in aliphatic compounds in BC samples is weak, indicating the presence of carboxylic acid and alcohol (Muigai et al., 2021). The spectra revealed a disappearance of an aromatic C=O stretching vibration in the produced BCs that appeared in the biomass samples at 1745 cm^{-1} (Uzoagba et al., 2024), probably due to the high pyrolysis temperature applied (600-800 °C). A strong band appeared at 1650 cm^{-1} assigned to the aromatic C=C stretching vibration, which was always present in the BCs manufactured until the temperature exceeded 800 °C (Rabichi et al., 2024a). The vibrations assigned to CH_2 deformation in aliphatic compounds, observed at 1460 cm^{-1}, also decreased as the pyrolysis temperature increased within this range, leading to the condensation and formation of aromatic structures (Uchimiya et al., 2011). Furthermore, the peak intensities within the 1000–1250 cm^{-1} range, corresponding to C–O, increased following pyrolysis, due to the breakdown of holocellulose and the cleavage of β-glycosidic bonds in the biomass samples (Muigai et al., 2021). Interestingly, the presence of functional groups such as hydroxyl, carboxyl, or aromatic groups plays a crucial role in the adsorption mechanism by facilitating hydrogen bonding, electrostatic interactions, or π-π stacking with adsorbate molecules like MB (Ji et al., 2025).

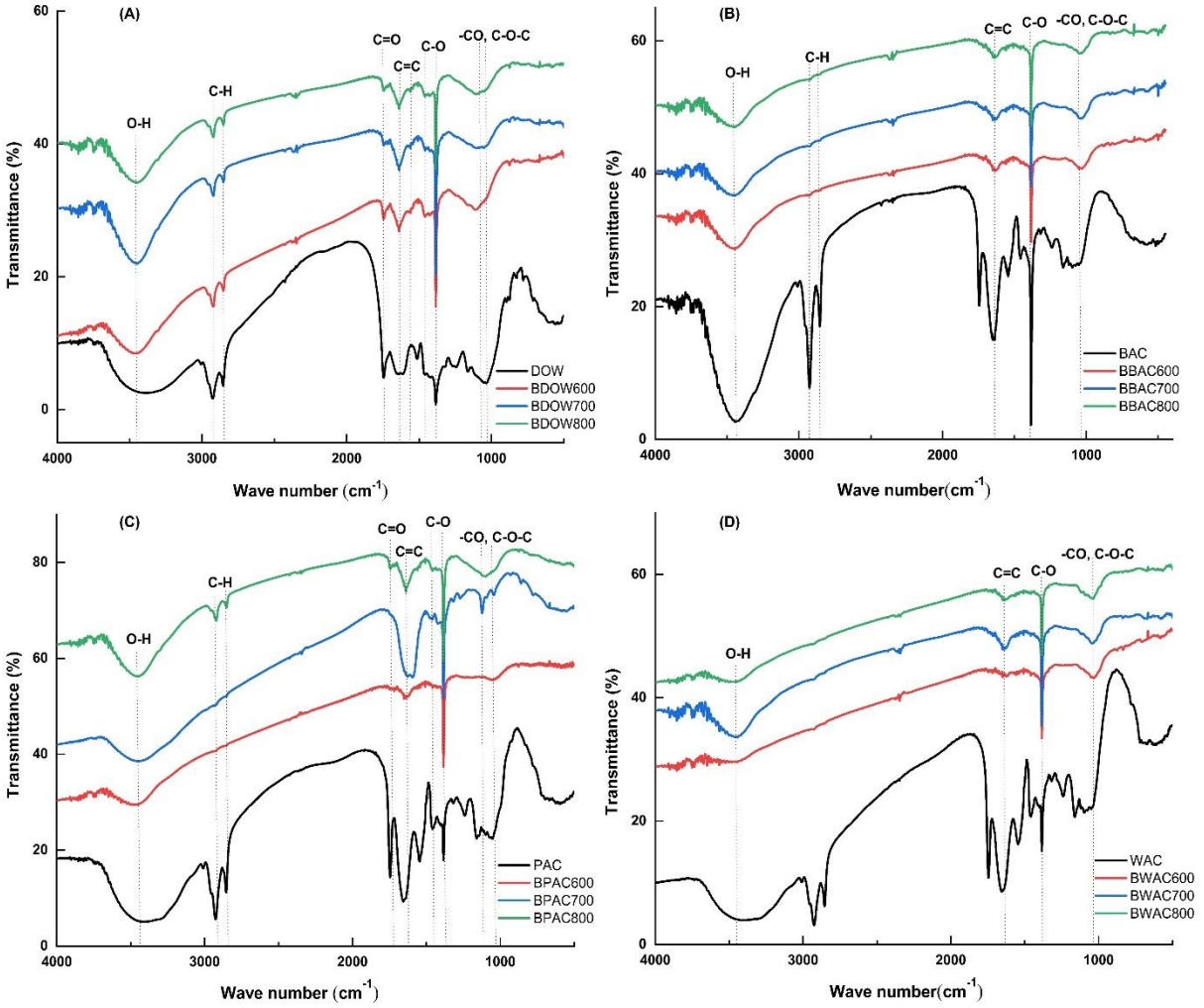

Figure II-15: Fourier transform infrared spectroscopy spectra in a range of 400 - 4000 cm-1 of the produced biochars derived from DOW: de-oiled olive mill waste (A), BAC: black argan press cake (B), PAC: pellet argan cake (C), and WAC: white argan press cake (D) at 600,700, and 800 °C, respectively.

Conclusion

This study demonstrated that the properties and performance of biochar derived from agro-residues are strongly influenced by both feedstock type and pyrolysis temperature. Increasing the temperature improved carbonisation, stability, and porosity, but reduced the yield. Of the materials tested, de-oiled olive mill waste (DOW) biochar produced at 800 °C exhibited the most favourable balance, with a yield of 31–33%, a BET surface area of 22 m^2/g and a maximum methylene blue adsorption capacity of 432 mg/g ($R^2 > 0.96$). In contrast, biochar from argan residues (PAC, WAC, and BAC) exhibited lower adsorption efficiencies. These findings highlight the potential of DOW-derived biochar as a sustainable, low-cost adsorbent for wastewater treatment. Future work should assess its performance in real effluents and evaluate its scalability for industrial applications.

References

Ahmed, A., Abu Bakar, M.S., Hamdani, R., Park, Y.-K., Lam, S.S., Sukri, R.S., Hussain, M., Majeed, K., Phusunti, N., Jamil, F., Aslam, M., 2020. Valorization of underutilized waste biomass from invasive species to produce biochar for energy and other value-added applications. Environ. Res. 186, 109596. https://doi.org/10.1016/j.envres.2020.109596

Albalasmeh, A., Gharaibeh, M.A., Mohawesh, O., Alajlouni, M., Quzaih, M., Masad, M., El Hanandeh, A., 2020. Characterization and Artificial Neural Networks Modelling of methylene blue adsorption of biochar derived from agricultural residues: Effect of biomass type, pyrolysis temperature, particle size. J. Saudi Chem. Soc. 24, 811–823. https://doi.org/10.1016/j.jscs.2020.07.005

Annadurai, G., Juang, R., Lee, D., 2002. Use of cellulose-based wastes for adsorption of dyes from aqueous solutions. J. Hazard. Mater. 92, 263–274. https://doi.org/10.1016/S0304-3894(02)00017-1

Baçaoui, A., Yaacoubi, A., Dahbi, A., Bennouna, C., Phan Tan Luu, R., Maldonado-Hodar, F.., Rivera-Utrilla, J., Moreno-Castilla, C., 2001. Optimization of conditions for the preparation of activated carbons from olive-waste cakes. Carbon N. Y. 39, 425–432. https://doi.org/10.1016/S0008-6223(00)00135-4

Bahsaine, K., Benzeid, H., Zari, N., Qaiss, A. el K., Bouhfid, R., 2024. Biochar-alginate beads derived from argan nutshells for effective methylene blue removal: A sustainable approach to wastewater treatment. Int. J. Biol. Macromol. 282, 136853. https://doi.org/10.1016/j.ijbiomac.2024.136853

Bakari, Z., Fichera, M., El Ghadraoui, A., Renai, L., Giurlani, W., Santianni, D., Fibbi, D., Bruzzoniti, M.C., Del Bubba, M., 2024. Biochar from co-pyrolysis of biological sludge and woody waste followed by chemical and thermal activation: end-of-waste procedure for sludge management and biochar sorption efficiency for anionic and cationic dyes. Environ. Sci. Pollut. Res. 31, 35249–35265. https://doi.org/10.1007/s11356-024-33577-3

Birhanu, A., Hailu, A.M., Worku, Z., Tessema, I., Angassa, K., Tibebu, S., 2025. Optimization of pyrolysis conditions for Catha edulis waste-based biochar production using response surface methodology. Bioresour. Bioprocess. 12, 62. https://doi.org/10.1186/s40643-025-00866-9

Bollinger, J.-C., Lima, E.C., Mouni, L., Salvestrini, S., Tran, H.N., 2025. Molecular properties of methylene blue, a common probe in sorption and degradation studies: a review. Environ. Chem. Lett. 23, 1403–1424. https://doi.org/10.1007/s10311-025-01856-1

Bracamontes-Ruelas, A.R., Ordaz-Díaz, L.A., Bailón-Salas, A.M., Ríos-Saucedo, J.C., Reyes-Vidal, Y., Reynoso-Cuevas, L., 2022. Emerging Pollutants in Wastewater, Advanced Oxidation Processes as an Alternative Treatment and Perspectives. Processes 10, 1041. https://doi.org/10.3390/pr10051041

Castiglioni, M., Rivoira, L., Ingrando, I., Meucci, L., Binetti, R., Fungi, M., El-Ghadraoui, A., Bakari, Z., Del Bubba, M., Bruzzoniti, M.C., 2022. Biochars intended for water filtration: A comparative study with activated carbons of their physicochemical properties and removal efficiency towards neutral and anionic organic pollutants. Chemosphere 288, 132538. https://doi.org/10.1016/j.chemosphere.2021.132538

Chafi, S., Cuevas-Aranda, M., Martínez-Cartas, M.L., Sánchez, S., 2025. Production of Bioadsorbents via Low-Temperature Pyrolysis of Exhausted Olive Pomace for the Removal of Methylene Blue from Aqueous Media. Molecules 30, 3254. https://doi.org/10.3390/molecules30153254

Charmas, B., Zięzio, M., Jedynak, K., 2023. Assessment of the Porous Structure and Surface Chemistry of Activated Biocarbons Used for Methylene Blue Adsorption. Molecules 28, 4922. https://doi.org/10.3390/molecules28134922

Chaudhuri, P., Pande, R., Baraiya, N.A., 2025. From char to flame: Evaluating bamboo bio-char combustion via cone calorimetry and thermogravimetric analysis. Energy 314, 134313. https://doi.org/10.1016/j.energy.2024.134313

Chauhan, S., Taksal, P.A., Chowdhury, S., Bhattacharya, J., Dubey, B.K., 2024. Unveiling Biochar Quality Index: A Factor Analysis Mediated Ranking Approach to Select Best Ranked Biochar for Adsorptive Removal of Sulfamethoxazole. Ind. Eng. Chem. Res. 63, 12126–12144. https://doi.org/10.1021/acs.iecr.4c00824

Chaves Fernandes, B.C., Ferreira Mendes, K., Dias Júnior, A.F., da Silva Caldeira, V.P., da Silva Teófilo, T.M., Severo Silva, T., Mendonça, V., de Freitas Souza, M., Valadão Silva, D., 2020. Impact of Pyrolysis Temperature on the Properties of Eucalyptus Wood-Derived Biochar. Materials (Basel). 13, 5841. https://doi.org/10.3390/ma13245841

Crombie, K., Mašek, O., Sohi, S.P., Brownsort, P., Cross, A., 2013. The effect of pyrolysis conditions on biochar stability as determined by three methods. GCB Bioenergy 5, 122–131. https://doi.org/10.1111/gcbb.12030

D'Eusanio, V., Lezza, A., Anderlini, B., Malferrari, D., Romagnoli, M., Roncaglia, F., 2024. Technological Prospects of Biochar Derived from Viticulture Waste: Characterization and Application Perspectives. Energies 17, 3421. https://doi.org/10.3390/en17143421

Dabare, S., Rajapaksha, S., Munaweera, I., 2025. Sustainable innovation in nanotechnology-based water treatment: aligning climate change adaptation with industrial ecology and CSR goals. Environ. Sci. Water Res. Technol. 11, 2100–2124. https://doi.org/10.1039/D5EW00557D

Déniel, M., Haarlemmer, G., Roubaud, A., Weiss-Hortala, E., Fages, J., 2016. Optimisation of bio-oil production by hydrothermal liquefaction of agro-industrial residues: Blackcurrant pomace (Ribes nigrum L.) as an example. Biomass and Bioenergy 95, 273–285. https://doi.org/10.1016/j.biombioe.2016.10.012

El Barkaoui, S., Mandi, L., Aziz, F., Del Bubba, M., Ouazzani, N., 2023. A critical review on using biochar as constructed wetland substrate: Characteristics, feedstock, design and pollutants removal mechanisms. Ecol. Eng. 190, 106927. https://doi.org/10.1016/j.ecoleng.2023.106927

El Barkaoui, S., Mandi, L., Ryah, H., El Ghadraoui, A., Del Bubba, M., Ouazzani, N., 2025a. Biochar-based filtration systems for wastewater treatment: performance, efficiency, and optimization. Int. J. Environ. Sci. Technol. https://doi.org/10.1007/s13762-025-06694-w

El Barkaoui, S., Mandi, L., Fichera, M., Ryah, H., Baçaoui, A., Del Bubba, M., Ouazzani, N., 2025b. Optimizing biochar-based column filtration systems for enhanced pollutant removal in wastewater treatment: A preliminary study. Chemosphere 372, 144067. https://doi.org/10.1016/j.chemosphere.2025.144067

El Barkaoui, S., Ouazzani, N., Mandi, L., Zafeiropoulos, J., Isari, E.A., Del Bubba, M., Kalavrouziotis, I.K., 2025c. Physicochemical and thermal characterization of argan residues for biofuel and biochar production: potential future prospects. Biomass Convers. Biorefinery 15, 17309–17319. https://doi.org/10.1007/s13399-024-06442-z

El kourdi, S., Chaabane, A., Abderafi, S., Abbassi, M.A., 2024. Valorizing argan residues into biofuels and chemicals through slow pyrolysis. Results Eng. 21, 101659. https://doi.org/10.1016/j.rineng.2023.101659

Enaime, G., Ennaciri, K., Ounas, A., Baçaoui, A., Seffen, M., Selmi, T., Yaacoubi, A., 2017. Preparation and characterization of activated carbons from olive wastes by physical and chemical activation: Application to Indigo carmine adsorption. J. Mater. Environ. Sci. 8, 4125–4137.

European Committee for Standardization, 2009 EN 12915, 2009. Products Used for the Treatment of Water Intended for Human Consumption – Granular Activated Carbon. In.

Gadipelly, C., Pérez-González, A., Yadav, G.D., Ortiz, I., Ibáñez, R., Rathod, V.K., Marathe, K. V., 2014. Pharmaceutical Industry Wastewater: Review of the Technologies for Water Treatment and Reuse. Ind. Eng. Chem. Res. 53, 11571–11592. https://doi.org/10.1021/ie501210j

Ghesti, G.F., Silveira, E.A., Guimarães, M.G., Evaristo, R.B.W., Costa, M., 2022. Towards a sustainable waste-to-energy pathway to pequi biomass residues: Biochar, syngas, and biodiesel analysis. Waste Manag. 143, 144–156. https://doi.org/10.1016/j.wasman.2022.02.022

Grich, A., Bouzid, T., Naboulsi, A., Regti, A., Tahiri, A.A., El Himri, M., El Haddad, M., 2024. Preparation of low-cost activated carbon from Doum fiber (Chamaerops humilis) for the removal of methylene blue: Optimization process by DOE/FFD design, characterization, and mechanism. J. Mol. Struct. 1295, 136534. https://doi.org/10.1016/j.molstruc.2023.136534

Hadey, C., Allouch, M., Alami, M., Boukhlifi, F., Loulidi, I., 2022. Preparation and Characterization of Biochars Obtained from Biomasses for Combustible Briquette Applications. Sci. World J. 2022, 1–13. https://doi.org/10.1155/2022/2554475

Hamieh, M., Tabaja, N., Tlais, S., Koubaissy, B., Hammoud, M., Chawraba, K., Hamieh, T., Toufaily, J., 2024. Development of a Novel Adsorbent Derived from Olive Mill Solid Wastes for Enhanced Removal of Methylene Blue. Materials (Basel). 17, 4326. https://doi.org/10.3390/ma17174326

Haris, M., Amjad, Z., Usman, M., Saleem, A., Dyussenova, A., Mahmood, Z., Dina, K., Guo, J., Wang, W., 2024. A review of crop residue-based biochar as an efficient adsorbent to remove trace elements from aquatic systems. Biochar 6, 47. https://doi.org/10.1007/s42773-024-00341-2

Hossain, N., Nizamuddin, S., Griffin, G., Selvakannan, P., Mubarak, N.M., Mahlia, T.M.I., 2020. Synthesis and characterization of rice husk biochar via hydrothermal carbonization for wastewater treatment and biofuel production. Sci. Rep. 10, 18851. https://doi.org/10.1038/s41598-020-75936-3

Ifguis, O., Bouhdadi, R., Ziat, Y., George, B., Mbarki, M., 2022. Characterization and Analysis of Argania spinosa Shells from Souss-Massa Area: Application in the Adsorption of Methylene Blue in Aqueous Solution. J. Nanomater. 2022, 1–14. https://doi.org/10.1155/2022/6403838

Ji, W., Jin, H., Wang, H., Tabassum, S., Lou, Y., Fan, X., Ren, M., Wang, J., 2025. Elucidating the dominant role of π–π interactions in methylene blue removal via porous biochar: A synergistic approach of experimental and theoretical mechanistic insights. Colloids Surfaces A Physicochem. Eng. Asp. 715, 136615. https://doi.org/10.1016/j.colsurfa.2025.136615

Kasambala, H.R., Rwiza, M.J., Mpumi, N., Mwema, M.F., Njau, K.K., 2025. Biochars derived from banana and mango peels in isolated systems revealed high removal efficiency of endocrine-disrupting compounds from water. Biomass Convers. Biorefinery 15, 13575–13588. https://doi.org/10.1007/s13399-024-06196-8

Kataya, G., Issa, M., Badran, A., Cornu, D., Bechelany, M., Jellali, S., Jeguirim, M., Hijazi, A., 2025. Dynamic removal of methylene blue and methyl orange from water using biochar derived from kitchen waste. Sci. Rep. 15, 29907. https://doi.org/10.1038/s41598-025-14133-6

Khater, E.-S., Bahnasawy, A., Hamouda, R., Sabahy, A., Abbas, W., Morsy, O.M., 2024. Biochar production under different pyrolysis temperatures with different types of agricultural wastes. Sci. Rep. 14, 2625. https://doi.org/10.1038/s41598-024-52336-5

Kundu, D., Sharma, P., Bhattacharya, S., Gupta, K., Sengupta, S., Shang, J., 2024. Study of methylene blue dye removal using biochar derived from leaf and stem of Lantana camara L. Carbon Res. 3, 22. https://doi.org/10.1007/s44246-024-00108-1

Lustosa Filho, J.F., da Silva, A.P.F., Costa, S.T., Gomes, H.T., de Figueiredo, T., Hernández, Z., 2024. Biochars Derived from Olive Mill Byproducts: Typology, Characterization, and Eco-Efficient Application in Agriculture—A Systematic Review. Sustain. 16. https://doi.org/10.3390/su16125004

Mahdi, Z., Hanandeh, A. El, Yu, Q., 2017. Influence of Pyrolysis Conditions on Surface Characteristics and Methylene Blue Adsorption of Biochar Derived from Date Seed Biomass. Waste and Biomass Valorization 8, 2061–2073. https://doi.org/10.1007/s12649-016-9714-y

Méndez, A., Paz-Ferreiro, J., Araujo, F., Gascó, G., 2014. Biochar from pyrolysis of deinking paper sludge and its use in the treatment of a nickel polluted soil. J. Anal. Appl. Pyrolysis 107, 46–52. https://doi.org/10.1016/j.jaap.2014.02.001

Mortada, W.I., Ghaith, M.M., Khedr, N.E., Ellethy, M.I., Mohsen, A.W., Shafik, A.L., 2024. Mesoporous magnetic biochar derived from common reed (Phragmites australis) for rapid and efficient removal of methylene blue from aqueous media. Environ. Sci. Pollut. Res. 31, 42330–42341. https://doi.org/10.1007/s11356-024-33860-3

Muigai, H.H., Bordoloi, U., Hussain, R., Ravi, K., Moholkar, V.S., Kalita, P., 2021. A comparative study on synthesis and characterization of biochars derived from lignocellulosic biomass for their candidacy in agronomy and energy applications. Int. J. Energy Res. 45, 4765–4781. https://doi.org/10.1002/er.6092

Nautiyal, P., Subramanian, K.A., Dastidar, M.G., 2017. Experimental Investigation on Adsorption Properties of Biochar Derived from Algae Biomass Residue of Biodiesel Production. Environ. Process. 4, 179–193. https://doi.org/10.1007/s40710-017-0230-2

Nawaz, A., & Razzak, S. A. 2025. Synergism, pyrolysis performance, product distribution and characteristics in the co-pyrolysis of date palm waste and polyethylene foam: Harnessing the potential of plastics and biomass valorization. Carbon Resources Conversion, 8(3), 100312. https://doi.org/10.1016/j.crcon.2025.100312

Nawaz, A., Rohman, G.A.N., Jameel, A.G.A., Ummer, A.C., Razzak, S.A., 2024. Engineered biochar-based catalytic pyrolysis of Spirulina plantensis microalgae for the production of high value compounds in microwave reactor. Algal Res. 81, 103583. https://doi.org/10.1016/j.algal.2024.103583

Nawaz, A., Singh, B. & Kumar, P. 2023. H3PO4-modified Lagerstroemia speciosa seed hull biochar for toxic Cr(VI) removal: isotherm, kinetics, and thermodynamic study. Biomass Conv. Bioref. 13, 7027–7041. https://doi.org/10.1007/s13399-021-01780-8

Panizio, R., Castro, C., Pacheco, N., Assis, A.C., Longo, A., Vilarinho, C., Teixeira, J.C., Brito, P., Gonçalves, M., Nobre, C., 2024. Investigation of biochars derived from waste lignocellulosic biomass and insulation electric cables: A comprehensive TGA and Macro-TGA analysis. Heliyon 10, e37882. https://doi.org/10.1016/j.heliyon.2024.e37882

Rabichi, I., Sekkouri, C., Yaacoubi, F.E., Ennaciri, K., Izghri, Z., Bouzid, T., El Fels, L., Baçaoui, A., Yaacoubi, A., 2024a. Experimental and Theoretical Investigation of Olive Mill Solid Waste Biochar for Vanillic Acid Adsorption Using DFT/B3LYP Analysis. Water, Air, Soil Pollut. 235, 369. https://doi.org/10.1007/s11270-024-07183-5

Rabichi, I., Yaacoubi, F.E., Sekkouri, C., Ezzahi, K., Ennaciri, K., Fels, L. El, Mohamed, H., Baçaoui, A., Yaacoubi, A., 2024b. Optimizing Biochar Preparation for Eco-friendly Adsorption of Polyphenols and Organic Compounds in Pilot-scale: an Application of Doehlert Designs. Biomass Convers. Biorefinery. https://doi.org/10.1007/s13399-024-06031-0

Rago, Y.P., Surroop, D., Mohee, R., 2018. Assessing the potential of biofuel (biochar) production from food wastes through thermal treatment. Bioresour. Technol. 248, 258–264. https://doi.org/10.1016/j.biortech.2017.06.108

Regti, A., Laamari, M.R., Stiriba, S.-E., El Haddad, M., 2017. Use of response factorial design for process optimization of basic dye adsorption onto activated carbon derived from Persea species. Microchem. J. 130, 129–136. https://doi.org/10.1016/j.microc.2016.08.012

Ren, Y., Geng, W., Xu, R., Wang, P., Zhao, H., 2025. Tuning Electronic and Pore Structures of Biochar via Nitrogen and Magnesium Doping for Superior Methylene Blue Adsorption: Synergistic Mechanisms and Kinetic Analysis. ACS Omega 10, 31679–31692. https://doi.org/10.1021/acsomega.5c02636

Saeed, A.A.H., Harun, N.Y., Sufian, S., Siyal, A.A., Zulfiqar, M., Bilad, M.R., Vagananthan, A., Al-Fakih, A., Ghaleb, A.A.S., Almahbashi, N., 2020. Eucheuma cottonii Seaweed-Based Biochar for Adsorption of Methylene Blue Dye. Sustainability 12, 10318. https://doi.org/10.3390/su122410318

Šarović, K., Klaić, Z.B., 2023. Effect of Climate Change on Water Temperature and Stratification of a Small, Temperate, Karstic Lake (Lake Kozjak, Croatia). Environ. Process. 10, 49. https://doi.org/10.1007/s40710-023-00663-6

Stamou, A., Mitsopoulos, G., Koutroulis, A., 2024. Proposed Methodology for Climate Change Adaptation of Water Infrastructures in the Mediterranean Region. Environ. Process. 11, 12. https://doi.org/10.1007/s40710-024-00691-w

Suganuma, S., Nakajima, K., Kitano, M., Yamaguchi, D., Kato, H., Hayashi, S., Hara, M., 2008. Hydrolysis of Cellulose by Amorphous Carbon Bearing SO 3 H, COOH, and OH Groups. J. Am. Chem. Soc. 130, 12787–12793. https://doi.org/10.1021/ja803983h

Tan, Z., Zou, J., Zhang, L., Huang, Q., 2018. Morphology, pore size distribution, and nutrient characteristics in biochars under different pyrolysis temperatures and atmospheres. J. Mater. Cycles Waste Manag. 20, 1036–1049. https://doi.org/10.1007/s10163-017-0666-5

Tran, H.N., You, S., Chao, H., 2016. Effect of pyrolysis temperatures and times on the adsorption of cadmium onto orange peel derived biochar. Waste Manag. Res. J. a Sustain. Circ. Econ. 34, 129–138. https://doi.org/10.1177/0734242X15615698

Uchimiya, M., Wartelle, L.H., Klasson, K.T., Fortier, C.A., Lima, I.M., 2011. Influence of Pyrolysis Temperature on Biochar Property and Function as a Heavy Metal Sorbent in Soil. J. Agric. Food Chem. 59, 2501–2510. https://doi.org/10.1021/jf104206c

Uzoagba, C.E.J., Okoroigwe, E., Kadivar, M., Anye, V.C., Bello, A., Ezealigo, U., Odette Ngasoh, F., Pereira, H., Azikiwe Onwualu, P., 2024. Characterization of Wood, Leaves, Barks, and pod wastes from Prosopis africana biomass for biofuel production. Waste Manag. Bull. 2, 172–182. https://doi.org/10.1016/j.wmb.2024.07.007

Vafakish, B., Babaei-Ghazvini, A., Acharya, B., 2025. Unraveling the mechanisms of methylene blue adsorption onto biochar: a robust and sustainable approach for water remediation. Int. J. Environ. Sci. Technol. 22, 7053–7064. https://doi.org/10.1007/s13762-024-06111-8

Wang, J., Tan, Y., Yang, H., Zhan, L., Sun, G., Luo, L., 2023. On the adsorption characteristics and mechanism of methylene blue by ball mill modified biochar. Sci. Rep. 13, 21174. https://doi.org/10.1038/s41598-023-48373-1

Wang, S., Dai, G., Yang, H., Luo, Z., 2017. Lignocellulosic biomass pyrolysis mechanism: A state-of-the-art review. Prog. Energy Combust. Sci. 62, 33–86. https://doi.org/10.1016/j.pecs.2017.05.004

Wang, Z., Nie, Q., Lei, Z., Zhang, Z., Shimizu, K., Yuan, T., 2024. Enhanced Pb(II) removal from wastewater by co-pyrolysis biochar derived from sewage sludge and calcium sulfate: Performance evaluation and quantitative mechanism analysis. Sep. Purif. Technol. 329, 125124. https://doi.org/10.1016/j.seppur.2023.125124

Yaacoubi, F.E., Sekkouri, C., Ennaciri, K., Rabichi, I., Izghri, Z., Baçaoui, A., Yaacoubi, A., 2024. Synthesis of composites from activated carbon based on olive stones and sodium alginate for the removal of methylene blue. Int. J. Biol. Macromol. 254, 127706. https://doi.org/10.1016/j.ijbiomac.2023.127706

Yang, X., Igalavithana, A.D., Oh, S.-E., Nam, H., Zhang, M., Wang, C.-H., Kwon, E.E., Tsang, D.C.W., Ok, Y.S., 2018. Characterization of bioenergy biochar and its utilization for metal/metalloid immobilization in contaminated soil. Sci. Total Environ. 640–641, 704–713. https://doi.org/10.1016/j.scitotenv.2018.05.298

Yazid, H., Grich, A., Naboulsi, A., Bouzid, T., El mersly, L., mountassir El mouchtari, E., Abdelmajid, R., El himri, M., Rafqah, S., El haddad, M., 2025. Enhancing adsorption efficiency of pharmaceutical pollutants using activatedcarbon derived from walnut shells: Investigating experimental design, mechanisms, and DFTCalculations. Diam. Relat. Mater. 153, 112077. https://doi.org/10.1016/j.diamond.2025.112077

Yu, S., Park, Jinje, Kim, M., Ryu, C., Park, Jungkeuk, 2019. Characterization of biochar and byproducts from slow pyrolysis of hinoki cypress. Bioresour. Technol. Reports 6, 217–222. https://doi.org/10.1016/j.biteb.2019.03.009

Zhang, H., Chen, C., Gray, E.M., Boyd, S.E., 2017. Effect of feedstock and pyrolysis temperature on properties of biochar governing end use efficacy. Biomass and Bioenergy 105, 136–146. https://doi.org/10.1016/j.biombioe.2017.06.024

Zhang, J., Liu, J., Liu, R., 2015. Effects of pyrolysis temperature and heating time on biochar obtained from the pyrolysis of straw and lignosulfonate. Bioresour. Technol. 176, 288–291. https://doi.org/10.1016/j.biortech.2014.11.011

Zhu, Y., Yi, B., Yuan, Q., Wu, Y., Wang, M., Yan, S., 2018. Removal of methylene blue from aqueous solution by cattle manure-derived low temperature biochar. RSC Adv. 8, 19917–19929. https://doi.org/10.1039/C8RA03018A

Chapter III – Integration of Biochar in Pilot-Scale Column Filtration Systems and Constructed Wetlands as low-cost and sustainable substrates for improving Wastewater Treatment

III-I. Optimizing Biochar-Based Column Filtration Systems for Enhanced Pollutant Removal in Wastewater Treatment: A Preliminary Study

This work was published as a research paper:

El Barkaoui, S., Mandi, L., Fichera, M., Ryah, H., Baçaoui, A., Del Bubba, M., & Ouazzani, N. (2025). Optimizing biochar-based column filtration systems for enhanced pollutant removal in wastewater treatment: A preliminary study. Chemosphere, 372, 144067. https://doi.org/10.1016/j.chemosphere.2025.144067.

Abstract

This study aims to test the efficiency of biochar-based substrates in removing chemical and bacteriological pollutants from wastewater and to determine the optimal percentage of biochar (BC) to implement for large-scale filters (e.g., constructed wetlands). So, a preliminary test was conducted on a lab column scale for wastewater treatment of decanted wastewater using column filtration systems (CFS) integrated with BC (BC-based CFSs) at different concentrations (0%, 10%, 25%, and 50%). The BC used here was produced from exhausted olive pomace (pyrolised at T 590 °C, residence time of 2 h, and a heating rate of 10 °C min^{-1}). The results revealed that the BC incorporated into the CFS improved the efficiency of nitrogen species removal (total nitrogen (TN) 64-65%, total kjeldahl nitrogen (TKN) 75% - 77%, organic nitrogen (ON) 78% - 87%, and NH_4^+-N 57% - 69%); phosphorus species (total phosphorus (TP) 39% - 44%, PO_4^{3-} 38% - 42%); total and soluble chemical oxygen demand (TCOD (44% - 56%), and SCOD (33% - 51%) respectively); and total suspended solids (TSS) 87% - 92%, compared to the control filter (CFS0). Bacteriological analysis focused on faecal bacteria indicators, including total coliforms (TC), faecal coliforms (FC), faecal streptococci (FS), as well as the pathogen *Staphylococcus* (SP) and total aerobic mesophilic flora (TAMF). The highest removal efficiencies were observed for CFS10. Based on this preliminary study, the efficiency of CFS in removing pollutants from wastewater is optimal with a small amount of BC (10%) from both water quality and economic points of view.

Keywords: Biochar concentration; Wastewater treatment; Column filtration systems; Optimization.

1. Introduction

In recent decades, biochar (BC) has become increasingly interesting as a low-cost adsorbent due to the abundance of surface functional groups and high surface area (El Barkaoui et al., 2023). BC derived from the pyrolysis of various feedstocks, such as agricultural waste, is a carbon-rich material. Its production cost is lower than that of activated carbon, due to the low-cost of the feedstock (Ahmad et al., 2014; Tran et al., 2016). Several research studies have demonstrated the ability of BC to remove various pollutants, including both organic and inorganic contaminants from wastewater, due to its porosity and chemical composition (Bakari et al., 2024; Ayadi et al., 2024).

The feedstock used to prepare the BC and the conditions under which the BC is prepared play an important role in the properties of the resulting BC, influencing its capacity to adsorb various pollutants (Yuan et al., 2011; Suliman et al., 2016; Yavari et al., 2016). The olive pomace (OP) is considered as one of the most available wastes in the Mediterranean area, due to the considerable production of olive oil. The OP is the waste product generated in the olive pomace oil industry following the OP drying and subsequent extraction of the OP oil, representing around 2% of its mass (Gómez-Cruz et al., 2020). The recycling of OP into BC can be a renewable solution for its

management. The analysis of the literature points out some papers dealing with the production of BC from OP via gasification or pyrolysis processes. Temperature, contact time, and heating rate of the thermal conversion process are key factors in determining the characteristics of BC and, consequently, the performance of wastewater treatment. Generally, the most commonly adopted methods for preparing OP-based BC for this purpose adopt temperatures between 400 and 600 °C and a contact time of 1-2 h, under an inert atmosphere, obtaining high yields of BC (El Barkaoui et al., 2023). For example, El Hanandeh et al., (2016) and Rbichi et al., (2024) prepared BC from OP under limited oxygen concentrations, at about 550-600 °C for 90 min, using a heating rate of 10-15 °C min^{-1}, obtaining yields as high as 25-30%.

To our knowledge, only a few papers have been published focusing on the application of OP-based BC for pollutant removal. Most of these articles deal with the removal of inorganic elements (Abdelhadi et al., 2017; Mannaï et al., 2022), methylene blue (Tayibi et al., 2021), polyphenols (Abid et al., 2022), and emerging contaminants (Delgado-Moreno et al., 2021) in lab-scale batch experiments, while only two studies focused on the integration of OP-based BC in filtering systems (El Hanandeh et al., 2017; 2018). In these researches the authors investigated the effect of the addition of OP-based BC into sand media of column filtration systems (CFSs) for the removal of phosphorus and ammonia. Their results demonstrated that the addition of BC into the CFS substrate had a slight effect on phosphate and ammonium elimination but significantly enhanced nitrate elimination. However, there is no information in the literature on the effect of adding different percentages of OP-based BC to the CFS substrate on the removal efficiency of these systems, and data on organic matter (i.e., organic carbon and nitrogen), nitrite nitrogen, and pathogen removal are completely missing.

Based on the aforementioned considerations, the main objective of this study was to evaluate the efficiency of incorporating different percentages of OP-derived BC into sand media as an interlayer in CFSs for the removal of several chemical and microbiological water quality parameters. In more detail, chemical oxygen demand (COD), the entire nitrogen and phosphorus cycles, hardness, total coliforms (TC), faecal coliforms (FC), faecal streptococci (FS), staphylococci (SP), and total aerobic mesophilic flora (TAMF) were investigated in influent and effluent wastewater of CFSs integrating 10%, 25%, and 50% OP-based BC, in comparison with control.

2. Materials and methods

2.1. Preparation and characterization of biochar

BC was obtained from exhausted olive pomace using a slow pyrolysis process, heating the biomass at about 10 °C min^{-1} up to 590 °C, which was maintained for 2 h. The BC produced was characterized for its environmental compatibility through the analysis of the parameters mentioned in the European regulation EN 12915-1 for materials intended for water treatment (European Committee for Standardization, 2009), i.e., ash content (AC) and water-leachable concentrations of selected elements. Other characterizations included elemental analysis (C, H, N, O, and S), Fourier-transform infrared spectroscopy (FT-IR), pH of zero-charge point (pH_{PZC}), BET specific surface area (SSA), microporous and mesoporous SSA, and scanning electron microscopy/energy dispersive X-ray spectroscopy (SEM-EDX). The full description of the methods used is reported in the *Supplementary Material 2 (SM2)*, while the results obtained are shown in **Figures SM2-1**, **SM2-2**, **SM2-3**, **SM2-4**, and **Tables SM2-1** and **SM2-2** of the same supplementary section.

2.2. Laboratory-scale microcosm

The experimental set-up is described in **Figure III-1** and consists of four polyvinyl chloride (PVC) filtration columns with an internal diameter of 7.5 cm, a surface area of 0.004 m^2, and a total height of 45 cm each. The columns contain a 30 cm filter bed, supported by two 8 cm drainage gravel layers, one at the top (2–6 mm diameter) and one at the bottom of the biofilter (2–8 mm diameter). A 14 cm layer of BC and sand (diameter: 2-5 mm, and 1-2 mm, respectively, **Figure SM2-5**) was placed as an interlayer substrate in all filter beds (except the control CFS with 100% sand) to prevent the BC from floating, with different BC doses (10%, 25%, and 50%). Sand was adopted as the main filling medium since it is inexpensive, characterized by higher hydraulic conductivity compared to soil, and therefore suitable to be used in biofilters treating wastewater (Martikainen, 2023). In this study, the sand was collected from a riparian zone in Rehamna. The lowest level of supernatant water was regulated using an overflow weir placed at a height of 15 cm above the filter bed.

The study started in July and lasted approximately 6 months. All CFS operated in sequential batch filling and empty mode (3 batches/d), with a total volume of 1 L/d, and an organic loading rate of approximately 51 g of COD/m^2/d (i.e., about 2.3 m^2/P.E., considering 1 P.E. = 120 g of COD).

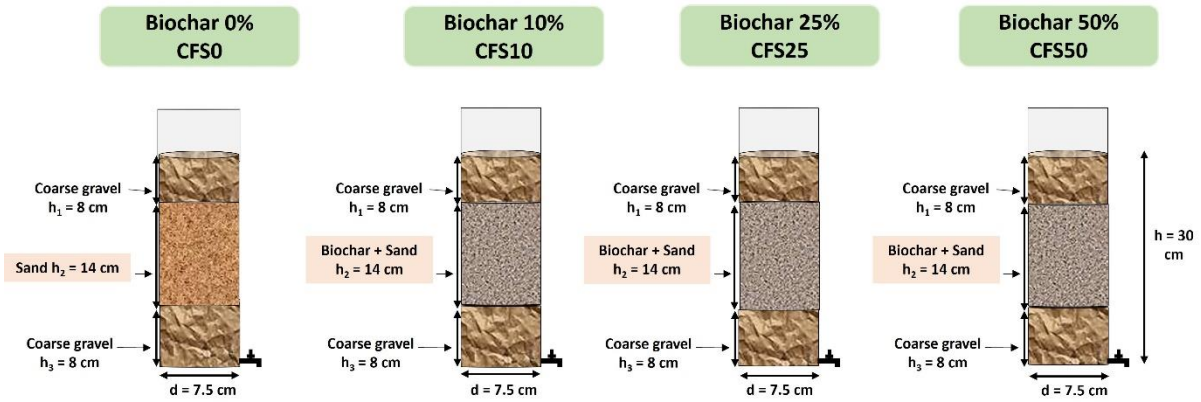

Figure III-1: Schematic illustration of the column filtration systems.

2.3. Water sampling and analysis

The sources of wastewater used for the operation in this study came from the Marrakech Wastewater Treatment Plant (WWTP) after primary sedimentation (decanted wastewater). The influent and effluent wastewater samples were collected every 15 days and immediately analysed after sampling. **Table III-1** shows the detailed characteristics of the influent throughout the entire experimental period.

Values of pH, electrical conductivity (EC), and dissolved oxygen (DO) were measured using a HI 9829 multi-parameter probe (HANNA, Woonsocket, RI, USA). For the determination of total suspended solids (TSS), samples were filtered through a Millipore (Burlington, MA, USA) glass fibre filter (0.45 µm), followed by drying of the collected residue at 105 °C until a stable weight was obtained (AFNOR-T90-105) (AFNOR, 1997); total and soluble COD (TCOD and SCOD, respectively) were determined through a digestion process, followed by the colorimetric method using dichromate after filtration of TSS for SCOD (AFNOR-T90-101) (AFNOR, 1997); TP was determined by using the molybdate and ascorbic acid method after potassium peroxydisulfate digestion (AFNOR-T90-023) (AFNOR, 1997); PO_4^{3-} was determined by the ascorbic acid and molybdate method (AFNOR-T90-022). Total Kjeldahl nitrogen (TKN) was measured using Kjeldahl mineralization followed by distillation of ammonium and a final acidimetric titration. The organic nitrogen (ON) was calculated as the difference between NH_4^+-N and TKN (ON = TKN - NH_4^+-N) (Rodier, 2009); the total nitrogen (TN) was determined by sum of ON, NH_4^+–N, NO_2^--N, and NO_3^--N (Rodier, 2009); NH_4^+–N was analysed using the indophenol method (AFNOR-T90-015) (AFNOR, 1997); NO_2^--N was determined by the colorimetric method after diazotation (AFNOR T 90-013) (AFNOR, 1997); NO_3^--N was transformed into NO_2^--N after passing through a copper and cadmium column (Rodier, 2009) and analysed as specified above.

Sulphates were analysed using the nephelometric method (Rodier, 2009). Total hardness (TH), calcium, and magnesium were determined simultaneously using the EDTA titrimetric method (Rodier, 2009).

Total and faecal coliform (TC and FC, respectively) were counted in accordance with AFNOR standard NF EN ISO 9308-1 (AFNOR, 1997) using TTC Tergitol medium. Petri dishes of TC and FC were incubated at 37°C and 44.5°C, respectively, for 24 hours, after which the number of colony-forming units was counted. Faecal streptococci (FS) enumeration was performed according to the AFNOR NF ISO 7899-2 method (AFNOR, 1997) using BEA medium. The Petri dishes were incubated at 44.5 °C for 24 h, and then the number of colonies was counted. Specific pathogens such as *Staphylococcus* (SP) and Total Aerobic Mesophilic Flora (TAMF) were also included, using Chapman and PCA agar as culture medium to enumerate SP and TAMF, respectively. And were both incubated at 37 °C for 24 h. Each test was repeated three times to ensure accuracy and to minimize errors. Bacterial concentrations in inlet and outlet samples were determined by using the dilution method, according to the Moroccan standard (2006). The bacterial removal efficiency was expressed by the following equation:

$$\log_{10} \text{removal} = \log (\text{influent/effluent})$$

2.4. Statistical analysis

All experimental data in this study were expressed as triplicate means with standard deviations. Statistical analyses were performed using Minitab (State College, PA, USA) version 17.1.0, which included analysis of variance (ANOVA). Significance levels were reported as insignificant or significant, according to a 5% probability level. The Fisher and Games-Howell tests were used depending on the results of the homogeneity tests for variance.

3. Results and discussion

3.1. Characteristics of biochar

The physicochemical and morphological properties of the BC are summarized in **Figures SM2-1**, **SM2-2**, **SM2-3**, and **SM2-4**, and **Tables SM2-1** and **SM2-2** of the *Supplementary Material 2*.

According to the data of proximate analyses, the BC had 13% volatile matter (VM) and 5% AC, the latter complying with the EN 12915-1 standard regulation concerning water treatment, which sets a limit of 15%, since a high AC in filter medium is predicted to decrease adsorption capacity

(Castiglioni et al., 2022). The elemental analysis showed that carbon was the main element in BC (> 90%, **Table SM2-1**), followed by O (6.6%), N (1.3%), and H (2%), thus pointing out the high quality of the material. Thus, OP-BC was characterized by low O/C (0.054), H/C (0.26), and (O + N)/C (0.067) ratios, indicating a high degree of carbonization with highly condensed aromatic ring systems (Zhu et al., 2015; Abdul et al., 2017), the hydrogen loss due to the breaking of weaker bonds within the BC structure (Li et al., 2018), and a limited number of functional groups. Consequently, OP-BC is expected to exhibit high chemical stability against microbial degradation and qualify it as a suitable filtration media for wastewater treatment (Kaetzl et al., 2020).

The SEM/EDX analysis substantially confirmed the results of the elemental analysis, since it highlighted that carbon was by far the most abundant element, as illustrated in **Figure SM2-2A** and **Table SM2-2**. The SEM images (**Figure SM2-1A**) clearly showed the existence of a heterogeneous structure and irregular forms of the BC surface. Moreover, the SEM image also showed some small granular and rough particles on the surface, as well as the presence of some mesopores (2-50 nm), which are important for determining a high surface area and adsorption ability of the material.

The OP-BC was characterized by a SSA of 106 m^2 g^{-1} (**Table SM2-1**), which is much higher than the range of data reported in literature for BC from OP (approximately 1-49 m^2 g^{-1}), used in wastewater treatment (Hanandeh et al., 2016; Tayibi et al., 2021). According to the BJH model, the OP-BC was mainly mesoporous, thus being suitable to retain a wide range of contaminants (Ayadi et al., 2024). SSA is a critical factor in assessing the suitability of a material for use in wastewater filtration, since a larger surface area indicates a higher potential for adsorption and biofilm development. Within this biofilm, processes such as biological degradation, mineralization of organic matter, nitrification, and denitrification can occur (Perez-Mercado et al., 2018).

The FT-IR spectrum of BC used in this work is reported in **Figure SM2-3**. The spectrum showed significantly wide bands in the 3700–3000 cm^{-1} region, indicating the presence of hydroxyl functional groups (-OH) and/or carboxylic acids originating from aliphatic and phenolic components (Liu et al., 2015). The presence of bands at 2842 cm^{-1} and 2916 cm^{-1} can be attributed to the stretching of the C-H bond in aliphatic compounds (Zhang et al., 2013). The appearance of a band at 1620 cm^{-1} can be attributed to the stretching of a C=O group conjugated with a C=C or an aromatic ring, as well as the aromatic ring itself (Del Bubba et al., 2020), while the one at 1550

cm^{-1} could be related to the stretching of C=C in an aliphatic structure (Rabichi et al., 2024). The band at 1374 cm^{-1} is in agreement with the presence of the stretching of C-O groups and confirms the oxygen content of the material (Rabichi et al., 2024). The existence of a band at 1030 cm^{-1} may be associated with C-O aliphatic ethers (Delgado-Moreno et al., 2021), while the signals between 831 and 872 cm^{-1} could be due to the presence of aromatic C-H and O-H deformation in carboxyls on aromatic ring. (Delgado-Moreno et al., 2021; Rabichi et al., 2024). Based on these findings, OP-BC contained aromatic and oxygenated moieties, thus being suitable to provide efficient sorption interactions.

The pH_{PZC} of the BC was 7.8 (**Figure SM2-4**), which is very close to the pH of the inlet wastewater used in this study (7.6). This results in a material exhibiting a minimal net surface charge under these experimental conditions, resulting in a neutral behaviour towards the sorption of charged species (Alhothali et al., 2021; Ayadi et al., 2024).

3.2. Treatment performance in different CFSs

3.2.1. Physicochemical parameters

Table III-1 illustrates the behaviour of the physicochemical parameters (pH, EC, DO, and TSS) studied in the inlet and outlet of the four columns (CFS0, CFS10, CFS25, and CFS50). The average inlet pH was around 7.6. After treatment, alkalization was observed in the CFSs, which increased with the BC concentration in the medium (CFS0 (7.9), CFS10 (8.0), CFS25 (8.1), and CFS50 (8.1)). This alkalization may be attributed to biological oxidation or dilution of carbonate salts from BC, hydroxyls, and its strong H^+ exchange capacity (Chen et al., 2015), due to the high carbon element content (90%). This finding is consistent with the findings of Chen et al. (2021a; b) and Chand et al. (2021), which indicated that BC had superior acid neutralizing capacity compared to sand and gravel when exposed at influent pH values of 4.0 and 7.8. EC exhibited very similar values in the inlet and effluents of the four CFSs, indicating that the BC neither adsorbed nor released ions during treatment. This finding is in agreement with data reported elsewhere for constructed wetlands (CWs) and CFSs integrated with BC from different origins (Kaetzl et al., 2019; Kaetzl et al., 2020; Ayadi et al., 2024). The inlet DO concentration was zero throughout the whole study period. After treatment, DO concentrations increased up to about 2 mg L^{-1}, even without any active aeration. The outlet DO concentration can be explained by the fact that oxygen is derived from the water inflow and air reoxygenation, which is a key source of oxygen supply (Ye et al., 2012; Kasak et al., 2018). In addition, oxygen is supplied to CFSs via

diffusion during dry periods. In general, the DO concentration of the influent would be lower than that of the effluent due to oxygen consumption during the simultaneous oxidation of organic matter and nitrification (Fan et al., 2013; Kizito et al., 2017). The improvement in DO levels reflects the improved quality of wastewater after treatment (Nguyen et al., 2020). The pH, EC, and DO results obtained during treatment correspond to the Moroccan standard for the reuse of treated wastewater in agriculture (S.E.E.E, 2007).

Table III-1: Values (mean ± standard deviation) of water quality parameters measured in influent wastewater and CFS0, CFS10, CFS25, and CFS10 effluents. Different letters in each row mean statistically significant differences (P<0.05) according to Fisher or Games.

Parameters	Influent	Systems			
		CFS0	CFS10	CFS25	CFS50
pH	7.6 ± 0.4^{a}	7.9 ± 0.2^{b}	8.0 ± 0.3^{b}	8.1 ± 0.3^{b}	8.1 ± 0.3^{b}
EC (µS cm^{-1})	2360 ± 380^{a}	2370 ± 357^{a}	2391 ± 331^{a}	2305 ± 361^{a}	2289 ± 388^{a}
DO (mg L^{-1})	0.00^{a}	2 ± 1^{b}	2.4 ± 0.8^{b}	2.3 ± 0.9^{b}	2.1 ± 0.8^{b}
TSS mg L^{-1})	218 ± 65^{a}	49 ± 19^{b}	17 ± 10^{c}	24 ± 14^{c}	27 ± 15^{bc}
TCOD (mg L^{-1})	205 ± 70^{a}	132 ± 37^{b}	85 ± 44^{c}	111 ± 43^{bc}	108 ± 34^{bc}
SCOD (mg L^{-1})	130 ± 31^{a}	92 ± 15^{b}	66 ± 31^{c}	86 ± 19^{bc}	82 ± 12^{bc}
TP (mg L^{-1})	12 ± 3^{a}	8 ± 2^{b}	6 ± 1^{c}	7 ± 1^{bc}	7 ± 1^{bc}
PO_4^{3-}-P (mg L^{-1})	9 ± 2^{a}	6 ± 1^{b}	5 ± 2^{c}	5 ± 1^{bc}	5 ± 1^{bc}
TN (mg L^{-1})	171 ± 7^{a}	94 ± 7^{b}	64 ± 6^{c}	61 ± 8^{c}	58 ± 4^{c}
TKN (mg L^{-1})	169 ± 7^{a}	72 ± 6^{b}	38 ± 3^{c}	41 ± 3^{c}	42 ± 2^{c}
Organic N (mg L^{-1})	112 ± 24^{a}	47 ± 8^{b}	22 ± 15^{c}	14 ± 9^{c}	19 ± 10^{c}
NH_4^{+}-N (mg L^{-1})	61 ± 24^{a}	26 ± 9^{b}	17 ± 14^{c}	24 ± 11^{bc}	22 ± 9^{bc}
NO_2^{-}-N (mg L^{-1})	0.13 ± 0.07^{a}	4.2 ± 1^{bc}	6.2 ± 2^{d}	5 ± 1^{b}	3.3 ± 0.9^{c}
NO_3^{-}-N (mg L^{-1})	2 ± 1^{a}	16 ± 5^{bc}	20 ± 8^{c}	15 ± 7^{b}	13 ± 6^{b}
SO_4^{2-} (mg L^{-1})	72 ± 38^{a}	78 ± 30^{a}	78 ± 30^{a}	79 ± 33^{a}	75 ± 28^{a}
Total hardness (mg L^{-1})	327 ± 101^{a}	548 ± 92^{b}	552 ± 124^{b}	484 ± 99^{bc}	441 ± 97^{c}
Calcium (mg L^{-1})	49 ± 15^{a}	111 ± 21^{b}	113 ± 31^{b}	88 ± 18^{c}	72 ± 18^{c}
Magnesium (mg L^{-1})	278 ± 87^{a}	438 ± 78^{b}	439 ± 100^{b}	395 ± 84^{bc}	368 ± 83^{c}

TSS is one of the key parameters in determining the quality of an effluent and its potential for treated wastewater reuse in agriculture. In this study, all CFSs provided a high TSS removal, ranging from 74 to 92% (**Figure III-2**). More in detail, BC-based filters exhibited a significantly higher removal (87% - 92%) compared to the control (74%); furthermore, the removal in these filters was much more homogeneous than in the one filled with sand only. These results can be explained by a greater removal by the BC-based substrates of the colloidal particles present in the wastewater, due to the higher sorption properties of biochar compared to sand.

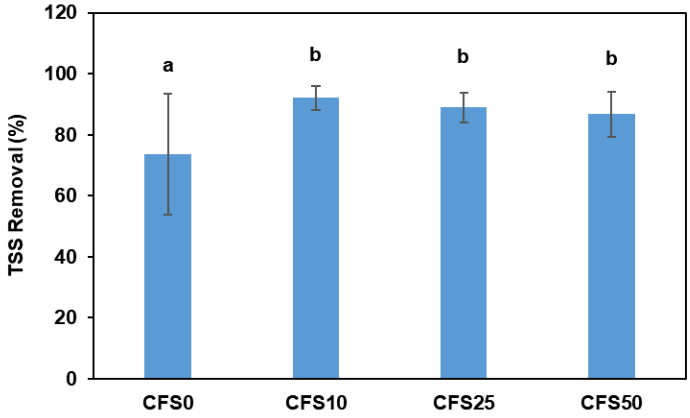

Figure III-2: Mean removal of total suspended solids in column filtration systems filled with sand (CFS0), and sand-biochar mixtures with 10% (CFS10), 25% (CFS25), and 50% (CFS50) of biochar.

3.2.2. COD removal

Figures III-3 and **SM2-6,** and **Table III-1** show the removal efficiency and the concentration of total and soluble organic carbon in the influent and effluent samples, evaluated through TCOD and SCOD. The trend of the TCOD is representative of some phenomena that occur in column filtration systems during different operating phases, i.e. (i) the initial lag phase of the biomass, which corresponds to very low efficiency of oxidation of organic matter, (ii) a summer phase of very good removal due to the very high temperatures that promote biological processes, and (iii) a winter phase with higher inlet concentrations of organic carbon, probably due to the higher tourist flow (**Figure SM2-6**). In overall terms, the mean concentrations of both parameters were significantly reduced by all systems, thus demonstrating the efficiency of CFSs in the removal of organic carbon, irrespective of the kind of substrate used for their implementation (**Table III-1**). Moreover, the systems filled with the sand-BC mixtures provided a general higher improvement of the removal efficiency (44% - 56% for TCOD and 33% - 51% for SCOD), compared to the CFS filled with sand only (33% and 27% for TCOD and SCOD, respectively). These results demonstrated the important role of BC addition in CFS, probably due to its porous structure, which promotes adsorption and creates a favourable environment for the microbial degradation of organic compounds (Deng et al., 2019). Moreover, the presence of functional groups on the surface of the material, such as chloro-, nitro-, hydroxyl, carbonyl, amine, and carboxylic acid, may improve the electrostatic adsorption of organic matter (de Rozari et al., 2015). Interestingly, CFS10 was (i) the best performing system, since it provided mean values of TCOD and SCOD removal higher than the other filters and (ii) the only one exhibiting a significantly better treatment

performance than the sand-based system (**Figure III-3**). The higher COD removal achieved with the lowest tested BC percentage is a result in accordance with findings reported elsewhere (Li et al., 2018; Zhou et al., 2018; Zhang et al., 2021), which pointed out a negative effect of increasing BC percentage on CFS treatment performance. This result could be ascribed to the release of soluble organic carbon from the BC (Deng et al., 2019) and/or to the toxicity of the material towards microorganisms. However, these effects are strongly dependent on the BC characteristics, as suggested by the positive correlation between BC percentage in the substrate and removal efficiency found by other authors (Deng et al., 2019) and the good results obtained also in the presence of 100% BC (Ayadi et al., 2024).

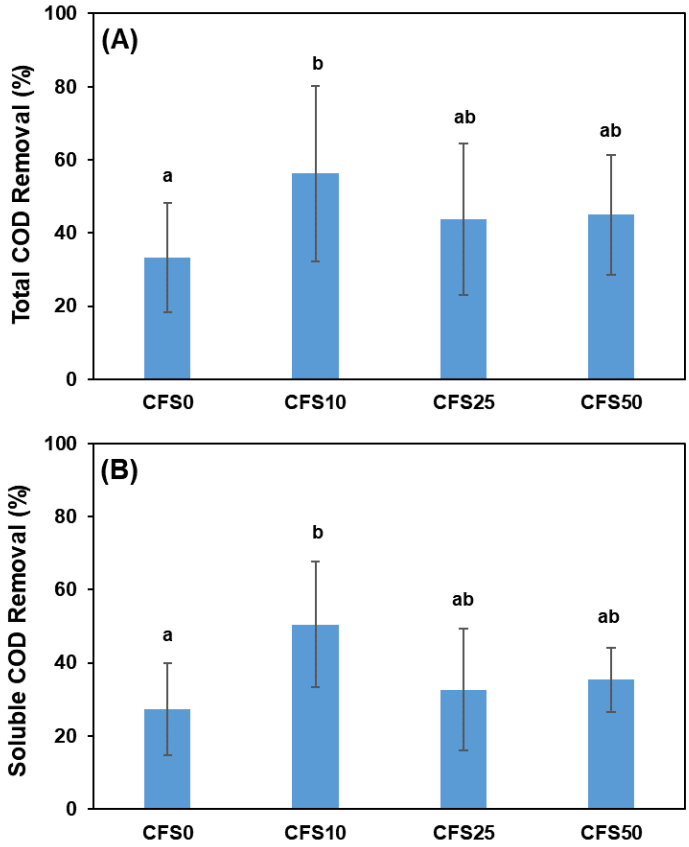

Figure III-3: Mean removal of total (A) and soluble (B) chemical oxygen demand in column filtration systems filled with sand (CFS0), and sand-biochar mixtures with 10% (CFS10), 25% (CFS25), and 50% (CFS50) of biochar.

3.2.3. Phosphorus removal

Figure III-4 illustrates the TP and PO_4^{3-} removal in the four CFSs, while **Table III-1** shows the

corresponding mean concentrations in the influent and effluent samples. The two phosphorus forms (TP and PO_4^{3-}) showed similar concentrations in the influent, pointing out a 25% contribution of the organic phosphorus to TP in settled wastewater. All BC-based systems provided P-removal slightly higher (about 10%) than the CFS filled with 100% sand, even though only CFS10 exhibited statistically significant differences compared to CFS0 for both TP and PO_4^{3-}, while for CFS50, a significantly higher removal was observed only for the latter parameter (**Figure III-4B**). These results are in agreement with findings reported elsewhere, which confirm the ability of BC to improve phosphorus removal (Yao et al., 2011; Ghezzehei et al., 2014; Zhang et al., 2021). For example, Zhang et al., (2021) investigated the removal of TP using four microcosms with different percentages of BC in the filling medium (25%, 50%, and 75% compared to a 100% gravel substrate), pointing out the positive effect of BC in slightly improving the performance of the treatment system. Indeed, many studies reported that BC has little ability to remove TP and PO_4^{3-} (Yao et al., 2012; de Rozari et al., 2016; El Barkaoui et al., 2023), and in some studies, no advantages for P removal were reported following the addition of BC to the substrate. For example, de Rozari et al., (2016) studied the removal of TP and PO_4^{3-} using BC-based microcosm with five ratios (5%, 10%, 15%, 20%, and 25% in comparison with 100% sand), showing no significant difference among the microcosms and even a slightly higher phosphorus removal of the 100% sandy microcosm. These conflicting results could be attributed to the fact that the properties of BC depend on the preparation conditions and raw material, which affect its ability to adsorb different chemicals (El Hanandeh et al., 2018).

In general, the main mechanisms of phosphorus removal in CFSs include physicochemical reactions due to substrates (such as precipitation, adsorption, ion exchange, and mineralization) and plant uptake (Wu et al., 2015). However, in this study, unplanted CFSs were tested, and therefore, the latter mechanism is not applicable. Based on concentrations of Ca, Mg, and P determined during the treatment and pH values of influent and effluent wastewater (**Table III-1**), precipitation of phosphorus as insoluble salts such as calcium apatite may be a plausible mechanism for P removal in all the investigated CFSs (Del Bubba et al., 2003). Furthermore, adsorption and ion exchange mechanisms can be responsible for the small increase in removal observed in BC-based filters (Li et al., 2016; Yin et al., 2017; Mohammadi et al., 2021).

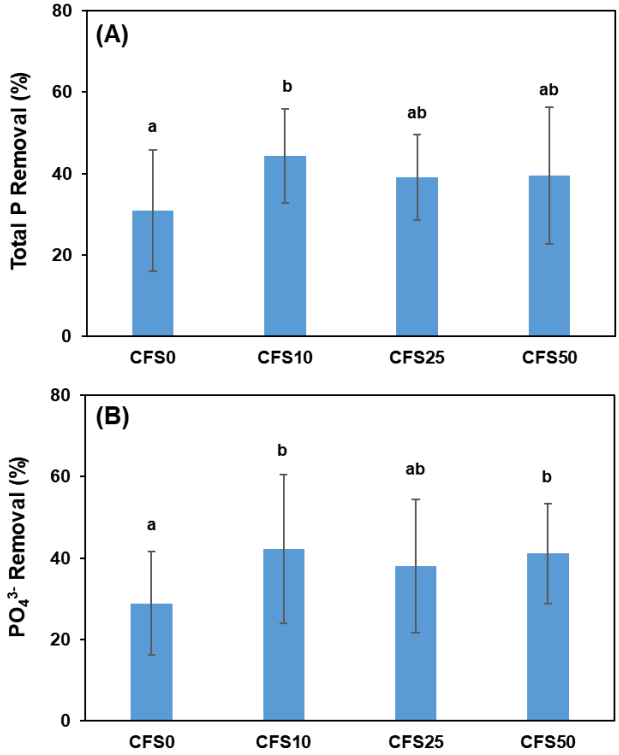

Figure III-4: Mean removal of total (A) and soluble (B) phosphorus in column filtration systems filled with sand (CFS0), and sand-biochar mixtures with 10% (CFS10), 25% (CFS25), and 50% (CFS50) of biochar.

3.2.4. Nitrogen Removal

Table III-1 illustrates how ON, NH_4^+-N, NO_2^--N, NO_3^--N, and TN change during the treatments. The data clearly highlighted that strong NH_4^+-N, ON (here determined as the difference between TKN and NH_4^+-N), and TN removal occurred in all systems (see **Figure III-5**). In general, the observed removal could be attributed to either biological or physicochemical mechanisms. However, it is well-known that in nature-based solutions for wastewater treatment, such as CW and CFSs, biological processes governing the nitrogen cycle are strongly active (Ma et al., 2023). Furthermore, the trend of NH_4^+-N removal as a function of operation time showed a short initial period of low performance, followed by a period of increasing treatment efficiency and a final phase of the experiment characterised by high and stable removal (**Figure SM2-7**). It should also be noted that, based on the biochar characteristics mentioned in section 3.1, the cation exchange mechanism should play a minor role in the removal of ionic species. Biological mechanisms should therefore be considered as responsible for the conversion of reduced and oxidised forms of nitrogen inside CFSs. The decrease observed for organic nitrogen can be attributed to the degradation of protein and other nitrogen-containing cell constituents. The nitrogen released may

be assimilated by the biomass and/or become ammonium nitrogen, which will undergo nitrification. Thus, the NH_4^+-N removal shown in **Figure III-5A**, which ranged from 53% to 69%, should be considered somewhat underestimated. In this context, BC played a significant role, as BC-based CFSs provided statistically lower TKN effluent concentrations (**Figure III-5B**), compared to control (i.e., CFS0). The nitrification of ammonia is a two-stage reaction that has nitrate and nitrite as final and intermediate products, respectively, the latter exhibiting a high toxicity to the fauna of water bodies (Ayadi et al., 2024). Therefore, nitrite concentrations in the effluent should be kept as low as possible and in any case below the legal limits of the interested country. In CFS effluents, nitrite and especially nitrate concentrations significantly increased, compared to the inlet, in accordance with the strong occurrence of the nitrification process. However, while effluent NO_3^--N concentrations (range 13-20 mg L^{-1}, see **Table III-1**) were below the toxicity levels reported for all aquatic species (Camargo et al., 2005), the concentrations of NO_2^--N (3.3-6.2 mg L^{-1}) were as high to exert toxic effects on fish fauna (Lewis and Morris, 1986). As reported by other authors, the incomplete oxidation of ammonia and the increased concentrations of nitrite ion are widely observed in CWs and CFSs, which can be explained by an insufficient availability of DO in the microcosms (Li et al., 2021; Lu et al., 2022; Ayadi et al., 2024), a condition that mainly influences the activity of nitrite-oxidising bacteria rather than microorganisms responsible for the conversion of ammonia into nitrite (Tan et al., 2013). Interestingly, for all the investigated microcosms, TN concentrations showed a decreasing trend during the treatment (**Table III-1**). It should also be noted that TN removal was significantly higher in BC-based microcosms than in the control system (**Figure III-5**). These findings demonstrated that denitrification occurred extensively in all systems and that BC significantly affected also this mechanism within the nitrogen cycle.

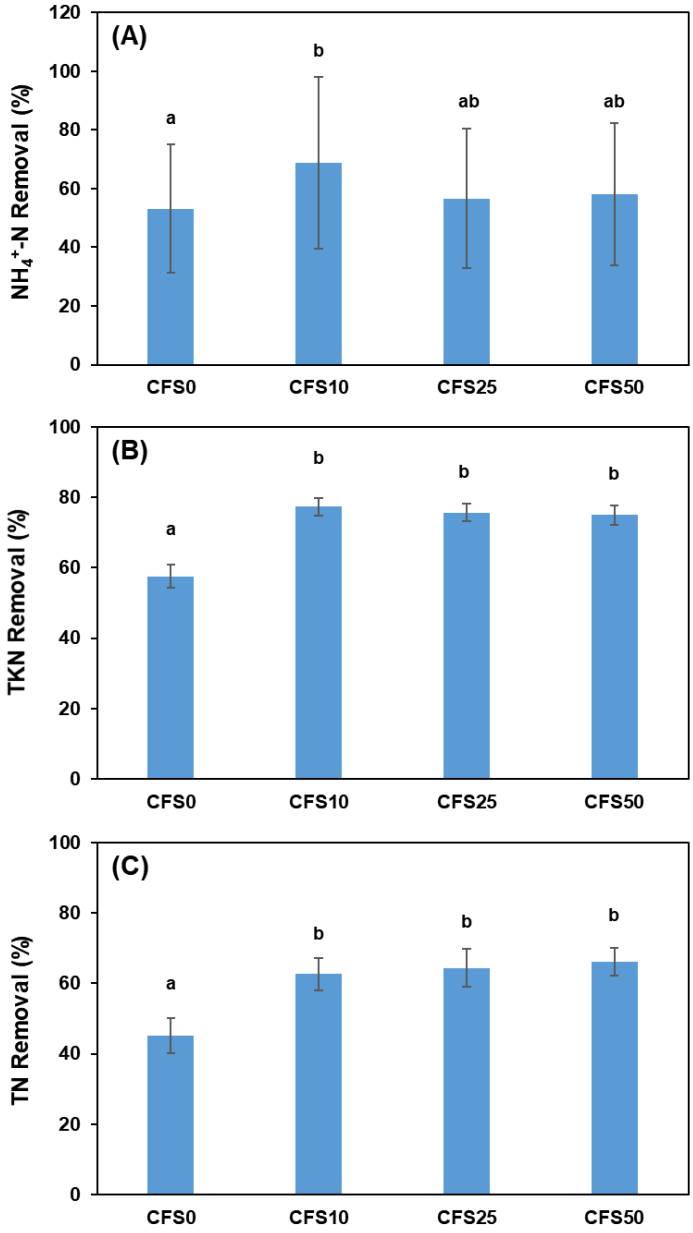

Figure III-5: Mean removal of ammonia (A) and total nitrogen (B) in column filtration systems filled with sand (CFS0), and sand-biochar mixtures with 10% (CFS10), 25% (CFS25), and 50% (CFS50) of biochar.

3.2.5. Sulphate, total hardness, Mg, and Ca removal

Table III-1 illustrates the sulphate, TH, Mg, and Ca concentrations in the influent and effluent samples. During the operation of CFSs, SO_4^{2-} showed no significant variation between the inlet and outlet samples. The slight increase in sulfate concentration after passing through the columns may be due to the oxidation of carbon-bound sulphur and the release of sulfate from the organic substrates used (Singh and Chakraborty, 2021).

In the present study, the concentration of TH, Ca, and Mg in the CFSs outlet samples significantly increased compared to the inlet concentrations (**Table III-1**), which contradicts some findings in the literature (Prajapati et al., 2018; Ghumra et al., 2021). Generally, the increase of TH, Ca, and Mg concentration could be due to dissolved minerals, or may be to the presence of carbonates and bicarbonates, contributing to temporary hardness, and sulphates and chlorides, which contribute to permanent hardness (Ramachandra et al., 2018). Otherwise, TH is caused by the dissolution of calcium and magnesium compounds present in the substrate (Prajapati et al., 2018; Ghumra et al., 2021).

The increase in TH, Ca, and Mg concentrations in the outlet samples corresponded to the increase in the amount of sand in the intermediate substrate (**Table III-1**). In addition, the EDX results show higher concentrations of calcium (6.68%) and magnesium (1.21%) (**Figure SM2-2B** and **Table SM2-2**). The release of these elements leads to an increase in Ca and Mg concentrations in the outlet samples, resulting in an increase in TH concentration.

3.2.6. Bacterial indicator and pathogens removal:

Bacterial pathogens, including TC, FC, FS, as well as the pathogen SP and TAMF, were monitored at the inlet and outlet of the four CFSs (**Table III-2**). These parameters showed higher concentrations in the influent sample; The effluent samples showed a not very significant decrease in TC, FC, FS, PS, and TAMF concentrations. All the filters showed very moderate removal efficiency that did not exceed 1 log unit. Normally, BC has a high specific surface area, high porosity, numerous pores of different sizes, and hydrophobicity that may make it more appropriate than gravel or sand for the elimination of microbial contaminants (El Barkaoui et al., 2023). Kaetzl et al., (2019) reported that CWs filled with rice husk-derived BC present better removal yield of bacteriophages and faecal indicator bacteria from municipal wastewater than CWs filled with sand. El Ghadraoui et al., (2020) investigated the removal efficiency of TC, FC, and FS using CW-based pozzolan, which removed 2.76 log units for TC, 2.56 log units for FC and 3.87 log units for FS. Sleytr et al., (2007) studied bacterial removal in CW and achieved a removal efficiency of 4,37 and 4,31 log units for FC and TC removal, respectively. According to Hijnen et al., (2004), E. coli and thermotolerant coliforms were removed at full-scale and in the pilot plant with 2-3 log units. In most cases, the removal of pathogens in the filter is achieved through the combined effects of chemical, physical, and biological processes. The main physical processes include filtration, sedimentation, and sorption onto organic matter and media. However, the chemical processes include oxidation. While the biological processes include biofilm retention,

natural die-off, competition under nutrient-limited conditions, and predation (Wu et al., 2016). The low efficacy to remove microbial pollutants in our case could be related to low biofilm development during the short time of the experiment. The development of the biofilm inside the filter could improve the filtration processes by decreasing the porosity of the filter. Particle deposition leads to progressively decreasing filter pore size, and the removal efficiency of screening increases with time and the maturity of the biofilm. Logan et al., (2001) reported that the size of the grain is a significant variable affecting the cryptosporidium cysts removal and potentially other pathogens in slow sand filters.

On the other hand, the depth of the filter and low retention time could also explain the findings. Torrens et al., (2009) achieved only 1.9 log units in vertical flow CW. According to the same authors, the depth of the filter affected the removal efficiency for all the pollutants; Deeper filters showed higher removals due to the higher hydraulic retention time.

Table III-2: Concentrations (C, mean ± standard deviation) and average removal (R, log units) of the microbiological parameters for inlet and outlet samples.

Parameters		Inlet	CFS0	CFS10	CFS25	CFS50
Total coliform	C	4.5 ± 0.1^{a}	3.85 ± 0.03^{b}	3.6 ± 0.1^{c}	3.8 ± 0.2^{b}	3.9 ± 0.2^{b}
	R	n.a.	0.7 ± 0.1^{a}	0.9 ± 0.2^{b}	0.7 ± 0.1^{a}	0.60 ± 0.07^{a}
Faecal coliform	C	4.26 ± 0.08^{a}	3.74 ± 0.06^{bc}	3.31 ± 0.08^{d}	3.8 ± 0.1^{b}	3.62 ± 0.06^{c}
	R	n.a.	0.51 ± 0.07^{a}	0.95 ± 0.05^{b}	0.5 ± 0.1^{a}	0.6 ± 0.1^{a}
Faecal streptococci	C	3.64 ± 0.08^{a}	3.5 ± 0.1^{ab}	3.48 ± 0.04^{b}	3.03 ± 0.09^{c}	2.9 ± 0.1^{c}
	R	n.a.	0.12 ± 0.1^{a}	0.16 ± 0.07^{a}	0.6 ± 0.1^{b}	0.8 ± 0.1^{b}
Staphylococcus	C	2.93 ± 0.07^{a}	2.60 ± 0.09^{b}	1.48 ± 0.09^{c}	2.16 ± 0.05^{d}	2.0 ± 0.1^{e}
	R	n.a.	0.3 ± 0.2^{a}	1.4 ± 0.2^{b}	0.8 ± 0.1^{c}	0.9 ± 0.2^{c}
Total aerobic mesophilic flora	C	5.61 ± 0.05^{a}	5.24 ± 0.03^{b}	4.87 ± 0.04^{c}	5.04 ± 0.06^{d}	4.68 ± 0.04^{e}
	R	n.a.	0.37 ± 0.04^{a}	0.7 ± 0.1^{b}	0.57 ± 0.05^{c}	0.9 ± 0.1^{d}

n.a. = not applicable.

Conclusion

This study investigated the preparation of BC from olive pomace and its application in BC-based CFS. The results show that the incorporation of BC into sand media significantly improves the removal efficiency of pollutants in CFS compared to conventional sand-based filters. The best results were achieved at lower BC concentrations (10%), which resulted in improved removal rates. In particular, the high efficiency in NH_4^+-N removal supported nitrification processes, explaining the release of NO_3^--N. However, increasing BC concentrations resulted in a decrease in HT, Ca, and Mg due to the reduced proportion of sand, which naturally contains higher levels

of these elements. Despite these improvements, the system's ability to remove bacterial indicators and pathogens remained moderate related to not yet mature filtration column and its low deep reducing the hydraulic retention time. Overall, BC played different roles in removing different contaminants, suggesting that higher BC additions do not necessarily improve treatment performance. These findings will contribute to the sustainable design and operation of BC-based CFS systems.

References

Abdelhadi, S.O., Dosoretz, C.G., Rytwo, G., Gerchman, Y., Azaizeh, H., 2017. Production of biochar from olive mill solid waste for heavy metal removal. Bioresour. Technol. 244, 759–767. https://doi.org/10.1016/j.biortech.2017.08.013

Abdul, G., Zhu, X., Chen, B., 2017. Structural characteristics of biochar-graphene nanosheet composites and their adsorption performance for phthalic acid esters. Chem. Eng. J. 319, 9–20. https://doi.org/10.1016/j.cej.2017.02.074

Abid, N., Masmoudi, M.A., Megdiche, M., Barakat, A., Ellouze, M., Chamkha, M., Ksibi, M., Sayadi, S., 2022. Biochar from olive mill solid waste as an eco-friendly adsorbent for the removal of polyphenols from olive mill wastewater. Chem. Eng. Res. Des. 181, 384–398. https://doi.org/10.1016/j.cherd.2022.02.029

AFNOR, 1997. AFNOR, Recueil de Norme Française: Eau, Méthodes D'essai,. 2nd ed., Paris Édition, Paris,.

Ahmad, M., Upamali, A., Eun, J., Zhang, M., Bolan, N., Mohan, D., Vithanage, M., Soo, S., Sik, Y., 2014. Chemosphere Biochar as a sorbent for contaminant management in soil and water : A review. Chemosphere 99, 19–33. https://doi.org/10.1016/j.chemosphere.2013.10.071

Alhothali, A., Haneef, T., Mustafa, M.R.U., Moria, K.M., Rashid, U., Rasool, K., Bamasag, O.O., 2021. Optimization of Micro-Pollutants' Removal from Wastewater Using Agricultural Waste-Derived Sustainable Adsorbent. Int. J. Environ. Res. Public Health 18, 11506. https://doi.org/10.3390/ijerph182111506

Ayadi, M., Passaseo, D., Bonaccorso, G., Fichera, M., Renai, L., Venturini, L., Colzi, I., Fibbi, D., Del Bubba, M., 2024. Biochar from co-pyrolysis of biological sludge and sawdust in comparison with the conventional filling media of vertical-flow constructed wetlands for the treatment of domestic-textile wastewater. Water Sci. Technol. 89, 1252–1263. https://doi.org/10.2166/wst.2024.056

Bakari, Z., Fichera, M., El Ghadraoui, A., Renai, L., Giurlani, W., Santianni, D., Fibbi, D., Bruzzoniti, M.C., Del Bubba, M., 2024. Biochar from co-pyrolysis of biological sludge and woody waste followed by chemical and thermal activation: end-of-waste procedure for sludge management and biochar sorption efficiency for anionic and cationic dyes. Environ. Sci. Pollut. Res. 31, 35249–35265. https://doi.org/10.1007/s11356-024-33577-3

Camargo, J.A., Alonso, A., Salamanca, A., 2005. Nitrate toxicity to aquatic animals: a review with new data for freshwater invertebrates. Chemosphere 58, 1255–1267. https://doi.org/10.1016/j.chemosphere.2004.10.044

Castiglioni, M., Rivoira, L., Ingrando, I., Meucci, L., Binetti, R., Fungi, M., El-Ghadraoui, A., Bakari, Z., Del Bubba, M., Bruzzoniti, M.C., 2022. Biochars intended for water filtration: A comparative study with activated carbons of their physicochemical properties and removal efficiency towards neutral and anionic organic pollutants. Chemosphere 288, 132538. https://doi.org/10.1016/j.chemosphere.2021.132538

Chand, N., Suthar, S., Kumar, K., Tyagi, V.K., 2021. Enhanced removal of nutrients and coliforms from domestic wastewater in cattle dung biochar-packed Colocasia esculenta-based vertical subsurface flow constructed wetland. J. Water Process Eng. 41, 101994. https://doi.org/10.1016/j.jwpe.2021.101994

Chen, J., Deng, S., Jia, W., Li, X., Chang, J., 2021a. Removal of multiple heavy metals from mining-impacted water by biochar-filled constructed wetlands: Adsorption and biotic removal routes. Bioresour. Technol. 331, 125061. https://doi.org/10.1016/j.biortech.2021.125061

Chen, J., Li, X., Jia, W., Shen, S., Deng, S., Ji, B., Chang, J., 2021b. Promotion of bioremediation performance in constructed wetland microcosms for acid mine drainage treatment by using organic substrates and supplementing domestic wastewater and plant litter broth. J. Hazard. Mater. 404, 124125. https://doi.org/10.1016/j.jhazmat.2020.124125

Chen, Z., Xiao, X., Chen, B., Zhu, L., 2015. Quantification of Chemical States, Dissociation Constants and Contents of Oxygen-containing Groups on the Surface of Biochars Produced at Different Temperatures.

Environ. Sci. Technol. 49, 309–317. https://doi.org/10.1021/es5043468
de Rozari, P., Greenway, M., El Hanandeh, A., 2016. Phosphorus removal from secondary sewage and septage using sand media amended with biochar in constructed wetland mesocosms. Sci. Total Environ. 569–570, 123–133. https://doi.org/10.1016/j.scitotenv.2016.06.096
de Rozari, P., Greenway, M., El Hanandeh, A., 2015. An investigation into the effectiveness of sand media amended with biochar to remove BOD5, suspended solids and coliforms using wetland mesocosms. Water Sci. Technol. 71, 1536–1544. https://doi.org/10.2166/wst.2015.120
Del Bubba, M., Anichini, B., Bakari, Z., Bruzzoniti, M.C., Camisa, R., Caprini, C., Checchini, L., Fibbi, D., El Ghadraoui, A., Liguori, F., Orlandini, S., 2020. Physicochemical properties and sorption capacities of sawdust-based biochars and commercial activated carbons towards ethoxylated alkylphenols and their phenolic metabolites in effluent wastewater from a textile district. Sci. Total Environ. 708, 135217. https://doi.org/10.1016/j.scitotenv.2019.135217
Del Bubba, M., Arias, C.., Brix, H., 2003. Phosphorus adsorption maximum of sands for use as media in subsurface flow constructed reed beds as measured by the Langmuir isotherm. Water Res. 37, 3390–3400. https://doi.org/10.1016/S0043-1354(03)00231-8
Delgado-Moreno, L., Bazhari, S., Gasco, G., Méndez, A., El Azzouzi, M., Romero, E., 2021. New insights into the efficient removal of emerging contaminants by biochars and hydrochars derived from olive oil wastes. Sci. Total Environ. 752, 141838. https://doi.org/10.1016/j.scitotenv.2020.141838
Deng, C., Huang, L., Liang, Y., Xiang, H., Jiang, J., Wang, Q., Hou, J., Chen, Y., 2019. Response of microbes to biochar strengthen nitrogen removal in subsurface flow constructed wetlands: Microbial community structure and metabolite characteristics. Sci. Total Environ. 694, 133687. https://doi.org/10.1016/j.scitotenv.2019.133687
El Barkaoui, S., Mandi, L., Aziz, F., Del Bubba, M., Ouazzani, N., 2023. A critical review on using biochar as constructed wetland substrate: Characteristics, feedstock, design and pollutants removal mechanisms. Ecol. Eng. 190, 106927. https://doi.org/10.1016/j.ecoleng.2023.106927
El Ghadraoui, A., Ouazzani, N., Ahmali, A., El Mansour, T.E.H., Aziz, F., Hejjaj, A., Del Bubba, M., Mandi, L., 2020. Treatment of olive mill and municipal wastewater mixture by pilot scale vertical flow constructed wetland. Desalin. WATER Treat. 198, 126–139. https://doi.org/10.5004/dwt.2020.26009
El Hanandeh, A., Bhuvaneswaran, A., de Rozari, P., 2017. Removal of nitrate, ammonia and phosphate from aqueous solutions in packed bed filter using biochar augmented sand media. MATEC Web Conf. 120, 05004. https://doi.org/10.1051/matecconf/201712005004
El Hanandeh, A., Gharaibeh, M., Albalasmeh, A.A., 2018. Phosphorus removal efficiency from wastewater under different loading conditions using sand biofilters augmented with biochar. Int. J. Environ. Sci. Technol. 15, 927–934. https://doi.org/10.1007/s13762-017-1474-0
European Committee for Standardization, 2009 EN 12915, 2009. Products Used for the Treatment of Water Intended for Human Consumption – Granular Activated Carbon. In.
Fan, J., Wang, W., Zhang, B., Guo, Y., Ngo, H.H., Guo, W., Zhang, J., Wu, H., 2013. Nitrogen removal in intermittently aerated vertical flow constructed wetlands: Impact of influent COD/N ratios. Bioresour. Technol. 143, 461–466. https://doi.org/10.1016/j.biortech.2013.06.038
Ghezzehei, T.A., Sarkhot, D. V, Berhe, A.A., 2014. Biochar can be used to capture essential nutrients from dairy wastewater and improve soil physico-chemical properties. Solid Earth 5, 953–962. https://doi.org/10.5194/se-5-953-2014
Ghumra, D.P., Agarkoti, C., Gogate, P.R., 2021. Improvements in effluent treatment technologies in Common Effluent Treatment Plants (CETPs): Review and recent advances. Process Saf. Environ. Prot. https://doi.org/10.1016/j.psep.2021.01.021
Gómez-Cruz, I., Cara, C., Romero, I., Castro, E., Gullón, B., 2020. Valorisation of Exhausted Olive Pomace by an Eco-Friendly Solvent Extraction Process of Natural Antioxidants. Antioxidants 9, 1010. https://doi.org/10.3390/antiox9101010
Hanandeh, A. El, Abu-Zurayk, R.A., Hamadneh, I., Al-Dujaili, A.H., 2016. Characterization of biochar prepared from slow pyrolysis of Jordanian olive oil processing solid waste and adsorption efficiency of Hg2+ ions in aqueous solutions. Water Sci. Technol. 74, 1899–1910. https://doi.org/10.2166/wst.2016.378
Hijnen, W.A.M., Schijven, J.F., Bonné, P., Visser, A., Medema, G.J., 2004. Elimination of viruses, bacteria and protozoan oocysts by slow sand filtration. Water Sci. Technol. 50, 147–154. https://doi.org/10.2166/wst.2004.0044
Kaetzl, K., Lübken, M., Nettmann, E., Krimmler, S., Wichern, M., 2020. Slow sand filtration of raw wastewater using biochar as an alternative filtration media. Sci. Rep. 10, 1229. https://doi.org/10.1038/s41598-020-57981-0
Kaetzl, K., Lübken, M., Uzun, G., Gehring, T., Nettmann, E., Stenchly, K., Wichern, M., 2019. On-farm wastewater treatment using biochar from local agroresidues reduces pathogens from irrigation water for safer food production in developing countries. Sci. Total Environ. 682, 601–610.

https://doi.org/10.1016/j.scitotenv.2019.05.142
Kasak, K., Truu, J., Ostonen, I., Sarjas, J., Oopkaup, K., Paiste, P., Kõiv-Vainik, M., Mander, Ü., Truu, M., 2018. Biochar enhances plant growth and nutrient removal in horizontal subsurface flow constructed wetlands. Sci. Total Environ. 639, 67–74. https://doi.org/10.1016/j.scitotenv.2018.05.146
Kizito, S., Lv, T., Wu, S., Ajmal, Z., Luo, H., Dong, R., 2017. Treatment of anaerobic digested effluent in biochar-packed vertical flow constructed wetland columns: Role of media and tidal operation. Sci. Total Environ. 592, 197–205. https://doi.org/10.1016/j.scitotenv.2017.03.125
Lewis, W.M., Morris, D.P., 1986. Toxicity of Nitrite to Fish: A Review. Trans. Am. Fish. Soc. 115, 183–195. https://doi.org/10.1577/1548-8659(1986)115<183:TONTF>2.0.CO;2
Li, J., Fan, J., Zhang, J., Hu, Z., Liang, S., 2018. Preparation and evaluation of wetland plant-based biochar for nitrogen removal enhancement in surface flow constructed wetlands. Environ. Sci. Pollut. Res. 25, 13929–13937. https://doi.org/10.1007/s11356-018-1597-y
Li, L., Feng, J., Zhang, L., Yin, H., Fan, C., Wang, Z., Zhao, M., Ge, C., Song, H., 2021. Enhanced nitrogen and phosphorus removal by natural pyrite–based constructed wetland with intermittent aeration. Environ. Sci. Pollut. Res. 28, 69012–69028. https://doi.org/10.1007/s11356-021-15461-6
Li, R., Wang, J.J., Zhou, B., Awasthi, M.K., Ali, A., Zhang, Z., Gaston, L.A., Lahori, A.H., Mahar, A., 2016. Enhancing phosphate adsorption by Mg/Al layered double hydroxide functionalized biochar with different Mg/Al ratios. Sci. Total Environ. 559, 121–129. https://doi.org/10.1016/j.scitotenv.2016.03.151
Liu, N., Charrua, A.B., Weng, C.-H., Yuan, X., Ding, F., 2015. Characterization of biochars derived from agriculture wastes and their adsorptive removal of atrazine from aqueous solution: A comparative study. Bioresour. Technol. 198, 55–62. https://doi.org/10.1016/j.biortech.2015.08.129
Logan, A.J., Stevik, T.K., Siegrist, R.L., Rønn, R.M., 2001. Transport and fate of Cryptosporidium parvum oocysts in intermittent sand filters. Water Res. 35, 4359–4369. https://doi.org/10.1016/S0043-1354(01)00181-6
Lu, J., Guo, Z., Pan, Y., Li, M., Chen, X., He, M., Wu, H., Zhang, J., 2022. Simultaneously enhanced removal of PAHs and nitrogen driven by Fe2+/Fe3+ cycle in constructed wetland through automatic tidal operation. Water Res. 215, 118232. https://doi.org/10.1016/j.watres.2022.118232
Ma, R., Ma, J., Chen, Y., Zhuo, Y., Cheng, L., Jiang, L., Mao, Y., Shen, Q., Liu, C., Ji, F., 2023. Efficient removal of nitrogen from tidal flow constructed wetlands based on the in-situ zeolite regeneration: Measures and mechanisms. Chem. Eng. J. 458, 141298. https://doi.org/10.1016/j.cej.2023.141298
Mannaï, I., Sayen, S., Arfaoui, A., Touil, A., Guillon, E., 2022. Copper removal from aqueous solution using raw pine sawdust, olive pomace and their derived traditional biochars. Int. J. Environ. Sci. Technol. 19, 6981–6992. https://doi.org/10.1007/s13762-021-03629-z
Martikainen, K., 2023. Wastewater treatment in rural areas – Functionality of sand filters and suitability offilter media for reuse.
Mohammadi, R., Hezarjaribi, M., Ramasamy, D.L., Sillanpää, M., Pihlajamäki, A., 2021. Application of a novel biochar adsorbent and membrane to the selective separation of phosphate from phosphate-rich wastewaters. Chem. Eng. J. 407, 126494. https://doi.org/10.1016/j.cej.2020.126494
Moroccan standard, 2006. Norme Marocaine homologuée par arrêté du ministre de l'Industrie, du commerce et de la mise à niveau de l'économie; Service de Normalisation Industrielle Marocaine (SNIMA).
Nguyen, X.C., Tran, T.C.P., Hoang, V.H., Nguyen, T.P., Chang, S.W., Nguyen, D.D., Guo, W., Kumar, A., La, D.D., Bach, Q., 2020. Combined biochar vertical flow and free-water surface constructed wetland system for dormitory sewage treatment and reuse. Sci. Total Environ. 713, 136404. https://doi.org/10.1016/j.scitotenv.2019.136404
Perez-Mercado, L.F., Lalander, C., Berger, C., Dalahmeh, S.S., 2018. Potential of Biochar Filters for Onsite Wastewater Treatment: Effects of Biochar Type, Physical Properties and Operating Conditions. Water 10, 1835. https://doi.org/10.3390/w10121835
Rabichi, I., Sekkouri, C., Yaacoubi, F.E., Ennaciri, K., Izghri, Z., Bouzid, T., El Fels, L., Baçaoui, A., Yaacoubi, A., 2024. Experimental and Theoretical Investigation of Olive Mill Solid Waste Biochar for Vanillic Acid Adsorption Using DFT/B3LYP Analysis. Water, Air, Soil Pollut. 235, 369. https://doi.org/10.1007/s11270-024-07183-5
Ramachandra, T. V, Sincy, V., Asulabha, K.S., Mahapatra, D.M., Bhat, S.P., Aithal, B.H., 2018. Optimal Treatment of Domestic Wastewater through Constructed Wetlands. J Biodivers. 9, 81–102. https://doi.org/11.258359/KRE-180
Rodier, J., 2009. L'analyse de l'eau _ Rodier 9e édition.pdf.
S.E.E.E, 2007. Moroccan water quality grid for irrigation purposes [WWW Document]. State Secr. Minist. Energy, Mines, Water Environ. Charg. Water Environ. Kingdom Morocco, Water Qual. Stand. Irrig. 2007. URL http://www.eau-tensift.net/fileadmin/user_files/pdf/publications/3_Irrigation.pdf
Singh, S., Chakraborty, S., 2021. Bioremediation of acid mine drainage in constructed wetlands: Aspect of vegetation (Typha latifolia), loading rate and metal recovery. Miner. Eng. 171, 107083. https://doi.org/10.1016/j.mineng.2021.107083

Sleytr, K., Tietz, A., Langergraber, G., Haberl, R., 2007. Investigation of bacterial removal during the filtration process in constructed wetlands. Sci. Total Environ. 380, 173–180. https://doi.org/10.1016/j.scitotenv.2007.03.001

Suliman, W., Harsh, J.B., Abu-Lail, N.I., Fortuna, A., Dallmeyer, I., Garcia-Perez, M., 2016. Influence of feedstock source and pyrolysis temperature on biochar bulk and surface properties. Biomass and Bioenergy 84, 37–48. https://doi.org/10.1016/j.biombioe.2015.11.010

Tan, C., Ma, F., Li, A., Qiu, S., Li, J., 2013. Evaluating the Effect of Dissolved Oxygen on Simultaneous Nitrification and Denitrification in Polyurethane Foam Contact Oxidation Reactors. Water Environ. Res. 85, 195–202. https://doi.org/10.2175/106143012X13503213812445

Tayibi, S., Monlau, F., Fayoud, N.-E., Abdeljaoued, E., Hannache, H., Zeroual, Y., Oukarroum, A., Barakat, A., 2021. Production and Dry Mechanochemical Activation of Biochars Derived from Moroccan Red Macroalgae Residue and Olive Pomace Biomass for Treating Wastewater: Thermodynamic, Isotherm, and Kinetic Studies. ACS Omega 6, 159–171. https://doi.org/10.1021/acsomega.0c04020

Torrens, A., Molle, P., Boutin, C., Salgot, M., 2009. Removal of bacterial and viral indicator in vertical flow constructed wetlands and intermittent sand filters. Desalination 246, 169–178. https://doi.org/10.1016/j.desal.2008.03.050

Tran, H.N., You, S., Chao, H., 2016. Effect of pyrolysis temperatures and times on the adsorption of cadmium onto orange peel derived biochar. Waste Manag. Res. 34, 129–138. https://doi.org/10.1177/0734242X15615698

Uday Bhan Prajapati, Arun Lal Srivastav, Shiraz A.Wajih, 2018. Eco-management of Wastewater by ZESTP. J. Chem. Environ. Sci. its Appl. 4, 51–57. https://doi.org/10.15415/jce.2018.42007

Wu, H., Zhang, J., Ngo, H.H., Guo, W., Hu, Z., Liang, S., Fan, J., Liu, H., 2015. A review on the sustainability of constructed wetlands for wastewater treatment: Design and operation. Bioresour. Technol. 175, 594–601. https://doi.org/10.1016/j.biortech.2014.10.068

Wu, S., Carvalho, P.N., Müller, J.A., Manoj, V.R., Dong, R., 2016. Sanitation in constructed wetlands: A review on the removal of human pathogens and fecal indicators. Sci. Total Environ. 541, 8–22. https://doi.org/10.1016/j.scitotenv.2015.09.047

Yao, Y., Gao, B., Inyang, M., Zimmerman, A.R., Cao, X., Pullammanappallil, P., Yang, L., 2011. Removal of phosphate from aqueous solution by biochar derived from anaerobically digested sugar beet tailings. J. Hazard. Mater. 190, 501–507. https://doi.org/10.1016/j.jhazmat.2011.03.083

Yao, Y., Gao, B., Zhang, M., Inyang, M., Zimmerman, A.R., 2012. Effect of biochar amendment on sorption and leaching of nitrate, ammonium, and phosphate in a sandy soil. Chemosphere 89, 1467–1471. https://doi.org/10.1016/j.chemosphere.2012.06.002

Yavari, S., Malakahmad, A., Sapari, N.B., 2016. Effects of production conditions on yield and physicochemical properties of biochars produced from rice husk and oil palm empty fruit bunches. Environ. Sci. Pollut. Res. 23, 17928–17940. https://doi.org/10.1007/s11356-016-6943-3

Ye, J., Wang, L., Li, D., Han, W., Ye, C., 2012. Vertical oxygen distribution trend and oxygen source analysis for vertical-flow constructed wetlands treating domestic wastewater. Ecol. Eng. 41, 8–12. https://doi.org/10.1016/j.ecoleng.2011.12.015

Yin, Q., Zhang, B., Wang, R., Zhao, Z., 2017. Biochar as an adsorbent for inorganic nitrogen and phosphorus removal from water: a review. Environ. Sci. Pollut. Res. 24, 26297–26309. https://doi.org/10.1007/s11356-017-0338-y

Yuan, J., Xu, R., Zhang, H., 2011. Bioresource Technology The forms of alkalis in the biochar produced from crop residues at different temperatures. Bioresour. Technol. 102, 3488–3497. https://doi.org/10.1016/j.biortech.2010.11.018

Zhang, P., Sun, H., Yu, L., Sun, T., 2013. Adsorption and catalytic hydrolysis of carbaryl and atrazine on pig manure-derived biochars: Impact of structural properties of biochars. J. Hazard. Mater. 244–245, 217–224. https://doi.org/10.1016/j.jhazmat.2012.11.046

Zhang, Y., Li, Mengqi, Dong, L., Han, C., Li, Ming, Wu, H., 2021. Effects of biochar dosage on treatment performance, enzyme activity and microbial community in aerated constructed wetlands for treating low C/N domestic sewage. Environ. Technol. Innov. 24, 101919. https://doi.org/10.1016/j.eti.2021.101919

Zhou, X., Liang, C., Jia, L., Feng, L., Wang, R., Wu, H., 2018. An innovative biochar-amended substrate vertical flow constructed wetland for low C/N wastewater treatment: Impact of influent strengths. Bioresour. Technol. 247, 844–850. https://doi.org/10.1016/j.biortech.2017.09.044

Zhu, L., Lei, H., Wang, L., Yadavalli, G., Zhang, X., Wei, Y., Liu, Y., Yan, D., Chen, S., Ahring, B., 2015. Biochar of corn stover: Microwave-assisted pyrolysis condition induced changes in surface functional groups and characteristics. J. Anal. Appl. Pyrolysis 115, 149–156. https://doi.org/10.1016/j.jaap.2015.07.012

III-II. Biochar-Based Filtration Systems for Wastewater Treatment: Performance, Efficiency, and Optimisation

This work was published as a research paper:

El Barkaoui, S., Mandi, L., Ryah, H., El Ghadraoui, A., Del Bubba, M., Ouazzani, N. (2025) . Biochar-based filtration systems for wastewater treatment: performance, efficiency, and optimization. Int. J. Environ. Sci. Technol. 22, 15843–15856 (2025). https://doi.org/10.1007/s13762-025-06694-w

Abstract

The aim of this work was to evaluate the role of four types of biochar (BC) derived from olive pomace (BOP), orange wood waste (BOW), filao (BF), and cypress (BCY) as unconventional filling interlayers of column filters (CFs) in the removal of contaminants from wastewater. Preliminary tests were carried out on five laboratory-scale CFs filled with sand (CF-S) and the aforementioned materials (CF-BOP, CF-BOW, CF-BF, and CF-BCY). The BOP was obtained by pyrolysis at a temperature of 590 °C for 2 h and at a heating rate of 10 °C min^{-1}, while the other BCs were produced at 400 °C for 12 h with a heating rate of 2 °C min^{-1}. The results highlighted that BCs integrated into the CFs enhanced the removal efficiency of most chemical and bacteriological pollutants. Notably, CF-BF exhibited the best removal performance for total suspended solids (90%), total COD (64%), PO_4^{3-} (45%), and NH_4^+-N (92%). CF-BCY demonstrated better performance in the removal of soluble COD (52%), total phosphorus (46%), and total Kjeldahl nitrogen (73%), while CF-BOP showed higher removal for total nitrogen (56%), and absorbance at 254 and 420 nm (40% and 39%, respectively). Faecal indicators monitored included total and faecal coliforms and faecal streptococci, which were largely removed by CF-BF, CF-BOP, and CF-BOW. The results demonstrated that the type of BC and its properties influence the treatment efficiency of CFs for the investigated parameters and that BF is the most effective type of BC for the removal of the target contaminants from wastewater.

Keywords: Wastewater treatment; Column filter; Biochar type; Properties; Optimisation.

1. Introduction

The main objectives of sustainable and renewable development are to guarantee universal access to water and to reduce environmental waste (Osborn et al. 2015). Combining the treatment and reuse of wastewater with agricultural waste recycling is an innovative and integrated approach. The conversion of agricultural waste into biochar (BC) and its use for wastewater treatment contributes to achieving a zero-waste cycle that conserves resources and protects the environment (Singh et al. 2022). Recently, there has been growing interest in using BC as a filling substrate in filter systems, such as constructed wetlands (CWs) and column filters (CFs), due to its many advantages. These include sustainability, cost-effectiveness, low environmental impact, and the ability to produce water suitable for irrigation (Stefanakis 2019). In addition, many authors reported that the BC has a high capacity in eliminating most pollutants, including inorganic and organic contaminants and heavy metals from wastewater (El Barkaoui et al. 2023), due to its high surface functionalization, porous structure, and high surface area, compared to conventional materials (e.g., soil, sand, and gravel) (Cha et al. 2016; Deng et al. 2019; El Barkaoui et al. 2023; Ayadi et al. 2024). Ayadi et al. (2024) investigated the influence of filling media on the performance of CWs by comparing systems with BC and gravel. The BC-based CW demonstrated superior treatment efficiency, achieving enhancements of 22% and 35% in chemical oxygen demand (COD) and ammonia removal, respectively. Additionally, greater reductions were

observed in UV–Vis absorbance, with decreases of 32–34% at 254 nm and 28% at 420 nm, compared to the gravel-based system. Similarly, Chen et al. (2024) compared the efficiency of gravel-based and BC-based CWs, pointing out a higher performance of the latter in removing various water quality parameters, particularly total phosphorus (TP), whose removal increased from 56% to 90%. In order to improve the efficiency of the treatment of BC-filled CWs and CFs, it is necessary to optimise several parameters, such as the type of biochar used, its position within the filter, and the percentage of biochar in the filling substrate. The type of plant used can also represent a further critical factor influencing the performance of CWs, since the rhizosphere provides an ideal surface for microbial colonization, improving the efficiency of biological degradation (Sacco et al. 2006). On the other hand, roots release organic carbon, which can limit the removal efficiency of the system through the adsorption mechanism (Ayadi et al. 2024). In fact, many studies have shown that the plant has a negligible or even negative impact on the performance of BC-based filter systems. For example, Janyasupab et al. (2023) and Ayadi et al. (2024) evaluated the effect of vegetation (*Typha latifolia* L. and *Phragmites australis* (Cav.) Trin. ex Steud., respectively) on the treatment efficiency of BC-based microcosms by comparing planted and unplanted systems. Their results pointed out a negligible or even negative effect of the presence of plants in the reduction of several water quality parameters, such as biochemical oxygen demand (BOD_5), chemical oxygen demand (COD), total suspended solids (TSS), NH_4^+-N, total nitrogen (TN), total Kjeldahl nitrogen (TKN), total phosphorus (TP), and absorbance at 254 and 420 nm.

As regards the percentage of BC in the filter substrate, many studies highlighted the lack of improvement in removal performance with an increase in the percentage of biochar in the filling medium, concluding that the introduction of 10% biochar may represent an optimal concentration in terms of removal efficiency, also taking into account the costs associated with the production and activation of the material (de Rozari et al. 2016; Li et al. 2018; El Barkaoui et al. 2025). For example, El Barkaoui et al. (2025) examined how increasing the percentage of olive pomace-derived biochar (BC) from 0% to 50% affected the performance of CFs for the removal of the aforementioned water quality parameters, showing that all systems containing BC performed better than the sand-filled system, although there were no statistically significant differences between the various BC percentages (10%, 25%, and 50%). Similar conclusions were drawn by Li et al. (2018) testing 10% and 20% percentages of BC from *Arundo donax* L. as filling medium of pilot-scale CWs, in comparison with a 100% sand-based control. de Rozari et al. (2016) highlighted even a negative effect of increasing the BC percentage in CFs in the removal of

phosphorus, which was better removed in the sand media (BC=0%) than in the BC-amended media (BC= 5%, 10%, 15%, 20%, and 25%). Conversely, Zhang et al. (2021) obtained opposite results testing three proportions of BC amendment (25%, 50%, and 75%) in comparison with 100% sand. These contrasting results can be explained by the different characteristics of the biochars used in the different studies. Biochar, in fact, may provide very low sorption properties, according to its surface area and porosity distribution and even act as a source of pollution, depending on its composition. This suggests the importance of an in-depth characterization of the materials intended to be used as filling media in CWs and/or CFs (Bakari et al. 2024). Furthermore, the different durations of the experiments may not be sufficient in some cases to highlight the different removal performances that can be obtained with increasing percentages of BC.

Regarding the position of the BC layer in the filter bed, the literature suggests its integration as an interposition layer between two inert materials (e.g., sand) to prevent BC floating and/or filter clogging (Ji et al. 2020; Liao et al. 2022; El Barkaoui et al. 2023).

Regarding the choice of the type of biomass to be used for BC production, the literature proposes an extremely wide range of feedstocks, whose composition will influence the BC performance. With regard to the choice of biomass for BC production, the literature proposes a wide range of feedstocks whose composition influences BC performance. In order to study the role that BC from different types of biomass can play in filtration systems, it is necessary to systematically compare the treatment performance of filters using different types of BC. However, only a few studies have focused on evaluating the effect of different types of BC-based substrates on the treatment performance of CFs. As an example, Perez-Mercado et al. (2018) tested the efficiency of two types of BC-based filters (willow BC and pine-spruce BC) in removing pollutants from wastewater, highlighting that during the first two months of operation the pine-spruce BC had the best removal efficiency towards COD (> 90%) and TN (> 50%), but lower removal performance for TP (32% – 60% vs 86%) and PO_4^{3-} (62% vs 89%), compared to the willow BC, showing a similar efficiency afterwards. Zheng et al. (2022) tested cattail litter- and sewage sludge-derived BC as CW filling media, showing that the latter provided significantly better removal efficiency for COD, nitrogen, and phosphorus removal. García-Ávila et al. (2023b) evaluated the efficiency of two CFs filled with BC derived from bamboo and eucalyptus, comparing their efficiency with that of systems based on sand, gravel and anthracite, fed with different types of wastewater (raw, settled and flocculated). The results of this study highlighted a greater capacity to mitigate

turbidity and colour pollution by both systems with BC and among them a better performance of the system filled with BC derived from bamboo, which presented the highest removal of turbidity (64%, 94% and 81%) and colour (45%, 91% and 69%), for raw, flocculated and settled water, respectively.

Generally, BC properties such as surface area, pore size and distribution, functional groups, and alkalinity are key factors influencing adsorption ability and, thus, the treatment performance of BC-based filter systems. In general, the characteristics of BC are related to both the feedstock properties and the experimental conditions adopted for BC production (e.g., carbonization time, temperature, and heating rate) (Enaime et al. 2020). Pyrolysis is more often used than gasification for the production of BCs to be integrated into CWs and/or CFs. Enaime et al. (2020) reported that high-temperature pyrolysis typically yields biochar with a high specific surface area (SSA), significant microporosity, and hydrophobic characteristics, making it more effective for the adsorption of organic pollutants. In contrast, biochars produced at lower pyrolysis temperatures exhibit reduced surface area and pore volume but possess a greater abundance of oxygen-containing functional groups, enhancing their affinity for inorganic contaminant removal (Enaime et al. 2020). As regards the feedstock used for BC production, it is suggested that it must be rich in carbon and low in mineral matter to produce good-quality biochar (El Barkaoui et al. 2024). Based on the previous literature, the raw materials most commonly used for BC production as filter substrates are bamboo, *maize cobs, Arundo donax straw*, tree branches, shells, and wooden containers, due to their composition, availability, and low cost (Zhang et al. 2021; Deng et al. 2021). In the Mediterranean area, the olive pomace (OP) is considered one of the most abundant types of waste, due to the considerable production of olive oil in this region. Nevertheless, the study of the integration of OP-based BC remains limited, with only three previous papers reported in the literature (El Hanandeh et al. 2018, 2017; El Barkaoui et al. 2025). El Hanandeh et al. (2018, 2017) evaluated the impact of adding OP-derived BC into sand media of CFs for nitrogen and phosphorus removal, pointing out that integrating BC from OP into CF significantly improved nitrate removal, while it slightly affected ammonium and phosphate removal. Similarly, El Barkaoui et al. (2025) tested the impact of the concentration of OP-derived BC integrated into CFs on treatment performance, showing that 10% is an optimal ratio for wastewater treatment. Furthermore, the use of agricultural waste such as orange wood (OW), cypress (CY), and filao (F) has never been tested in BC-integrated filter systems for wastewater treatment. In addition, there is still insufficient available information on the effect of the type and characteristics of BC integrated into CFs on the treatment performance of these systems. Moreover, data regarding

absorbance at 254 and 420 nm and faecal bacteria indicators removal are completely absent.

Based on these considerations, the main aim of this work is to assess the performance of incorporating various types of BC into a sandy medium as an interlayer in CFs for removing a number of microbiological and chemical water quality parameters. This evaluation was conducted by analysing the influent and effluent wastewater of CFs integrated with BOP (CF-BOP), BOW (CF-BOW), BF (CF-BF), and BCY (CF-BCY), in comparison with the control (CF-S).

2. Methodology

2.1. Biochar production conditions and characterisation

The BC types used in this study were obtained from four different biomasses: olive pomace (BOP), orange wood waste (BOW), filao (BF), and cypress (BCY). BOP was prepared as described in the study of El Barkaoui et al. (2025). BOW, BF, and BCY were produced under similar conditions using a semi-pilot scale system of slow pyrolysis at 400 °C for 12 h with a heating rate of 2 °C min^{-1}. The environmental compatibility of the four types of BCs was assessed according to the parameters specified in the European standard EN 12915-1 for materials designed for the treatment of water (European Committee for Standardisation 2009). Additional characterisations included proximate and elemental analysis, determination of the pH at the point of zero charge (pH_{PZC}), specific surface area (SSA), mesoporous and microporous distribution, and scanning electron microscopy (SEM). A complete description of the techniques and the methods used is reported in the *Supplementary Material 3 (SM3)*.

2.2. Description of the experimental setup of the filters

The experimental setup consisted of five PVC column filters (CFs), each measuring 45 cm in height and 7.5 cm in internal diameter (**Figure III-6)**. The filtration section (30 cm) comprised two 8 cm layers of gravel (2–8 mm and 2–6 mm grain diameter, respectively) at the top and bottom of the filter bed, and a 14 cm interlayer filled with a 1:10 BC and sand mixture (grain diameter: 1–2 mm and 2–5 mm, respectively) to prevent BC from floating or clogging the filter system. Conversely, the control filter (CF-S) was filled with 100% sand. The experiments started in February 2024 and lasted approximately five months. They involved sequential batch filling and rest modes of three batches per day, with a total volume of one litre per day and an organic loading rate of 88 g COD/m^2 day.

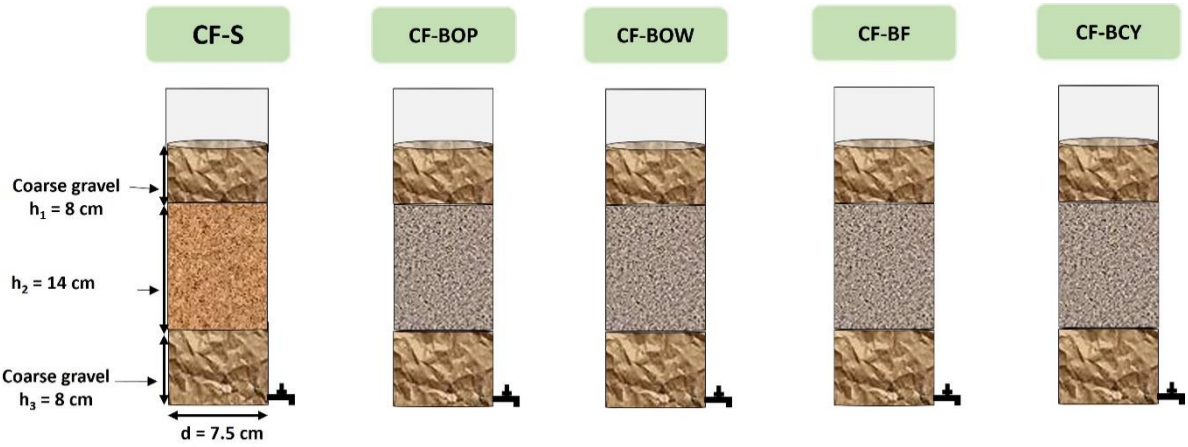

Figure III-6: Schematic diagram of the column filters experiment based on sand (CF-S), biochar from olive pomace (CF-BOP), biochar from orange wood waste (CF-BOW), biochar from filao (CF-BF), and biochar from cypress (CF-BCY).

2.3. Sample collection and analysis

In the present study, the influent was collected from the Marrakech wastewater treatment plant after primary settling. Every week, the effluent and influent samples were collected and immediately analysed. **Table III-4** provides the mean influent characteristics over the whole experimental period.

A multi-parameter HI 9829 probe (HANNA, Woonsocket, RI, USA) was used to measure pH, dissolved oxygen (DO), and electrical conductivity (EC). The absorbance of the influent and effluent samples was measured at 254 and 420 nm. Total suspended solids (TSS), soluble and total COD (SCOD and TCOD, respectively), TP, PO_4^{3-}, TN, NH_4^+–N, total Kjeldahl nitrogen (TKN), NO_3^--N, NO_2^--N, SO_4^{2-}, total hardness (TH), calcium, and magnesium were determined according to the standard methods indicated in AFNOR, (1997) and Rodier, (2009). The bacterial indicators of faecal contamination determined in this study using the AFNOR Standard (AFNOR 1997) included faecal streptococci (FS), faecal coliforms (FC), and total coliform (TC). The analysis of the aforementioned physicochemical and bacteriological parameters was performed in triplicate to minimize errors and ensure accuracy. The details of the aforementioned methods of the analysed parameters have been reported by El Barkaoui et al. (2025).

2.4. Statistical and data analysis

Statistical analysis to test the significance of the data collected in this study was performed using

the Games-Howell non-parametric test with Minitab 17 software, version 17.1.0 (State College, PA, USA).

3. Results and discussion

3.1. Properties of biochar

Figure III-7 shows the pH_{PZC} curves of the four types of BCs. Generally, the pH of the water medium is considered a crucial factor in the adsorption process (Alhothali et al. 2021). The pH_{PZC} curves demonstrate that BCY has the highest pH_{PZC} value (8.8), followed by BOP (7.8), BF (6.4), and BOW (6.2). The influent wastewater had a pH of 7.5 (**Table III-4**), which is very close to the pH_{PZC} of BOP. Hence, under these experimental conditions, BOP exhibited a minimal net surface charge, thus leading to a neutral sorption behaviour for charged species (Ayadi et al. 2024). Conversely, BCY, which had the highest pH_{PZC}, was characterized by a positively charged surface, which will facilitate the adsorption of anions. On the other hand, BOW and BF exhibited the lowest pH_{PZC} values, leading to a negatively charged surface, thus being more efficient for sorption of cations (Alhothali et al. 2021).

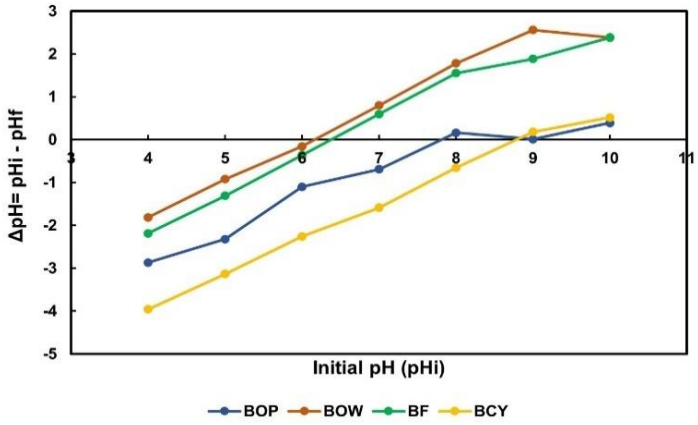

Figure III-7: Point of zero charge of the four types of biochar derived from olive pomace (BOP), orange wood waste (BOW), filao (BF), and cypress (BCY).

The physicochemical and morphological characteristics of the studied BCs are reported in **Table III-3** and **Figure III-8**. The proximate analysis revealed a low ash content (AC < 5%) for all BCs investigated, in accordance with the EN 12915-1 standard for water treatment, which specifies a limit of 15%, given that a high AC content in the filter medium is likely to reduce its adsorption efficiency (Bakari et al. 2024). BOW and BF showed higher volatile matter (VM), around 32%, followed by BCY (21%), and BOP with a lower value (13%). However, BOP showed higher fixed

carbon (FC 82%), compared to BCY (75%), BOW (62%), and BF (62%). The elemental analysis confirmed the high carbon content for BOP (90%), BCY (89%), BOW (76%), and BF (75%), indicating high material quality. Notably, the BC derived from cypress exhibited the highest SSA (152 m^2/g), followed by BOP (106 m^2/g), while BOW and BF showed much less porosity (6 - 7 m^2/g). The SSA of an adsorbent is a crucial factor in assessing the material's suitability and cost-effectiveness for wastewater treatment (Zeghioud et al. 2022). Moreover, a larger SSA indicates a greater potential for extensive biofilm formation, facilitating processes such as nitrification, denitrification, biological degradation of organic carbon, and organic matter mineralisation (El Barkaoui et al. 2023). SEM showed longitudinal hollow tubes with a high degree of porosity, especially for BCs derived from lignocellulosic raw materials, such as orange wood waste, filao, and cypress wood (**Figure III-8**). These findings are consistent with the literature (Kizito et al. 2017; Xin et al. 2021; Zheng et al. 2022; Chang et al. 2022; Rabichi et al. 2024).

Table III-3: Physicochemical characteristics of biochar derived from olive pomace (BOP), orange wood waste (BOW), filao (BF), and cypress (BCY).

Parameters	**BOP**	**BOW**	**BF**	**BCY**
Ash content (%)	4.92	3.64	4.24	1.95
Volatile matter (%)	12.93	31.73	31.96	21.15
Fixed carbon (%)	82.15	61.79	61.62	75.10
C (%)	90.11	76.27	74.65	88.61
N (%)	1.31	0.62	1.05	0.47
H (%)	2.00	3.93	3.91	2.62
S (%)	0.00	0.00	0.00	0.00
O[a] (%)	6.57	19.18	20.39	8.30
BET surface area (m^2/g)	106 ± 1	6.0 ± 0.1	6.71 ±0.06	152 ± 3
Micropore surface area (m^2/g)	n.d.	n.d.	n.d.	68.50
Mesopore surface area (m^2/g)	113	6.10	6.65	82.20

[a] calculated by difference.

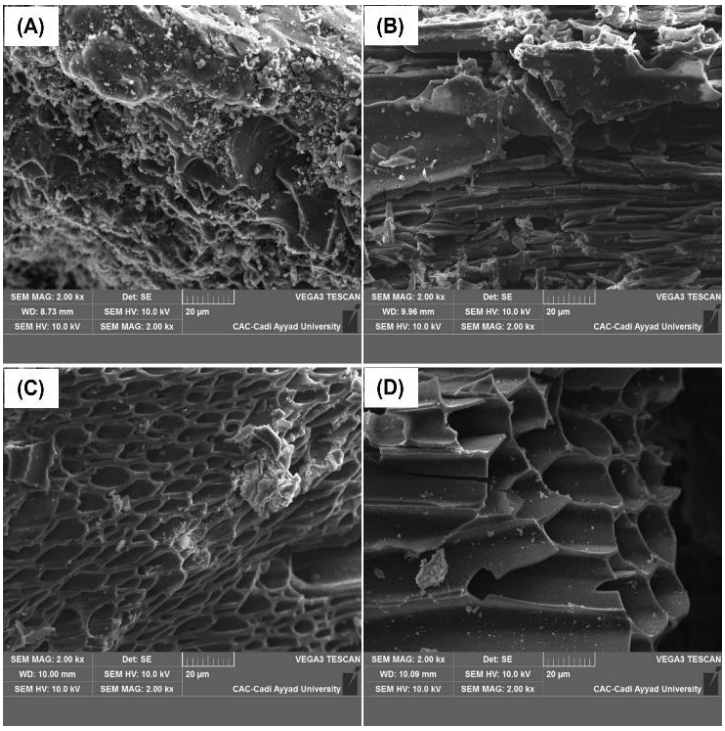

Figure III-8: SEM surface scan of the four types of biochar derived from olive pomace (A), orange wood waste (B), filao (C), and cypress (D).

3.2. Overall treatment performance of CFs

3.2.1. Wastewater quality parameters

Table III-4 shows the results of the analysis of DO, EC, pH, and TSS in the influent and effluent samples of CF-S, CF-BOP, CF-BOW, CF-BF, and CF-BCY. No statistically significant difference was observed for EC between influent and effluent samples, suggesting that the BC did not provide any net adsorption or release of ions throughout the treatment process. For pH, a significant increase was observed for all CFs after treatment, without statistically significant differences among the different CFs tested. This may be due to the alkaline properties of Moroccan sand used as filling media of CFs (Mghaiouini et al. 2024). The influent pH and EC obtained during the treatment are in line with the Moroccan standard for agricultural reuse (pH 6.5–8.4 and EC < 12 mS/cm) (S.E.E.E 2007). The DO concentrations of the effluent samples increased significantly compared to the influent, reflecting the improved effluent quality (Nguyen et al. 2020). This increase can be attributed to multiple sources, primarily the inflow of water and atmospheric reoxygenation, which serve as major contributors to oxygen availability. Additionally, during dry periods, oxygen is supplied to filter systems through diffusion processes (Ye et al. 2012; Kasak et al. 2018; El Barkaoui et al. 2025). Significant removal performance,

ranging from 76% to 90%, was observed in all the investigated CFs. However, BC-amended filters achieved higher TSS removal rates (84–90%) compared to the sand-based control system (76%). This improved performance is likely due to the peculiar sorption properties of BC, which promote more efficient retention of colloidal particles from the wastewater (El Barkaoui et al. 2025). Generally, TSS in the effluent wastewaters showed low and stable concentrations, irrespective of the concentration levels determined in the influent, thus highlighting the remarkable sedimentation occurring through the filtration substrate (Khalifa et al. 2020; El Ghadraoui et al. 2020).

Table III-4: Measured water quality parameters (mean value ± standard deviation) in the inlet and outlet of CFs based on sand (CF-S), biochar from olive pomace (CF-BOP), biochar from orange wood waste (CF-BOW), biochar from filao (CF-BF), and biochar from cypress (CF-BCY). Values with different letters are statistically different according to Games or Fisher ($P<0.05$).

Parameters	Influent	Systems				
		CF-S	CF-BOP	CF-BOW	CF-BF	CF-BCY
pH	7.5 ± 0.3^{a}	8.3 ± 0.4^{b}	8.3 ± 0.3^{b}	8.2 ± 0.4^{b}	7.8 ± 0.4^{b}	8.3 ± 0.4^{b}
EC (µS cm^{-1})	2457 ± 242^{a}	2379 ± 197^{a}	2380 ± 272^{a}	2462 ± 263^{a}	2329 ± 161^{a}	2466 ± 100^{a}
DO (mg L^{-1})	0 ± 0^{a}	2 ± 1^{b}	1.8 ± 0.9^{b}	1.8 ± 0.8^{b}	1.8 ± 0.8^{b}	1.6 ± 0.8^{b}
TSS (mg L^{-1})	195 ± 41^{a}	45 ± 24^{b}	25 ± 19^{c}	31 ± 23^{bc}	19 ± 15^{c}	30 ± 21^{bc}
TCOD (mg L^{-1})	353 ± 96^{a}	182 ± 52^{b}	148 ± 40^{bc}	127 ± 47^{c}	123 ± 60^{c}	140 ± 58^{c}
SCOD (mg L^{-1})	168 ± 19^{a}	104 ± 28^{b}	100 ± 35^{bc}	89 ± 27^{bc}	83 ± 28^{c}	79 ± 24^{c}
TP (mg L^{-1})	13 ± 2^{a}	7 ± 1^{b}	7.7 ± 0.9^{b}	7.8 ± 0.9^{b}	7 ± 1^{b}	7 ± 1^{b}
PO_4^{3-} (mg L^{-1})	11 ± 2^{a}	6 ± 1^{b}	6 ± 2^{b}	7 ± 2^{b}	6 ± 2^{b}	6 ± 2^{b}
TN (mg L^{-1})	165 ± 12^{a}	65 ± 10^{b}	73 ± 14^{bc}	94 ± 22^{c}	82 ± 27^{bc}	64 ± 19^{b}
TKN (mg L^{-1})	160 ± 12^{a}	44 ± 9^{b}	50 ± 11^{b}	68 ± 10^{c}	56 ± 21^{bc}	44 ± 10^{b}
NH_4^{+}-N (mg L^{-1})	98 ± 19^{a}	15 ± 10^{b}	21 ± 14^{b}	11 ± 9^{b}	10 ± 11^{b}	17 ± 12^{b}
NO_2^{-}-N (mg L^{-1})	0.11 ± 0.03^{a}	3 ± 4^{ab}	5 ± 9^{b}	5 ± 9^{b}	6 ± 9^{b}	4 ± 9^{ab}
NO_3^{-}-N (mg L^{-1})	4 ± 1^{a}	18 ± 14^{b}	18 ± 6^{b}	22 ± 14^{b}	20 ± 12^{b}	16 ± 8^{b}
SO_4^{2-} (mg L^{-1})	56 ± 42^{a}	72 ± 24^{ab}	74 ± 26^{ab}	75 ± 26^{b}	80 ± 31^{b}	73 ± 24^{ab}
Hardness (mg L^{-1})	358 ± 46^{a}	522 ± 67^{b}	528 ± 67^{b}	536 ± 73^{b}	549 ± 70^{b}	531 ± 97^{b}
Calcium (mg L^{-1})	68 ± 15^{a}	110 ± 33^{bc}	103 ± 25^{b}	123 ± 28^{bc}	126 ± 30^{c}	119 ± 31^{bc}
Magnesium (mg L^{-1})	291 ± 48^{a}	412 ± 46^{b}	425 ± 53^{b}	413 ± 56^{b}	424 ± 65^{b}	413 ± 87^{b}
ABS 254 nm (mAu)	538 ± 5^{a}	354 ± 18^{bc}	325 ± 39^{b}	325 ± 31^{b}	342 ± 42^{b}	406 ± 76^{c}
ABS 420 nm (mAu)	90 ± 18^{a}	57 ± 30^{b}	58 ± 35^{ab}	54 ± 20^{b}	64 ± 27^{ab}	62 ± 18^{ab}

3.2.2. COD removal

Table III-4 illustrates the concentrations of SCOD and TCOD in the influent and effluent samples, while **Figure III-9** shows their removal efficiencies in different CFs. Generally, the mean concentrations of TCOD and SCOD decreased after treatment, irrespective of the CF considered. Moreover, CFs filled with BC provided higher removal performance (57% - 64% for TCOD and 41% - 52% for SCOD), compared to CF-S (47% for TCOD and 38% for SCOD),

demonstrating the positive role of BC added to the CFs, due to its surface and porous structure, enabling higher adsorption ability and providing a suitable medium for the microbial degradation of organic carbon (Li et al. 2021b). In addition, its surface, which is rich in functional groups (e.g., nitro-, chloro-, amine, carbonyl, hydroxyl, and carboxylic acid), may enhance the electrostatic adsorption of organic matter (Ambaye et al. 2021). Liang et al. (2020) reported that the higher TCOD removal may be due to the presence of chemo-heterotrophic microorganisms in BC-filled systems, while Ayadi et al. (2024) attributed this phenomenon to adsorption processes by BC rather than biological mechanisms. Interestingly, CF-BOW and CF-BF showed higher removal efficiencies of TCOD (63% - 64%), while CF-BCY was the best-performing substrate for the removal of SCOD (53%). The difference in removal performance between the CFs filled with BCs could be strongly dependent on the specific characteristics of the BC used.

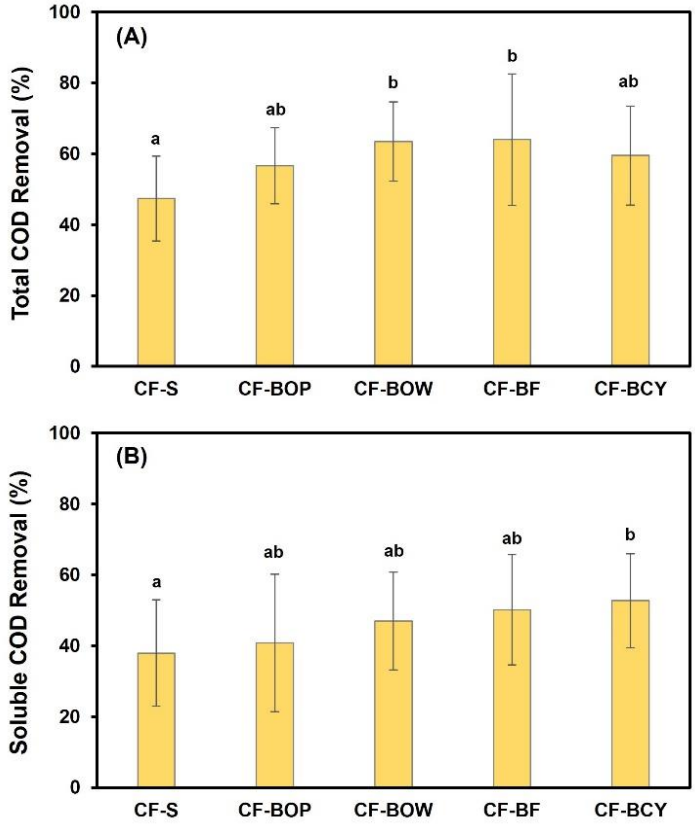

Figure III-9: Average elimination of total (A) and soluble (B) COD in CFs based on sand (CF-S), biochar from olive pomace (CF-BOP), biochar from orange wood waste (CF-BOW), biochar from filao (CF-BF), and biochar from cypress (CF-BCY).

3.2.3. Phosphorus removal

Both forms of phosphorus showed a significant reduction in their concentrations due to the

treatment performed by CFs (**Table III-4**). All systems provided similar P-removal, ranging approximately from 40% to 45%, irrespective of the presence of BC in the systems, thus pointing out the lack of BC effect on phosphorus elimination (**Figure III-10**). Numerous studies mentioned the limited effectiveness of BC in removing TP and PO_4^{3-} (Yao et al. 2012; de Rozari et al. 2016; El Barkaoui et al. 2023). For instance, de Rozari et al. (2016) found that sand was more effective than BC-amended CWs in removing phosphorus. Similarly, Zhou et al. (2019) reported that incorporating BC into gravel-filled CW showed no effect on phosphorus removal. This may be due to the fact that BCs often possess hydrophobic or very weakly charged groups on their surface (Almanassra et al. 2021), thus providing a higher affinity towards competing organic compounds and resulting in poor phosphate adsorption capacity. Indeed, the main removal mechanisms for phosphorus in filtration systems include plant uptake and especially physicochemical reactions of substrates (e.g., adsorption, precipitation, mineralisation, and ion exchange), which need the use of tailored materials (Vohla et al. 2011; Kamilya et al. 2022).

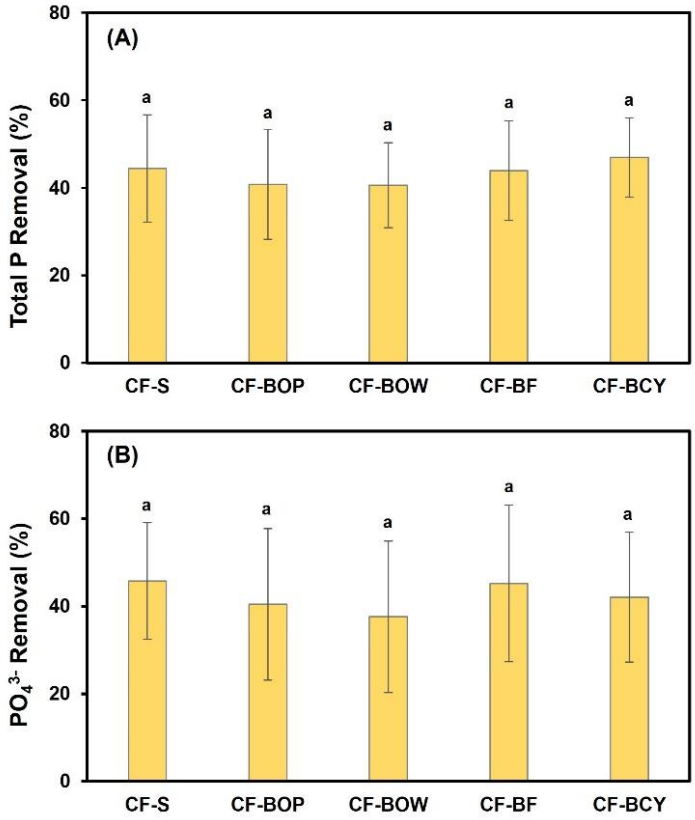

Figure III-10: Average elimination of TP (A) and PO_4^{3-} (B) in CFs based on sand (CF-S), biochar from olive pomace (CF-BOP), biochar from orange wood waste (CF-BOW), biochar from filao (CF-BF), and biochar from cypress (CF-BCY).

3.2.4. Nitrogen removal

Table III-4 shows the evolution of nitrogen forms (TN, TKN, NH_4^+-N, NO_2^--N, NO_3^--N) during the treatment period. The results show that high removal of TN, NH_4^+-N, and TKN occurred in all CFs (**Figure III-11**). Generally, either biological or physicochemical mechanisms can be invoked to explain the observed removal (Yousaf et al. 2021). Biological mechanisms controlling the cycle of nitrogen are known to be very active in nature-based wastewater treatment processes such as CFs and CWs (Ma et al. 2023), which may be involved in the conversion of oxidised and reduced forms of nitrogen within the systems. Moreover, the NH_4^+-N removal trend as a function of operating time showed two distinct phases: a short initial phase (3 weeks) of low efficiency, followed by a phase of improved treatment performance stabilising at a high removal rate (data not shown). Based on the characteristics of each type of BC (section **3.1**), the cation exchange mechanism is expected to play a relatively limited role in eliminating ionic substances. The nitrogen released can be taken up by the biomass and/or converted to NH_4^+-N and then undergo nitrification. The removal performance of NH_4^+-N in all CFs was higher, ranging from 83% to 91%, with slightly better performance of CF-BF and CF-BOW compared to the other BC-amended filters (**Figure III-11C**). However, the sand-based system behaved similarly to those filled with BC, without any statistically significant difference. In addition, CF-BF and CF-BOW provided lower removal of TKN and TN (**Figures III-6B** and **III-6C**) compared to the other systems, probably due to lower removal of organic nitrogen resulting from lower degradation of protein and other nitrogenous cell constituents. In general, ammonia nitrification is a two-step reaction whose intermediate and final products are nitrite and nitrate, respectively, the former being highly toxic to aquatic fauna (Ayadi et al. 2024). For this reason, the concentration of nitrite in the effluent samples should be reduced as much as possible, complying with the legal limits in the studied region. In the CF effluents, the concentrations of NO_2^--N and NO_3^--N increased significantly compared to the influent, in line with the high nitrification. The nitrate concentrations of the effluents (16 - 22 mg L^{-1}) were within the regulation limits, remaining below the toxicity thresholds reported for all aquatic organisms (Camargo et al. 2005), while the concentrations of nitrite (3 - 6 mg L^{-1}) were sufficiently high to pose toxic effects on the fish population (Lewis and Morris 1986). According to the literature, the incomplete NH_4^+-N oxidation and the release of NO_2^--N ions are common findings in CFs and CWs, caused by insufficient DO availability in the filters (Li et al., 2021; Lu et al., 2022; Ayadi et al., 2024), a condition that primarily affects the nitrite-oxidizing bacteria activity instead of the microorganisms involved in the conversion of nitrite/ammonia (Vymazal 2007; Tan et al. 2013). However, Kizito et al. (2017) reported that the higher release of NO_3^--N in BC-packed CWs may be due to the high level of oxygen in the filter.

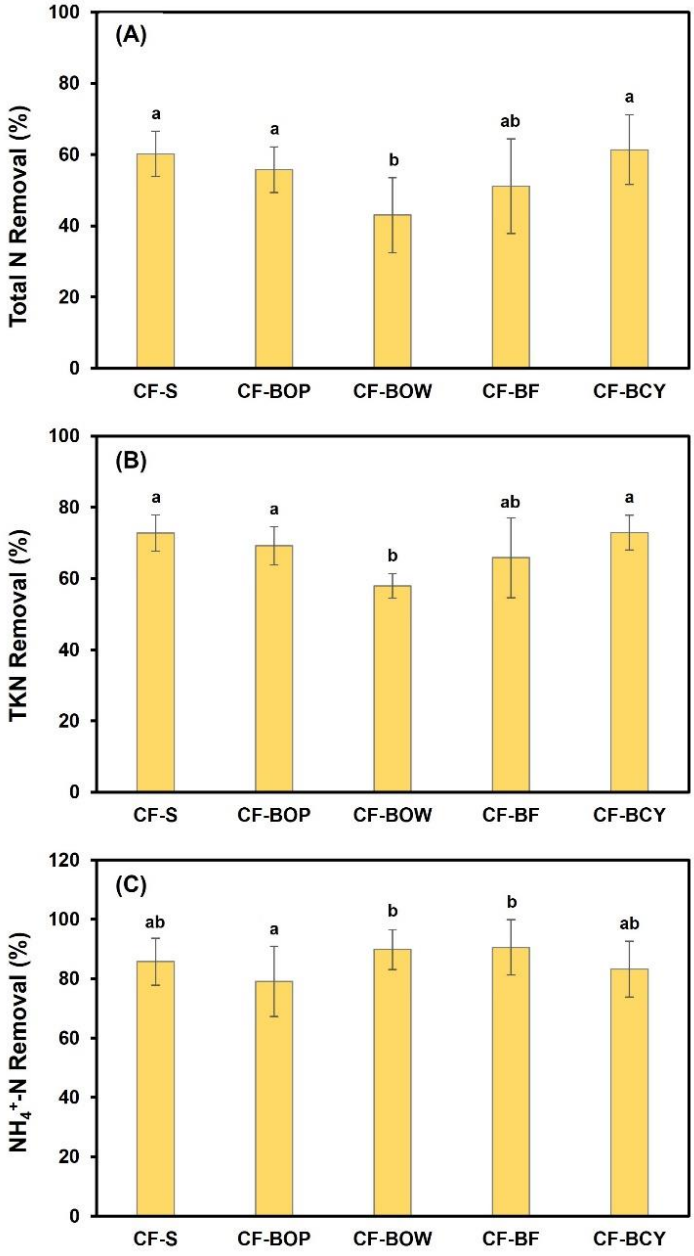

Figure III-11: Average elimination of TN (A), TKN (B), and NH_4^+-N (C) in CFs based on sand (CF-S), biochar from olive pomace (CF-BOP), biochar from orange wood waste (CF-BOW), biochar from filao (CF-BF), and biochar from cypress (CF-BCY).

3.2.5. Sulphate, total hardness, calcium, and magnesium removal

Table III-4 shows the concentrations of SO_4^{2-}, TH, Ca, and Mg in the inlet and outlet samples of CFs. The effluent samples showed significantly higher concentrations of sulphate compared to the influent concentration. This increase observed after the passage through the CFs could be attributed to the oxidation of sulphur bound to carbon and/or the release of SO_4^{2-} from the organic media used (Singh and Chakraborty 2021). However, no statistical difference in SO_4^{2-}

concentration was observed among the effluents during this experiment.

During the CFs operation, TH, Ca, and Mg concentrations were significantly increased after passing through the columns (**Table III-4**). This increase could be attributed to solubilised minerals and/or the presence of bicarbonates and carbonates, which contribute to temporary hardness, and chlorides and sulphates for permanent hardness (Ramachandra et al. 2018). Typically, TH results from dissolving magnesium and calcium substances present in the media. These results contradict some findings reported in the literature (Prajapati et al. 2018; Ghumra et al. 2021).

3.2.6. Absorbance removal

Figure III-12 and **Table III-4** illustrate the trends of absorbance at 254 and 420 nm. Absorbance values at 254 nm and 420 nm reflect the organic micropollutant concentrations, including aromatic halves and/or chromophores, which represent the reliable and rapid screening parameters for studying their removal performance (Ciardelli and Ranieri 2001; Altmann et al. 2016). The effluent samples showed significantly lower concentrations compared to the influent at both wavelengths, highlighting the role of the different types of substrates in the removal of organic micropollutants (**Figure III-12**). At 254 nm, CF-BOP, CF-BOW, and CF-BF showed significantly higher removal performance (range of 36% - 40%) than CF-BCY (25%), while at 420 nm the effluent samples illustrate no significant difference in treatment performance. The removal of absorbance is a topic poorly described in the literature. Ayadi et al. (2024) found a higher range of removal in the BC-based microcosm, about 59% and 31% at 254 and 420 nm, respectively, with statistically significant differences compared to the gravel-based control.

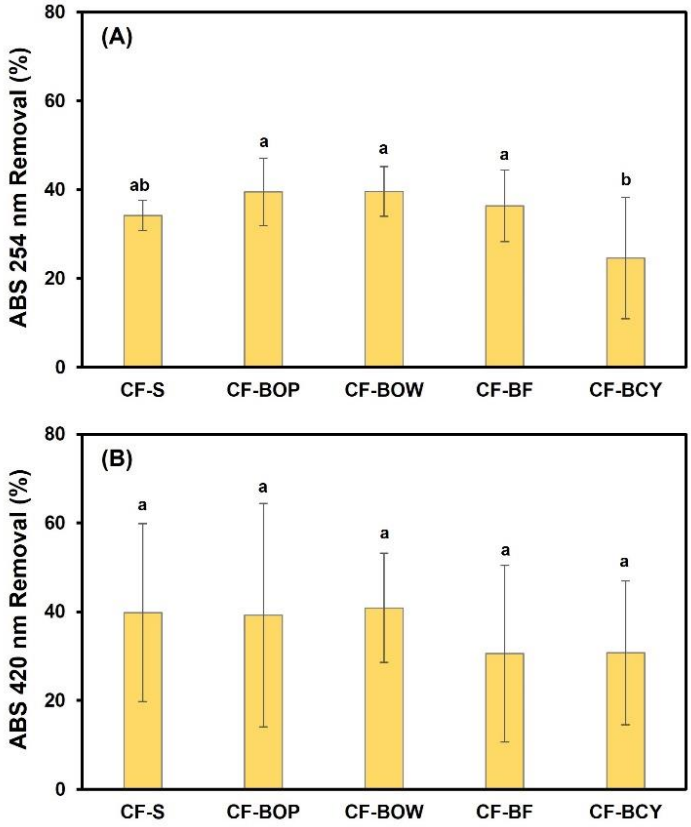

Figure III-12: Average elimination of absorbance measured at 254 (A) and 420 nm (B) in CFs based on sand (CF-S), biochar from olive pomace (CF-BOP), biochar from orange wood waste (CF-BOW), biochar from filao (CF-BF), and biochar from cypress (CF-BCY).

3.2.7. Removal of faecal bacteria indicators

Figure III-13 shows the removal of bacterial indicators, including TC, FC, and FS, measured at the outlet of all CFs. All filters illustrated a very moderate level of elimination for total and faecal coliforms (**Figures III-13A** and **III-13B**), while the removal level of faecal streptococcus was high enough in all CFs, with no statistically significant differences in terms of removal observed between them (**Figure III-13C**). Furthermore, CFs integrated BC showed a significantly higher removal of TC and FC compared to the control filter. Generally, BC has a high porosity, distribution, specific surface area, functional groups, and hydrophobicity, making it more adequate than sand and/or gravel for the removal of microbial fractions (El Barkaoui et al. 2023). Kaetzl et al. (2019) reported that rice-husk BC-filled CWs exhibited better removal of FS, TC, and FC compared to sand-filled CWs. El Ghadraoui et al. (2021, 2020) studied bacterial removal using pozzolan-based CW, resulting in the removal of 2.76, 2.56, and 3.87 log units for TC, FC, and FS, respectively. Moreover, Sleytr et al. (2007) studied the removal of faecal indicators in CW based on conventional materials (sand and gravel), achieving a removal efficiency of 4,37

log units for FC and 4,31 log units for TC. Hijnen et al. (2004) reported a removal of 2-3 log units of E. Coli and thermotolerant coliform at the full-scale and planted pilot. In general, the elimination of bacteria in filters is performed by the combined effects of biological, chemical, and physical processes. The latter includes sedimentation, filtration, and sorption onto media and organic matter. However, the biological processes could include natural die-off, biofilm retention, predation, and competition under nutrient-limited conditions, while the chemical processes are based mostly on oxidation (Wu et al. 2016). The limited effectiveness in removing microbial contaminants in our study may be due to minimal biofilm development within the short experimental duration. Biofilm formation within the filter can enhance filtration by reducing its porosity; as particles accumulate, the filter pore size decreases, thereby improving screening efficiency as the biofilm matures over time. Logan et al. (2001) noted that grain size is a critical factor influencing the removal of Cryptosporidium cysts, as well as probably other pathogens in slow sand-based filters. In addition, the filter depth and short retention time may also help explain the observed results. Similarly, Torrens et al. (2009) reported that filter depth significantly influenced pollutant removal efficiency; deeper filters demonstrated higher removal rates due to increased hydraulic retention time.

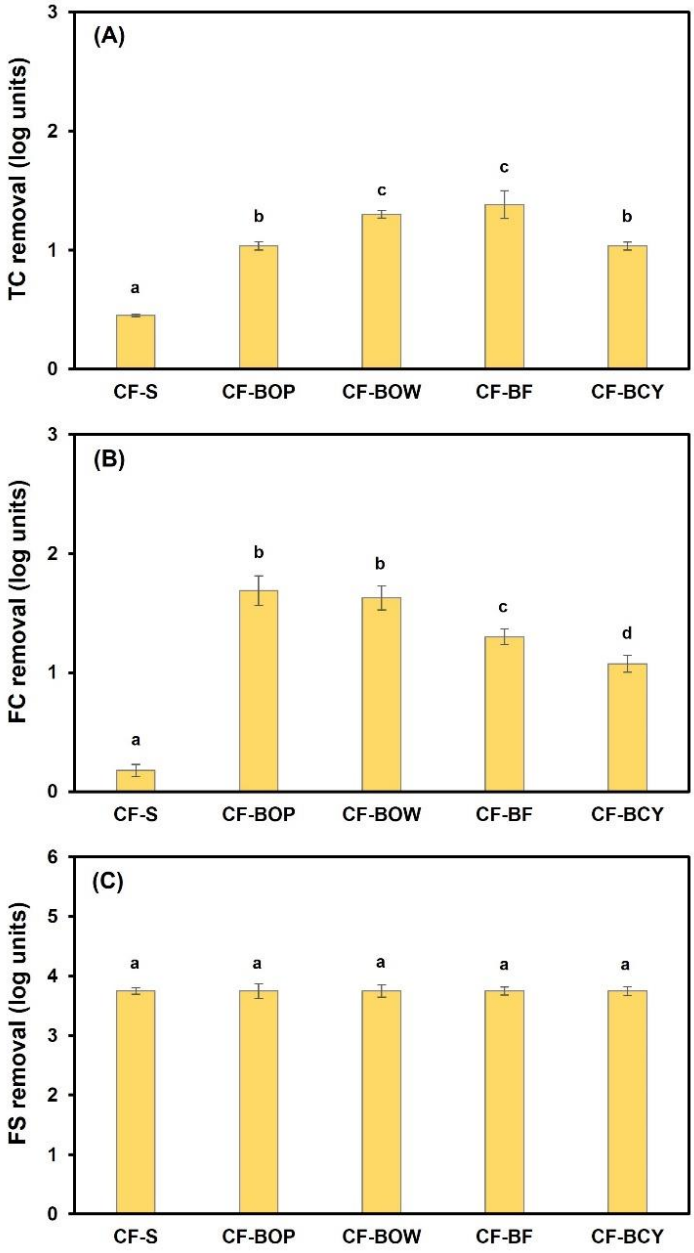

Figure III-13: Average elimination of bacterial indicators: A: total coliform (TC), B: faecal coliforms (FC), and C: faecal streptococci (FS) in CFs based on sand (CF-S), biochar from olive pomace (CF-BOP), biochar from orange wood waste (CF-BOW), biochar from filao (CF-BF), and biochar from cypress (CF-BCY).

Conclusion and future directions

This study comprehensively evaluated the use of biochar (BC) derived from olive pomace, orange wood waste, filao, and cypress as substrates in column filters for wastewater treatment. The results clearly showed that the integration of BC significantly enhances the removal performance of total suspended solids, soluble and total COD, NH_4^+-N, and total and faecal coliforms compared to sand-only filters. Among the tested biochars, filao biochar (CF-BF) showed superior performance,

achieving remarkable removal efficiencies, particularly for ammonium nitrogen, total suspended solids, and total COD. Its ability to support nitrification processes was further highlighted by the conversion of NH_4^+-N to nitrates, a critical step in the nitrogen removal cycle.

Cypress biochar (CF-BCY) was particularly effective in removing total phosphorus and total Kjeldahl nitrogen, while olive pomace biochar (CF-BOP) stood out for its ability to attenuate total nitrogen (TN) and UV-absorbing organic compounds, indicating the removal of organic micropollutants. Orange wood biochar (CF-BOW) also contributed positively to contaminant removal, albeit with varying efficiencies.

This being said, biochar substrates did not improve phosphorus removal compared to conventional sand filters. In addition, their use led to an increase in effluent concentrations of hardness-related ions (e.g. calcium, magnesium, and sulphate), which could affect downstream applications such as irrigation or ecosystem compatibility. These observations highlight the need for careful consideration of biochar properties and potential trade-offs when designing biochar-based treatment systems.

The study confirms the feasibility of biochar as a low-cost, environmentally friendly alternative for improving wastewater treatment performance, particularly in decentralised and rural settings. The tunable properties of biochar, such as pH at the point of zero charge, specific surface area, and porosity, were critical in influencing pollutant adsorption and biological interactions. These findings are invaluable for advancing the design and optimisation of large-scale systems, such as constructed wetlands, to ensure higher pollutant removal efficiencies while meeting sustainability goals.

Future studies should investigate the long-term stability and regeneration of biochar under real operating conditions. Exploring combinations of biochar with different feedstocks and pyrolysis conditions may further enhance multi-pollutant removal capabilities. In addition, the integration of biochar-based systems with other treatment technologies could mitigate some identified limitations, such as increased hardness ion concentrations, thereby improving their overall applicability.

References

AFNOR, 1997. AFNOR, Recueil de Norme Française: Eau, Méthodes D'essai,. 2nd ed., Paris Édition, Paris,.

Alhothali, A., Haneef, T., Mustafa, M.R.U., Moria, K.M., Rashid, U., Rasool, K., Bamasag, O.O., 2021. Optimization of Micro-Pollutants' Removal from Wastewater Using Agricultural Waste-Derived Sustainable Adsorbent. Int. J. Environ. Res. Public Health 18, 11506. https://doi.org/10.3390/ijerph182111506

Altmann, J., Massa, L., Sperlich, A., Gnirss, R., Jekel, M., 2016. UV254 absorbance as real-time monitoring and control parameter for micropollutant removal in advanced wastewater treatment with powdered activated carbon. Water Res. 94, 240–245. https://doi.org/10.1016/j.watres.2016.03.001

Ambaye, T.G., Vaccari, M., van Hullebusch, E.D., Amrane, A., Rtimi, S., 2021. Mechanisms and adsorption capacities of biochar for the removal of organic and inorganic pollutants from industrial wastewater. Int. J. Environ. Sci. Technol. 18, 3273–3294. https://doi.org/10.1007/s13762-020-03060-w

Ayadi, M., Passaseo, D., Bonaccorso, G., Fichera, M., Renai, L., Venturini, L., Colzi, I., Fibbi, D., Del Bubba, M., 2024. Biochar from co-pyrolysis of biological sludge and sawdust in comparison with the conventional filling media of vertical-flow constructed wetlands for the treatment of domestic-textile wastewater. Water Sci. Technol. 89, 1252–1263. https://doi.org/10.2166/wst.2024.056

Bakari, Z., Fichera, M., El Ghadraoui, A., Renai, L., Giurlani, W., Santianni, D., Fibbi, D., Bruzzoniti, M.C., Del Bubba, M., 2024. Biochar from co-pyrolysis of biological sludge and woody waste followed by chemical and thermal activation: end-of-waste procedure for sludge management and biochar sorption efficiency for anionic and cationic dyes. Environ. Sci. Pollut. Res. 31, 35249–35265. https://doi.org/10.1007/s11356-024-33577-3

Camargo, J.A., Alonso, A., Salamanca, A., 2005. Nitrate toxicity to aquatic animals: a review with new data for freshwater invertebrates. Chemosphere 58, 1255–1267. https://doi.org/10.1016/j.chemosphere.2004.10.044

Cha, J.S., Park, S.H., Jung, S.-C., Ryu, C., Jeon, J.-K., Shin, M.-C., Park, Y.-K., 2016. Production and utilization of biochar: A review. J. Ind. Eng. Chem. 40, 1–15. https://doi.org/10.1016/j.jiec.2016.06.002

Chang, J., Peng, D., Deng, S., Chen, J., Duan, C., 2022. Efficient treatment of mercury(II)-containing wastewater in aerated constructed wetland microcosms packed with biochar. Chemosphere 290, 133302. https://doi.org/10.1016/j.chemosphere.2021.133302

Chen, Z., Xiao, X., Chen, B., Zhu, L., 2015. Quantification of Chemical States, Dissociation Constants and Contents of Oxygen-containing Groups on the Surface of Biochars Produced at Different Temperatures. Environ. Sci. Technol. 49, 309–317. https://doi.org/10.1021/es5043468

Ciardelli, G., Ranieri, N., 2001. The treatment and reuse of wastewater in the textile industry by means of ozonation and electroflocculation. Water Res. 35, 567–572. https://doi.org/10.1016/S0043-1354(00)00286-4

de Rozari, P., Greenway, M., El Hanandeh, A., 2016. Phosphorus removal from secondary sewage and septage using sand media amended with biochar in constructed wetland mesocosms. Sci. Total Environ. 569–570, 123–133. https://doi.org/10.1016/j.scitotenv.2016.06.096

Deng, C., Huang, L., Liang, Y., Xiang, H., Jiang, J., Wang, Q., Hou, J., Chen, Y., 2019. Response of microbes to biochar strengthen nitrogen removal in subsurface flow constructed wetlands: Microbial community structure and metabolite characteristics. Sci. Total Environ. 694, 133687. https://doi.org/10.1016/j.scitotenv.2019.133687

Deng, S., Chen, J., Chang, J., 2021. Application of biochar as an innovative substrate in constructed wetlands/biofilters for wastewater treatment: Performance and ecological benefits. J. Clean. Prod. 293, 126156. https://doi.org/10.1016/j.jclepro.2021.126156

El Barkaoui, S., Mandi, L., Aziz, F., Del Bubba, M., Ouazzani, N., 2023. A critical review on using biochar as constructed wetland substrate: Characteristics, feedstock, design and pollutants removal mechanisms. Ecol. Eng. 190, 106927. https://doi.org/10.1016/j.ecoleng.2023.106927

El Barkaoui, S., Mandi, L., Fichera, M., Ryah, H., Baçaoui, A., Del Bubba, M., Ouazzani, N., 2025. Optimizing biochar-based column filtration systems for enhanced pollutant removal in wastewater treatment: A preliminary study. Chemosphere 372, 144067. https://doi.org/10.1016/j.chemosphere.2025.144067

El Ghadraoui, A., Ouazzani, N., Ahmali, A., El Mansour, T.E.H., Aziz, F., Hejjaj, A., Del Bubba, M., Mandi, L., 2020. Treatment of olive mill and municipal wastewater mixture by pilot scale vertical flow constructed wetland. Desalin. Water Treat. 198, 126–139. https://doi.org/10.5004/dwt.2020.26009

El Ghadraoui, A., Ouazzani, N., Saf, C., Ahmali, A., Hejjaj, A., Aziz, F., Del Bubba, M., Mandi, L., 2021. Behaviour of physicochemical and microbiological characteristics of vertical flow constructed wetland substrate after treating a mixture of urban and olive mill wastewaters. Environ. Sci. Pollut. Res. 28, 55433–55445. https://doi.org/10.1007/s11356-021-14874-7

El Hanandeh, A., Bhuvaneswaran, A., de Rozari, P., 2017. Removal of nitrate, ammonia and phosphate from aqueous solutions in packed bed filter using biochar augmented sand media. MATEC Web Conf. 120, 05004. https://doi.org/10.1051/matecconf/201712005004

El Hanandeh, A., Gharaibeh, M., Albalasmeh, A.A., 2018. Phosphorus removal efficiency from wastewater under different loading conditions using sand biofilters augmented with biochar. Int. J. Environ. Sci. Technol. 15, 927–934. https://doi.org/10.1007/s13762-017-1474-0

Enaime, G., Baçaoui, A., Yaacoubi, A., Lübken, M., 2020. Biochar for Wastewater Treatment—Conversion Technologies and Applications. Appl. Sci. 10, 3492. https://doi.org/10.3390/app10103492

European Committee for Standardization, 2009 EN 12915, 2009. Products Used for the Treatment of Water Intended for Human Consumption – Granular Activated Carbon. In.

García-Ávila, F., Galarza-Guamán, A., Barros-Bermeo, M., Alfaro-Paredes, E.A., Avilés-Añazco, A., Iglesias-Abad, S., 2023. Integration of high-rate filtration using waste-derived biochar as a potential sustainable

technology for drinking water supply. Biochar 5, 62. https://doi.org/10.1007/s42773-023-00256-4
Ghumra, D.P., Agarkoti, C., Gogate, P.R., 2021. Improvements in effluent treatment technologies in Common Effluent Treatment Plants (CETPs): Review and recent advances. Process Saf. Environ. Prot. https://doi.org/10.1016/j.psep.2021.01.021
Hijnen, W.A.M., Schijven, J.F., Bonné, P., Visser, A., Medema, G.J., 2004. Elimination of viruses, bacteria and protozoan oocysts by slow sand filtration. Water Sci. Technol. 50, 147–154. https://doi.org/10.2166/wst.2004.0044
Ji, B., Chen, J., Mei, J., Chang, J., Li, X., Jia, W., Qu, Y., 2020. Roles of biochar media and oxygen supply strategies in treatment performance, greenhouse gas emissions, and bacterial community features of subsurface-flow constructed wetlands. Bioresour. Technol. 302, 122890. https://doi.org/10.1016/j.biortech.2020.122890
Kaetzl, K., Lübken, M., Uzun, G., Gehring, T., Nettmann, E., Stenchly, K., Wichern, M., 2019. On-farm wastewater treatment using biochar from local agroresidues reduces pathogens from irrigation water for safer food production in developing countries. Sci. Total Environ. 682, 601–610. https://doi.org/10.1016/j.scitotenv.2019.05.142
Khalifa, M.E., El-Reash, Y.G.A., Ahmed, M.I., Rizk, F.W., 2020. Effect of media variation on the removal efficiency of pollutants from domestic wastewater in constructed wetland systems. Ecol. Eng. 143, 105668. https://doi.org/10.1016/j.ecoleng.2019.105668
Kizito, S., Lv, T., Wu, S., Ajmal, Z., Luo, H., Dong, R., 2017. Treatment of anaerobic digested effluent in biochar-packed vertical flow constructed wetland columns: Role of media and tidal operation. Sci. Total Environ. 592, 197–205. https://doi.org/10.1016/j.scitotenv.2017.03.125
Lewis, W.M., Morris, D.P., 1986. Toxicity of Nitrite to Fish: A Review. Trans. Am. Fish. Soc. 115, 183–195. https://doi.org/10.1577/1548-8659(1986)115<183:TONTF>2.0.CO;2
Li, J., Fan, J., Zhang, J., Hu, Z., Liang, S., 2018. Preparation and evaluation of wetland plant-based biochar for nitrogen removal enhancement in surface flow constructed wetlands. Environ. Sci. Pollut. Res. 25, 13929–13937. https://doi.org/10.1007/s11356-018-1597-y
Li, Liya, Feng, J., Zhang, L., Yin, H., Fan, C., Wang, Z., Zhao, M., Ge, C., Song, H., 2021. Enhanced nitrogen and phosphorus removal by natural pyrite–based constructed wetland with intermittent aeration. Environ. Sci. Pollut. Res. 28, 69012–69028. https://doi.org/10.1007/s11356-021-15461-6
Li, Lei, Guo, X., Zhao, T., Li, T., 2021. Green waste composting with bean dregs, tea residue, and biochar: Effects on organic matter degradation, humification and compost maturity. Environ. Technol. Innov. 24, 101887. https://doi.org/10.1016/j.eti.2021.101887
Liang, Y., Wang, Q., Huang, L., Liu, M., Wang, N., Chen, Y., 2020. Insight into the mechanisms of biochar addition on pollutant removal enhancement and nitrous oxide emission reduction in subsurface flow constructed wetlands: Microbial community structure, functional genes and enzyme activity. Bioresour. Technol. 307, 123249. https://doi.org/10.1016/j.biortech.2020.123249
Liao, Y., Jiang, L., Cao, X., Zheng, H., Feng, L., Mao, Y., Zhang, Q., Shen, Q., Ji, F., 2022. Efficient removal mechanism and microbial characteristics of tidal flow constructed wetland based on in-situ biochar regeneration (BR-TFCW) for rural gray water. Chem. Eng. J. 431, 134185. https://doi.org/10.1016/j.cej.2021.134185
Logan, A.J., Stevik, T.K., Siegrist, R.L., Rønn, R.M., 2001. Transport and fate of Cryptosporidium parvum oocysts in intermittent sand filters. Water Res. 35, 4359–4369. https://doi.org/10.1016/S0043-1354(01)00181-6
Lu, J., Guo, Z., Pan, Y., Li, M., Chen, X., He, M., Wu, H., Zhang, J., 2022. Simultaneously enhanced removal of PAHs and nitrogen driven by Fe2+/Fe3+ cycle in constructed wetland through automatic tidal operation. Water Res. 215, 118232. https://doi.org/10.1016/j.watres.2022.118232
Ma, R., Ma, J., Chen, Y., Zhuo, Y., Cheng, L., Jiang, L., Mao, Y., Shen, Q., Liu, C., Ji, F., 2023. Efficient removal of nitrogen from tidal flow constructed wetlands based on the in-situ zeolite regeneration: Measures and mechanisms. Chem. Eng. J. 458, 141298. https://doi.org/10.1016/j.cej.2023.141298
Nguyen, X.C., Tran, T.C.C.P.P., Hoang, V.H., Nguyen, T.P., Chang, S.W., Nguyen, D.D., Guo, W., Kumar, A., La, D.D., Bach, Q.V., 2020. Combined biochar vertical flow and free-water surface constructed wetland system for dormitory sewage treatment and reuse. Sci. Total Environ. 713, 136404. https://doi.org/10.1016/j.scitotenv.2019.136404
Osborn, D., Cutter, A., Ullah, F., 2015. Universal Sustainable Development Goals: Understanding the transformational challenge for developed countries, Universal Sustainable Development Goals.
Perez-Mercado, L.F., Lalander, C., Berger, C., Dalahmeh, S.S., 2018. Potential of Biochar Filters for Onsite Wastewater Treatment: Effects of Biochar Type, Physical Properties and Operating Conditions. Water 10, 1835. https://doi.org/10.3390/w10121835
Rabichi, I., Sekkouri, C., Yaacoubi, F.E., Ennaciri, K., Izghri, Z., Bouzid, T., El Fels, L., Baçaoui, A., Yaacoubi, A., 2024. Experimental and Theoretical Investigation of Olive Mill Solid Waste Biochar for Vanillic Acid Adsorption Using DFT/B3LYP Analysis. Water, Air, Soil Pollut. 235, 369.

https://doi.org/10.1007/s11270-024-07183-5
Ramachandra, T. V, Sincy, V., Asulabha, K.S., Mahapatra, D.M., Bhat, S.P., Aithal, B.H., 2018. Optimal Treatment of Domestic Wastewater through Constructed Wetlands. J Biodivers. 9, 81–102. https://doi.org/11.258359/KRE-180
Rodier, J., 2009. L'analyse de l'eau _ Rodier 9e édition.pdf.
S.E.E.E, 2007. Moroccan water quality grid for irrigation purposes, State Secretariat at the Ministry of Energy, Mines, Water and Environment, Charge of Water and Environment, Kingdom of Morocco, Water Quality Standards for Irrigation, 2007.
Singh, E., Mishra, R., Kumar, A., Shukla, S.K., Lo, S.-L., Kumar, S., 2022. Circular economy-based environmental management using biochar: Driving towards sustainability. Process Saf. Environ. Prot. 163, 585–600. https://doi.org/10.1016/j.psep.2022.05.056
Singh, S., Chakraborty, S., 2021. Bioremediation of acid mine drainage in constructed wetlands: Aspect of vegetation (Typha latifolia), loading rate and metal recovery. Miner. Eng. 171, 107083. https://doi.org/10.1016/j.mineng.2021.107083
Sleytr, K., Tietz, A., Langergraber, G., Haberl, R., 2007. Investigation of bacterial removal during the filtration process in constructed wetlands. Sci. Total Environ. 380, 173–180. https://doi.org/10.1016/j.scitotenv.2007.03.001
Stefanakis, A., 2019. The Role of Constructed Wetlands as Green Infrastructure for Sustainable Urban Water Management. Sustainability 11, 6981. https://doi.org/10.3390/su11246981
Tan, C., Ma, F., Li, A., Qiu, S., Li, J., 2013. Evaluating the Effect of Dissolved Oxygen on Simultaneous Nitrification and Denitrification in Polyurethane Foam Contact Oxidation Reactors. Water Environ. Res. 85, 195–202. https://doi.org/10.2175/106143012X13503213812445
Torrens, A., Molle, P., Boutin, C., Salgot, M., 2009. Removal of bacterial and viral indicator in vertical flow constructed wetlands and intermittent sand filters. Desalination 246, 169–178. https://doi.org/10.1016/j.desal.2008.03.050
Uday Bhan Prajapati, Arun Lal Srivastav, Shiraz A.Wajih, 2018. Eco-management of Wastewater by ZESTP. J. Chem. Environ. Sci. its Appl. 4, 51–57. https://doi.org/10.15415/jce.2018.42007
Vohla, C., Kõiv, M., Bavor, H.J., Chazarenc, F., Mander, Ü., 2011. Filter materials for phosphorus removal from wastewater in treatment wetlands—A review. Ecol. Eng. 37, 70–89. https://doi.org/10.1016/j.ecoleng.2009.08.003
Vymazal, J., 2007. Removal of nutrients in various types of constructed wetlands. Sci. Total Environ. 380, 48–65. https://doi.org/10.1016/j.scitotenv.2006.09.014
Werner, S., Kätzl, K., Wichern, M., Buerkert, A., Steiner, C., Marschner, B., 2018. Agronomic benefits of biochar as a soil amendment after its use as waste water filtration medium. Environ. Pollut. 233, 561–568. https://doi.org/10.1016/j.envpol.2017.10.048
Wu, S., Carvalho, P.N., Müller, J.A., Manoj, V.R., Dong, R., 2016. Sanitation in constructed wetlands: A review on the removal of human pathogens and fecal indicators. Sci. Total Environ. 541, 8–22. https://doi.org/10.1016/j.scitotenv.2015.09.047
Xin, X., Liu, S., Qin, J., Ye, Z., Liu, W., Fang, S., Yang, J., 2021. Performances of simultaneous enhanced removal of nitrogen and phosphorus via biological aerated filter with biochar as fillers under low dissolved oxygen for digested swine wastewater treatment. Bioprocess Biosyst. Eng. 44, 1741–1753. https://doi.org/10.1007/s00449-021-02557-z
Yao, Y., Gao, B., Zhang, M., Inyang, M., Zimmerman, A.R., 2012. Effect of biochar amendment on sorption and leaching of nitrate, ammonium, and phosphate in a sandy soil. Chemosphere 89, 1467–1471. https://doi.org/10.1016/j.chemosphere.2012.06.002
Yousaf, A., Khalid, N., Aqeel, M., Noman, A., Naeem, N., Sarfraz, W., Ejaz, U., Qaiser, Z., Khalid, A., 2021. Nitrogen Dynamics in Wetland Systems and Its Impact on Biodiversity. Nitrogen 2, 196–217. https://doi.org/10.3390/nitrogen2020013
Zhang, Q., Yang, Y., Chen, F., Zhang, L., Ruan, J., Wu, S., Zhu, R., 2021. Effects of hydraulic loading rate and substrate on ammonium removal in tidal flow constructed wetlands treating black and odorous water bodies. Bioresour. Technol. 321, 124468. https://doi.org/10.1016/j.biortech.2020.124468
Zheng, F., Fang, J., Guo, F., Yang, X., Liu, T., Chen, M., Nie, M., Chen, Y., 2022. Biochar based constructed wetland for secondary effluent treatment: Waste resource utilization. Chem. Eng. J. 432, 134377. https://doi.org/10.1016/j.cej.2021.134377
Zhou, X., Wang, R., Liu, H., Wu, S., Wu, H., 2019. Nitrogen removal responses to biochar addition in intermittent-aerated subsurface flow constructed wetland microcosms: Enhancing role and mechanism. Ecol. Eng. 128, 57–65. https://doi.org/10.1016/j.ecoleng.2018.12.028

III-III. Effect of Organic Loading Rates on Olive Pomace Biochar-Enhanced Vertical Flow Constructed Wetlands for Wastewater Treatment

This work was published as a research paper:

El Barkaoui, **S.,** Ouazzani, N., Ryah, H., Sbahi, S., Rabichi, I., Del Bubba, M., Mandi, L. (2025). Effect of Organic Loading Rates on Olive Pomace Biochar-Enhanced Vertical Flow Constructed Wetlands for Wastewater Treatment. Environ Sci Pollut Res (2025). https://doi.org/10.1007/s11356-025-37083-y.

Abstract

This study investigates the performance of vertical flow constructed wetlands (VF-CWs) using olive pomace biochar (CW-B) versus a sand-only control (CW-C) under two organic loading rates (OLR): low (20 g COD/m².d) and high (70 g COD/m².d). At low OLR, CW-B achieved higher removal efficiencies than CW-C, with 60% vs. 50% for COD, 85% vs. 71% for NH_4^+-N, 74% vs. 52% for TKN, 81% vs. 67% for TSS, and over 3-log unit reductions in faecal indicators. Increasing OLR led to an overall decrease in treatment efficiency, although CW-B remained superior. Biochar had a limited effect on phosphorus, sulphate, and hardness removal. Release of NO_2 and NO_3 confirmed active nitrification, which decreased at high OLR. These results highlight the potential of olive pomace biochar as a sustainable and effective VF-CW substrate, especially under moderate organic loads.

Keywords: Biochar-based filters; Domestic wastewater treatment; Organic matter removal; Nutrient removal; Pathogen removal.

1. Introduction

With the rapid growth of the global population and urbanization, the demand for clean water is increasing while freshwater resources are becoming scarce. Industrialization and agricultural activities contribute to wastewater generation, often containing pollutants such as heavy metals, inorganic and organic compounds, and pathogens (Saravanan et al., 2021). Wastewater treatment is one of the best ways to preserve water for reuse in different sectors, such as agriculture. Unfortunately, the traditional wastewater treatment plants using conventional material-based biofilters (e.g., sand, gravel) are in most cases not 100% efficient in removing most pollutants, making a major concern for the safety of water resources (Gadipelly et al., 2014). Eco-friendly technologies such as biochar-based vertical flow-constructed wetlands (VF-CWs) could be an adequate solution (sustainable, cheap, and environmental) to treat wastewater (Stefanakis, 2019), due to the large benefits of biochar (BC) as an efficient adsorbent material (high specific area, porous structure, and large functional groups on the surface) (El Barkaoui et al., 2025a). An efficient treatment of wastewater requires the optimisation of several parameters, such as the characteristics of BC, which are strictly dependent on the origin of raw material and the pyrolysis conditions used (El Barkaoui et al., 2025b; Wang et al., 2024). The literature pointed out that the BC should be prepared from biomass containing a high carbon content and low minerals, and pyrolysis it under an inert atmosphere in a range of temperature from 400 to 600 °C and a contact time of 1–2h, maintaining a large surface functionalization and high yield (El Barkaoui et al., 2023). Furthermore, the availability and cost of biomass could present real economic challenges. In the Mediterranean region, olive pomace (OP) is one of the most abundant residues due to the area's high production and consumption of olive oil. In 2021/22, Spain produced 1,300 tonnes,

Italy produced 315 tonnes, Turkey produced 228 tonnes, Greece produced 225 tonnes, Tunisia produced 240 tonnes, and Morocco produced 200 tonnes (EU Olive Oil Production, 2021). The transformation of OP into BC could be a sustainable and low-cost solution in terms of environmental and economic value. According to the literature, only three papers have used the BC derived from OP as a filter substrate for wastewater treatment, producing it in a range of temperature of 550-600 °C under an inert atmosphere for 90 min of contact time, obtaining BC with good quality and high yields (25–30%) (El Hanandeh et al., 2018, 2017; El Barkaoui et al., 2025c).

Secondly, it is necessary to think deeply about optimizing the configuration of the OP-BC substrate-based filter (e.g., position and concentrations of BC, plantation, and organic loading rate (OLR)) for efficient wastewater treatment. Regardless of the type of BC, it is believed that the best position for the BC substrate is between two inert media (e.g., gravel, sand) to prevent the BC from floating or clogging the filter (Visiy et al., 2022; El Barkaoui et al., 2023; Karki, 2024). El Barkaoui et al., (2025c) investigated the impact of increasing the percentage of OP-derived BC (0%, 10%, 25%, and 50%) on the treatment performance of unplanted column filtration systems. They found that systems containing BC performed better than the sand-filled system, though there were no significant differences among the various BC percentages. While the impact of increasing the OLR on the treatment performance of planted VF-CWs integrated with OP-derived BC has never been investigated. Furthermore, there is limited information in the literature on using BC from OP as a VF-CW substrate, and its removal performance toward nitrogen, organic carbon, nitrite nitrogen, absorbance at 254 nm and 420 nm, and pathogens.

Therefore, this study aims to evaluate the effect of increasing organic loading rates (from 20 to 70 g COD/m².d) on the performance of vertical flow constructed wetlands (VF-CWs) amended with biochar derived from olive pomace. The evaluation focuses on the removal efficiencies of chemical pollutants (e.g., COD, nitrogen species, phosphorus, sulphates, hardness) and microbiological pollutants (e.g., total and faecal coliforms, faecal streptococci), with the aim of determining the potential of this low-cost biochar substrate to improve wastewater treatment under different operating conditions.

2. Materials and methods

2.1. Experimental design of VF-CWs

Two VF-CWs were established using cylindrical polyethylene containers, each with identical dimensions: 0.45 meters in height, 0.30 meters in diameter, and a surface area of 0.07 m² **(Figure III-14)**. The bed frame structure of each VF-CW is 0.30 m, supported by packed substances consisting from the bottom with 8 cm of gravel (particle size: 2–8 cm), BC–sand mixture (particle size: 2–5 cm and 1–2 cm respectively) of volume ratios 1:10 for CW-B and sand alone for the control CW-C, and a top layer of gravel (particle size: 2–6 cm). Each system was fitted with two aeration tubes to provide oxygen during the filtration process and planted with young *Phragmites australis* shoots at a density of 4 plants m^{-2} (El Ghadraoui et al., 2020).

The BC used in this study was derived from exhausted olive pomace. It was heated at 590 °C for two hours and at a heating rate of 10 °C per minute. This process resulted in the following properties: a specific surface area of 106 m^2 g^{-1}, a mesopore surface area of 113 m^2 g^{-1}, a pore volume of 0.130402 cm^3/g, a carbon content of 90% nm, an ash content of 4.9%, and a pH at the point of zero charge of 7.8. A full description of the BC characteristics is reported in the previous work in El Barkaoui et al. (2025c).

The experimental period was divided into two distinct phases based on OLRs. The low OLR phase (20 g COD/m²·d), from June 2023 to March 2024, operated in a sequential batch filling and rest mode, with five batches per day and a total influent volume of 5 L/day, incorporating a one-day drying period. The high OLR phase (70 g COD/m²·d), from April 2024 to January 2025, maintained the same batch frequency but increased the total influent volume to 15 L/day while preserving the one-day drying period. Further design criteria details are provided in **Table III-5**.

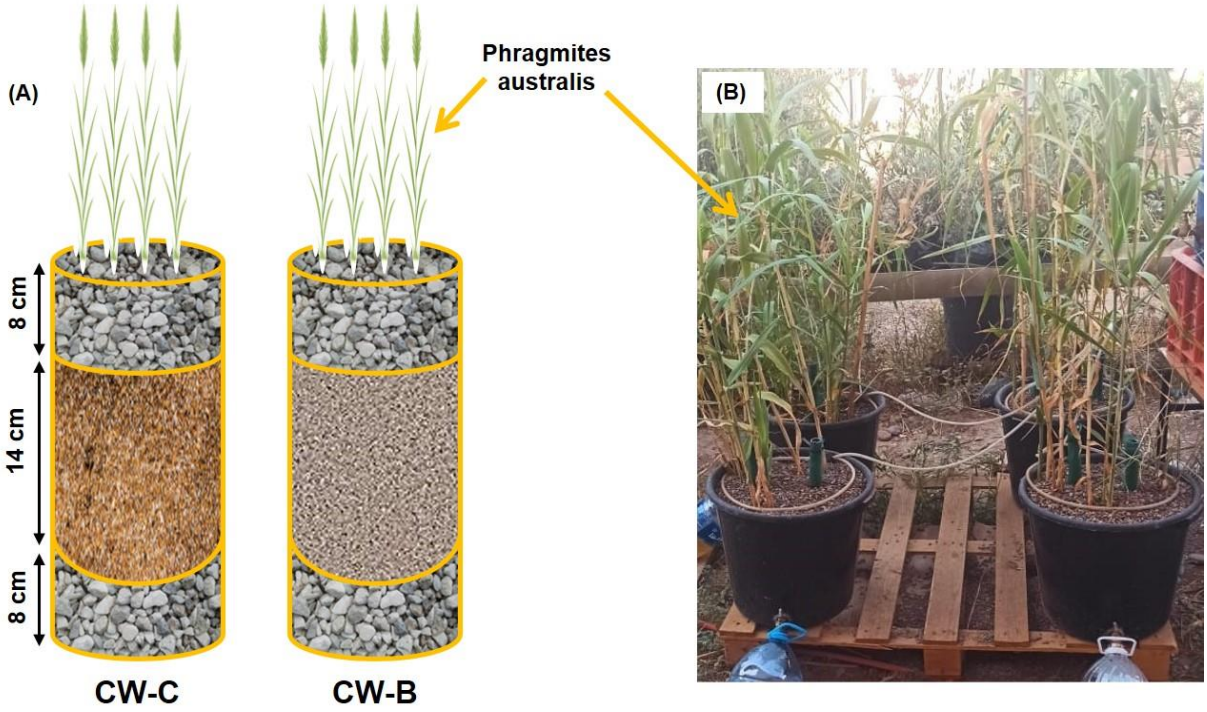

Figure III-14: Schematic illustration (A) and photograph (B) of the pilot-scale vertical flow constructed wetlands filled with biochar (CW-B) and without biochar (CW-C).

Table III-5: Design criteria for pilot-scale vertical flow constructed wetlands filled with (CW-B) and without (CW-C) biochar.

Setup	CW-C		CW-B	
OLR	20	70	20	70
Flow rate (L/h)	0.54	10.52	4.02	19.12
Cross-sectional velocity (m/h)	0.0077	0.1503	0.0574	0.2731
Hydraulic retention time (h)	38.9	2	5.22	1.10

2.2. Sample collection and analytical methodology

The wastewater used in the experiment was collected biweekly from the Marrakech Wastewater Treatment Plant (WWTP) after primary decantation and analysed immediately after sampling. **Table III-6** shows the full characteristics of the influent samples throughout the whole experimental duration.

Water quality parameters were determined using the standard methods of AFNOR (1997) and Rodier (2009). Total suspended solids (TSS) were measured by filtering the samples through a 0.45 µm Millipore (Burlington, MA, USA) glass fiber filter, followed by drying at 105 °C until a constant weight was achieved (AFNOR T90-105). Chemical oxygen demand (COD) was

determined via dichromate digestion and colorimetry (AFNOR T90-101). Total phosphorus (TP) was analyzed using the molybdate-ascorbic acid method following potassium peroxydisulfate digestion (AFNOR T 90-023), and orthophosphate (PO_4^{3-}) was quantified using the same method (AFNOR T 90-022). Total Kjeldahl nitrogen (TKN) was measured via Kjeldahl mineralization, ammonium distillation, and acidimetric titration. Ammoniacal nitrogen (NH_4^+-N) was determined using the indophenol method (AFNOR T 90-015); nitrite (NO_2^-–N) was determined using the diazotation method (AFNOR T 90-013); and nitrate (NO_3^-–N) was determined after reduction to nitrite via a copper–cadmium column (Rodier, 2009). Total nitrogen (TN) was calculated as the sum of TKN, NO_2^-–N, and NO_3^-–N. Sulphates were measured nephelometrically, and total hardness, calcium, and magnesium were determined simultaneously using the EDTA titrimetric method.

Dissolved oxygen (DO), electrical conductivity (EC), and pH were measured in situ with a multi-parameter HI 9829 probe (HANNA, Woonsocket, RI, USA). The absorbance of the influent and effluent samples was measured at 254 and 420 nm. Pathogen indicators of faecal pollution, such as faecal streptococci (FS), faecal coliforms (FC), and total coliforms (TC), were quantified according to AFNOR standard methods (AFNOR, 1997).

TC and FC were grown on TTC Tergitol medium and incubated at 37 °C and 44.5 °C, respectively, for 24 h before colony counting. FS were enumerated on BEA medium at 44.5 °C for 24 h.

2.3. Statistical analysis

Statistical analysis was conducted using the Games-Howell non-parametric test and analysis of variance (ANOVA), with Minitab 17 software (version 17.1.0, State College, PA, USA). The significance of results was assessed with p-values, where $p > 0.05$ was considered non-significant and $p < 0.05$ was considered significant. Principal component analysis (PCA) was used to explore the information contained within the entire database, to identify potential relationships between variables, and to better understand the influence of various factors on water quality parameters. Meanwhile, Pearson's correlation coefficient was applied to measure linear relationships between water quality indicators, helping to gauge the degree of convergence or divergence of water quality indicators in their behaviour.

3. Results and discussion

3.1. Overall treatment performance

3.1.1. Physicochemical parameters

Table III-6 presents the EC, pH, DO, and TSS data analysed at the inlet and outlet of CW-C and CW-B during low and high OLR periods. The influent pH was approximately 7.6–7.7. After treatment, the outlet samples of CW-C and CW-B showed a significant increase during the low OLR period (8.1-8.2), while at high OLR showed insignificant differences, which could be attributed to the excessive feeding volume, leading to less contact time between the influent and the material substrate. The alkalization observed for the treated samples may be due to biological oxidation or dilution of carbonate salts from bed-filled CWs, hydroxyls, and/or their strong H^+ exchange capacity (Chen et al., 2015). The EC showed a statistical increase after treatment at high and low OLR in all effluent samples. This increase may be attributed to the oxidation of organic compounds during the treatment. In general, EC reflects the overall concentration of dissolved ions in solution. Its elevation can be attributed both to the leaching of ions from the substrate into the pretreated solution and to the generation of ionic species during the biodegradation of organic matter (Achak et al., 2023). Throughout the experiment, the influent DO concentration remained consistently low (0.3–0.4 mg L^{-1}), likely due to the high oxygen demand associated with the concurrent oxidation of organic matter and nitrification processes (Fan et al., 2013; Kizito et al., 2017). However, without active aeration, the DO concentrations after treatment increased significantly to 1.1 mg L^{-1} under low OLR, reflecting the improved quality of wastewater after treatment (Nguyen et al., 2020a). During the second period under high OLR, the DO concentration of the effluent samples (0.6 – 0.7 mg L^{-1}) decreased and became significantly closer to the influent concentration (0.3 mg L^{-1}). This decline could be due to higher microbial oxygen consumption, limited oxygen transfer, and increased biofilm thickness. Furthermore, an excess of organic matter can also cause clogging, further restricting aeration. As a result, lower DO levels may shift microbial processes toward anaerobic pathways, affecting treatment efficiency (Maina et al., 2011). Generally, the key sources of oxygen supply are air reoxygenation, water inflow, and oxygen diffusion during dry periods (Ye et al., 2012; Kasak et al., 2018). The pH, EC, and DO parameters recorded during the treatment process fall within the permissible limits set by Moroccan regulations for the reuse of treated wastewater in agricultural applications (S.E.E.E, 2007).

Table III-6: Values (mean ± standard deviation) of water quality parameters measured in the inlet and outlet samples of the vertical flow-constructed wetlands filled with sand (CW-C) and biochar (CW-B) during the low and high organic loading rates (OLR) periods. Different letters (a, b, c) in each row mean statistically significant differences (P<0.05) according to Fisher or Games.

Parameters	OLR	Influent	Effluents	
			CW-C	CW-B
pH	Low	7.7 ± 0.2^{a}	8.1 ± 0.1^{b}	8.1 ± 0.1^{b}
	High	7.6 ± 0.2^{a}	7.8 ± 0.3^{b}	7.6 ± 0.1^{ab}
EC	Low	2.3 ± 0.3^{a}	4 ± 1^{b}	4 ± 1^{b}
(mS/cm)	High	2.4 ± 0.6^{a}	4 ± 1^{b}	3.5 ± 0.7^{b}
DO	Low	0.4 ± 0.3^{a}	1.1 ± 0.8^{b}	1.1 ± 0.6^{b}
(mg/L)	High	0.3 ± 0.4^{a}	0.6 ± 0.5^{ab}	0.7 ± 0.5^{b}
TSS	Low	212 ± 105^{a}	69 ± 37^{b}	37 ± 25^{b}
(mg/L)	High	332 ± 82^{a}	90 ± 35^{b}	54 ± 45^{b}
COD	Low	272 ± 77^{a}	131 ± 29^{b}	106 ± 25^{b}
(mg/L)	High	332 ± 71^{a}	200 ± 47^{b}	170 ± 41^{b}
TP	Low	12 ± 2^{a}	5 ± 2^{b}	6 ± 2^{b}
(mg/L)	High	12 ± 2^{a}	9 ± 1^{b}	8.4 ± 0.7^{b}
PO_4^{3-}	Low	9 ± 1^{a}	4 ± 1^{b}	5 ± 1^{b}
(mg/L)	High	10 ± 2^{a}	7.4 ± 0.9^{b}	7 ± 1^{b}
TN	Low	142 ± 31^{a}	84 ± 22^{b}	64 ± 14^{b}
(mg/L)	High	157 ± 36^{a}	101 ± 39^{b}	104 ± 36^{b}
TKN	Low	139 ± 29^{a}	62 ± 16^{b}	34 ± 9^{c}
(mg/L)	High	154 ± 35^{a}	86 ± 32^{b}	81 ± 29^{b}
NH_4^{+}	Low	69 ± 21^{a}	18 ± 4^{b}	9 ± 4^{b}
(mg/L)	High	92 ± 10^{a}	38 ± 15^{b}	33 ± 11^{b}
NO_2^{-}	Low	0.10 ± 0.04^{a}	4 ± 3^{b}	5 ± 3^{b}
(mg/L)	High	0.12 ± 0.03^{a}	1 ± 1^{b}	1.3 ± 0.9^{b}
NO_3^{-}	Low	3 ± 2^{a}	18 ± 9^{b}	25 ± 13^{b}
(mg/L)	High	3 ± 2^{a}	13 ± 10^{b}	22 ± 14^{b}
SO_4^{2-}	Low	75 ± 27^{a}	83 ± 23^{a}	80 ± 23^{a}
(mg/L)	High	89 ± 33^{a}	98 ± 39^{a}	103 ± 27^{a}
Total hardness	Low	369 ± 34^{a}	735 ± 153^{b}	700 ± 129^{b}
(mg/L)	High	365 ± 23^{a}	599 ± 103^{b}	621 ± 116^{b}
Calcium	Low	61 ± 9^{a}	150 ± 27^{b}	141 ± 23^{b}
(mg/L)	High	71 ± 8^{a}	125 ± 32^{b}	127 ± 44^{b}
Magnesium	Low	308 ± 34^{a}	584 ± 149^{b}	558 ± 114^{b}
(mg/L)	High	295 ± 28^{a}	474 ± 75^{b}	494 ± 82^{b}
ABS 254 nm	Low	633 ± 101^{a}	329 ± 95^{b}	313 ± 94^{b}
(mAu)	High	625 ± 24^{a}	433 ± 39^{b}	401 ± 38^{b}
ABS 420 nm	Low	96 ± 20^{a}	41 ± 14^{b}	29 ± 16^{b}
(mAu)	High	100 ± 7^{a}	69 ± 13^{b}	57 ± 16^{b}
Total coliform	Low	8 ± 1^{a}	3 ± 1^{b}	3 ± 1^{b}
(Log unit)	High	4.9 ± 0.7^{a}	2.9 ± 0.4^{b}	2.8 ± 0.4^{b}
Faecal coliforms	Low	6.3 ± 0.9^{a}	2 ± 2^{b}	2 ± 1^{b}
(Log unit)	High	4.2 ± 0.5^{a}	2.8 ± 0.4^{b}	2.7 ± 0.7^{b}
Faecal streptococci	Low	6.4 ± 0.5^{a}	3.9 ± 0.2^{b}	3.18 ± 0.05^{c}
(Log unit)	High	5.3 ± 0.4^{a}	4.8 ± 0.2^{a}	3.97 ± 0.09^{c}

TSS is a crucial parameter in determining the quality of the effluent and its possibility of reuse in agriculture. Regardless of the OLR and the media filling the VF-CWs, the filter systems showed

high reductions in TSS concentrations (**Table III-6**). In addition, CW-B had a lower TSS concentration than CW-C throughout the experimental study (**Figure III-15**). Moreover, BC-filled CWs showed significantly higher removal (81% – 84%) than the control CW-C (67% – 71%) (**Table III-7**). The latter was less homogeneous than the VF-CW filled with BC. These findings can be attributed to the fact that BC has a greater ability to remove the colloidal particles present in the influent due to biochar's higher sorption properties than sand (El Barkaoui et al., 2025c). The influent TSS concentration in the second period under higher OLR was higher compared to the first period under low OLR (333 and 212 mg L^{-1}, respectively). Even when a high OLR is applied, the TSS removal efficiency remains stable throughout the experiment, demonstrating that the removal rate is strongly related to the inlet concentration.

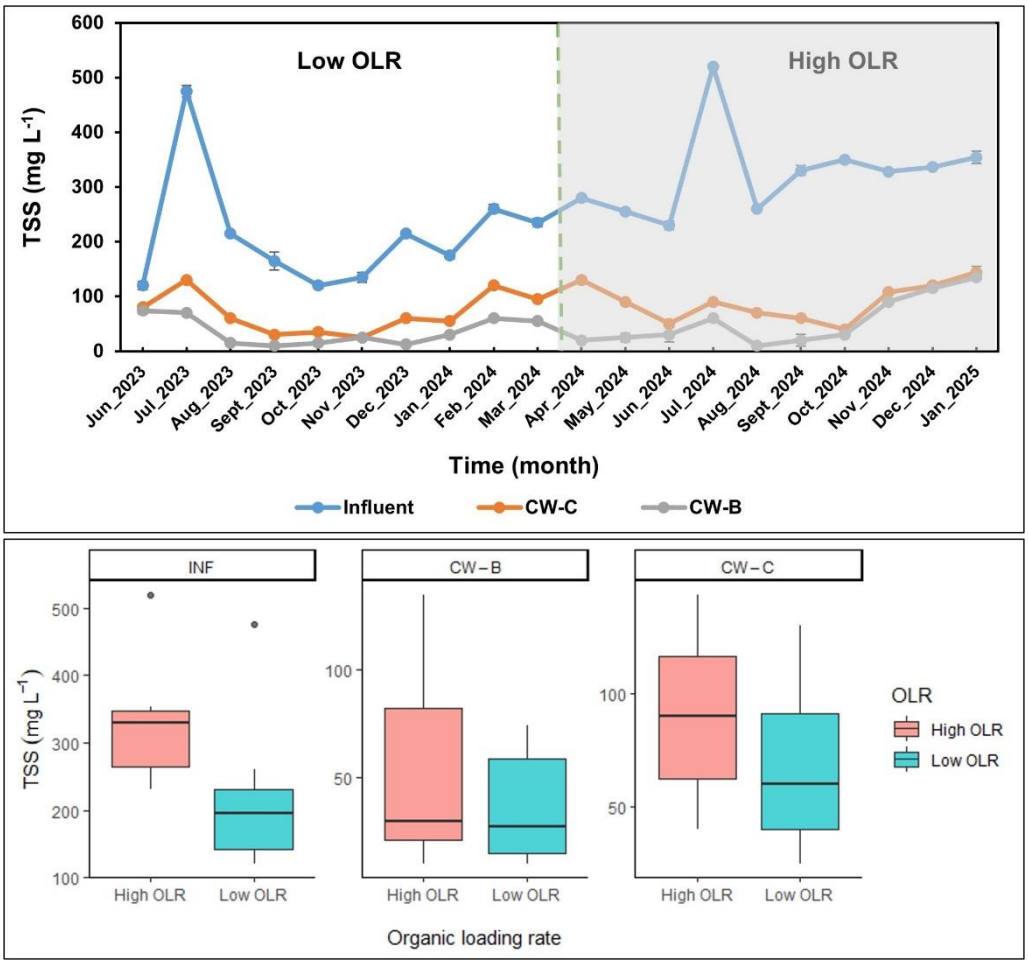

Figure III-15: Evolution of the total suspended solids (TSS) concentration in the influent and effluent samples of the vertical flow-constructed wetlands filled with sand (CW-C) and biochar (CW-B) during the low and high organic loading rates (OLR) periods. The box chart represents the mean TSS values at the influent and effluent of each system (CW-C and CW-B), based on monthly averages.

3.1.2. COD removal

Figure III-16 illustrates the kinetic evolution of the COD concentration in the inlet and outlet samples of CW-C and CW-B during the whole experimental period. However, **Tables III-6** and **III-7** show their corresponding average concentrations and removal efficiencies throughout the low and high OLR periods. Regardless of the OLR and composition of substrate-based VF-CWs, the average concentrations of COD significantly decreased after treatment (**Table III-6**). The evolution of COD in both VF-CWs reflects distinct operational phases: (i) an initial lag phase characterized by limited biomass activity and low organic matter oxidation efficiency; (ii) an adaptation phase marked by enhanced removal performance, attributed to stimulating biological activity; and (iii) a high organic loading rate phase associated with increased influent organic carbon concentrations, likely resulting a low removal efficiency. In addition, CW-B showed a higher ability to reduce the COD concentration than CW-C throughout the operational periods (**Figure III-16**). Furthermore, CW-B exhibited high removal efficiencies of COD compared to CW-C (49% – 60% and 39% – 50%, respectively), highlighting the positive impact of BC addition, due to its porous structure and rich surface functionalization, which enhances the electrostatic adsorption capacity of organic matter and provides a favourable microbial environment for the degradation of organic carbon (de Rozari et al., 2015; Deng et al., 2019). Ayadi et al. (2024) reported that the adsorption mechanisms by BC involve the degradation of the COD rather than biological processes. Similarly, El Barkaoui et al. (2025c) reported that the addition of OP-derived BC into the microcosms provided higher removal of total and soluble COD compared with the column filter filled with conventional materials (e.g., sand and gravel). This finding is in accordance with other studies reported in the literature (El Hanandeh et al., 2018, 2017; Deng et al., 2019). Interestingly, the results presented in **Figure III-16** indicate that COD is the most significant parameter influencing the OLR throughout the treatment period. Furthermore, the increase in OLR leads to a reduction in the removal efficiency of both VF-CWs by approximately 10%. This decline may be attributed to the increased feed volume, which elevates oxygen demand and promotes the formation of anaerobic zones where COD degradation is less effective. Additionally, the high OLR reduces the hydraulic retention time, limiting the contact time necessary for efficient COD removal (Xu et al., 2020).

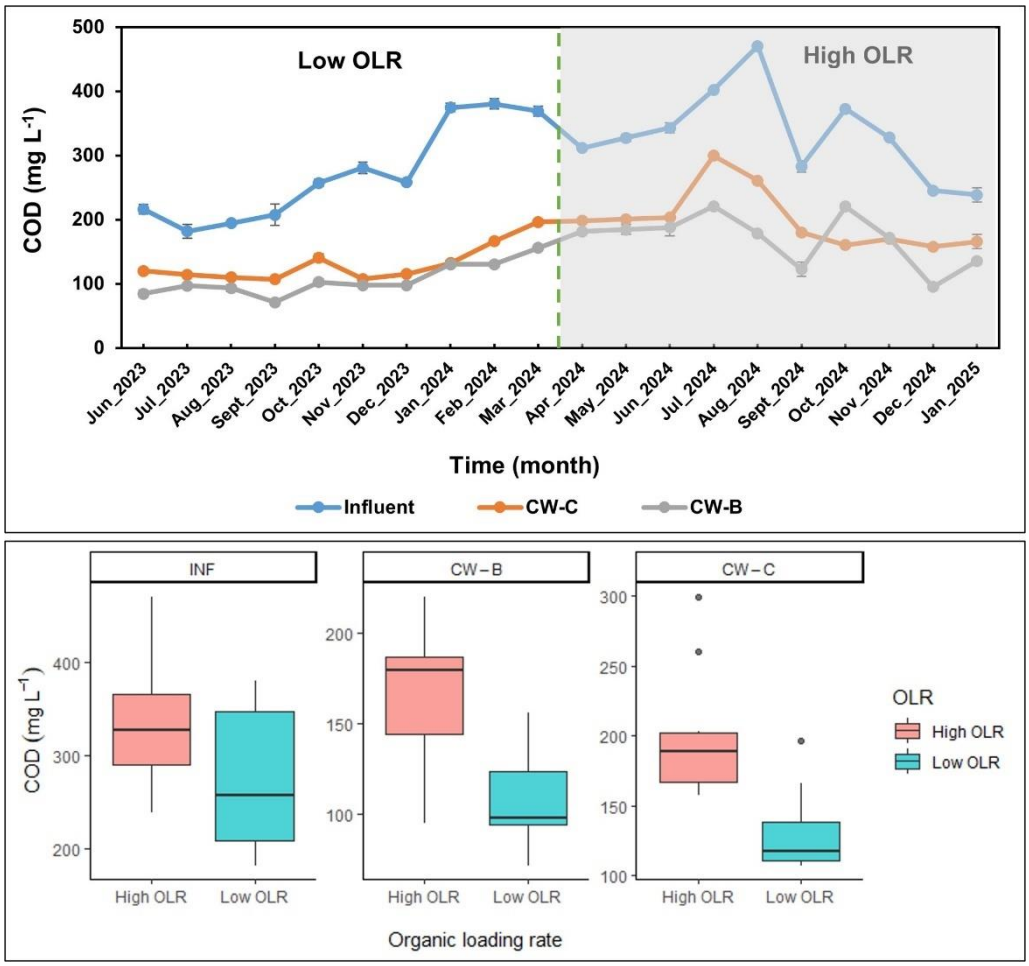

Figure III-16: Evolution of the total chemical oxygen demand (COD) concentration in the influent and effluent samples of the vertical flow-constructed wetlands filled with sand (CW-C) and biochar (CW-B) during the low and high organic loading rates (OLR) periods. The box chart represents the mean COD values at the influent and effluent of each system (CW-C and CW-B), based on monthly averages.

3.1.3. Phosphorus removal

Table III-6 shows the TP and PO_4^{3-} concentrations in the inlet and outlet samples of CW-C and CW-B, **Table III-7** presents their corresponding mean removal efficiencies, while **Figure III-17** illustrates their kinetic trend throughout the whole operational duration. The kinetic curves of TP and PO_4^{3-} concentrations change in a parallel way, exhibiting a high reduction in their concentrations, irrespective of the material media filled VF-CWs (**Figure III-17**). The average concentrations of phosphorus forms in the effluent samples after treatment showed a significant decrease compared to the influent, irrespective of the OLR. Furthermore, the removal efficiency in the VF-CWs ranged from 49% to 58% for TP and from 49% to 51% for PO_4^{3-} under a low OLR period, and from 24% to 28% for TP and from 28% to 35% for PO_4^{3-} under a high OLR. The increase in the OLR showed a significant reduction in the removal efficiency of both phosphorus

forms through both systems, which could be due to the excessive organic matter, limiting adsorption and precipitation processes, as well as shifting microbial communities toward anaerobic conditions, reducing microbial assimilation of phosphorus (Chazarenc et al., 2007). However, the results demonstrate the lack of the BC effect on phosphorus elimination. In general, BC is known to have limited effectiveness in removing phosphorus and negatively charged compounds due to its surface characteristics (e.g., low affinity, surface charge). This finding is in accordance with other studies (Yao et al., 2012; de Rozari et al., 2016; Werner et al., 2018; El Barkaoui et al., 2023). For example, de Rozari et al. (2016) found that sand exhibited better phosphorus performance than the BC-amended media due to the negative surface charge and low affinity of BC towards phosphorus forms, as well as competition from other negatively charged molecules in wastewater, such as organic compounds, for exchange sites on the surface of BC. Similarly, Zhou et al. (2019) reported that the integration of BC into CW did not affect phosphorus removal. Generally, the primary mechanisms for phosphorus removal in CWs include microbial oxidation and decomposition, plant, and physicochemical reactions of substrates (e.g., mineralization, precipitation, ion exchange, and adsorption) (Wu et al., 2015).

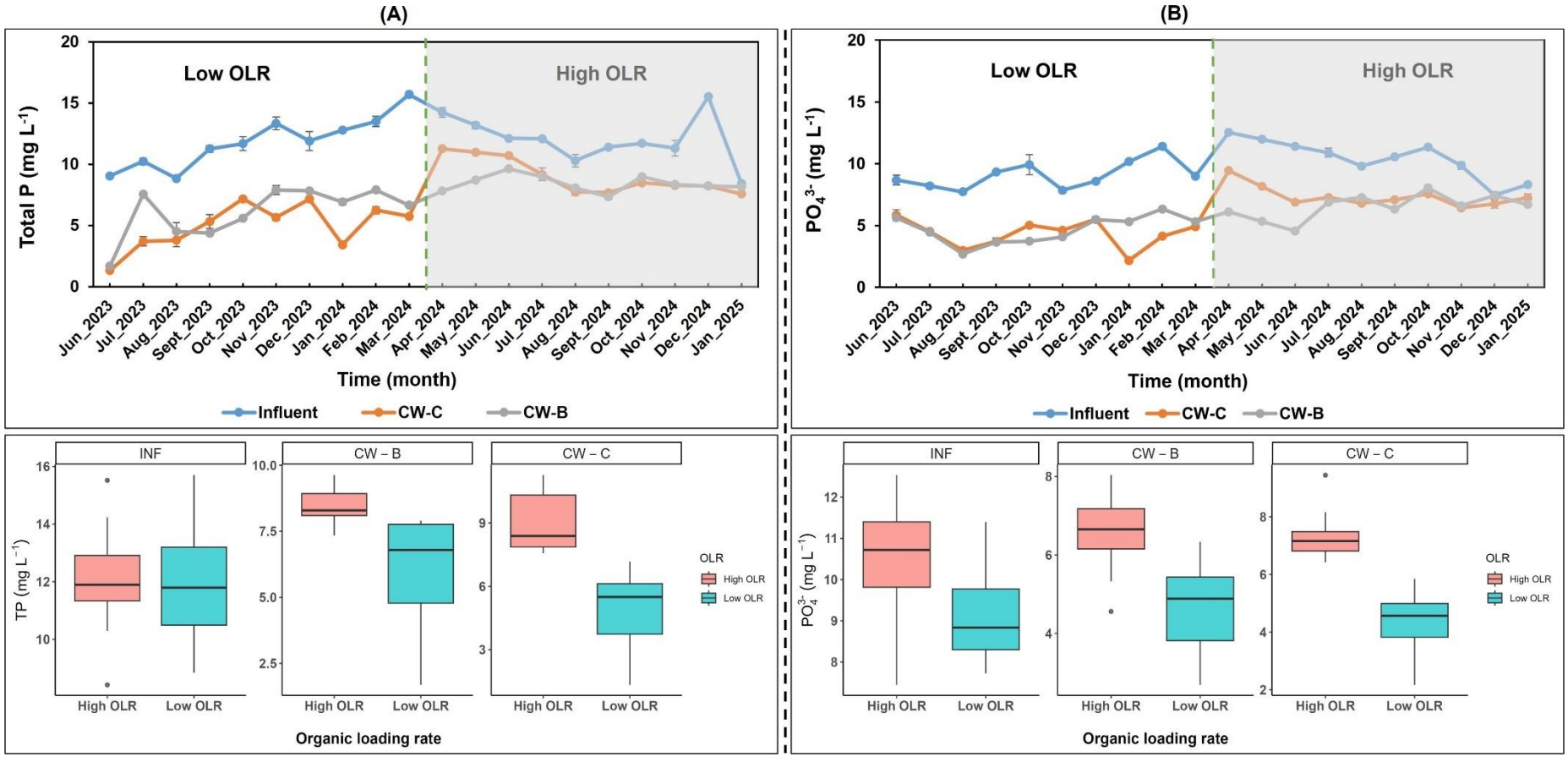

Figure III-17: Evolution of the total phosphorus (A) and orthophosphate (B) concentration in the influent and effluent samples of the vertical flow-constructed wetlands filled with sand (CW-C) and biochar (CW-B) during the low and high organic loading rates (OLR) periods. The box chart represents the mean TP and PO_4^{3-} values at the influent and effluent of each system (CW-C and CW-B), based on monthly averages.

3.1.4. Nitrogen Removal

Table III-6 illustrates the concentrations of different nitrogen forms in the influent and effluent samples, **Table III-7** shows the efficiencies of CW-C and CW-B in removing NH_4^+-N, TKN, and TN during low and high OLR periods, and **Figure III-18** illustrates the kinetic evolution of NH_4^+-N, TN, and nitrate concentrations during the whole experimental period. The results highlight a significant decrease in TKN, NH_4^+-N, and TN concentrations in effluent samples compared to influent, irrespective of the OLR applied. In the first period under low OLR, CW-B showed a significantly higher removal of TN (53%), TKN (74%), and NH_4^+-N (85%) than the control CW-C (38% for TN, 52% for TKN, and 71% for NH_4^+-N), suggesting that the ammonia-oxidising bacteria grew dynamically and performed optimally in the BC-based substrate (Odedishemi Ajibade et al., 2021). This performance decreased strongly in the second period under high OLR, especially for NH_4^+-N removal, to 61% for CW-B and 59% for CW-C. Generally, the observed removal of NH_4^+-N, TKN, and TN could be due to either physicochemical or biological processes. However, it is well established that biological processes are responsible for driving the nitrogen cycle in VF-CWs, mediating the conversion between various nitrogen oxidation states (Ma et al., 2023).

During the whole experimental period, the NH_4^+-N curves showed a low concentration for the effluent coming from CW-B compared to CW-C, combined with a high release of NO_3^--N (**Figure III-18C**), exceeding an average concentration of 18 – 25 mg L^{-1} and 13 – 22 mg L^{-1} under low and high OLR, respectively for NO_3^--N, and 4 – 5 mg L^{-1} and 1 – 1.3 mg L^{-1} under low and high OLR, respectively for NO_2^--N, due to the nitrification process (**Table III-6**). In particular, nitrite is highly toxic to aquatic fauna (Ayadi et al., 2024) and hence should be minimized and must always remain within the legal limits of the respective country. Fortunately, in the present study, the concentrations of NO_3^--N and NO_2^--N are below the reported toxicity limits for all aquatic species and fish fauna (Camargo et al., 2005; Lewis and Morris, 1986). Numerous studies have indicated that the release of NO_2^--N ions in CWs is primarily due to the incomplete oxidation of NH_4^+-N, resulting from limited DO availability (Li et al., 2021; Lu et al., 2022; Ayadi et al., 2024), a condition that primarily affects the activity of nitrite-oxidizing bacteria instead of the microorganisms responsible for nitrite/ammonia conversion (Vymazal, 2007; Tan et al., 2013). However, Kizito et al. (2017) reported that the higher release of NO_3^--N in BC-packed CWs may be due to the high level of oxygen in the filter. The increase in OLR during the second period results in a lower release of nitrite, while ammoniacal nitrogen concentration increases, possibly

due to the overloading of the system with organic matter and the insufficient amount of oxygen required for nitrification processes, and shifts microbial processes towards anaerobic pathways, favouring ammonium retention rather than removal, causing accumulation of NH_4^+-N, leading to poor effluent quality (Ilyas and Masih, 2017). Interestingly, the observed reduction in TN concentrations throughout the treatment process (**Table III-6**) indicates that denitrification occurred extensively in CW-C and CW-B, especially with BC playing a significant role in enhancing this mechanism within the nitrogen cycle.

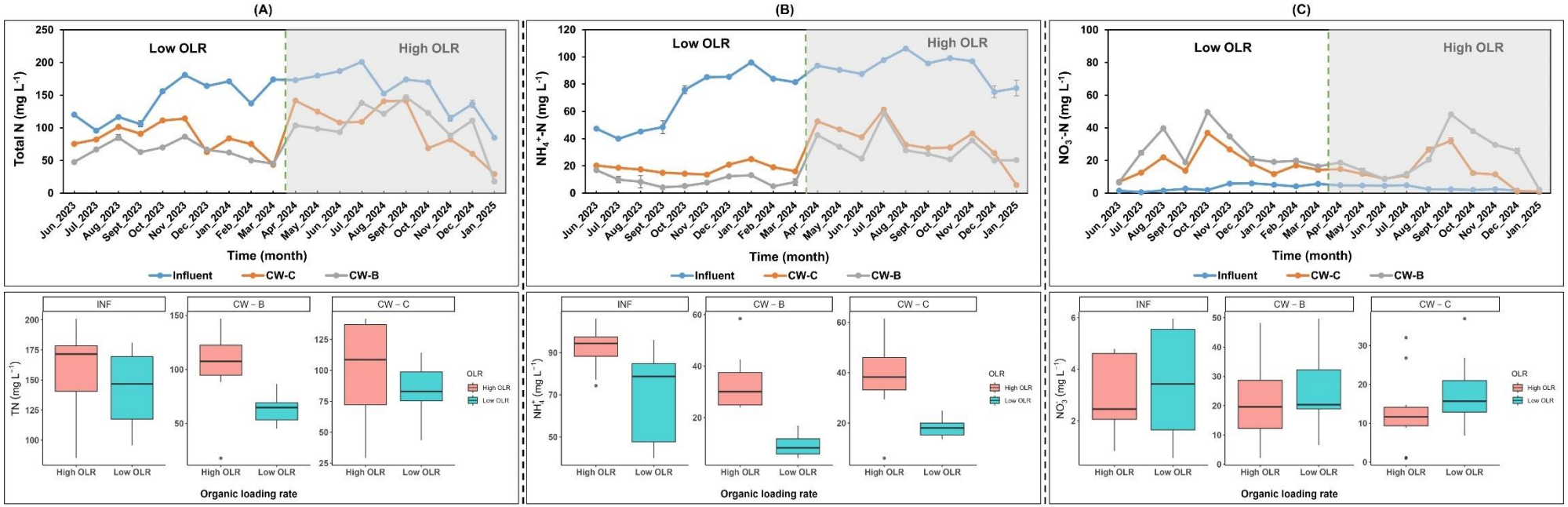

Figure III-18: Evolution of the total nitrogen (A), ammoniacal nitrogen (B), and nitrate (C) concentration in the influent and effluent samples of the vertical flow-constructed wetlands filled with sand (CW-C) and biochar (CW-B) during the low and high organic loading rates (OLR) periods. The box chart represents the mean TN, NH_4^+, and NO_3^- values at the influent and effluent of each system (CW-C and CW-B), based on monthly averages.

3.1.5. Hardness and sulfate removal

Table III-6 illustrates the concentrations of total hardness (TH), magnesium (Mg), calcium (Ca), and sulfate in the inlet and outlet samples of CW-C and CW-B. Regardless of the OLR, the mean concentrations of TH, Ca, and Mg were 365 – 369, 61 – 71, and 295 – 308 mg L^{-1}, respectively. After treatment, these concentrations significantly increased to 599 – 735 mg L^{-1} for TH, 125 – 150 mg L^{-1} for Ca, and 474 – 584 mg L^{-1} for Mg. This finding could be attributed to mineral dissolution, where water percolation through the filter bed releases these ions (Prajapati et al., 2018; Ghumra et al., 2021). Ion exchange processes in the substrate can further contribute to Ca^{2+} and Mg^{2+} release (Ramachandra et al., 2018). Additionally, the filter systems were installed under external climate conditions in Marrakech, which is characterized by high temperatures during the whole year (> 40 °C), leading to higher evapotranspiration, which concentrates dissolved ions, while anaerobic conditions promote the mobilization of Ca^{2+} and Mg^{2+} from sediments (Basílico et al., 2024). In addition, the effluent samples showed no significant difference in concentrations of TH, Ca, and Mg throughout the experiment (under low and high OLR), demonstrating the absence of BC and OLR effects.

During the whole experiment period, there was no significant difference in the concentration of SO_4^{2-} between the influent and effluent samples (**Table III-6**). Furthermore, the effluent samples showed an insignificant increase in the concentration of SO_4^{2-}, which could be due to the oxidation of sulfur bound to carbon and the release of SO_4^{2-} from the organic substrates used (Singh and Chakraborty, 2021). A similar observation was reported by El Barkaoui et al. (2025c), who attributed the slight increase in effluent concentrations to the oxidation of carbon-bound sulfur and subsequent sulfate release from the column media. The limited performance of SO_4^{2-} in the present study could be due to the immobilization of reduced sulfide in sediments in the absence of active aeration (Johnston et al., 2014). On the other hand, a high removal efficiency of SO_4^{2-} was reported in the study of Chand et al., (2021), exciding 85% using a Colocasia esculenta derived-BC-based vertical subsurface flow constructed wetland, referring this performance to some processes such as nitrate reduction process, sulfur oxidation mediated by sulfur-oxidizing bacteria, chemical oxidation reactions, precipitation with metal ions, dissimilatory sulfate reduction, and plant uptake.

3.1.6. Absorbance removal

Table III-7 shows the performance of CW-C and CW-B in removing absorbance (ABS) at 254 and 420 nm, and **Table III-6** shows the corresponding mean concentrations at the inlet and outlets of both VF-CWs under low and high OLR. The absorbance at 254 nm and 420 nm serves as an indicator of organic micropollutant concentrations, particularly associated with aromatic and unsaturated organic compounds (e.g., aromatic and organic compounds) and colored dissolved organic matter (e.g., humic-like substances), respectively. These parameters provide a rapid and reliable means for assessing their removal efficiency (Ciardelli and Ranieri, 2001; Altmann et al., 2016). The finding data highlighted significantly low concentrations of ABS 254 and 420 nm in the effluent samples compared to the influent, irrespective of the OLR. In addition, the removal efficiency of ABS 254 nm showed no significant difference between effluent samples provided from both filters, with a slight superiority of CW-B during both OLR periods. On the other hand, the addition of BC into VF-CW leads to a statistically high removal (71% and 52% under low and high OLR, respectively) of ABS 420 nm than the control CW-C (58% and 37% under low and high OLR, respectively) during both periods, demonstrating the key role of BC in the removal of organic micropollutants. Similarly, Ayadi et al. (2024) found a higher absorbance reduction in the BC-based microcosm than in the gravel-filled microcosm. On the other hand, the excessive OLR may affect oxygen depletion, biofilm overloading, substrate saturation, and reduce absorbance removal efficiency at both wavelengths.

Table III-7: Removal (Main value ± standard deviation) efficiency of water quality parameters in outlet samples of the vertical flow-constructed wetlands filled with sand (CW-C) and biochar (CW-B) during the low and high organic loading rates (OLR) periods. Different letters in each row mean statistically significant differences (P<0.05) according to Fisher or Games.

	Outlet CW-C		**Outlet CW-B**	
Parameters	**Low OLR**	**High OLR**	**Low OLR**	**High OLR**
Total suspended solids (%)	67 ± 14^{a}	71 ± 11^{ab}	81 ± 16^{bc}	84 ± 12^{c}
Chemical oxygen demand (%)	50 ± 9^{a}	39 ± 9^{b}	60 ± 6^{c}	49 ± 8^{a}
Total phosphorus (%)	58 ± 14^{a}	24 ± 11^{b}	49 ± 15^{a}	28 ± 13^{b}
Orthophosphate (%)	51 ± 14^{a}	28 ± 10^{b}	49 ± 11^{a}	35 ± 18^{b}
Total nitrogen (%)	38 ± 21^{ab}	37 ± 20^{ab}	53 ± 15^{a}	35 ± 19^{b}
Total Kjeldahl nitrogen (%)	52 ± 17^{a}	46 ± 15^{a}	74 ± 9^{b}	47 ± 15^{a}
Ammonium (%)	71 ± 11^{a}	59 ± 15^{b}	85 ± 9^{c}	61 ± 14^{ab}
Absorbance at 254 nm (%)	48 ± 15^{a}	38 ± 15^{a}	50 ± 15^{a}	42 ± 14^{a}
Absorbance at 420 nm (%)	58 ± 8^{ab}	37 ± 12^{c}	71 ± 10^{a}	52 ± 13^{b}
Total coliforms (log unit)	5 ± 3^{a}	1.9 ± 0.3^{b}	5 ± 2^{a}	2.1 ± 0.3^{b}
Faecal coliforms (log unit)	4 ± 3^{a}	1.41 ± 0.05^{b}	4 ± 2^{a}	1.6 ± 0.1^{b}
FS (log unit)	2.5 ± 0.3^{a}	0.5 ± 0.2^{b}	3.2 ± 0.6^{c}	1.3 ± 0.3^{d}

3.1.7. Removal of faecal bacteria indicators

The concentrations of faecal bacteria indicators (e.g., TC, FC, and FS) monitored at the inlet and outlet of CW-C and CW-B under low and high OLR periods are shown in **Table III-6**, and their corresponding removal rates are illustrated in **Table III-7**. The statistical data showed a significant reduction in the concentration of the three indicators after treatment, mainly when a low OLR was applied. Applying a higher OLR in the second period significantly reduced the performance of CW-C and CW-B in removing TC (from 5 to 1.9-2.1 log units), FC (from 4-5 to 1.4-1.6 log units), and FS (from 2.5-3.2 to 0.5-1.3 log units), which can be explained by the fact that the higher OLR limits aeration, leading to anaerobic conditions that lower pathogen inactivation. Chand et al. (2021) reported that the removal efficiency of faecal coliforms using CWs was strongly influenced by DO, pH, medium texture, influent load, and root structure. The results demonstrate the limited effect of BC on the removal of FC and TC while showing the significant role of BC in improving the removal of FS. Similarly, Nguyen et al. (2020b) considered that the hydraulic loading rate is the most influential factor on the removal of coliform bacteria, in addition to other mechanisms, including filter materials, vegetation, seasonal fluctuations, oxygenation, pH, and water composition. There are limited studies available in the literature discussing the contribution of BC-based CW for the removal of pathogen contaminants. Kaetzl et al. (2019) reported that CWs filled with BC derived from rice-husk BC showed a higher removal of faecal indicator bacteria from municipal wastewater compared to sand-based CWs. El Barkaoui et al. (2025c) evaluated the performance of biochar-based column filters for the removal of FS, FC, and TC. Their findings demonstrated that biochar exhibited a significantly higher bacterial removal efficiency compared to conventional sand filtration. On the other hand, Visiy et al. (2022) reported that there was no significant difference in the reduction of faecal coliforms between CWs based on sand or BC, suggesting that the removal of pathogens in CWs is mainly a physical process that is not significantly affected by the composition of the substrate. These contradictory findings are probably due to the characteristics of BC, such as the high porosity, surface functionalization, specific surface area, and hydrophobicity (El Barkaoui et al., 2023).

The results obtained in the present study are consistent with those reported in the literature. For example, Sleytr et al. (2007) studied bacterial removal in CW based on conventional materials (sand and gravel), achieving a removal efficiency of 4,37 log units for FC and 4,31 log units for TC. In addition, Hijnen et al. (2004) reported a removal of 2-3 log units of *E. coli* and thermotolerant coliforms at the full-scale and pilot plants. In general, the removal of pathogen indicators in CW occurs through biological, physical, and chemical mechanisms. Physical processes involve sedimentation, filtration, and sorption onto media and organic matter.

Biological mechanisms include biofilm retention, natural die-off, competition in nutrient-limited environments, and predation (Mandi et al., 2022). Meanwhile, chemical processes primarily rely on oxidation (Wu et al., 2016). Although the level of microbial removal in our study remains moderate, this may be attributed to the minimal biofilm development that occurred during the experiment. Biofilm formation within the filter improves filtration by reducing its porosity. As particles accumulate, the pore size decreases, resulting in enhanced filtration efficiency as the biofilm continues to develop over time. Grain size can also affect the removal of pathogens in slow sand filters (Logan et al., 2001). Additionally, the filter depth and short retention time may also help explain the observed results, especially in the second period under high OLR. Similarly, Torrens et al. (2009) reported that filter depth significantly influenced contaminant removal efficiency, with deeper filters showing higher removal rates due to increased hydraulic retention time.

3.2. Statistical analysis

By identifying individuals based on the concentration dataset, Principal Component Analysis (PCA) was used to investigate the effect of the bed-filled VF-CWs and organic loading rate on the removal efficiency of various pollutants (**Figure III-19**). The PCA was performed on a data matrix consisting of 21 variables, which mainly correlated along two axes (Dim1 and Dim2), which accounted for 71.2% of the total variability in the data, representing 63.1% for Dim1 and 8.9% for Dim2. Thus, **Figure III-19A** illustrates the squared cosines (cos^2) for dimensions 1 and 2, representing the quality of the representation of the variables on the principal components, with a higher squared cos^2 (close to 1) indicating that the principal component represents the variable well. In the present study, it can be noted that the indicator variables of organic matter (COD), nitrogen (TKN and $N\text{-}NH_4^+$), phosphorus (TP and PO_4^{3-}), UV-absorbance at 254 and 420 nm (ABS254 and ABS420), and coliforms (TC, FC, and FS) present a strong positive correlation with Dim1. Conversely, the variables $N\text{-}NO_2^-$, $N\text{-}NO_3^-$, TH, Ca, Mg, pH, EC, and DO present a strong negative correlation with Dim1. This (Dim1) positively indicates a source of organic and bacteriological pollution, while negatively, Dim1 indicates a source of mineralogical pollution and increased oxygen consumption. For Dim2, the results show the presence of nitrification processes, which, through their intensification, release H_3O^+, which decreases the pH of the environment, as indicated by a negative correlation between $N\text{-}NO_3^-$ and pH on Dim2.

Figure III-19B represents the confidence ellipses illustrating the dispersion of individuals according to the OLR variable. It can be seen that the low and high OLR groups are not well

separated in the PCA space. This indicates that individuals in these two categories provide similar information. Therefore, OLR does not appear to explain the variance captured by the principal axes (Dim1 and Dim2). However, **Figure III-19C** shows the ellipse representing the influent (INF) on the principal axis. The INF group highlights physicochemical and bacteriological characteristics distinct from those observed in the two CW-B and CW-C outlets. The two effluents present similar information, suggesting that they have comparable efficiency. They significantly reduced the organic load, particularly in TSS, COD, nitrogen, phosphorus, coliforms, and adsorbents. On the other hand, the effluents of CW-C and CW-B are characterised by the residual presence of minerals (Ca, Mg, and TH) and oxidised forms of nitrogen (NO_2 and NO_3), as well as by parameters such as pH, EC, and DO. These results indicate that they reduce the rate of organic load in the INF, transforming the treated wastewater into water containing mineral residues and oxidised nitrogen elements.

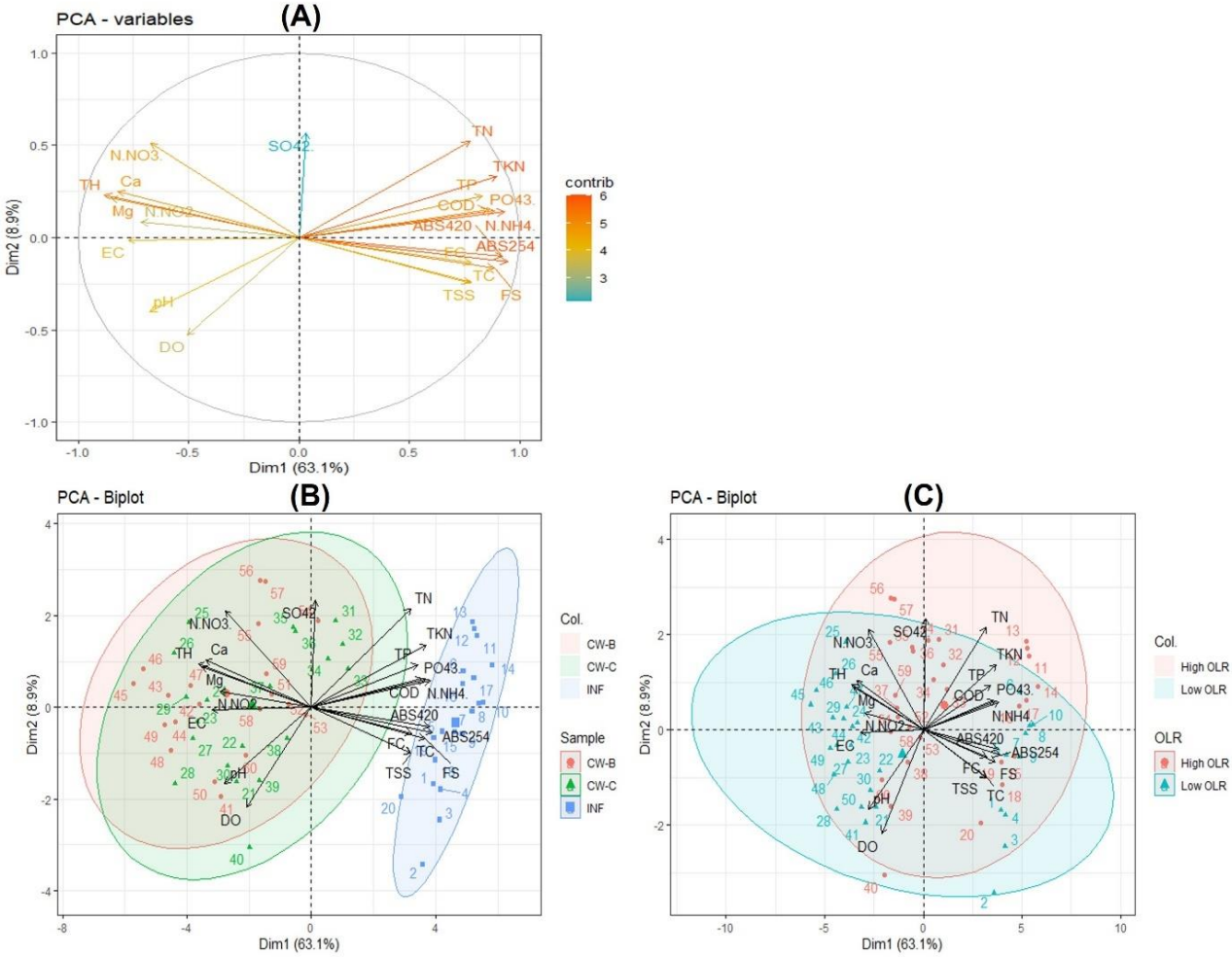

Figure III-19: Principal component analyses (PCA) perspective. A: Variables-PCA shows the relationships between the variables and the principal components. B: PCA Biplot visualises the relationships between variables and observations in the dataset across the inlet (INF) and outlets of the vertical flow-constructed wetlands filled with sand (CW-C) and biochar (CW-B). C: PCA Biplot visualises the relationships between variables and observations in the dataset across the organic loading rate (OLR).

Correlation analysis is a statistical method used to evaluate the strength and direction of linear relationships between quantitative variables, typically quantified by the Pearson correlation coefficient, which ranges from −1 to +1. A coefficient of ±1 indicates a perfect linear relationship, while a value of 0 denotes no linear correlation (Gogtay and Thatte, 2017). The monitoring campaign comprised 20 observations over 20 months under low and high OLR conditions. **Figure III-20** illustrates the Pearson correlation coefficients that quantify the linear relationships between the parameters investigated at the inlet and outlet of CW-C and CW-B. According to the linear correlation analysis result, TP is highly correlated with organic matter (e.g., r = 0.767), nitrogen (e.g., r = 0.793 with NH_4^+), UV-absorbance (e.g., r = 0.727 with ABS254), and coliforms (e.g., r

= 0.713 with FS). This suggests that these parameters tend to increase together due to organic pollution and domestic discharge. Similarly, NH_4^+ shows a high correlation with COD (r = 0.918), PO_4^{3-} (r = 0.856), TKN (r = 0.903), and ABS254 (r = 0.864), indicating a common source of nitrogen and organic contamination. Regarding TKN and TN, these water quality indicators have a strong relationship (r = 0.961), which is expected since TKN is a component of TN. As for TH, it is highly correlated with Ca (r = 0.863) and Mg (r = 0.988), confirming their key role in water hardness. As for the absorbance at 254 and 420 nm (ABS254 and ABS420) also exhibit a significant relationship (r = 0.914), reflecting their common origin linked to the UV-visible absorbance of organic matter. Regarding TH, PO_4^{3-}, COD, TKN, and NH_4^+, they exhibit negative correlations with NO_2^- and NO_3^-, which could indicate the coexistence of nitrogen transformation processes, mainly nitrification and denitrification, potentially intensified by the presence of organic matter and microbial activity.

Regarding TH, Ca, and Mg are negatively correlated with TP, COD, and TKN, which could reflect differences between pollution sources. Furthermore, pH is negatively correlated with TP, COD, and TKN, suggesting an acidic environment associated with organic pollution. Finally, the strong correlations between organic parameters (COD, ABS254, TSS) and nutrients (TP, TKN, NH_4^+) support the hypothesis of anthropogenic pollution, such as wastewater discharge or agricultural runoff. Negative correlations with oxidized nitrogen forms (NO_2^- and NO_3^-) could indicate incomplete nitrification or the predominance of anaerobic conditions.

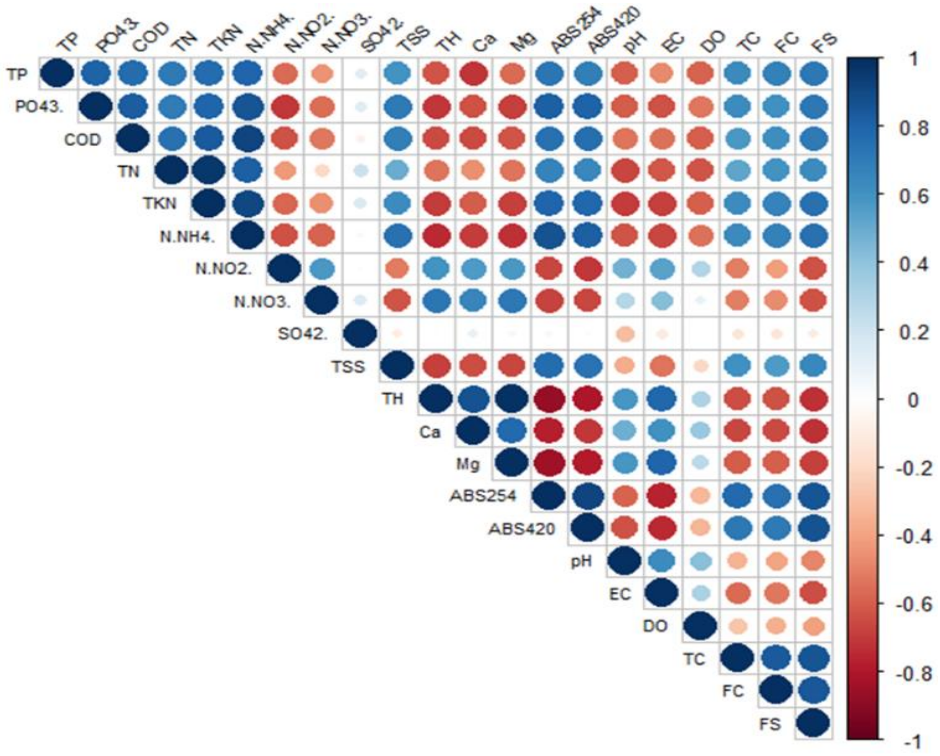

Figure III-20: Analysing correlations between physicochemical and bacteriological pollutants during monitoring.

Conclusion and Future Directions

This study demonstrated the potential of olive pomace-derived biochar (BC) as an effective and sustainable substrate amendment in vertical flow constructed wetlands (VF-CWs) for domestic wastewater treatment. The results showed that the integration of BC into the VF-CW system (CW-B) significantly improved the removal of key pollutants, particularly NH_4^+-N (up to 85%), TKN, COD, TSS, and faecal indicators, compared to the sand-only control (CW-C), especially under low organic loading conditions (20 g COD/m²-d). However, although CW-B consistently outperformed CW-C at high organic loads (70 g COD/m².d), overall treatment performance declined. Notably, the biochar had limited phosphorus, sulphate, and hardness removal capacity, probably due to surface charge limitations.

The study also confirmed active nitrification through the detection of NO_2^- and NO_3^-, although this process was inhibited at high OLR due to potential oxygen limitations. Despite this, CW-B maintained higher nitrogen removal, suggesting improved microbial activity supported by the biochar structure.

These results highlight the viability of olive pomace biochar as a low-cost, locally available, and environmentally friendly amendment to improve VF-CW performance, particularly in

Mediterranean and arid regions where wastewater reuse is critical.

Future research should focus on:

- Long-term system performance and stability under continuous high OLR.
- Evaluate shock load resilience of biochar-amended systems.
- Improving phosphorus removal through co-addition with mineral-rich materials (e.g., Fe-based compounds).
- Investigate the dynamics of microbial communities within biochar-enhanced wetlands.
- Integration of biochar-amended VF-CWs with tidal flow operation and bio-electrochemical processes.
- Scale up the system for real field applications and assess cost-benefit and life cycle impacts.

Such findings will help to optimise nature-based wastewater treatment technologies and promote circular economy approaches through the valorisation of agricultural waste.

References

Achak M, Boumya W, Elamraoui S, et al (2023) Performance of olive mill wastewater treatment using hybrid system combining sand filtration and vertical flow constructed wetlands. J Water Process Eng 53:103737. https://doi.org/10.1016/j.jwpe.2023.103737

AFNOR (1997) AFNOR, Recueil de Norme Française: Eau, Méthodes D'essai,. 2nd ed, Paris Édition, Paris.

Altmann, J., Massa, L., Sperlich, A., Gnirss, R., Jekel, M., 2016. UV254 absorbance as real-time monitoring and control parameter for micropollutant removal in advanced wastewater treatment with powdered activated carbon. Water Res. 94, 240–245. https://doi.org/10.1016/j.watres.2016.03.001

Ayadi, M., Passaseo, D., Bonaccorso, G., Fichera, M., Renai, L., Venturini, L., Colzi, I., Fibbi, D., Del Bubba, M., 2024. Biochar from co-pyrolysis of biological sludge and sawdust in comparison with the conventional filling media of vertical-flow constructed wetlands for the treatment of domestic-textile wastewater. Water Sci. Technol. 89, 1252–1263. https://doi.org/10.2166/wst.2024.056

Basílico, G., Casares, M.V., de Cabo, L., 2024. Performance of vertical flow wetland in the treatment of medium organic strength synthetic wastewater. Discov. Water 4, 77. https://doi.org/10.1007/s43832-024-00142-5

Camargo, J.A., Alonso, A., Salamanca, A., 2005. Nitrate toxicity to aquatic animals: a review with new data for freshwater invertebrates. Chemosphere 58, 1255–1267. https://doi.org/10.1016/j.chemosphere.2004.10.044

Chand, N., Suthar, S., Kumar, K., Tyagi, V.K., 2021. Enhanced removal of nutrients and coliforms from domestic wastewater in cattle dung biochar-packed Colocasia esculenta-based vertical subsurface flow constructed wetland. J. Water Process Eng. 41, 101994. https://doi.org/10.1016/j.jwpe.2021.101994

Chazarenc, F., Maltais-Landry, G., Troesch, S., Comeau, Y., Brisson, J., 2007. Effect of loading rate on performance of constructed wetlands treating an anaerobic supernatant. Water Sci. Technol. 56, 23–29. https://doi.org/10.2166/wst.2007.500

Chen, Z., Xiao, X., Chen, B., Zhu, L., 2015. Quantification of Chemical States, Dissociation Constants and Contents of Oxygen-containing Groups on the Surface of Biochars Produced at Different Temperatures. Environ. Sci. Technol. 49, 309–317. https://doi.org/10.1021/es5043468

Ciardelli, G., Ranieri, N., 2001. The treatment and reuse of wastewater in the textile industry by means of ozonation and electroflocculation. Water Res. 35, 567–572. https://doi.org/10.1016/S0043-1354(00)00286-4

de Rozari, P., Greenway, M., El Hanandeh, A., 2016. Phosphorus removal from secondary sewage and septage using sand media amended with biochar in constructed wetland mesocosms. Sci. Total Environ. 569–570, 123–133. https://doi.org/10.1016/j.scitotenv.2016.06.096

de Rozari, P., Greenway, M., El Hanandeh, A., 2015. An investigation into the effectiveness of sand media amended with biochar to remove BOD5, suspended solids and coliforms using wetland mesocosms. Water Sci. Technol. 71, 1536–1544. https://doi.org/10.2166/wst.2015.120

Deng, C., Huang, L., Liang, Y., Xiang, H., Jiang, J., Wang, Q., Hou, J., Chen, Y., 2019. Response of microbes to biochar strengthen nitrogen removal in subsurface flow constructed wetlands: Microbial community structure and metabolite characteristics. Sci. Total Environ. 694, 133687. https://doi.org/10.1016/j.scitotenv.2019.133687

El Barkaoui, S., Mandi, L., Aziz, F., Del Bubba, M., Ouazzani, N., 2023. A critical review on using biochar as constructed wetland substrate: Characteristics, feedstock, design and pollutants removal mechanisms. Ecol. Eng. 190, 106927. https://doi.org/10.1016/j.ecoleng.2023.106927

El Barkaoui, S., Ouazzani, N., Mandi, L., Zafeiropoulos, J., Isari, E.A., Del Bubba, M., Kalavrouziotis, I.K., 2025a. Physicochemical and thermal characterization of argan residues for biofuel and biochar production: potential future prospects. Biomass Convers. Biorefinery 15, 17309–17319. https://doi.org/10.1007/s13399-024-06442-z

El Barkaoui, S., Mandi, L., Ryah, H., El Ghadraoui, A., Del Bubba, M., Ouazzani, N., 2025b. Biochar-based filtration systems for wastewater treatment: performance, efficiency, and optimization. Int. J. Environ. Sci. Technol. https://doi.org/10.1007/s13762-025-06694-w

El Barkaoui, S., Mandi, L., Fichera, M., Ryah, H., Baçaoui, A., Del Bubba, M., Ouazzani, N., 2025c. Optimizing biochar-based column filtration systems for enhanced pollutant removal in wastewater treatment: A preliminary study. Chemosphere 372, 144067. https://doi.org/10.1016/j.chemosphere.2025.144067

El Ghadraoui, A., Ouazzani, N., Ahmali, A., El Mansour, T.E.H., Aziz, F., Hejjaj, A., Del Bubba, M., Mandi, L., 2020. Treatment of olive mill and municipal wastewater mixture by pilot scale vertical flow constructed wetland. Desalin. Water Treat. 198, 126–139. https://doi.org/10.5004/dwt.2020.26009

El Hanandeh, A., Bhuvaneswaran, A., de Rozari, P., 2017. Removal of nitrate, ammonia and phosphate from aqueous solutions in packed bed filter using biochar augmented sand media. MATEC Web Conf. 120, 05004. https://doi.org/10.1051/matecconf/201712005004

El Hanandeh, A., Gharaibeh, M., Albalasmeh, A.A., 2018. Phosphorus removal efficiency from wastewater under different loading conditions using sand biofilters augmented with biochar. Int. J. Environ. Sci. Technol. 15, 927–934. https://doi.org/10.1007/s13762-017-1474-0

EU Olive Oil Production, 2021. International olive council. https://www.internationaloliveoil.org/what-we-do/economic-affairs-promotion-unit/.

Fan, J., Wang, W., Zhang, B., Guo, Y., Ngo, H.H., Guo, W., Zhang, J., Wu, H., 2013. Nitrogen removal in intermittently aerated vertical flow constructed wetlands: Impact of influent COD/N ratios. Bioresour. Technol. 143, 461–466. https://doi.org/10.1016/j.biortech.2013.06.038

Gadipelly, C., Pérez-González, A., Yadav, G.D., Ortiz, I., Ibáñez, R., Rathod, V.K., Marathe, K. V., 2014. Pharmaceutical Industry Wastewater: Review of the Technologies for Water Treatment and Reuse. Ind. Eng. Chem. Res. 53, 11571–11592. https://doi.org/10.1021/ie501210j

Ghumra, D.P., Agarkoti, C., Gogate, P.R., 2021. Improvements in effluent treatment technologies in Common Effluent Treatment Plants (CETPs): Review and recent advances. Process Saf. Environ. Prot. https://doi.org/10.1016/j.psep.2021.01.021

Gogtay, N.J., Thatte, U.M., 2017. Principles of Correlation Analysis. J. Assoc. Physicians India 65, 78–81.

Hijnen, W.A.M., Schijven, J.F., Bonné, P., Visser, A., Medema, G.J., 2004. Elimination of viruses, bacteria and protozoan oocysts by slow sand filtration. Water Sci. Technol. 50, 147–154. https://doi.org/10.2166/wst.2004.0044

Ilyas, H., Masih, I., 2017. The performance of the intensified constructed wetlands for organic matter and nitrogen removal: A review. J. Environ. Manage. 198, 372–383. https://doi.org/10.1016/j.jenvman.2017.04.098

Johnston, S.G., Burton, E.D., Aaso, T., Tuckerman, G., 2014. Sulfur, iron and carbon cycling following hydrological restoration of acidic freshwater wetlands. Chem. Geol. 371, 9–26. https://doi.org/10.1016/j.chemgeo.2014.02.001

Kaetzl, K., Lübken, M., Uzun, G., Gehring, T., Nettmann, E., Stenchly, K., Wichern, M., 2019. On-farm wastewater treatment using biochar from local agroresidues reduces pathogens from irrigation water for safer food production in developing countries. Sci. Total Environ. 682, 601–610. https://doi.org/10.1016/j.scitotenv.2019.05.142

Karki, B.K., 2024. Amended biochar in constructed wetlands: Roles, challenges, and future directions removing pharmaceuticals and personal care products. Heliyon 10, e39848. https://doi.org/10.1016/j.heliyon.2024.e39848

Kasak, K., Truu, J., Ostonen, I., Sarjas, J., Oopkaup, K., Paiste, P., Kõiv-Vainik, M., Mander, Ü., Truu, M., 2018. Biochar enhances plant growth and nutrient removal in horizontal subsurface flow constructed wetlands. Sci. Total Environ. 639, 67–74. https://doi.org/10.1016/j.scitotenv.2018.05.146

Kizito, S., Lv, T., Wu, S., Ajmal, Z., Luo, H., Dong, R., 2017. Treatment of anaerobic digested effluent in biochar-packed vertical flow constructed wetland columns: Role of media and tidal operation. Sci. Total Environ. 592, 197–205. https://doi.org/10.1016/j.scitotenv.2017.03.125

Lewis, W.M., Morris, D.P., 1986. Toxicity of Nitrite to Fish: A Review. Trans. Am. Fish. Soc. 115, 183–195.

https://doi.org/10.1577/1548-8659(1986)115<183:TONTF>2.0.CO;2
Li, L., Feng, J., Zhang, L., Yin, H., Fan, C., Wang, Z., Zhao, M., Ge, C., Song, H., 2021. Enhanced nitrogen and phosphorus removal by natural pyrite–based constructed wetland with intermittent aeration. Environ. Sci. Pollut. Res. 28, 69012–69028. https://doi.org/10.1007/s11356-021-15461-6
Logan, A.J., Stevik, T.K., Siegrist, R.L., Rønn, R.M., 2001. Transport and fate of Cryptosporidium parvum oocysts in intermittent sand filters. Water Res. 35, 4359–4369. https://doi.org/10.1016/S0043-1354(01)00181-6
Lu, J., Guo, Z., Pan, Y., Li, M., Chen, X., He, M., Wu, H., Zhang, J., 2022. Simultaneously enhanced removal of PAHs and nitrogen driven by Fe2+/Fe3+ cycle in constructed wetland through automatic tidal operation. Water Res. 215, 118232. https://doi.org/10.1016/j.watres.2022.118232
Ma, R., Ma, J., Chen, Y., Zhuo, Y., Cheng, L., Jiang, L., Mao, Y., Shen, Q., Liu, C., Ji, F., 2023. Efficient removal of nitrogen from tidal flow constructed wetlands based on the in-situ zeolite regeneration: Measures and mechanisms. Chem. Eng. J. 458, 141298. https://doi.org/10.1016/j.cej.2023.141298
Maina, C.W., Mutua, B.M., Oduor, S.O., 2011. Evaluating performance of vertical flow constructed wetland under various hydraulic loading rates in effluent polishing. J. Water, Sanit. Hyg. Dev. 1, 144–151. https://doi.org/10.2166/washdev.2011.025
Mandi, L., Ouazzani, N., Aziz, F. (2022). Constructed Wetlands as a Green and Sustainable Technology for Domestic Wastewater Treatment Under the Arid Climate of Rural Areas in Morocco. In: Stefanakis, A. (eds) Constructed Wetlands for Wastewater Treatment in Hot and Arid Climates. Wetlands: Ecology, Conservation and Management, vol 7. Springer, Cham. https://doi.org/10.1007/978-3-031-03600-2_1
Nguyen, X.C., Nguyen, D.D., Tran, Q.B., Nguyen, T.T.H., Tran, T.K.A., Tran, T.C.P., Nguyen, T.H.G., Tran, T.N.T., La, D.D., Chang, S.W., Balasubramani, R., Chung, W.J., Yoon, Y.S., Nguyen, V.K., 2020a. Two-step system consisting of novel vertical flow and free water surface constructed wetland for effective sewage treatment and reuse. Bioresour. Technol. 306, 123095. https://doi.org/10.1016/j.biortech.2020.123095
Nguyen, X.C., Tran, T.C.C.P.P., Hoang, V.H., Nguyen, T.P., Chang, S.W., Nguyen, D.D., Guo, W., Kumar, A., La, D.D., Bach, Q.V., 2020b. Combined biochar vertical flow and free-water surface constructed wetland system for dormitory sewage treatment and reuse. Sci. Total Environ. 713, 136404. https://doi.org/10.1016/j.scitotenv.2019.136404
Odedishemi Ajibade, F., Wang, H.-C.C., Guadie, A., Fausat Ajibade, T., Fang, Y.-K.K., Muhammad Adeel Sharif, H., Liu, W.-Z.Z., Wang, A.-J.J., Odedishemi, F., Wang, H.-C.C., Guadie, A., Fausat, T., Fang, Y.-K.K., Muhammad, H., Sharif, A., 2021. Total nitrogen removal in biochar amended non-aerated vertical flow constructed wetlands for secondary wastewater effluent with low C/N ratio: Microbial community structure and dissolved organic carbon release conditions. Bioresour. Technol. 322, 124430. https://doi.org/10.1016/j.biortech.2020.124430
Ramachandra, T. V, Sincy, V., Asulabha, K.S., Mahapatra, D.M., Bhat, S.P., Aithal, B.H., 2018. Optimal Treatment of Domestic Wastewater through Constructed Wetlands. J Biodivers. 9, 81–102. https://doi.org/11.258359/KRE-180
Rodier J (2009) L'analyse de l'eau _ Rodier 9e édition.pdf. 3–675 et 1187–1390
S.E.E.E, 2007. Moroccan water quality grid for irrigation purposes, State Secretariat at the Ministry of Energy, Mines, Water and Environment, Charge of Water and Environment, Kingdom of Morocco, Water Quality Standards for Irrigation, 2007. http://www.eau-tensift.net/fileadmin/user_files/pdf/publications/3_Irrigation.pdf.
Saravanan, A., Senthil Kumar, P., Jeevanantham, S., Karishma, S., Tajsabreen, B., Yaashikaa, P.R., Reshma, B., 2021. Effective water/wastewater treatment methodologies for toxic pollutants removal: Processes and applications towards sustainable development. Chemosphere 280, 130595. https://doi.org/10.1016/j.chemosphere.2021.130595
Singh, S., Chakraborty, S., 2021. Bioremediation of acid mine drainage in constructed wetlands: Aspect of vegetation (Typha latifolia), loading rate and metal recovery. Miner. Eng. 171, 107083. https://doi.org/10.1016/j.mineng.2021.107083
Sleytr, K., Tietz, A., Langergraber, G., Haberl, R., 2007. Investigation of bacterial removal during the filtration process in constructed wetlands. Sci. Total Environ. 380, 173–180. https://doi.org/10.1016/j.scitotenv.2007.03.001
Stefanakis, A., 2019. The Role of Constructed Wetlands as Green Infrastructure for Sustainable Urban Water Management. Sustainability 11, 6981. https://doi.org/10.3390/su11246981
Tan, C., Ma, F., Li, A., Qiu, S., Li, J., 2013. Evaluating the Effect of Dissolved Oxygen on Simultaneous Nitrification and Denitrification in Polyurethane Foam Contact Oxidation Reactors. Water Environ. Res. 85, 195–202. https://doi.org/10.2175/106143012X13503213812445
Torrens, A., Molle, P., Boutin, C., Salgot, M., 2009. Removal of bacterial and viral indicator in vertical flow constructed wetlands and intermittent sand filters. Desalination 246, 169–178. https://doi.org/10.1016/j.desal.2008.03.050

Visiy, E.B., Djousse, B.M.K., Martin, L., Zangue, C.N., Sangodoyin, A., Gbadegesin, A.S., Fonkou, T., 2022. Effectiveness of biochar filters vegetated with Echinochloa pyramidalis in domestic wastewater treatment. Water Sci. Technol. 85, 2613–2624. https://doi.org/10.2166/wst.2022.147

Vymazal, J., 2007. Removal of nutrients in various types of constructed wetlands. Sci. Total Environ. 380, 48–65. https://doi.org/10.1016/j.scitotenv.2006.09.014

Wang, M., Xie, Y., Gao, Y., Huang, X., Chen, W., 2024. Machine learning prediction of higher heating value of biochar based on biomass characteristics and pyrolysis conditions. Bioresour. Technol. 395, 130364. https://doi.org/10.1016/j.biortech.2024.130364

Werner, S., Kätzl, K., Wichern, M., Buerkert, A., Steiner, C., Marschner, B., 2018. Agronomic benefits of biochar as a soil amendment after its use as waste water filtration medium. Environ. Pollut. 233, 561–568. https://doi.org/10.1016/j.envpol.2017.10.048

Wu, H., Zhang, J., Ngo, H.H., Guo, W., Hu, Z., Liang, S., Fan, J., Liu, H., 2015. A review on the sustainability of constructed wetlands for wastewater treatment: Design and operation. Bioresour. Technol. 175, 594–601. https://doi.org/10.1016/j.biortech.2014.10.068

Wu, S., Carvalho, P.N., Müller, J.A., Manoj, V.R., Dong, R., 2016. Sanitation in constructed wetlands: A review on the removal of human pathogens and fecal indicators. Sci. Total Environ. 541, 8–22. https://doi.org/10.1016/j.scitotenv.2015.09.047

Xu, Q.L., Yuan, T., Qiao, Z.W., Wang, P., Wang, L., Zhang, F., 2020. The Influence Of Combinations of Operation Parameters on Sewage Treatment in Vertical-Flow Constructed Wetlands. Appl. Ecol. Environ. Res. 18, 7941–7951. https://doi.org/10.15666/aeer/1806_79417951

Yao, Y., Gao, B., Zhang, M., Inyang, M., Zimmerman, A.R., 2012. Effect of biochar amendment on sorption and leaching of nitrate, ammonium, and phosphate in a sandy soil. Chemosphere 89, 1467–1471. https://doi.org/10.1016/j.chemosphere.2012.06.002

Ye, J., Wang, L., Li, D., Han, W., Ye, C., 2012. Vertical oxygen distribution trend and oxygen source analysis for vertical-flow constructed wetlands treating domestic wastewater. Ecol. Eng. 41, 8–12. https://doi.org/10.1016/j.ecoleng.2011.12.015

Zhou, X., Wang, R., Liu, H., Wu, S., Wu, H., 2019. Nitrogen removal responses to biochar addition in intermittent-aerated subsurface flow constructed wetland microcosms: Enhancing role and mechanism. Ecol. Eng. 128, 57–65. https://doi.org/10.1016/j.ecoleng.2018.12.028

Chapter IV– Removal of Contaminants of Emerging Concern in Constructed Wetlands

IV-I. Performance of Biochar-Enhanced Vertical Flow Constructed Wetlands for Wastewater Treatment: Influence of Biochar Concentration on the Removal of Organic Matter, Nutrients, Pathogens, and Emerging Contaminants

This work is in the preparation state to be submitted as a research paper:

Abstract

This study evaluates the performance of vertical flow constructed wetlands (VF-CWs) amended with different proportions of biochar (BC), 0% (CW-0), 10% (CW-10), and 50% (CW-50) in treating domestic wastewater containing conventional pollutants, pathogens, and pharmaceutical compounds (PhCs). Monitoring inlet and outlet parameters revealed significant improvements in effluent quality. BC-amended systems (CW-10, CW-50) enhanced removals to 79–81% for suspended solids, 71–72% for UV-absorbance, 60–61% for organic matter, 53% for total nitrogen, 66–74% for Kjeldahl nitrogen, 81–85% for NH4+-N, and 3.2–3.3 Log units for faecal streptococci, compared with CW-0 (67%, 58%, 50%, 38%, 52%, 71%, and 2.5 Log units, respectively). Meanwhile, increases in the BC percentage have no significant effect on the conventional pollutant removal. From 36 PhCs compounds, only 18 compounds were identified in the PM and 19 in the aqueous wastewater samples, with non-steroidal anti-inflammatory drugs dominating due to their high usage and excretion. Treatment achieved near-complete removal of Clarithromycin, Furosemide, Atenolol, Bisoprolol, Erythromycin, 4'-Hydroxydiclofenac, and Ketoprofen, while compounds such as carbamazepine and fluoxetine exhibited poor or negative removal, likely due to desorption, persistence, low biodegradability, or release from PM. Contrary to expectations, the BC addition did not significantly enhance the removal of PhCs, possibly reflecting variability in BC properties and compound-specific interactions. These findings highlight the complexity of PhCs' behaviour in CWs and the need for optimised system designs to improve treatment efficiency.

Keywords: Micropollutants removal; Particulate matter; Constructed wetlands; Pharmaceutical compounds; Olive pomace-derived biochar.

1. Introduction

The occurrence of emerging contaminants (CECs) in wastewater, such as pharmaceutical compounds (PhCs), pesticides, industrial chemicals, and personal care products, poses a major environmental concern, as wastewater is a primary pathway through which these substances enter natural ecosystems (Renai et al., 2020; Santos et al., 2023). These substances, particularly PhCs, are widely detected in both rural and urban settings due to their extensive use and persistence in the environment, irrespective of geographical location (Renai et al., 2020). Growing concern surrounds their potential adverse impacts on ecosystems and human health, particularly their involvement in endocrine disruption (e.g., oestrogens) and the spread of antimicrobial resistance (e.g., antibiotics) (Varatharajan et al., 2025).

Mitigating the spread of PhCs into aquatic environments requires effective wastewater treatment. It is well known that conventional wastewater treatment plants (WWTPs) are not originally designed to target these pollutants and therefore often fail to remove them effectively (Belete et al., 2023). Constructed wetlands (CWs) have been proposed as a sustainable, nature-

based solution for wastewater treatment, particularly well-suited for the secondary treatment of domestic sewage in small communities and for refining effluents from larger urban facilities (Prabhu et al., 2022; Valipour and Ahn, 2016). CWs are widely valued for being simple, low-cost, and environmentally friendly systems that use natural processes, such as adsorption, precipitation, biodegradation of organic matter, nitrification, and denitrification (Kataki et al., 2021). Thus, they are highly effective in removing conventional water quality parameters such as nitrogen compounds, biodegradable organic matter, and suspended solids (El Barkaoui et al., 2023; Vymazal et al., 2021). Their ability to eliminate PhCs remains limited, especially when traditional media are used, such as sand, gravel, zeolite, quartz (Alsubih et al., 2022; Delgado et al., 2020; Petrie et al., 2018; Vymazal et al., 2017; Yuan et al., 2020a; Zhang et al., 2011). Consequently, this limitation raises significant concerns about the safety and quality of reclaimed water resources, emphasising the need for sustainable strategies to mitigate wastewater pollution and protect water resources (Gadipelly et al., 2014). Recently, biochar (BC) has been proposed as an alternative, low-cost, and sustainable material to improve filter media and enhance the treatment efficiency of CWs (El Barkaoui et al., 2025d). BC-based CWs have demonstrated a high ability in removing various wastewater pollutants, including both conventional and emerging contaminants (El Barkaoui et al., 2023; Kushwaha et al., 2024), due to the distinct physicochemical properties of BC, including its high specific surface area and well-developed porous structure, which provide abundant active sites for the adsorption of organic pollutants (El Barkaoui et al., 2025c; Maleki Shahraki and Mao, 2022; Zehouani et al., 2026; Zhang et al., 2022). Generally, the adsorption efficiency largely depends on the nature of the physical and chemical interactions between BC and PhCs (Czech et al., 2021). For instance, rich in surface functional groups (e.g., hydroxyl and carboxyl), BC facilitates chemical bonding with PhCs, such as hydrogen bonding (Keerthanan et al., 2022; Li et al., 2023). Furthermore, electrostatic interactions and van der Waals forces contribute to the overall adsorption process, effectively decreasing PhCs concentrations in constructed wetlands (Wu et al., 2022). The negatively charged surface of BC further promotes electrostatic interactions with positively charged PhCs (Nakarmi et al., 2022), while its functional groups enable complexation mechanisms (Liang et al., 2020; Xue et al., 2022), collectively enhancing the removal efficiency of PhCs. In general, the removal process of PhCs begins with their separation from organic materials with identical chemical characteristics. Subsequently, these compounds are adsorbed onto the surface of the substrate, where their extractability, toxicity, and bioavailability progressively diminish with extended contact time (Salah et al., 2023).

Literature review reveals that only a few studies have examined the impact of incorporating BC into substrate-based CWs, particularly regarding its effectiveness in removing PhCs. For instance, Ofiera et al. (2025) examined the effect of adding BC (from undefined biomass) into CWs, finding that BC-enhanced CWs effectively reduced all target PhCs to below quantification limits. In contrast, conventional CWs showed inconsistent removal, with maximum efficiencies of 86% for metoprolol, 62% for clarithromycin (CLA), and 48% for diclofenac (DIC), while candesartan, carbamazepine (CBZ), and hydrochlorothiazide were not removed (Ofiera et al., 2025). Yuan et al. (2020) demonstrated that integrating BC derived from fruit stones into zeolite-based CWs significantly enhanced the removal efficiency of antibiotics, achieving removal rates of approximately 88% for CIP and 56% for sulfamethazine. Chand et al. (2022) evaluated the performance of vertical flow constructed wetlands (VF-CWs) incorporating BC derived from cow dung pats for the removal of pharmaceutical contaminants, including amoxicillin (AMX), caffeine (CF), and ibuprofen (IBU). The BC-amended VF-CW demonstrated significantly enhanced removal efficiencies, achieving 75.5% for AMX, 87.5% for CF, and 79.9% for IBU, compared to 53.82%, 69.8%, and 63.98%, respectively, in VF-CWs utilizing conventional filter media. Similarly, Ajibade et al. (2023) highlighted that adding bamboo-derived BC to CWs markedly improved the elimination of sulfamethoxazole (SMZ), with a removal efficiency of 65% compared to 28% in sand-filled CWs. Moreover, Ilyas and Hosney (2024) assessed the role of softwood-bagasse BC-added CWs in addressing some PhCs, including SMZ, irbesartan, erythromycin (ERY), DIC, and CBZ, showing a high performance exceeding 91% compared to conventional CWs filled with gravel (72%, 50%, 84%, 22%, and 36%, respectively). On the other hand, Venditti et al. (2022) reported that VF-CWs amended with plant-derived BC exhibited lower performance than sand-based VF-CWs, which achieved average removal efficiencies exceeding 91% and 94% for a range of PhCs, respectively. The variations in removal efficiencies can be attributed to several factors, including the BC intrinsic properties, operation conditions of the CWs, and the vegetation (El Barkaoui et al., 2023). To date, no studies have addressed the efficiency of olive pomace-derived BC in VF-CWs or the effect of BC proportion in substrate-based CWs on PhCs removal. Furthermore, comprehensive studies addressing the occurrence of PhCs in particulate matter (PM) in wastewater and the mechanisms governing their removal are lacking.

Based on the above considerations, this study aims to evaluate the impact of integrating BC derived from olive pomace into VF-CWs and its substrate percentage on the removal efficiency

of conventional pollutants, pathogens, and pharmaceutical substances. In addition, investigate the occurrence of PhCs in both the aqueous and PM samples of the influent wastewater.

2. Materials and Methods

2.1. Design and operation of VF-CW systems

The experiment utilised three identical vertical flow constructed wetlands (VF-CWs), each constructed from cylindrical polyethylene with uniform dimensions: 0.45 m in height, 0.30 m in diameter, and a surface area of 0.07 m² (**Figure IV-1**). The bed frame structure of each microcosm is 0.30 m, supported by packed substances consisting from the bottom with 8 cm of gravel (particle size: 2–8 cm), sand (particle size: 1–2 cm) mixed with different ratios 0% (CW-0), 10% (CW-10), and 50% (CW-50) of BC (particle size: 2–5 cm), and another layer of gravel at the top (particle size: 2–6 cm). Each system was equipped with two ventilation pipes to ensure adequate oxygen supply during filter operation and was planted with P. australis seedlings at a density of 4 plants per m^2. The experiment was conducted over 10 months (June 2023–March 2024) under a sequential batch operation mode, consisting of five daily batches with a total influent volume of 5 L/day and an organic loading rate of 20 g COD/m² d, incorporating a one-day drying period.

In this study, the BC was prepared as described in the study of El Barkaoui et al. (2025b), from exhausted olive pomace via pyrolysis at 590 °C for a contact time of 2 h, under a heating rate of 10 °C min^{-1} (El Barkaoui et al. 2025). The resulting material exhibited an SSA of 106 m^2/g^1, a carbon content of 90%, an ash content of 4.9%, and a point of zero charge (pH_{pzc}) of 7.8. The full characterisation of the BC can be found in section 1 (**Table SM4-1** and **Figure SM4-1**) of the *supplementary material 4 (SM4)* and also reported in the previous study of El Barkaoui et al. (2025b).

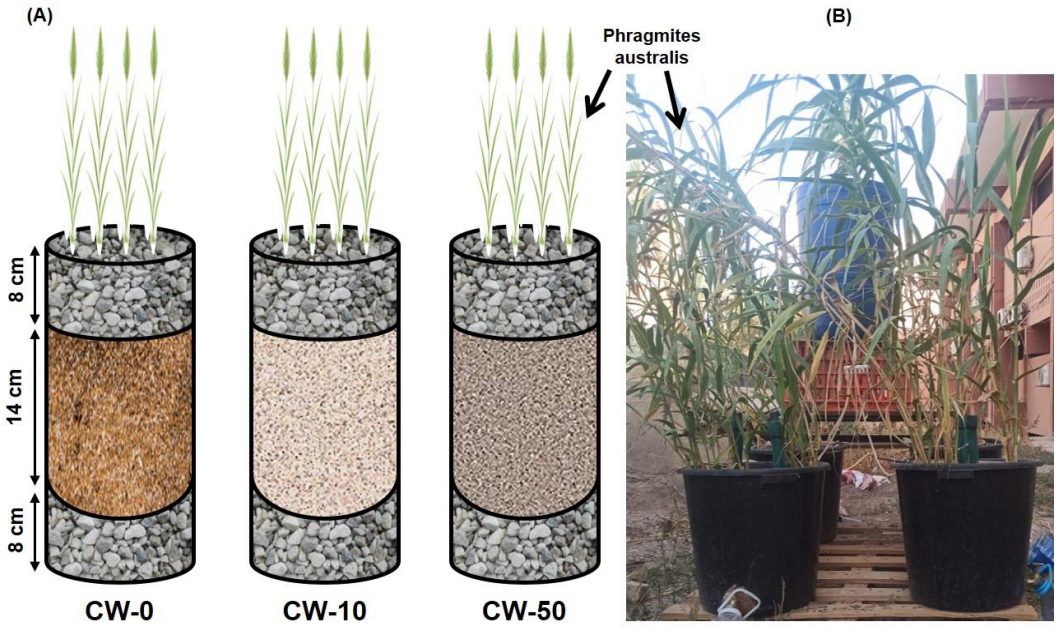

Figure IV-1: Schematic illustration of the pilot-scale vertical flow constructed wetlands (A) and a photograph of the real CWs (B) with different percentages of biochar 0% (CW-0), 10% (CW-10), and 50% (CW-50).

2.2. Sampling and analysis

2.2.1. Wastewater source

Wastewater samples were collected biweekly from the Marrakech Wastewater Treatment Plant (WWTP) after primary treatment (decantation) and analysed immediately after sampling. **Table IV-1** summarises the physicochemical characteristics of the influent over the entire study duration.

2.2.2. Conventional water quality parameters

The physicochemical and Pathogen indicators of faecal contaminations, including total suspended solids (TSS), chemical oxygen demand (COD), total nitrogen (TN), total Kjeldahl nitrogen (TKN), ammonium nitrogen (NH_4^+-N), nitrate nitrogen (NO_3^--N), nitrite nitrogen (NO_2^--N), total phosphorus (TP), phosphate (PO_4^{3-}), total hardness (TH), calcium, magnesium, faecal streptococci (FS), faecal coliforms (FC), and total coliforms (TC), were analysed following the standard procedures outlined by Standard of AFNOR, (1997) and Rodier, (2009). The UV absorbance of both the influent and effluent samples was quantified at wavelengths of 254 nm and 420 nm (Ayadi et al. 2024). The complete methodology for analysing the

aforementioned parameters is provided in the *supplementary material 4*.

2.2.3. Analysis of pharmaceutical compounds in particulate and aqueous samples

2.2.3.1. Extraction procedure

After collecting, the particulate samples were freeze-dried and finally stored in the dark at -20°C. They were subjected to Quick, Easy, Cheap, Effective, Rugged and Safe (QuEChERS) extraction and subsequent analysis according to the method developed by Rossini et al. (2016) (full description in *supplementary material 4*). Wastewater samples were collected and stored at -20°C until analysis. All samples were filtered with a 0.2 mm RC membrane, pretreated by adding EDTA as a chelating agent, then analysed by liquid chromatography coupled to a mass spectrometer (LC-MS/MS).

2.2.3.2. LC-MS/MS analysis

Instrumental analysis was performed on a Shimadzu (Kyoto, Japan) chromatographic system coupled with a 5500 QTrap mass spectrometer (Sciex, Framingham, MA, USA), equipped with a Turbo V® interface by an ESI probe. Pharmaceutical compounds were determined according to the method developed. Full details of this analytical protocol are reported in Renai et al. (2021). Target compounds and internal standards of this study (Sigma-Aldrich), including the analgesics, antibiotics, beta-blockers, antibiotics, antifungals, psychiatric drugs, diuretics, statins, gastric protectors, analgesics, antihypertensives, Urinary α-Blockers, and transformation products are reported in **Table SM4-2** of the *supplementary material 4*.

2.3. Statistical analysis

Statistical analysis to assess the significance of the data in this study was conducted using the Games-Howell non-parametric test and analysis of variance (ANOVA) through Minitab 17 software (version 17.1.0, State College, PA, USA). Significance levels were categorised as non-significant ($p > 0.05$) or significant ($p < 0.05$).

3. Results and discussion

3.1. Conventional pollutant removal

Table IV-1 summarises the physicochemical parameters measured at the inlet and the outlet of

CW-0, CW-10, and CW-50. Throughout the experiment, the influent consistently exhibited low dissolved oxygen (DO) levels (0.4 mg L^{-1}), likely due to oxygen depletion associated with the concurrent oxidation of organic matter and nitrification processes (Fan et al. 2013; Kizito et al. 2017). However, without active aeration, the DO concentrations after treatment increased significantly to 1.1 mg L^{-1}, reflecting the improved quality of the wastewater after treatment (Nguyen et al. 2020b). As a result, lower DO levels may shift microbial processes toward anaerobic pathways, affecting treatment efficiency (Maina et al. 2011). Generally, the key sources of oxygen supply are air reoxygenation, water inflow, and oxygen diffusion during dry periods (Ye et al. 2012; Kasak et al. 2018). The influent pH was approximately 7.7, while the effluent pH of all three systems increased significantly to 8.1–8.2. This rise may be attributed to the biological oxidation processes and the release or dilution of carbonate salts, hydroxyl ions, and the strong H^+ exchange capacity of the bed materials within the CWs (Chen et al. 2015). In addition, the increase in the effluent's pH may be due to the alkaline properties of Moroccan sand used as filling media of CWs (Mghaiouini et al. 2024). EC significantly increased after treatment across all three VF-CWs, reaching 4 mS cm^{-1} compared to a mean influent value of 2.3 mS cm^{-1}. This rise is likely attributed to the oxidation of organic compounds, nitrification processes, and elevated temperatures in Marrakech (>40 °C), which enhance evapotranspiration and ion concentration (Licata et al. 2021; De Sanctis et al. 2025). Additionally, the increase in EC may be influenced by ions released from sand and the biodegradation of organic matter, reflecting a higher concentration of dissolved anions and cations in the treated effluent (Achak et al. 2023). The pH and EC results of the effluent samples obtained after treatment correspond to the Moroccan standard for the reuse of treated wastewater in agriculture (pH 6.5–8.4 and EC < 12 mS/cm) (S.E.E.E 2007).

Calcium and magnesium are essential macronutrients that support the growth, development, and reproduction of both plants and animals, and their presence contributes to water hardness (Azad et al. 2024). At the inlet of the three VF-CWs, the mean concentrations of TH, Ca, and Mg were 369, 61, and 308 mg L^{-1}, respectively. Post-treatment, a significant increase in these concentrations was observed at the outlet, with TH ranging from 645 to 735 mg L^{-1}, Ca from 120 to 150 mg L^{-1}, and Mg from 525 to 584 mg L^{-1}. This finding could be attributed to mineral dissolution, where water percolation through the filter bed releases these ions (Prajapati et al., 2018; Ghumra et al., 2021). Ion exchange processes in the substrate can further contribute to Ca^{2+} and Mg^{2+} release, contributing to the increase in the EC (Ramachandra et al. 2018).

Additionally, the filter systems were installed under external climate conditions in Marrakech, which is characterised by high temperatures during most periods of the year, leading to higher evapotranspiration, which concentrates dissolved ions, while anaerobic conditions promote the mobilisation of Ca^{2+} and Mg^{2+} from sediments (Basílico et al. 2024). Moreover, the rise in TH, Ca, and Mg concentrations in the effluent correlated with the higher sand content in the interlayer substrate. These results are consistent with the literature (Prajapati et al., 2018; Ghumra et al., 2021; El Barkaoui et al. 2025b).

TSS is a crucial parameter that determines the quality of the effluent and whether it can be reused for agricultural purposes. In this study, the three CWs exhibited high removal efficiencies, ranging from 67% to 83%, with CW-10 and CW-50 outperforming the control CW-0, which was less homogeneous than the BC-filled systems. These findings can be attributed to the fact that BC has a greater ability to remove the colloidal particles present in the influent due to biochar's higher sorption properties than sand (El Barkaoui et al. 2025b).

Table IV-1 presents the performance of CW-0, CW-10, and CW-50 in reducing absorbance at 254 nm and 420 nm, which are commonly used as surrogate indicators for the presence of aromatic and unsaturated organic compounds, as well as coloured dissolved organic matter such as humic substances. These parameters offer a rapid and effective method for assessing the removal of organic micropollutants (Ciardelli and Ranieri, 2001; Altmann et al., 2016). The results reveal a notable reduction in absorbance at both wavelengths after treatment. For absorbance at 254 nm, the results showed no significant removal efficiency among the three filter systems, although the VF-CWs containing BC showed slightly higher efficiencies. In contrast, BC-based VF-CWs demonstrated a significantly greater reduction in absorbance at 420 nm compared to the control VF-CW, with removal efficiencies of 58%, 71%, and 72% for CW-0, CW-10, and CW-50, respectively. These findings emphasise the key role of BC in the effective removal of organic micropollutants. In contrast, they revealed that increasing the percentage of BC had no impact on the removal performance at either wavelength. Ayadi et al. (2024) reported a greater reduction in absorbance at 254 and 420 nm in BC-based microcosms compared to gravel-filled microcosms, being about 51–59% and 18–31%, respectively. However, El Barkaoui et al. (2025c) demonstrated that adding BC to substrate-based filter columns did not significantly improve performance at either wavelength.

Throughout the experiment, there was no significant variation in SO_4^{2-} concentrations between

the influent and effluent samples, indicating the limited performance of the VF-CWs towards sulphates (**Table IV-1**). A comparable observation was reported by El Barkaoui et al. (2025b), who attributed the slight increase in effluent concentrations from unplanted columns relative to influent to the oxidation of carbon-bound sulphur and subsequent sulphate release from the column media. The limited performance of SO_4^{2-} in the present study could be due to the immobilisation of reduced sulphide in sediments in the absence of active aeration (Johnston et al. 2014). On the other hand, a high removal efficiency of SO_4^{2-} was reported in the study of Chand et al., (2021), exceeding 85% using a BC-packed Colocasia esculenta-based vertical subsurface flow constructed wetland, referring this performance to some processes such as the nitrate reduction process, sulphur oxidation by sulphur-oxidising bacteria, plant uptake, chemical oxidation processes, precipitating with metal ions, and dissimilatory sulfate reduction.

As regards the phosphorus, **Table IV-1** presents the TP and PO_4^{3-} concentrations in the inlet and outlet samples of the three VF-CWs. The behaviour of TP and PO_4^{3-} exhibited a similar trend throughout the treatment process. Consequently, their mean concentrations in the effluent were significantly lower than those in the influent, indicating effective phosphorus removal, ranging from 49% to 58% for TP and from 49% to 53% for PO_4^{3-}. Furthermore, there was no significant difference in phosphorus removal between the effluents of CW-0, CW-10, and CW-50 during the whole experimental period, indicating a lack of role for BC. In general, it is well known that the BC has a limited effect on the removal of phosphorus, as well as negatively charged compounds, due to its surface characteristics (e.g., low affinity, surface charge). This finding is in accordance with other studies (Yao et al., 2012; de Rozari et al., 2016; Werner et al., 2018; El Barkaoui et al., 2023). For example, de Rozari et al. (2016) found that sand exhibited better phosphorus performance than the BC-amended media due to the negative surface charge and low affinity of BC towards phosphorus forms, as well as competition from other negatively charged molecules in wastewater, such as organic compounds, for exchange sites on the surface of BC. Similarly, Zhou et al. (2019) reported that the integration of BC into CW did not affect phosphorus removal. Generally, the primary mechanisms for phosphorus removal in CWs include microbial oxidation and decomposition, physicochemical reactions of substrates (e.g., precipitation, adsorption, ion exchange, and mineralisation), and plant uptake (Wu et al. 2015).

Regarding the organic matter, **Table IV-1** presents the COD concentrations in the inlet and outlet samples of CW-0, CW-10, and CW-50, along with their respective removal efficiencies.

The results showed a significant decrease in average concentrations of COD after treatment. Furthermore, the BC-filled planted VF-CWs exhibited high statistical removal efficiencies (60 – 61%) compared to the control VF-CW (50%), highlighting the positive impact of BC addition, due to its various benefits (e.g., porous structure and rich surface functionalization, pores with different sizes and distributions), enhancing the electrostatic adsorption capacity of organic matter and providing a favourable microbial environment for the degradation of organic carbon (de Rozari et al., 2015; Deng et al., 2019). Ayadi et al. (2024) reported that the adsorption mechanisms by BC involve the degradation of the COD rather than biological processes. Interestingly, the increase in BC concentration up to 50% did not affect COD removal, likely resulting in the release of soluble organic carbon from the BC and/or the toxicity of the material toward microorganisms (Deng et al. 2019). This finding is consistent with previous research recommending a lower BC percentage (Li et al., 2018; Zhou et al., 2018a, 2018b; Zhang et al., 2021; El Barkaoui et al. 2025b).

A particularly noteworthy aspect is the removal of nitrogen forms (**Table IV-1**). The results highlight a strong removal of NH_4^+-N, TKN, and TN in the three VF-CWs, especially those integrated BC showed a significantly higher removal of TN (53%), TKN (66 – 74%), and NH_4^+-N (81 – 85%) than the control filer (38% for TN, 52% for TKN, and 71% for NH_4^+-N), demonstrating the positive effect of BC adding, due to its cation exchange mechanism, which play a minor role in the removal of ionic species (El Barkaoui et al. 2025b). The high removal observed of NH_4^+-N, TKN, and TN was probably due to either physicochemical or biological processes. Furthermore, it is well established that biological processes are responsible for driving the nitrogen cycle and the conversion of reduced and oxidised forms of nitrogen inside the VF-CWs (Ma et al. 2023). Furthermore, increasing the concentration of BC-based substrate (up to 50%) showed no effect on the removal of NH_4^+-N, TKN, and TN, indicating that a lower ratio of BC (10%) is an additional advantage from an economic and performance point of view. The higher removal of NH_4^+-N was combined with the release of NO_3^--N (16 – 25 mg L^{-1}) and NO_2^--N (4 – 5 mg L^{-1}) due to the nitrification process. Fortunately, in the present study, the concentrations of NO_3^--N and NO_2^--N are below the reported toxicity limits for all aquatic species and the fish fauna (Lewis and Morris 1986; Camargo et al. 2005). Many studies reported this phenomenon, which may be attributed to the incomplete oxidation of NH_4^+-N, caused by the insufficient availability of DO in CWs (Li et al. 2021; Lu et al. 2022; Ayadi et al. 2024; El Barkaoui et al. 2025a), a condition that primarily affects the activity of nitrite-oxidising bacteria

instead of the microorganisms responsible for nitrite/ammonia conversion (Vymazal, 2007; Tan et al., 2013). However, Kizito et al. (2017) reported that the higher release of NO_3^--N in BC-packed CWs may be due to the high level of oxygen in the filter. The TN concentrations in all three VF-CWs exhibited a notable reduction throughout the treatment process, with a more pronounced decline in BC-based VF-CWs compared to CW-0. This suggests that denitrification was a predominant process in all VF-CWs, with BC playing a significant role in enhancing this mechanism within the nitrogen cycle. Generally, the different forms of nitrogen and their conversion depend on filter material, plant type, oxygen availability, and substrates (Nguyen et al. 2020a).

Monitoring of faecal bacteria indicators (e.g., TC, FC, and FS) at the inlet and outlet of CW-0, CW-10, and CW-50 revealed a significant decrease in the concentrations of the effluent samples (3 log units for TC, 2 log units for FC, and 3.1 – 3.9 log units for FS) compared to the influent (8 log units for TC, 6.3 log units for FC, and 6.4 log units for FS). Furthermore, the three filters showed no statistically significant differences in the removal efficiency of TC and FC. However, FS elimination was notably higher in CW-10 (3.2 log units) and CW-50 (3.3 log units) compared to CW-0 (2.5 log units), highlighting the crucial role of biochar (BC). This improvement is attributed to BC's favourable properties, such as high hydrophobicity and porous structure, which make it more effective than conventional materials like gravel or sand (El Barkaoui et al. 2023). The reduction in microbial contaminant concentrations in the present study remains moderate after treatment, which may be attributed to the limited biofilm development during the experimental period. Because its formation within the filter enhances filtration efficiency by progressively reducing porosity as accumulated particles decrease pore size. This process improves contaminant removal over time. Additionally, grain size can influence pathogen removal in slow sand filters (Logan et al. 2001). Besides, retention time and filter depth also play a crucial role. Consistent with these findings, Torrens et al. (2009) reported that increasing filter depth enhances contaminant removal efficiency due to prolonged hydraulic retention time. Additionally, the removal efficiency of faecal coliforms in CWs can also be affected by several factors, including DO, pH, medium texture, influent load, and rhizome root structure (Chand et al. 2021). There are conflicting results in the literature regarding the effect of BC on the removal efficiency of faecal indicator organisms. For instance, Kaetzl et al. (2019) demonstrated that CWs incorporating rice-husk-derived BC exhibited superior ability in removing faecal indicator bacteria from municipal wastewater compared to conventional sand-

based CWs. Similarly, El Barkaoui et al. (2025b) investigated the effect of BC-based column filters on the removal of TC, FC, and FS, mentioning the high capacity of BC in reducing bacterial contamination compared to sand. Another study conducted by El Barkaoui et al. (2025c) evaluated the efficiency of five substrate-based column filters (sand, olive pomace BC, orange wood waste BC, filao BC, and cypress BC) in removing bacterial indicators (TC, FC, and FS). The results showed that while all filters achieved only moderate removal of TC and FC, they consistently exhibited high removal of FS, with no significant differences among them. Notably, BC-amended filters demonstrated significantly greater removal of TC and FC compared to the sand control. This enhanced performance was attributed to the unique properties of BC, including its high surface area, porosity, functional groups, and hydrophobicity, which make it more effective than sand or gravel in reducing microbial loads.

According to Chand et al. (2021), the use of BC-based media in planted CWs significantly improved TC removal compared to systems with conventional substrates. This improvement was mainly due to the enhanced filtration properties of the biochar's porous structure, which promoted more efficient microbial retention and removal. Nevertheless, Visiy et al. (2022) demonstrated that faecal coliform reduction in CWs was comparable between sand and BC substrates, indicating that pathogen removal is mainly governed by physical processes with minimal influence from substrate composition. There is a scarcity of research on the impact of governing the removal of microbial contaminants in BC-based CWs. The removal performance of faecal coliform indicators using conventional filter media such as pozzolan, gravel, and sand was comparable. The removal performance of faecal coliform indicators using conventional filter media such as pozzolan, gravel, and sand has shown consistent and similar results. For instance, El Ghadraoui et al. (2020) reported removal efficiencies of 2.76, 2.56, and 3.87 log units for TC, FC, and FS, respectively, in pozzolan-based constructed wetlands (CWs). Similarly, Sleytr et al. (2007) observed high removal rates in sand- and gravel-based CWs, with 4.37 log units for FC and 4.31 log units for TC.

Table IV-1: Values (mean ± standard deviation) of water quality parameters measured in the influent (INF) and effluent (EFF) samples of the three CWs filled with different percentages of biochar: 0% (CW-0), 10% (CW-10), and 50% (CW-50).

Parameters	INF concentration	Outlet of CW-0		Outlet of CW-10		Outlet of CW-50	
		EFF concentration	Removal (%)	EFF concentration	Removal (%)	EFF concentration	Removal (%)
DO (mg/L)	0.4 ± 0.9^{a}	1.1 ± 0.8^{ab}	–	1.1 ± 0.6^{ab}	–	1.1 ± 0.7^{b}	–
EC (mS/cm)	2.3 ± 0.3^{a}	4 ± 1^{b}	–	4 ± 1^{b}	–	4 ± 1^{b}	–
pH	7.7 ± 0.2^{a}	8.1 ± 0.1^{b}	–	8.1 ± 0.2^{b}	–	8.2 ± 0.2^{b}	–
Total hardness (mg/L)	369 ± 34^{a}	735 ± 153^{b}	–	700 ± 129^{b}	–	645 ± 126^{b}	–
Calcium (mg/L)	61 ± 9^{a}	150 ± 27^{b}	–	141 ± 23^{bc}	–	120 ± 36^{c}	–
Magnesium (mg/L)	308 ± 34^{a}	584 ± 149^{b}	–	558 ± 114^{b}	–	525 ± 110^{b}	–
TSS (mg/L)	212 ± 105^{a}	69 ± 37^{b}	67 ± 14^{a}	37 ± 25^{b}	81 ± 16^{b}	38 ± 19^{b}	79 ± 15^{ab}
ABS 254 nm (mAu)	633 ± 101^{a}	329 ± 95^{b}	48 ± 15^{a}	313 ± 94^{b}	50 ± 15^{a}	315 ± 93^{b}	50 ± 15^{a}
ABS 420 nm (mAu)	96 ± 20^{a}	41 ± 14^{b}	58 ± 8^{a}	29 ± 16^{b}	71 ± 10^{b}	28 ± 14^{b}	72 ± 10^{b}
SO_4^{2-} (mg/L)	75 ± 27^{a}	83 ± 23^{a}	–	80 ± 23^{a}	–	75 ± 24^{a}	–
COD (mg/L)	272 ± 77^{a}	131 ± 29^{b}	50 ± 9^{a}	106 ± 25^{b}	60 ± 6^{b}	103 ± 25^{b}	61 ± 8^{b}
TP (mg/L)	12 ± 2^{a}	5 ± 2^{b}	58 ± 14^{a}	6 ± 2^{b}	49 ± 15^{a}	5 ± 1^{b}	57 ± 9^{a}
PO_4^{3-} (mg/L)	9 ± 1^{a}	4 ± 1^{b}	51 ± 14^{a}	5 ± 1^{b}	49 ± 11^{a}	4 ± 1^{b}	53 ± 10^{a}
TN (mg/L)	142 ± 31^{a}	84 ± 22^{b}	38 ± 21^{a}	64 ± 14^{c}	53 ± 15^{b}	66 ± 11^{c}	53 ± 9^{b}
TKN (mg/L)	139 ± 29^{a}	62 ± 16^{b}	52 ± 17^{a}	34 ± 9^{c}	74 ± 9^{b}	45 ± 6^{c}	66 ± 6^{b}
NH_4^{+}-N (mg/L)	69 ± 21^{a}	18 ± 4^{b}	71 ± 11^{a}	9 ± 4^{b}	85 ± 9^{b}	10 ± 7^{b}	81 ± 18^{ab}
NO_2^{-}-N (mg/L)	0.10 ± 0.04^{a}	4 ± 3^{b}	–	5 ± 3^{b}	–	4 ± 3^{b}	–
NO_3^{-}-N (mg/L)	3 ± 2^{a}	18 ± 9^{bc}	–	25 ± 13^{b}	–	16 ± 8^{c}	–
Total coliform (Log unit)	8 ± 1^{a}	3 ± 1^{b}	–	3 ± 1^{b}	–	3 ± 1^{b}	–
Faecal coliforms (Log unit)	6.3 ± 0.9^{a}	2 ± 2^{b}	–	2 ± 1^{b}	–	2 ± 1^{b}	–
Faecal streptococci (Log unit)	6.4 ± 0.5^{a}	3.9 ± 0.2^{b}	–	3.18 ± 0.05^{c}	–	3.1 ± 0.2^{c}	–

Different letters in each row mean statistically significant differences ($P<0.05$) according to Fisher or Games.

3.2. Overall removal of pharmaceutical compounds

3.2.1. Occurrence of pharmaceutical compounds in wastewater

PhCs are persistent and complex substances commonly detected in wastewater, both in dissolved form and adsorbed onto particulate matter (PM), making their removal challenging. **Table IV-2** lists the mean concentrations of the selected PhCs detected in PM. The data indicate the presence of 18 compounds with a total concentration of 35 ng g^{-1}, including CBZ, SMZ, O-DES, FLC, CLA, FUR, AZI, TMP, CLT, MCL, 4-HYDIC, KET, IBU, 2H-IBU, 3H-IBU, FLU, O-DMNAP, and ACE. The highest concentration detected was 12 ng g^{-1} for KET, followed by ACE (5.5 ng g^{-1}), CBZ (3.7 ng g^{-1}), AZI (2.6 ng g^{-1}), 3H-IBU (2.2 ng g^{-1}), 4-HYDIC and MCL (2 ng g^{-1}), and O-DMNAP (1.7 ng g^{-1}). However, the following compounds were undetectable as they were below the detection limit: ATE, VEN, BIS, PAN, RMP, ATO, DIC, DZP, TAM, ERY, CIP, 1H-IBU, FEN, and NAP.

Conversely, the analysis of the PhCs in the influent wastewater revealed the presence of various compounds, notably CLA, FUR, ATE, BIS, ERI, 4-HYDIC, KET, DIC, IBU, NAP, OVEN, 1H-IBU, 3H-IBU, SMZ, VEN, 2H-IBU, CIP, CBZ, and FLU, with a total concentration (ΣPhCs) of 18163 ng L^{-1} (**Table IV-3**). In addition, the analysis of PhCs in the influent water samples showed the appearance of some of the undetectable compounds in PM, such as ATE, BIS, OVEN, ERY, DIC, NAP, 1H-IBU, VEN, and CIP, suggesting that those compounds are primarily present in the dissolved phase rather than being associated with PM. This indicates their higher water solubility and lower affinity for adsorption onto suspended solids, affecting their environmental mobility and potential bioavailability in aquatic systems. Many studies have reported that there are higher concentrations of PhCs in the dissolved phase of influent wastewater than in suspended solids (PM) and sediments (Silva et al. 2011; Aminot et al. 2015). On the other hand, the data revealed the absence of several compounds (e.g., O-DES, FLC, AZI, TMP, CLT, MCL, O-DMNAP, ACE) in the dissolved phase of the influent wastewater, although they were previously detected in the PM. This absence can be attributed to the high affinity of these compounds toward PM. A similar finding was reported by Silva et al. (2011), who observed that certain compounds were preferentially bound to PM rather than being detected in river water. Those compounds are generally characterised by a basic behaviour (pKa > 7).

Table IV-2: Concentration (mean values (n=3) ± standard deviation) of selected pharmaceutical compounds detected in particulate matter (PM) in the inlet samples.

Compound	Abbreviation	Concentration (ng g^{-1})	CV%
Carbamazepine	CBZ	3.7 ± 0.4	10
Sulfamethoxazole	SMZ	0.26 ± 0.05	19
O-Desmethylvenlafaxinec	O-DES	0.18 ± 0.03	17
Fluconazole	FLC	0.73 ± 0.08	11
Clarithromycin	CLA	0.36 ± 0.07	18
Furosemide	FUR	0.5 ± 0.1	18
Azithromycin	AZI	2.6 ± 0.6	23
Trimethoprim	TMP	0.05 ± 0.01	31
Clotrimazole	CLT	0.38 ± 0.08	21
Miconazole	MCL	2.0 ± 0.3	15
4'-Hydroxydiclofenac	4-HYDIC	2.0 ± 0.2	11
Ketoprofen	KET	12 ± 1	8
Ibuprofen	IBU	0.6 ± 0.1	22
2-Hydroxyibuprofenc	2H-IBU	0.3 ± 0.1	34
3-Hydroxyibuprofenc	3H-IBU	2.2 ± 0.1	7
Flurbiprofen	FLU	0.18 ± 0.07	39
O-Desmethylnaproxen	O-DMNAP	1.7 ± 0.3	17
Acetaminophen	ACE	5.5 ± 0.9	16
Atenolol	ATE	<0.003	-
Venlafaxine	VEN	<0.1	-
Bisoprolol	BIS	<0.003	-
Pantoprazole	PAN	<0.014	-
Ramipril	RMP	<0.37	-
Atorvastatin	ATO	<0.06	-
Diclofenac	DIC	<0.05	-
Diazepam	DZP	<0.01	-
Tamsulosin	TAM	<0.001	-
Erythromycin	ERY	<0.36	-
Ciprofloxacin	CIP	<1.38	-
1-Hydroxyibuprofenc	1H-IBU	<0.028	-
Fenbufen	FEN	<0.110	-
Naproxen	NAP	<0.014	-
ΣPhCs	-	35.24	-

3.2.2. Performance of VF-CWs in removing pharmaceutical compounds

Table IV-3 summarises the average concentrations of the selected PhCs measured at the inlet and outlet of CW-0, CW-10, and CW-50, while **Figure IV-2** illustrates their corresponding mean removal efficiencies throughout the experiment duration. Among 36 PhCs (**Table SM4-2**), only 19 compounds had concentrations above the limits of quantification, including CLA, FUR, ATE, BIS, ERY, 4-HYDIC, KET, DIC, IBU, NAP, OVEN, 1H-IBU, 3H-IBU, SMZ, VEN, 2H-IBU, CIP, CBZ, and FLU. Furthermore, analysis of influent samples revealed high concentrations of non-steroidal anti-inflammatory drugs (NSAIDs) such as IBU, KET, DIC, NAP, and their

metabolites (e.g., 1H-IBU, 2H-IBU, 3H-IBU, 4-HYDIC), ranging from 176 to 3992 ng/L. The high level of NSAIDs in the influent samples is mainly attributed to their widespread use, partial metabolism in the human body, and improper disposal. These compounds are frequently excreted unchanged or as active metabolites and enter municipal wastewater systems (Massano 2025). However, ERY, BIS, VEN, and CLA have the lowest concentration (< 100 ng/L).

Regardless of the CW's substrate type (with or without BC), the data indicated in **Table IV-3** illustrate a significant decrease in the concentrations of the selected compounds following treatment, except CBZ and FLU, which exhibited an increase in their concentrations, especially in the effluent from CW-0, due to their persistent nature, low biodegradability, and resistance to microbial degradation (Oulton et al. 2010; Chen et al. 2018; Fernandes et al. 2021). Similarly, Qing et al., (2011) reported that CBZ is one of the most recalcitrant PhCs, attributing its low removal efficiency in CWs to its high hydrophobicity. This behaviour may be linked to the conversion of the transformation products into the parent compound via photochemical or biological processes (Ilyas and van Hullebusch 2020). Another hypothesis is that the increased concentrations of these compounds after filtration may be due to their release from the PM retained in the filter systems, since these compounds were already present in the PM (see **Table IV-2**). In addition, the observed negative removal of PhCs like CBZ can also be attributed to the desorption of previously retained compounds from the substrate, which provides only temporary retention (Wang et al. 2018; Venditti et al. 2022). Venditti et al. (2022) further suggested that the observed rebound in removal efficiency may result from the regeneration of sorption sites becoming available again. Moreover, Phan et al. (2018) and Vassalle et al. (2020) linked the negative removal of these compounds to their desorption from the filter bed, which was likely induced by increased pH levels that diminished their adsorption potential. Numerous studies have highlighted the limited effectiveness of CWs in removing CBZ. Reported removal efficiencies include 0% (Ofiera et al. 2025), 0–2% (Petrie et al. 2018), and <10% (Delgado et al. 2020), highlighting a recalcitrant behaviour in these treatment systems.

Table IV-3: Concentrations (mean value ± standard deviation) of selected pharmaceutical compounds at the inlet and outlet samples of the three CWs filled with different percentages of biochar: 0% (CW-0), 10% (CW-10), and 50% (CW-50) throughout the entire period of treatment (10 months).

Analyte	Inlet ($ng\ L^{-1}$)	Outlet CW-0 ($ng\ L^{-1}$)	Outlet CW-10 ($ng\ L^{-1}$)	Outlet CW-50 ($ng\ L^{-1}$)
CLA	85 ± 39	6 ± 1	< 5 ± -	5 ± -
FUR	341 ± 124	< 20 ± -	< 20 ± -	< 20 ± -
ATE	217 ± 65	52 ± -	< 50 ± -	52 ± -
BIS	54 ± 22	< 20 ± -	< 20 ± -	< 20 ± -
ERY	36 ± 19	5 ± -	< 5 ± -	< 5 ± -
4-HYDIC	983 ± 363	< 300 ± -	< 300 ± -	< 300 ± -
KET	1200 ± 462	< 200 ± -	< 200 ± -	< 200 ± -
DIC	955 ± 232	271 ± 194	272 ± 106	229 ± 113
IBU	3438 ± 1439	1068 ± 647	996 ± 473	865 ± 483
NAP	568 ± 288	272 ± 132	238 ± 113	209 ± 119
OVEN	190 ± 83	57 ± 48	47 ± 23	27 ± 4
1H-IBU	3992 ± 4497	193 ± 94	203 ± 69	136 ± 89
3H-IBU	976 ± 721	390 ± 285	258 ± 227	261 ± 298
SMZ	291 ± 133	84 ± 62	59 ± 27	56 ± 17
VEN	71 ± 20	38 ± 17	32 ± 6	31 ± 12
2H-IBU	3184 ± 822	1388 ± 629	1677 ± 1249	1417 ± 901
CIP	806 ± 197	333 ± 219	336 ± 89	350 ± 136
CBZ	600 ± 225	666 ± 323	477 ± 242	453 ± 247
FLU	176 ± 66	329 ± 206	226 ± 142	231 ± 162
ΣPhCs	18163 ± 1213	5152 ± 406	4821 ± 477	4322 ± 392

[a] Method detection limit; [b] Method quantification limit.

Furthermore, over the experimental period, the three treatment systems achieved approximately a complete removal of CLA, FUR, ATE, BIS, ERY, 4-HYDIC, and KET, above 70% for DIC, OVEN, 1H-IBU, and SMZ, above 50% for IBU, VEN, and CIP, and lower than 50% for NAP and 2H-IBU, as shown in **Figure IV-2**. The obtained removal performances of PhCs vary across compounds, being higher, comparable, or lower than those reported in previous studies. For example, Zhang et al. (2012) reached a removal efficiency of 52% for CBZ, 80% for IBU, 91% for NAP, and 55% for DIC in planted CWs. In a study conducted by Vymazal et al. (2017), the removal efficiency of IBU and DIC reached approximately 55% and 41%, respectively. Ravichandran and Philip, (2022) demonstrated that CWs filled with wood charcoal or zeolite effectively remove CBZ, DIC, and ATE (>90%). Rühmland et al. (2015) tested the removal of ATE, VEN, CBZ, and CLA using sand-based CWs and achieved removal efficiencies of up to 99%, 57%, 80%, and 89%, respectively. Ávila et al. (2021) tested the efficiency of an aerated gravel-filled CW in removing DIC and KET from influent wastewater, exceeding an elimination performance of >83%. Alsubih et al. (2022) investigated the efficiency of treating hospital wastewater using CWs filled with conventional substrates (e.g., gravel and sand) across pre-

monsoon, monsoon, and post-monsoon periods, reaching moderate removal efficiencies of SMZ and CBZ, which varied seasonally from 39% to 64% and 22% to 48%, respectively. Khan et al., (2023) observed poor removal efficiencies of 25%, 36%, and 21% for IBU, CBZ, and ERY, respectively, attributing their limited removal performance to their low influent concentration. In contrast, PhCs with higher concentrations, such as CIP, exhibited high removal efficiencies of up to 84%.

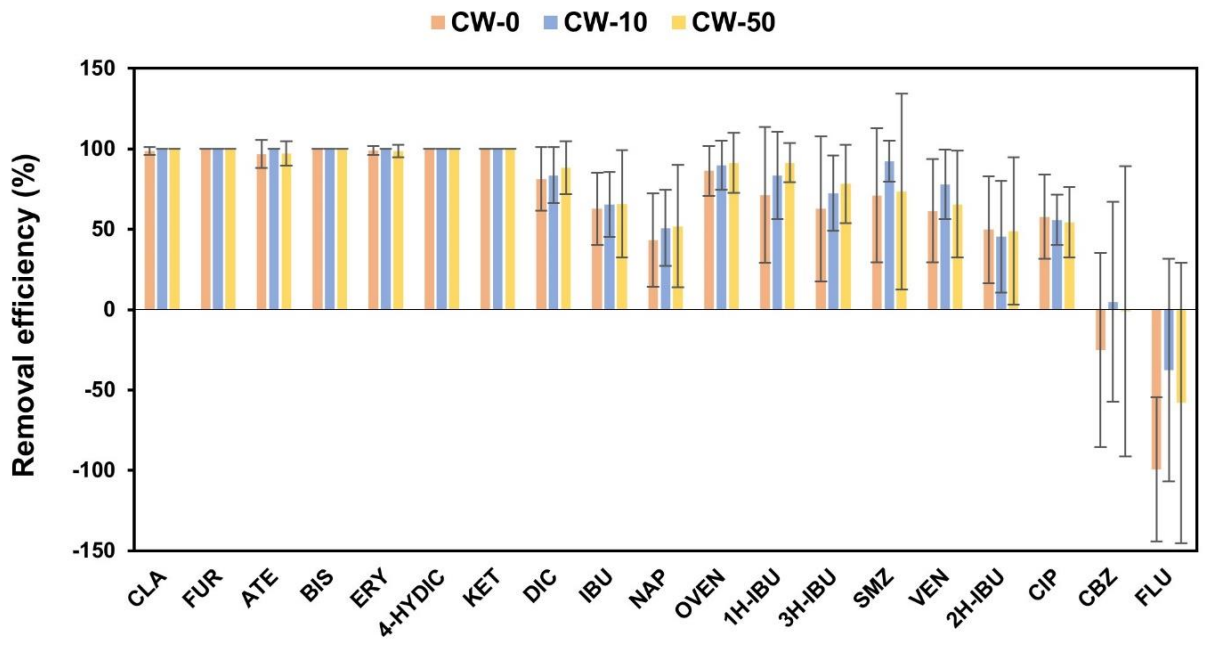

Figure IV-2: Removal efficiency of pharmaceutical compounds in vertical-flow constructed wetlands filled with 0% (CW-0), 10% (CW-10), and 50% (CW-50) biochar throughout the entire treatment period (10 months). Different letters in each row indicate statistically significant differences ($P<0.05$) according to Fisher's or Games' tests.

Unexpectedly, the results showed no significant difference in removal efficiency between CW-0, CW-10, and CW-50, demonstrating the lack of BC effect (**Figure IV-2**). This finding may be due to the physicochemical characteristics of BC, including its ash content, SSA, pore volume, hydrophobicity, affinity, polarity, and surface charge, as well as the speciation of PhCs, all of which can affect BC's adsorption capacity towards PhCs (Lin et al. 2017). The presence of vegetation in BC-based CWs could be critical, as the root system may reduce BC's sorption ability for multiple reasons (Ayadi et al. 2024). One hypothesis suggests that plant exudates may saturate the sorption capacity of BC, while another points to the formation of hydraulic short-circuits within the planted system, which reduce contact between wastewater and BC. Additionally, the presence of BC may lower the plants' effectiveness in promoting the degradation of PhCs (Nweze

et al. 2024). Contradictory findings on the impact of adding BC into CWs and its fusibility on the removal performance of PhCs have been reported in the literature. For instance, Ofiera et al. (2025) reported that BC-amended CWs successfully reduced all targeted pharmaceutical compounds (PhCs) to below quantification limits. In contrast, traditional CWs exhibited variable removal performance, achieving maximum efficiencies of 62% for CLA and 48% for DIC, while showing no removal of carbamazepine (CBZ). Parallelly, Chand et al. (2022) evaluated the performance of VF-CWs incorporating BC derived from cow dung pats for the removal of IBU. The BC-amended VF-CW demonstrated significantly enhanced removal efficiencies, achieving 79.9% compared to 63.98% in VF-CWs utilizing conventional filter media. Similarly, Ajibade et al. (2023) highlighted that adding bamboo-derived BC to CWs markedly improved the elimination of SMZ, with a removal efficiency of 65% compared to 28% in sand-filled CWs. Moreover, Ilyas and Hosney (2024) assessed the role of softwood-bagasse BC-added CWs in addressing some PhCs, including SMZ, ERY, DIC, and CBZ, showing a high performance exceeding 91% compared to conventional CWs filled with gravel (72%, 84%, 22%, and 36%, respectively). In addition, Dalahmeh et al. (2018) revealed that CBZ adsorption capacity using BC-active-biofilm filters was high (>98%), whereas biodegradation in sand-active-biofilm filters was very low (7%). On the other hand, Venditti et al. (2022) reported that VF-CWs amended with plant-derived BC exhibited lower performance than sand-based VF-CWs, which achieved average removal efficiencies exceeding 91% and 94% for a range of PhCs, respectively.

In general, in planted CW systems, it is well known that the dominant removal mechanisms are adsorption onto the sediment bed, uptake by plants, and biodegradation (Petrie et al. 2018; Khan et al. 2023). This suggests that plant-assisted systems offer a synergistic advantage by improving the overall efficiency of PhCs removal through physical-chemical and biological pathways. Likewise, Zhang et al., (2011) confirmed that the planted CWs significantly enhanced the removal of IBU and NAP, reaching 80% and 91%, respectively, compared to unplanted CWs, which reached 60% and 52%, respectively.

Conclusion and future directions

This study highlights the potential of vertical flow constructed wetlands (VF-CWs) amended with biochar (BC) as an effective, nature-based solution for treating domestic wastewater, particularly pharmaceutical compounds (PhCs). Biochar addition significantly improved the removal of some conventional pollutants, such as TSS (79%–81%), COD (60%–61%), UV-absorbance at 420 nm

(71%–72%), TN (53%), TKN (66%–74%), NH_4^+-N (81%–85%), and FS (3.2–3.3 Log unit), compared to the control system (67%, 58%, 50%, 38%, 52%, 71%, and 2.5%, respectively). However, the BC addition into CWs showed no significant improvement in removing phosphorus, TC, FC, and UV-absorbance at 254 nm. Furthermore, the increase in the BC concentration in the CWs substrate did not affect the treatment efficiencies of the conventional pollutants. In summary, the CW-0, CW-10, and CW-50 systems significantly reduced the concentrations of various pollutants, except sulfate, hardness, nitrite, and nitrate, which exhibited limited or poor removal efficiency.

In terms of pharmaceutical compounds (PhCs), the analysis reveals that many compounds predominantly occur in the aqueous phase due to their high solubility, while others associate strongly with particulate matter (PM). The treatment of PhCs based on the VF-CW systems achieved high removal efficiencies for several widely used drugs, particularly antibiotics and beta-blockers, reaching a complete elimination for CLA, FUR, ATE, BIS, ERY, 4-HYDIC, and KET, above than 70% for DIC, OVEN, 1H-IBU, and SMZ, above 50% for IBU, VEN, and CIP, and lower than 50% for NAP and 2H-IBU.

Yet, the integration of BC into CWs did not significantly enhance overall PhCs removal, likely due to variability in both BC properties and compound-specific behaviours. Persistent pollutants like CBZ and FLU remained poorly removed, underscoring the need for more targeted treatment approaches. These findings highlight both the potential and limitations of BC-amended VF-CWs and emphasize the need for tailored system designs to optimize pollutant removal, particularly for emerging contaminants such as PhCs.

In summary, while VF-CWs are effective for general wastewater treatment and the removal of many PhCs, their performance against certain resilient compounds remains limited. Future efforts should focus on optimizing system design, including substrate selection and biochar characteristics, and integrating plant-based and microbial processes to achieve broader and more consistent micropollutant removal.

References

Achak, M., Boumya, W., Elamraoui, S., Asdiou, N., Taoufik, N., Barka, N., Aboulkas, A., Lamy, E., 2023. Performance of olive mill wastewater treatment using hybrid system combining sand filtration and vertical flow constructed wetlands. J. Water Process Eng. 53, 103737. https://doi.org/10.1016/j.jwpe.2023.103737

AFNOR, 1997. AFNOR, Recueil de Norme Française: Eau, Méthodes D'essai,. 2nd ed., Paris Édition, Paris,.

Ajibade, F.O., Yin, W., Guadie, A., Ajibade, T.F., Liu, Y., Kumwimba, M.N., Liu, W., Han, J.-L., Wang, H.-C., Wang, A.-J., 2023. Impact of biochar amendment on antibiotic removal and ARGs accumulation in constructed wetlands for low C/N wastewater treatment. Chem. Eng. J. 459, 141541. https://doi.org/10.1016/j.cej.2023.141541

Alsubih, M., El Morabet, R., Khan, R.A., Khan, N.A., Khan, A.R., Khan, S., Mushtaque, N., Hussain, A., Yousefi,

M., 2022. Performance evaluation of constructed wetland for removal of pharmaceutical compounds from hospital wastewater: Seasonal perspective. Arab. J. Chem. 15, 104344. https://doi.org/10.1016/j.arabjc.2022.104344
Altmann, J., Massa, L., Sperlich, A., Gnirss, R., Jekel, M., 2016. UV254 absorbance as real-time monitoring and control parameter for micropollutant removal in advanced wastewater treatment with powdered activated carbon. Water Res. 94, 240–245. https://doi.org/10.1016/j.watres.2016.03.001
Aminot, Y., Litrico, X., Chambolle, M., Arnaud, C., Pardon, P., Budzindki, H., 2015. Development and application of a multi-residue method for the determination of 53 pharmaceuticals in water, sediment, and suspended solids using liquid chromatography-tandem mass spectrometry. Anal. Bioanal. Chem. 407, 8585–8604. https://doi.org/10.1007/s00216-015-9017-3
Ávila, C., García-Galán, M.J., Uggetti, E., Montemurro, N., García-Vara, M., Pérez, S., García, J., Postigo, C., 2021. Boosting pharmaceutical removal through aeration in constructed wetlands. J. Hazard. Mater. 412, 125231. https://doi.org/10.1016/j.jhazmat.2021.125231
Ayadi, M., Passaseo, D., Bonaccorso, G., Fichera, M., Renai, L., Venturini, L., Colzi, I., Fibbi, D., Del Bubba, M., 2024. Biochar from co-pyrolysis of biological sludge and sawdust in comparison with the conventional filling media of vertical-flow constructed wetlands for the treatment of domestic-textile wastewater. Water Sci. Technol. 89, 1252–1263. https://doi.org/10.2166/wst.2024.056
Azad, A.A., Chiddiq, A.B., Miah, R., 2024. Heliyon Temporal assessment of water and soil quality near Barapukuria coal mine , Bangladesh. Heliyon 10, e40722. https://doi.org/10.1016/j.heliyon.2024.e40722
Basílico, G., Casares, M.V., de Cabo, L., 2024. Performance of vertical flow wetland in the treatment of medium organic strength synthetic wastewater. Discov. Water 4, 77. https://doi.org/10.1007/s43832-024-00142-5
Belete, B., Desye, B., Ambelu, A., Yenew, C., 2023. Micropollutant Removal Efficiency of Advanced Wastewater Treatment Plants: A Systematic Review. Environ. Health Insights 17. https://doi.org/10.1177/11786302231195158
Camargo, J.A., Alonso, A., Salamanca, A., 2005. Nitrate toxicity to aquatic animals: a review with new data for freshwater invertebrates. Chemosphere 58, 1255–1267. https://doi.org/10.1016/j.chemosphere.2004.10.044
Chand, N., Suthar, S., Kumar, K., Singh, V., 2022. Removal of pharmaceuticals by vertical flow constructed wetland with different configurations: Effect of inlet load and biochar addition in the substrate. Chemosphere 307, 135975. https://doi.org/10.1016/j.chemosphere.2022.135975
Chand, N., Suthar, S., Kumar, K., Tyagi, V.K., 2021. Enhanced removal of nutrients and coliforms from domestic wastewater in cattle dung biochar-packed Colocasia esculenta-based vertical subsurface flow constructed wetland. J. Water Process Eng. 41, 101994. https://doi.org/10.1016/j.jwpe.2021.101994
Chen, X., Hu, Z., Zhang, Y., Zhuang, L., Zhang, J., Li, J., Hu, H., 2018. Removal Processes of Carbamazepine in Constructed Wetlands Treating Secondary Effluent: A Review. Water 10, 1351. https://doi.org/10.3390/w10101351
Chen, Z., Xiao, X., Chen, B., Zhu, L., 2015. Quantification of Chemical States, Dissociation Constants and Contents of Oxygen-containing Groups on the Surface of Biochars Produced at Different Temperatures. Environ. Sci. Technol. 49, 309–317. https://doi.org/10.1021/es5043468
Ciardelli, G., Ranieri, N., 2001. The treatment and reuse of wastewater in the textile industry by means of ozonation and electroflocculation. Water Res. 35, 567–572. https://doi.org/10.1016/S0043-1354(00)00286-4
Czech, B., Kończak, M., Rakowska, M., Oleszczuk, P., 2021. Engineered biochars from organic wastes for the adsorption of diclofenac, naproxen and triclosan from water systems. J. Clean. Prod. 288, 125686. https://doi.org/10.1016/j.jclepro.2020.125686
Dalahmeh, S., Ahrens, L., Gros, M., Wiberg, K., Pell, M., 2018. Potential of biochar filters for onsite sewage treatment: Adsorption and biological degradation of pharmaceuticals in laboratory filters with active, inactive and no biofilm. Sci. Total Environ. 612, 192–201. https://doi.org/10.1016/j.scitotenv.2017.08.178
de Rozari, P., Greenway, M., El Hanandeh, A., 2016. Phosphorus removal from secondary sewage and septage using sand media amended with biochar in constructed wetland mesocosms. Sci. Total Environ. 569–570, 123–133. https://doi.org/10.1016/j.scitotenv.2016.06.096
de Rozari, P., Greenway, M., El Hanandeh, A., 2015. An investigation into the effectiveness of sand media amended with biochar to remove BOD5, suspended solids and coliforms using wetland mesocosms. Water Sci. Technol. 71, 1536–1544. https://doi.org/10.2166/wst.2015.120
De Sanctis, M., El Barkaoui, S., Mondal, S., Murgolo, S., Pellegrino, M., Slavik, E., Mascolo, G., Di Iaconi, C., 2025. An advanced biological system for per-and poly-fluoroalkyl substances (PFASs) removal from landfill leachate. J. Water Process Eng. 78, 108740. https://doi.org/10.1016/j.jwpe.2025.108740
Delgado, N., Bermeo, L., Hoyos, D.A., Peñuela, G.A., Capparelli, A., Marino, D., Navarro, A., Casas-Zapata, J.C., 2020. Occurrence and removal of pharmaceutical and personal care products using subsurface horizontal flow constructed wetlands. Water Res. 187, 116448. https://doi.org/10.1016/j.watres.2020.116448
Deng, C., Huang, L., Liang, Y., Xiang, H., Jiang, J., Wang, Q., Hou, J., Chen, Y., 2019. Response of microbes to

biochar strengthen nitrogen removal in subsurface flow constructed wetlands: Microbial community structure and metabolite characteristics. Sci. Total Environ. 694, 133687. https://doi.org/10.1016/j.scitotenv.2019.133687
El Barkaoui, S., De Sanctis, M., Mondal, S., Murgolo, S., Pellegrino, M., Franz, S., Slavik, E., Mascolo, G., Di Iaconi, C., 2025a. A Comparative Study of Biological and Ozonation Approaches for Conventional and Per- and Polyfluoroalkyl Substances Contaminant Removal from Landfill Leachate. Water 17, 2501. https://doi.org/10.3390/w17172501
El Barkaoui, S., Mandi, L., Aziz, F., Del Bubba, M., Ouazzani, N., 2023. A critical review on using biochar as constructed wetland substrate: Characteristics, feedstock, design and pollutants removal mechanisms. Ecol. Eng. 190, 106927. https://doi.org/10.1016/j.ecoleng.2023.106927
El Barkaoui, S., Mandi, L., Fichera, M., Ryah, H., Baçaoui, A., Del Bubba, M., Ouazzani, N., 2025b. Optimizing biochar-based column filtration systems for enhanced pollutant removal in wastewater treatment: A preliminary study. Chemosphere 372, 144067. https://doi.org/10.1016/j.chemosphere.2025.144067
El Barkaoui, S., Ouazzani, N., Mandi, L., Zafeiropoulos, J., Isari, E.A., Del Bubba, M., Kalavrouziotis, I.K., 2025c. Physicochemical and thermal characterization of argan residues for biofuel and biochar production: potential future prospects. Biomass Convers. Biorefinery 15, 17309–17319. https://doi.org/10.1007/s13399-024-06442-z
El Barkaoui, S., Mandi, L., Ryah, H., El Ghadraoui, A., Del Bubba, M., Ouazzani, N., 2025d. Biochar-based filtration systems for wastewater treatment: performance, efficiency, and optimization. Int. J. Environ. Sci. Technol. https://doi.org/10.1007/s13762-025-06694-w
El Ghadraoui, A., Ouazzani, N., Ahmali, A., El Mansour, T.E.H., Aziz, F., Hejjaj, A., Del Bubba, M., Mandi, L., 2020. Treatment of olive mill and municipal wastewater mixture by pilot scale vertical flow constructed wetland. Desalin. Water Treat. 198, 126–139. https://doi.org/10.5004/dwt.2020.26009
Fan, J., Wang, W., Zhang, B., Guo, Y., Ngo, H.H., Guo, W., Zhang, J., Wu, H., 2013. Nitrogen removal in intermittently aerated vertical flow constructed wetlands: Impact of influent COD/N ratios. Bioresour. Technol. 143, 461–466. https://doi.org/10.1016/j.biortech.2013.06.038
Fernandes, J.P., Almeida, C.M.R., Salgado, M.A., Carvalho, M.F., Mucha, A.P., 2021. Pharmaceutical Compounds in Aquatic Environments—Occurrence, Fate and Bioremediation Prospective. Toxics 9, 257. https://doi.org/10.3390/toxics9100257
Gadipelly, C., Pérez-González, A., Yadav, G.D., Ortiz, I., Ibáñez, R., Rathod, V.K., Marathe, K. V., 2014. Pharmaceutical Industry Wastewater: Review of the Technologies for Water Treatment and Reuse. Ind. Eng. Chem. Res. 53, 11571–11592. https://doi.org/10.1021/ie501210j
Ghumra, D.P., Agarkoti, C., Gogate, P.R., 2021. Improvements in effluent treatment technologies in Common Effluent Treatment Plants (CETPs): Review and recent advances. Process Saf. Environ. Prot. https://doi.org/10.1016/j.psep.2021.01.021
Ilyas, H., Hosney, H., 2024. Biochar - Integrated Constructed Wetlands for Organic Micropollutants Removal Biochar - Integrated Constructed Wetlands for Organic Micropollutants Removal.
Ilyas, H., van Hullebusch, E.D., 2020. Performance Comparison of Different Constructed Wetlands Designs for the Removal of Personal Care Products. Int. J. Environ. Res. Public Health 17, 3091. https://doi.org/10.3390/ijerph17093091
Johnston, S.G., Burton, E.D., Aaso, T., Tuckerman, G., 2014. Sulfur, iron and carbon cycling following hydrological restoration of acidic freshwater wetlands. Chem. Geol. 371, 9–26. https://doi.org/10.1016/j.chemgeo.2014.02.001
Kaetzl, K., Lübken, M., Uzun, G., Gehring, T., Nettmann, E., Stenchly, K., Wichern, M., 2019. On-farm wastewater treatment using biochar from local agroresidues reduces pathogens from irrigation water for safer food production in developing countries. Sci. Total Environ. 682, 601–610. https://doi.org/10.1016/j.scitotenv.2019.05.142
Kasak, K., Truu, J., Ostonen, I., Sarjas, J., Oopkaup, K., Paiste, P., Kõiv-Vainik, M., Mander, Ü., Truu, M., 2018. Biochar enhances plant growth and nutrient removal in horizontal subsurface flow constructed wetlands. Sci. Total Environ. 639, 67–74. https://doi.org/10.1016/j.scitotenv.2018.05.146
Kataki, S., Chatterjee, S., Vairale, M.G., Dwivedi, S.K., Gupta, D.K., 2021. Constructed wetland, an eco-technology for wastewater treatment: A review on types of wastewater treated and components of the technology (macrophyte, biolfilm and substrate). J. Environ. Manage. 283, 111986. https://doi.org/10.1016/j.jenvman.2021.111986
Keerthanan, S., Jayasinghe, C., Bolan, N., Rinklebe, J., Vithanage, M., 2022. Retention of sulfamethoxazole by cinnamon wood biochar and its efficacy of reducing bioavailability and plant uptake in soil. Chemosphere 297, 134073. https://doi.org/10.1016/j.chemosphere.2022.134073
Khan, R.A., Khan, N.A., El Morabet, R., Alsubih, M., Khan, A.R., Khan, S., Mubashir, M., Balakrishnan, D., Khoo, K.S., 2023. Comparison of constructed wetland performance coupled with aeration and tubesettler for pharmaceutical compound removal from hospital wastewater. Environ. Res. 216, 114437.

https://doi.org/10.1016/j.envres.2022.114437
Kizito, S., Lv, T., Wu, S., Ajmal, Z., Luo, H., Dong, R., 2017. Treatment of anaerobic digested effluent in biochar-packed vertical flow constructed wetland columns: Role of media and tidal operation. Sci. Total Environ. 592, 197–205. https://doi.org/10.1016/j.scitotenv.2017.03.125
Kushwaha, A., Goswami, L., Kim, B.S., Lee, S.S., Pandey, S.K., Kim, K.-H., 2024. Constructed wetlands for the removal of organic micropollutants from wastewater: Current status, progress, and challenges. Chemosphere 360, 142364. https://doi.org/10.1016/j.chemosphere.2024.142364
Lewis, W.M., Morris, D.P., 1986. Toxicity of Nitrite to Fish: A Review. Trans. Am. Fish. Soc. 115, 183–195. https://doi.org/10.1577/1548-8659(1986)115<183:TONTF>2.0.CO;2
Li, J., Fan, J., Zhang, J., Hu, Z., Liang, S., 2018. Preparation and evaluation of wetland plant-based biochar for nitrogen removal enhancement in surface flow constructed wetlands. Environ. Sci. Pollut. Res. 25, 13929–13937. https://doi.org/10.1007/s11356-018-1597-y
Li, L., Feng, J., Zhang, L., Yin, H., Fan, C., Wang, Z., Zhao, M., Ge, C., Song, H., 2021. Enhanced nitrogen and phosphorus removal by natural pyrite–based constructed wetland with intermittent aeration. Environ. Sci. Pollut. Res. 28, 69012–69028. https://doi.org/10.1007/s11356-021-15461-6
Li, N., Liu, Y., Du, C., Wang, Y., Wang, L., Li, X., 2023. A novel role of various hydrogen bonds in adsorption, desorption and co-adsorption of PPCPs on corn straw-derived biochars. Sci. Total Environ. 861, 160623. https://doi.org/10.1016/j.scitotenv.2022.160623
Liang, G., Hu, Z., Wang, Z., Yang, X., Xie, X., Zhao, J., 2020. Effective removal of carbamazepine and diclofenac by CuO/Cu2O/Cu-biochar composite with different adsorption mechanisms. Environ. Sci. Pollut. Res. 27, 45435–45446. https://doi.org/10.1007/s11356-020-10284-3
Licata, M., Rossini, F., Virga, G., Ruggeri, R., Farruggia, D., Iacuzzi, N., 2021. Performance of a Pilot-Scale Constructed Wetland and Medium-Term Effects of Treated Wastewater Irrigation of Arundo donax L. on Soil and Plant Parameters. Water 13, 1994. https://doi.org/10.3390/w13151994
Lin, L., Jiang, W., Xu, P., 2017. Science of the Total Environment Comparative study on pharmaceuticals adsorption in reclaimed water desalination concentrate using biochar : Impact of salts and organic matter. Sci. Total Environ. 601–602, 857–864. https://doi.org/10.1016/j.scitotenv.2017.05.203
Logan, A.J., Stevik, T.K., Siegrist, R.L., Rønn, R.M., 2001. Transport and fate of Cryptosporidium parvum oocysts in intermittent sand filters. Water Res. 35, 4359–4369. https://doi.org/10.1016/S0043-1354(01)00181-6
Lu, J., Guo, Z., Pan, Y., Li, M., Chen, X., He, M., Wu, H., Zhang, J., 2022. Simultaneously enhanced removal of PAHs and nitrogen driven by Fe2+/Fe3+ cycle in constructed wetland through automatic tidal operation. Water Res. 215, 118232. https://doi.org/10.1016/j.watres.2022.118232
Ma, R., Ma, J., Chen, Y., Zhuo, Y., Cheng, L., Jiang, L., Mao, Y., Shen, Q., Liu, C., Ji, F., 2023. Efficient removal of nitrogen from tidal flow constructed wetlands based on the in-situ zeolite regeneration: Measures and mechanisms. Chem. Eng. J. 458, 141298. https://doi.org/10.1016/j.cej.2023.141298
Maina, C.W., Mutua, B.M., Oduor, S.O., 2011. Evaluating performance of vertical flow constructed wetland under various hydraulic loading rates in effluent polishing. J. Water, Sanit. Hyg. Dev. 1, 144–151. https://doi.org/10.2166/washdev.2011.025
Maleki Shahraki, Z., Mao, X., 2022. Biochar application in biofiltration systems to remove nutrients, pathogens, and pharmaceutical and personal care products from wastewater. J. Environ. Qual. 51, 129–151. https://doi.org/10.1002/jeq2.20331
Massano, M., 2025. Analytical methods for monitoring pharmaceutical and illicit drugs in wastewater and biological matrices.
Mghaiouini, R., Labrim, H., Saad, A., El Bouayadi, R., Salah, M., 2024. Moroccan sand characteristics and their effect on mortar quality. Results Chem. 7, 101520. https://doi.org/10.1016/j.rechem.2024.101520
Nakarmi, K.J., Daneshvar, E., Eshaq, G., Puro, L., Maiti, A., Nidheesh, P.V., Wang, H., Bhatnagar, A., 2022. Synthesis of biochar from iron-free and iron-containing microalgal biomass for the removal of pharmaceuticals from water. Environ. Res. 214, 114041. https://doi.org/10.1016/j.envres.2022.114041
Nguyen, X.C., Nguyen, D.D., Tran, Q.B., Nguyen, T.T.H., Tran, T.K.A., Tran, T.C.P., Nguyen, T.H.G., Tran, T.N.T., La, D.D., Chang, S.W., Balasubramani, R., Chung, W.J., Yoon, Y.S., Nguyen, V.K., 2020a. Two-step system consisting of novel vertical flow and free water surface constructed wetland for effective sewage treatment and reuse. Bioresour. Technol. 306, 123095. https://doi.org/10.1016/j.biortech.2020.123095
Nguyen, X.C., Tran, T.C.C.P.P., Hoang, V.H., Nguyen, T.P., Chang, S.W., Nguyen, D.D., Guo, W., Kumar, A., La, D.D., Bach, Q.V., 2020b. Combined biochar vertical flow and free-water surface constructed wetland system for dormitory sewage treatment and reuse. Sci. Total Environ. 713, 136404. https://doi.org/10.1016/j.scitotenv.2019.136404
Nweze, J.E., Nweze, J.A., Akor, J., Gupta, S., Nwuche, C.O., 2024. Bioremediation of pharmaceutical waste waters, in: Development in Wastewater Treatment Research and Processes. Elsevier, pp. 289–336. https://doi.org/10.1016/B978-0-323-99278-7.00015-8

Ofiera, L.M., Wintgens, T., Kazner, C., 2025. Comparative analysis of conventional and modified constructed wetlands for the removal of trace organic compounds from municipal wastewater effluent. Sci. Total Environ. 987, 179796. https://doi.org/10.1016/j.scitotenv.2025.179796

Oulton, R.L., Kohn, T., Cwiertny, D.M., 2010. Pharmaceuticals and personal care products in effluent matrices: A survey of transformation and removal during wastewater treatment and implications for wastewater management. J. Environ. Monit. 12, 1956. https://doi.org/10.1039/c0em00068j

Petrie, B., Rood, S., Smith, B.D., Proctor, K., Youdan, J., Barden, R., Kasprzyk-Hordern, B., 2018. Biotic phase micropollutant distribution in horizontal sub-surface flow constructed wetlands. Sci. Total Environ. 630, 648–657. https://doi.org/10.1016/j.scitotenv.2018.02.242

Phan, H. V, Wickham, R., Xie, S., McDonald, J.A., Khan, S.J., Ngo, H.H., Guo, W., Nghiem, L.D., 2018. The fate of trace organic contaminants during anaerobic digestion of primary sludge: A pilot scale study. Bioresour. Technol. 256, 384–390. https://doi.org/10.1016/j.biortech.2018.02.040

Prabhu, S.D., Lekshmi, B., Asolekar, S.R., 2022. Potential for Constructed Wetlands Aimed at Sustainable Wastewater Treatment, Reuse, and Disposal in Dyestuff and Textile Sectors, in: Sustainable Textiles: Production, Processing, Manufacturing & Chemistry. pp. 187–233. https://doi.org/10.1007/978-981-19-0526-1_9

Ramachandra, T. V, Sincy, V., Asulabha, K.S., Mahapatra, D.M., Bhat, S.P., Aithal, B.H., 2018. Optimal Treatment of Domestic Wastewater through Constructed Wetlands. J Biodivers. 9, 81–102. https://doi.org/11.258359/KRE-180

Ravichandran, M.K., Philip, L., 2022. Assessment of the contribution of various constructed wetland components for the removal of pharmaceutically active compounds. J. Environ. Chem. Eng. 10, 107835. https://doi.org/10.1016/j.jece.2022.107835

Renai, L., Scordo, C.V.A., Ghadraoui, A. El, Santana-Viera, S., Rodriguez, J.J.S., Orlandini, S., Furlanetto, S., Fibbi, D., Lambropoulou, D., Bubba, M. Del, 2021. Quality by design optimization of a liquid chromatographic-tandem mass spectrometric method for the simultaneous analysis of structurally heterogeneous pharmaceutical compounds and its application to the rapid screening in wastewater and surface water sam. J. Chromatogr. A 1649, 462225. https://doi.org/10.1016/j.chroma.2021.462225

Renai, L., Tozzi, F., Checchini, L., Del Bubba, M., 2020. Impact of the use of treated wastewater for agricultural need: Behavior of organic micropollutants in soil, transfer to crops, and related risks, in: Advances in Chemical Pollution, Environmental Management and Protection. Elsevier Inc., pp. 103–135. https://doi.org/10.1016/bs.apmp.2020.07.008

Rodier, J., 2009. L'analyse de l'eau _ Rodier 9e édition.pdf.

Rossini, D., Ciofi, L., Ancillotti, C., Checchini, L., Bruzzoniti, M.C., Rivoira, L., Fibbi, D., Orlandini, S., Del Bubba, M., 2016. Innovative combination of QuEChERS extraction with on-line solid-phase extract purification and pre-concentration, followed by liquid chromatography-tandem mass spectrometry for the determination of non-steroidal anti-inflammatory drugs and their metaboli. Anal. Chim. Acta 935, 269–281. https://doi.org/10.1016/j.aca.2016.06.023

Rühmland, S., Wick, A., Ternes, T.A., Barjenbruch, M., 2015. Fate of pharmaceuticals in a subsurface flow constructed wetland and two ponds. Ecol. Eng. 80, 125–139. https://doi.org/10.1016/j.ecoleng.2015.01.036

S.E.E.E, 2007. Moroccan water quality grid for irrigation purposes, State Secretariat at the Ministry of Energy, Mines, Water and Environment, Charge of Water and Environment, Kingdom of Morocco, Water Quality Standards for Irrigation, 2007.

Salah, M., Zheng, Y., Wang, Q., Li, C., Li, Y., Li, F., 2023. Insight into pharmaceutical and personal care products removal using constructed wetlands: A comprehensive review. Sci. Total Environ. 885, 163721. https://doi.org/10.1016/j.scitotenv.2023.163721

Santos, A.F., Alvarenga, P., Gando-Ferreira, L.M., Quina, M.J., 2023. Urban Wastewater as a Source of Reclaimed Water for Irrigation: Barriers and Future Possibilities. Environments 10, 17. https://doi.org/10.3390/environments10020017

Silva, B.F. da, Jelic, A., López-Serna, R., Mozeto, A.A., Petrovic, M., Barceló, D., 2011. Occurrence and distribution of pharmaceuticals in surface water, suspended solids and sediments of the Ebro river basin, Spain. Chemosphere 85, 1331–1339. https://doi.org/10.1016/j.chemosphere.2011.07.051

Sleytr, K., Tietz, A., Langergraber, G., Haberl, R., 2007. Investigation of bacterial removal during the filtration process in constructed wetlands. Sci. Total Environ. 380, 173–180. https://doi.org/10.1016/j.scitotenv.2007.03.001

Tan, C., Ma, F., Li, A., Qiu, S., Li, J., 2013. Evaluating the Effect of Dissolved Oxygen on Simultaneous Nitrification and Denitrification in Polyurethane Foam Contact Oxidation Reactors. Water Environ. Res. 85, 195–202. https://doi.org/10.2175/106143012X13503213812445

Torrens, A., Molle, P., Boutin, C., Salgot, M., 2009. Removal of bacterial and viral indicator in vertical flow constructed wetlands and intermittent sand filters. Desalination 246, 169–178.

https://doi.org/10.1016/j.desal.2008.03.050
Uday Bhan Prajapati, Arun Lal Srivastav, Shiraz A.Wajih, 2018. Eco-management of Wastewater by ZESTP. J. Chem. Environ. Sci. its Appl. 4, 51–57. https://doi.org/10.15415/jce.2018.42007
Valipour, A., Ahn, Y.-H., 2016. Constructed wetlands as sustainable ecotechnologies in decentralization practices: a review. Environ. Sci. Pollut. Res. 23, 180–197. https://doi.org/10.1007/s11356-015-5713-y
Varatharajan, G.R., Ndayishimiye, J.C., Nyirabuhoro, P., 2025. Emerging Contaminants: A Rising Threat to Urban Water and a Barrier to Achieving SDG-Aligned Planetary Protection. Water 17, 2367. https://doi.org/10.3390/w17162367
Vassalle, L., García-Galán, M.J., Aquino, S.F., Afonso, R.J. de C.F., Ferrer, I., Passos, F., R Mota, C., 2020. Can high rate algal ponds be used as post-treatment of UASB reactors to remove micropollutants? Chemosphere 248, 125969. https://doi.org/10.1016/j.chemosphere.2020.125969
Venditti, S., Brunhoferova, H., Hansen, J., 2022. Behaviour of 27 selected emerging contaminants in vertical flow constructed wetlands as post-treatment for municipal wastewater. Sci. Total Environ. 819, 153234. https://doi.org/10.1016/j.scitotenv.2022.153234
Visiy, E.B., Djousse, B.M.K., Martin, L., Zangue, C.N., Sangodoyin, A., Gbadegesin, A.S., Fonkou, T., 2022. Effectiveness of biochar filters vegetated with Echinochloa pyramidalis in domestic wastewater treatment. Water Sci. Technol. 85, 2613–2624. https://doi.org/10.2166/wst.2022.147
Vymazal, J., 2007. Removal of nutrients in various types of constructed wetlands. Sci. Total Environ. 380, 48–65. https://doi.org/10.1016/j.scitotenv.2006.09.014
Vymazal, J., Dvořáková Březinová, T., Koželuh, M., Kule, L., 2017. Occurrence and removal of pharmaceuticals in four full-scale constructed wetlands in the Czech Republic – the first year of monitoring. Ecol. Eng. 98, 354–364. https://doi.org/10.1016/j.ecoleng.2016.08.010
Vymazal, J., Zhao, Y., Mander, Ü., 2021. Recent research challenges in constructed wetlands for wastewater treatment: A review. Ecol. Eng. 169, 106318. https://doi.org/10.1016/j.ecoleng.2021.106318
Wang, W., Du, Z., Deng, S., Vakili, M., Ren, L., Meng, P., Maimaiti, A., Wang, B., Huang, J., Wang, Y., Yu, G., 2018. Regeneration of PFOS loaded activated carbon by hot water and subsequent aeration enrichment of PFOS from eluent. Carbon N. Y. 134, 199–206. https://doi.org/10.1016/j.carbon.2018.04.005
Werner, S., Kätzl, K., Wichern, M., Buerkert, A., Steiner, C., Marschner, B., 2018. Agronomic benefits of biochar as a soil amendment after its use as waste water filtration medium. Environ. Pollut. 233, 561–568. https://doi.org/10.1016/j.envpol.2017.10.048
Wu, B., Xu, D., Wang, H., Xu, R., Qin, N., Han, J., 2022. Wetland plant-derived biochar enhances the diclofenac treatment performance in vertical subsurface flow constructed wetlands. Environ. Res. 215, 114326. https://doi.org/10.1016/j.envres.2022.114326
Wu, H., Zhang, J., Ngo, H.H., Guo, W., Hu, Z., Liang, S., Fan, J., Liu, H., 2015. A review on the sustainability of constructed wetlands for wastewater treatment: Design and operation. Bioresour. Technol. 175, 594–601. https://doi.org/10.1016/j.biortech.2014.10.068
Xue, Y., Guo, Y., Zhang, X., Kamali, M., M. Aminabhavi, T., Appels, L., Dewil, R., 2022. Efficient adsorptive removal of ciprofloxacin and carbamazepine using modified pinewood biochar – A kinetic, mechanistic study. Chem. Eng. J. 450, 137896. https://doi.org/10.1016/j.cej.2022.137896
Yao, Y., Gao, B., Zhang, M., Inyang, M., Zimmerman, A.R., 2012. Effect of biochar amendment on sorption and leaching of nitrate, ammonium, and phosphate in a sandy soil. Chemosphere 89, 1467–1471. https://doi.org/10.1016/j.chemosphere.2012.06.002
Ye, J., Wang, L., Li, D., Han, W., Ye, C., 2012. Vertical oxygen distribution trend and oxygen source analysis for vertical-flow constructed wetlands treating domestic wastewater. Ecol. Eng. 41, 8–12. https://doi.org/10.1016/j.ecoleng.2011.12.015
Yuan, Y., Yang, B., Wang, H., Lai, X., Li, F., Salam, M.M.A., Pan, F., Zhao, Y., 2020a. The simultaneous antibiotics and nitrogen removal in vertical flow constructed wetlands: Effects of substrates and responses of microbial functions. Bioresour. Technol. 310, 123419. https://doi.org/10.1016/j.biortech.2020.123419
Yuan, Y., Yang, B., Wang, H., Lai, X., Li, F., Salam, M.M.A., Pan, F., Zhao, Y., 2020b. The simultaneous antibiotics and nitrogen removal in vertical flow constructed wetlands: Effects of substrates and responses of microbial functions. Bioresour. Technol. 310, 123419. https://doi.org/10.1016/j.biortech.2020.123419
Zhang, D.Q., Gersberg, R.M., Hua, T., Zhu, J., Tuan, N.A., Tan, S.K., 2012. Pharmaceutical removal in tropical subsurface flow constructed wetlands at varying hydraulic loading rates. Chemosphere 87, 273–277. https://doi.org/10.1016/j.chemosphere.2011.12.067
Zhang, D.Q., Tan, S.K., Gersberg, R.M., Sadreddini, S., Zhu, J., Tuan, N.A., 2011. Removal of pharmaceutical compounds in tropical constructed wetlands. Ecol. Eng. 37, 460–464. https://doi.org/10.1016/j.ecoleng.2010.11.002
Zhang, M., Shen, J., Zhong, Y., Ding, T., Dissanayake, P.D., Yang, Y., Tsang, Y.F., Ok, Y.S., 2022. Sorption of pharmaceuticals and personal care products (PPCPs) from water and wastewater by carbonaceous materials: A review. Crit. Rev. Environ. Sci. Technol. 52, 727–766.

https://doi.org/10.1080/10643389.2020.1835436
Zhang, Y., Li, Mengqi, Dong, L., Han, C., Li, Ming, Wu, H., 2021. Effects of biochar dosage on treatment performance, enzyme activity and microbial community in aerated constructed wetlands for treating low C/N domestic sewage. Environ. Technol. Innov. 24, 101919. https://doi.org/10.1016/j.eti.2021.101919
Zhou, X., Jia, L., Liang, C., Feng, L., Wang, R., Wu, H., 2018a. Simultaneous enhancement of nitrogen removal and nitrous oxide reduction by a saturated biochar-based intermittent aeration vertical flow constructed wetland: Effects of influent strength. Chem. Eng. J. 334, 1842–1850. https://doi.org/10.1016/j.cej.2017.11.066
Zhou, X., Liang, C., Jia, L., Feng, L., Wang, R., Wu, H., 2018b. An innovative biochar-amended substrate vertical flow constructed wetland for low C/N wastewater treatment: Impact of influent strengths. Bioresour. Technol. 247, 844–850. https://doi.org/10.1016/j.biortech.2017.09.044
Zhou, X., Wang, R., Liu, H., Wu, S., Wu, H., 2019. Nitrogen removal responses to biochar addition in intermittent-aerated subsurface flow constructed wetland microcosms: Enhancing role and mechanism. Ecol. Eng. 128, 57–65. https://doi.org/10.1016/j.ecoleng.2018.12.028

IV-II. Behaviour of pharmaceutical compounds in the quaternary treatment of urban wastewater by vertical-flow constructed wetlands filled with biochar from co-pyrolysis of sewage sludge and sawdust.

This work is in the preparation state to be submitted as a research paper:

Abstract

Constructed wetlands (CWs) are an effective, low-cost, and environmentally friendly technology for treating wastewater. However, they have a limited capacity to remove poorly biodegradable organic micropollutants, particularly pharmaceuticals (PhCs), which remains a major challenge. This study investigated the use of sewage sludge-derived biochar (SSBC) as a filling medium in vertical subsurface flow constructed wetlands (VSSF-CWs) to enhance their performance. The VSSF-CWs were operated in both planted and unplanted configurations. The systems were tested under real outdoor conditions for 221 days using real urban wastewater as the inflow, and their efficiency was compared with that of conventional gravel-based wetlands. A total of 35 pharmaceutical compounds representing various therapeutic classes, including priority substances listed in recent European Monitoring Watch Lists and the 2024/3019 Urban Wastewater Directive, were monitored. The results showed that integrating SSBC markedly improved the removal efficiency of PhCs, achieving average removal rates of around 70%. This improvement was sustained over eight months and was effective immediately after start-up. This enhanced performance is attributed to the combined effects of adsorption and biofilm-supported biodegradation, which are facilitated by the high porosity and microbial affinity of the biochar. Overall, this study provides comprehensive evidence for the first time of the potential of SSBC to significantly improve CW performance in advanced wastewater treatment. This addresses emerging regulatory requirements and contributes to the circular and sustainable management of sewage sludge resources.

Keywords: Emerging contaminants; Sewage sludge valorization; Particulate matter; Constructed wetlands; Pharmaceutical compounds occurrence.

1. Introduction

Constructed wetlands (CWs) are well-established nature-based solutions for wastewater depuration, particularly appropriate for the secondary treatment of domestic sewage from small communities (Valipour and Ahn, 2016), but also for refining urban wastewaters from larger treatment facilities (Verlicchi and Zambello, 2014). CWs have traditionally been considered as a simple, low-impact, and low-cost technology for wastewater treatment that takes advantage of the removal mechanisms active in natural ecosystems, such as adsorption, precipitation, biodegradation of organic carbon, nitrification, and denitrification (Kataki et al., 2021). CWs can be implemented as a series of flooded planted channels or basins (free-water surface flow) or as systems in which water flows through a substrate a few cm below the filling medium (subsurface flow, SSF-CWs). Furthermore, for SSF-CWs, the wetland can be fed by horizontal flow (HSSF-CW), being constantly saturated with the wastewater, or the wastewater can be introduced with vertical flow and subjected to alternating filling and drying cycles (VSSF-CWs). While CWs have proven to be very effective in removing conventional water quality parameters such as suspended solids, organic and inorganic nitrogen, and biodegradable organic matter (Vymazal et al., 2021),

their removal efficiency for organic micropollutants is limited, unless it is adopted a hydraulic retention time much higher than those commonly used in wastewater treatment plants (Gorito et al., 2017). It should also be noted that the biological mechanisms responsible for the removal of poorly biodegradable organic matter in CWs are active only after adequate biomass acclimatization, making these systems inefficient in the first weeks following their start-up (Coppini et al., 2019; Su-qing et al., 2012). These problems clearly represent a limitation in the use of CWs, especially considering the widespread presence of organic micropollutants in all types of wastewater, including domestic ones, and the importance of their removal, also certified by the recent 2024/3019 Urban Wastewater Directive (European Parliament and the Council, 2024).

Among the many classes of organic micropollutants that have been widely identified in all aquatic compartments, pharmaceutical compounds (PhCs) are undoubtedly of great environmental concern because of their widespread use, the incomplete removal often observed in conventional wastewater treatment plants (Renai et al., 2021), and their high biological activity, which can pose a risk to the environment and humans. Indeed, PhCs present in fresh water can contaminate the drinking water production chain or the agricultural products through irrigation, causing various types of toxic effects, including neurotoxicity, reproductive and developmental toxicity, metabolic disorders, and antimicrobial resistance phenomena (Cizmas et al., 2015).

The removal of PhCs in CWs is a fairly well-studied topic in the literature, mainly in HSSF, VFSS, and hybrid systems (HS) filled with conventional substrates (i.e., sand and gravel) (Ilyas and Van Hullebusch, 2020). An overview of the literature revealed that the study of PhCs removal in CWs has involved numerous molecules, belonging to various therapeutic classes and characterized by a wide range of physicochemical properties (e.g., log D and acid-base properties) (Salah et al., 2023). These studies highlighted compound-dependent removals, which, however, appear to be generally quite low, being below 60% for most analytes or even much lower in some specific cases, such as for carbamazepine and clarithromycin (Ilyas and Van Hullebusch, 2020). The insufficient removal of PhCs has been attributed to their poor degradability in CWs, due to their chronic oxygen deficiency and consequently limited biodegradation capacity (Liu et al., 2016). In this context, high hydraulic retention times (HRTs), as high as several days, were adopted, attempting to increase the removal performance of HSSF systems (Auvinen et al., 2017). Furthermore, VSSF systems with intermittent feeding provided better removal efficiencies compared to HSSF, ascribable to the higher oxygenation of the bed (Ilyas and Van Hullebusch,

2020).

In such systems, it is claimed that the plant and in particular the filling material play an important role in the removal of chemical and biological pollutants (Borsetto et al., 2025; El Barkaoui et al., 2023). Recently, innovative materials, such as lightweight expanded clay aggregates (LECA) (Delgado et al., 2020), zeolites (Ravichandran and Philip, 2022; Venditti et al., 2022), steel slag (Petrie et al., 2018), pozzolan (El Ghadraoui et al., 2020), and biochar (BC) (Ajibade et al., 2023; Ayadi et al., 2024; Venditti et al., 2022) were proposed as unconventional, highly porous filling materials of CWs, arguing for these materials a dual role in PhC removal, either providing the direct adsorption of micropollutants or enhancing their biodegradation by supporting bacterial growth. These advanced applications have confirmed their effectiveness in removing various types of micropollutants, achieving significantly higher removal rates, particularly for poorly degradable compounds such as carbamazepine, compared to conventional CWs filled with gravel and/or sand.

Among the above-mentioned materials, BC is receiving increasing attention from the scientific community as it can be obtained through well-established thermal conversion processes of waste biomass (i.e., pyrolysis or gasification) and subsequent chemical and/or thermal activation of the resulting carbon material. In this way, it is possible to obtain BC with good adsorptive capacity and, at the same time, high environmental compatibility, the latter being related to (i) the low release of organic and inorganic micropollutants and (ii) the long-term carbon sequestration, which offers a crucial benefit for climate change mitigation (Bakari et al., 2024). Furthermore, published literature agrees that BC acts as an optimal adhesion support for the growth of microorganisms, thereby helping to improve the efficiency of biological removal processes such as nitrification, denitrification, and even the degradation of organic micropollutants, including pharmaceutical compounds (Pandey et al., 2025; Zhuang et al., 2022). It should also be noted that BC, once its adsorptive capacity is saturated, can be easily regenerated through thermal treatments (Dai et al., 2019), similarly to what happens for activated carbon used in drinking water purification plants.

The use of BC for wastewater treatment is even more advantageous when this material is obtained from the thermal conversion of sewage sludge (SS), as a high level of circularity is provided to the wastewater treatment sector in accordance with the European Directive 2024/3019 (European Parliament and the Council, 2024). Moreover, this process allows to inhibit the intrinsic chemical and biological risks related to the management and disposal of SS (Bakari et al., 2024). Despite

the numerous positive aspects of integrating BC from SS (SSBC) into CWs, this topic has been poorly explored in the literature, as to the best of our knowledge, only four articles describe the use of this kind of material as CW substrate (Ayadi et al., 2024; Yao et al., 2025; Zhang et al., 2025; Zhong et al., 2025). This literature indicates that SSBC is also capable of boosting the growth of nitrifying and denitrifying bacterial populations (Yao et al., 2025) and may represent a suitable substrate for the adsorption of organic micropollutants (Bakari et al., 2024; Zhang et al., 2025; Zhong et al., 2025). Nevertheless, the available studies regarding the removal of these micropollutants focused only on sulphadiazine (Zhong et al., 2025) or perfluorobutanesulfonic acid (Zhang et al., 2025), and were, in most cases, short-term experiments (95-120 days), performed at lab-scale, in a controlled environment, using synthetic wastewater, thus restricting the scope of the information obtained (Yao et al., 2025; Zhang et al., 2025; Zhong et al., 2025). In addition, the SSBCs employed were characterized by very low values of specific surface area (18 – 43 m2/g) (Zhang et al., 2025; Zhong et al., 2025), thus suggesting the need of improved methodologies for biochar preparation and activation. In this regard, a recent study demonstrated that the integration into planted and unplanted VSSF-CWs of a SSBC produced and activated under specific and optimized experimental conditions allows to provide a significantly higher removal of chemical oxygen demand, nitrogen, and absorbance in VSSF-CWs, compared to gravel-based systems, also showing a negligible role of plants (Ayadi et al., 2024).

To fill the above-mentioned gaps in the current literature, regarding the behaviour of PhCs in SSBC-based CWs, planted and unplanted pilot-scale VSSF-CWs filled with SSBC were monitored for the removal of 35 target analytes, during a 227-day open-air study on the quaternary treatment of real urban wastewater, using gravel-based systems as control.

2. Materials and methods

2.1. Standards, reagents, and materials

Ultrapure water (conductivity ≤ 0.055 µS/cm) was produced in the laboratory using a Milli-Q system (Millipore, Billerica, MA, USA). Glass fibre filters, featuring a nominal porosity of 0.7 µm, were purchased from Whatman (Maidstone, England). All reagents employed for monitoring conventional water quality parameters (see Section 2.4) were supplied by HACH (Loveland, CO, USA). Reagent-grade ammonium chloride was obtained from Sigma-Aldrich (St. Louis, MO,

USA). LC-MS grade water, methanol, and acetonitrile were obtained from Carlo Erba (Milan, Italy). All reference standards of PhCs and related transformation products (TPs) were supplied by Sigma-Aldrich, with the only exception of venlafaxine-d6, which was purchased from Supelco (Bellefonte, PA, USA); the complete list of target analytes and their abbreviations is reported in **Table IV-4** and **Table SM5-1**, Section 1 of the *Supplementary material 5*, the latter showing also selected physicochemical properties.

Table IV-4: List of pharmaceutical compounds and transformation products investigated in this study, their abbreviations, detection frequencies (D.F.), concentration ranges (ng/L) found in the VSSF inlet samples, and consumption in 2022 expressed as Defined Daily Doses per 1000 inhabitants.

Compound	Abbreviation	D.F.	Range	Consumption
Atenolol	ATE	14/14	<15[b] – 69	n.r.
Bisoprolol	BIS	14/14	19 – 44	12.8
Carbamazepine	CBZ	14/14	75 – 200	1.2
Diclofenac	DIC	14/14	113 – 984	4.4
Fluconazole	FLU	14/14	15 – 72	0.3
Furosemide	FUR	14/14	27 – 285	23.3
Levofloxacin	LVF	14/14	64 – 300	0.7
Ramipril	RMP	14/14	40 – 197	61.5
Sulfamethoxazole	SMX	14/14	45 – 162	n.r.
Venlafaxine	VEN	14/14	28 – 115	3.7
O-Desmethylvenlafaxine[c]	O-DVEN	14/14	71 – 278	n.a.
Clarithromycin	CLA	10/14	<13[b] – 49	1.8
Atorvastatin	ATO	6/14	<7[b] – 21	50.9
Trimethoprim	TMP	5/14	7 – 16	n.r.
2-Hydroxyibuprofen[c]	2-HYIBU	4/14	709 – 1025	n.a.
4'-Hydroxydiclofenac[c]	4'-HYDIC	2/14	21 – 62	n.a.
Ketoprofen	KET	1/14	<68[b]	9.9
Erythromycin	ERY	0/14	<47[a]	n.r.
Pantoprazole	PAN	0/14	<252[a]	29.0
Ciprofloxacin	CIP	0/14	<100[a]	0.7
Tamsulosin	TAM	0/14	<1[a]	11.2
Diazepam	DZP	0/14	<10[a]	n.r.
Ranitidine	RNT	0/14	<0.3[a]	n.r.
Azithromycin	AZI	0/14	<6[a]	1.8
Clotrimazole	CLT	0/14	<10[a]	n.r.
Miconazole	MCL	0/14	<10[a]	n.r.
Ibuprofen	IBU	0/14	<90[a]	6.9
1-Hydroxyibuprofen[c]	1-HYIBU	0/14	<20[a]	n.a.
3-Hydroxyibuprofen[c]	3-HYIBU	0/14	<20[a]	n.a.
Flurbiprofen	FLU	0/14	<10[a]	0.6
Fenbufen	FEN	0/14	<80[a]	n.r.
Acetylsalicylic acid	ASA	0/14	<3[a]	67.2
Naproxen	NAP	0/14	<10[a]	n.r.
O-Desmethylnaproxen	O-DMNAP	0/14	<10[a]	n.a.
Acetaminophen	ACE	0/14	<10[a]	11.1

[a] Method detection limit; [b] Method quantification limit; [c] Transformation products; n.a.=not applicable; n.r.=not reported

2.2. Wastewater origin

The study utilized wastewater derived from the clariflocculation stage downstream of the activated sludge treatment of the Baciacavallo WWTP (GIDA S.p.A., Prato, Italy). This facility receives urban wastewater from the city of Prato and its textile industrial district (Section 2 of the Supplementary material). Notably, the wastewater treated in this study was collected prior to the final ozone-based advanced oxidation stage, which is pivotal in eliminating organic micropollutants, including those responsible for residual colour, before the treated effluent is

discharged into the receiving water body. In this regard, the VSSF-CWs acted as the final quaternary treatment stage. Approximately 1.5 m3 of wastewater was transferred on a weekly basis from the Baciacavallo WWTP to the outdoor laboratory of the Department of Chemistry at the University of Florence (Natural Wastewater Treatment Laboratory, NatLab), where the experimental setup for this study is located (**Figure SM5-1** in Section 3 of the *Supplementary material 5*). Since the wastewater supplied by GIDA contained a very low concentration of ammonia, it was enriched with reagent-grade ammonium chloride (Sigma-Aldrich, St. Louis, MO, USA), to study the nitrification and denitrification processes, as described elsewhere (Ayadi et al., 2024).

2.3. Design and operation of VSSF-CW systems

The experimental setup at the NatLab comprised twelve laboratory-scale systems, each consisting of high-density polyethylene tanks with a height of 25 cm and a surface area of 0.04 m2. To prevent light from reaching the inside of CWs, the outer walls of the tanks were painted, except for a water level control band inside the tank equipped with a removable lid. Six out of the twelve tanks were filled from the top to the bottom with coarse sand (3 cm, Ø=1-2 mm), fine gravel (12 cm, Ø=7-10 mm), medium gravel (5 cm, Ø=10-14 mm), and cobblestone (5 cm, Ø=30-50 mm), following the European VF-CWs design (Tsihrintzis, 2017). The vertical profile of the filling media used in CWs is also schematically illustrated in **Figure IV-3 (A and B)** for conventional and biochar-based systems, respectively. Among these systems, three were planted with P. australis (G-P), while the remaining three were left unplanted (G-U). The remaining six tanks – three planted with P. australis (SSBC-P) and three left unplanted (SSBC-U) – were filled with SSBC (range 1.808-1.921 kg, corresponding to about 3 L), medium gravel, and cobblestone, adopting the following grain size profile: 3 cm of SSBC, Ø=1-2 mm; 6 cm of SSBC, Ø=2-4 mm; 6 cm of SSBC, Ø=4-10 mm; 5 cm of medium gravel, and 5 cm of cobblestones. Plantation was carried out using young plantlets and their rhizomes, with two individuals per tank, collected from a real natural wetland in the "Parco di Travalle" area (Calenzano, 43°52'38.5"N 11°09'21.0"E).

A peristaltic pump with fifteen channels (Watson-Marlow model 313, Marlow, UK) was employed to feed CWs at a flow rate of 21 mL/min through a 1.5 mm perforated distribution comb positioned at the top of each mesocosm. Twelve out of the fifteen distribution pipes of the multi-channel pump were used to supply wastewater to the mesocosms, while a further pipe was employed to collect inlet wastewater. This approach ensured that all VSSF-CWs received an equal

amount of wastewater, and representative inlet samples of the treated wastewater could be collected. Each system was equipped with an outlet tap and a zero-pressure time-controlled solenoid valve, enabling the adjustment of the opening interval and duration, thus allowing for the automatic drainage of the CWs.

The mesocosms were fed according to the tidal approach by a timer controlling the peristaltic pump, with a 6-h cycle, repeated four times a day. The cycle comprised the following steps: (i) loading at 21 mL/min for 145 minutes with the solenoid valve closed, (ii) maintaining hydraulic saturation for 60 minutes, (iii) opening the solenoid valve with the complete emptying of the systems, and (iv) empty phase for 145 minutes. This cycle allowed for the complete filling of gravel-based constructed wetlands (CWs) up to the substrate's upper limit, while for SSBC systems, the water level was maintained approximately 2 cm below the top of the substrate. Under these conditions, each mesocosm received approximately 12 L of wastewater per day. Considering a hydraulic loading of 200 L per population equivalent (p.e.), the design size was around 0.7 m2/p.e.

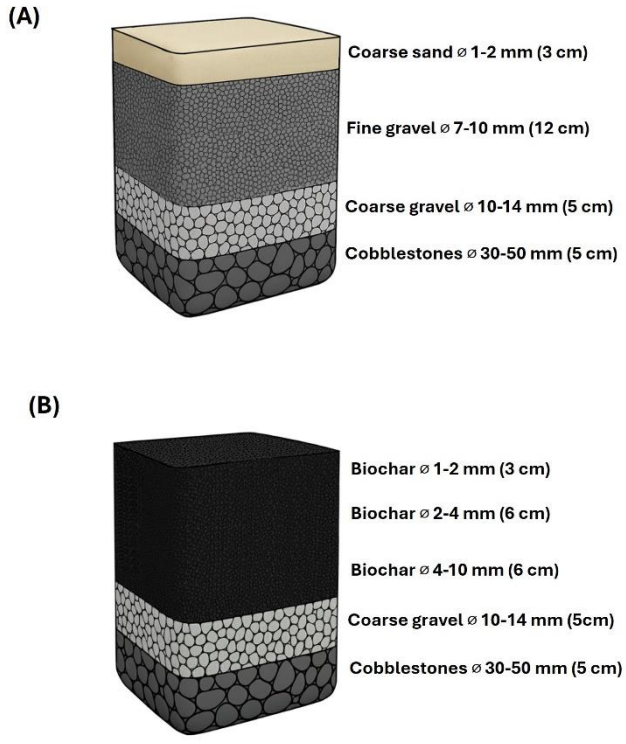

Figure IV-4: Schematic representation of the pilot-scale microcosms filled (A) with sand and gravel (VSSF-G) and (B) with biochar (VSSF-SSBC).

2.4. Biochar production and characterization

The SSBC used in this study was produced from a mixture of sawdust (derived from the cutting of forests, mainly consisting of oak and poplar) and biological sludge (70:30 w/w), supplied by Romana Maceri Centro Italia S.r.l. (Civitella in Val di Chiana, Italy) and Gestione Impianti di Depurazione Acque S.p.A. (GIDA, Prato, Italy), respectively. The feedstock underwent co-pyrolysis at 850 °C for 60 minutes under N_2-saturated conditions in a muffle furnace (Bioclass, Pistoia, Italy). The resulting BC was chemically activated by washing with BioDea® acid solution (Bio-Esperia S.r.l., Umbertide, Italy), a by-product of wood waste gasification (see **Table SM5-2**, section 4 of the *Supplementary material 5* for its characterization), at the 1/10 (w/w) biochar/BioDea® ratio for 30 minutes. Finally, the BC was rinsed with deionized water until a stable pH was reached and sieved using ASTM sieves with mesh sizes of 10, 4, 2, and 1 mm (ENCO S.r.l., Venezia, Italy). The physicochemical properties of the obtained material were determined, including specific surface area (SSA), pH at the point of zero charge (pHPZC). Moreover, environmental compatibility was assessed (i.e., ash content, leachable polycyclic aromatic hydrocarbons (PAHs), and selected trace elements) in accordance with the EN 12915-1 European Standard for materials intended for drinking water production (European Committee for Standardization, 2009). Full information on methodologies for BC production and characterisation has been detailed elsewhere (Bakari et al., 2024), while the results are shown in **Table SM5-3**, Section 3 of the *Supplementary material 5*.

2.5. Sample collection and analysis

The study spanned approximately 8 months, from July 2022 to February 2023, and included weekly and biweekly samplings for the analysis of conventional water quality parameters and PhCs, respectively. In more detail, the sampling chrono program for the analysis of PhCs is shown in **Table SM5-4**, Section 5 of the *Supplementary material* 5.

During the first three samplings, for each CW configuration (GP, GU, SSBC-P, and SSBC-U), the concentrations of water quality parameters and PhCs exiting each of the three mesocosms were analysed individually, verifying that the results were affected by a variability less than or equal to 16% (data not shown). Accordingly, for each CW configuration, equal aliquots of the effluents from the individual mesocosms were mixed to obtain pooled samples, which were then subjected to analysis.

An entire and homogeneous sample series, which includes one inlet sample and twelve outlet samples (one from each mesocosm), was collected for the determination of water quality

parameters (see Section 2.5.2) and PhCs (see Section 2.5.3).

For each sample collected, the following conventional water quality parameters were determined immediately after sampling or in any case within 24 hours from the collection: pH, dissolved oxygen (DO), electrical conductivity (EC), total suspended solids (TSS), chemical oxygen demand (COD), total nitrogen (TN), ammonium nitrogen (NH4+-N), nitrite nitrogen (NO2--N), nitrate nitrogen (NO3--N), total phosphorus (TP), orthophosphate (PO43-), and absorbance at 254 and 420 nm. During this period, the samples were stored in the fridge at +4°C.

For PhCs, an aliquot of 10 mL was taken from each sample immediately after collection and stored as five sub-aliquots in 2 mL-Eppendorf tubes at a temperature of -18 °C. The analysis of PhCs was carried out approximately at the end of each month of the study.

2.5.1. Analysis of conventional water quality parameters

Temperature (T), pH, EC, and DO were measured on unfiltered samples in the VSSF-CWs inlet and outlets using the following portable meters: (i) model 3310 (WTW, Weilheim, Germany) equipped with a temperature sensor and coupled with a SenTix® 61 pH-electrode (WTW), (ii) model HQ40D (HACH Instruments, Loveland, CO, USA) equipped with an LDO10110 sensor coupled with an integrated temperature sensor, and (iii) model COND340i conductivity meter (WTW). The values of temperature measured in the inlet and outlet were averaged in order to highlight possible correlations with removal efficiency.

TSS were evaluated according to the method 2540 D of the Standard Methods for the Examination of Water and Wastewater (American Public Health Association & American Water Works Association, 1995).

COD, TN, NH4+-N, NO2--N, NO3--N, TP, and PO43- were colorimetrically determined on wastewater samples after filtration at 0.7 µm, using a DR/4000U UV-Vis spectrophotometer (HACH Instruments) and USEPA-approved methods based on HACH reagent kits (for full details see Section 2 of the Supplementary material).

The results of the analysis of the water quality parameters are reported in **Table SM5-5**, Section 5 of the *Supplementary material 5*, and were previously discussed with full details elsewhere (Ayadi et al., 2024).

2.5.2. Analysis of pharmaceutical compounds

Liquid chromatographic (LC) analysis of PhCs was performed on a Shimadzu (Kyoto, Japan) chromatographic system Nexera X2 consisting of a low-pressure gradient quaternary pump LC-30AD, a DGU-20A 5R degassing unit, a SIL-30AC autosampler equipped with a 100 µL loop, a CTO/20AC thermostatted column compartment, and a CBM-20A module controller. The LC system was coupled with a 5500 QTrap mass spectrometer (Sciex, Framingham, MA, USA), equipped with a Turbo V® interface by an ESI probe. The MS/MS analysis was carried out in Multiple Reaction Monitoring (MRM) mode, performing two different chromatographic runs for the acquisition in negative and positive ionization, under the same chromatographic conditions. The chromatographic conditions, optimized in a previous study (Renai et al., 2021), are summarized below. Chromatographic column: Kinetex® PFP; eluent "A": acidic water (0.011% HCOOH); eluent "B": ACN/MeOH ratio 1.75 (v/v); flow rate: 0.50 ml/min; temperature: 32°C; elution gradient: initial isocratic at percent "B" 11.0% for 1 min and increasing eluent "B" to 11.5% per minute for 8.7 min. The injection volume was 100 µL. In order to minimize contamination of the MS source, from 0 min to 1 min and from 10 min to the end of the chromatographic run, the LC eluate was diverted to waste via a two-position six-port valve (model HT, Vici, Schenkon, Switzerland) installed upstream of the mass spectrometer.

2.6. Mass of pharmaceuticals in the inlet and outlets of mesocosm

The cumulative mass of pharmaceutical compounds (M, µmol) in the inlet and outlet samples collected in the mesocosms was calculated according to two different approaches.

The first one (following identified as "mean" approach) used equation 1,

$$M=\frac{\Sigma_{i,j}\left(\frac{C_{i,j}\times V}{MW_i}\right)}{14}\times 227 \qquad \text{(Equation 1)}$$

where V is the volume entering or leaving the plant (here approximated at 12 L in both cases), $C_{i,j}$ is the concentration expressed in µg/L of the i-th PhC in the j-th sample of influent or effluent wastewater, MW_i is the molecular weight of the i-th PhC, 14 is the number of inlet and outlet sampling days and 227 are the total number of days of the study. Note that with the "mean" approach it is possible to calculate the standard deviation (S.D.) according to the equation 2,

$$S.D.=\sqrt{\frac{\Sigma_j\left(M_j-\overline{M}\right)^2}{13}} \qquad \text{(Equation 2)}$$

where M_j and $\overline{M}$ are the total mass of PhCs in the j-th sample of the influent and effluent wastewaters and the corresponding mean value referred to the 14 samples analysed, respectively. M_j and $\overline{M}$ are calculated by the following equations:

$$M_j = \sum_i \left(\frac{C_{i,j} \times V}{MW_i}\right) \quad \text{(Equation 3)}$$

$$\overline{M} = \frac{\sum_j M_j}{14} \quad \text{(Equation 4)}$$

The second approach (following identified as "integral" approach) consisted in the integration of sixth degree polynomial equations that approximated the trends observed in the masses entering and leaving the mesocosms between t=0 and t=227 days.

The mass of each individual PhC entering in the inlet and outlet of the mesocosms was also calculated for each sampling date, in order to evaluate any differences in the behaviour of each target analyte during treatment.

2.7. Statistical analysis

Statistical analysis used for the comparison of mean values of the data obtained was performed by means of ANOVA followed by the Games-Howell test, using the Minitab® software package version 17.1.0 (Minitab Inc., State College, PA, USA). Games-Howell post-hoc test was used to determine which specific groups have significantly different means since it does not assume equal variances for the different groups of data. Regression analyses aimed at identifying the equation that best fits the masses of PhCs in the inlet and outlet of the various mesocosms as a function of days after VSSF-CW start-up were carried out with Microsoft® Excel® for Microsoft 365 MSO (Version 2510 Build 16.0.19328.20178), using sixth-degree polynomial approximations.

3. Results and discussion

3.1. Environmental assessment of SSBC for wastewater treatment

During the thermal conversion process for biochar production, toxic compounds such as benzene derivatives and PAHs can be generated (Krzyszczak et al., 2021), thus involving potential hazards when biochar is used as a sorbent material in wastewater treatment (Del Bubba et al., 2020).

Previous studies reported PAH concentrations in SSBC up to 800 μg kg^{-1} (Feng et al., 2023), thus suggesting that the material itself could become a potential pollution source when used as a sorbent for wastewater treatment. Moreover, SS may contain significant amounts of toxic metals, which are retained in the resulting biochar and then potentially released during wastewater treatment (Vause et al., 2018). It is therefore of fundamental importance to thoroughly characterize biochar before its use as an adsorbent material for wastewater treatment, in order to assess the environmental risks associated with this application (Castiglioni et al., 2021). To this purpose, the EN 12915-1 standard was adopted as a reference, by evaluating leachable PAHs and selected trace elements, and the results obtained are illustrated in **Table SM5-3**. The results of the leaching tests demonstrated the environmental compatibility of SSBC in terms of the release of PAHs and inorganic elements into the treated effluent. The biochar also complied with the limits specified by the aforementioned standard regarding ash content, a key parameter for evaluating the adsorption efficiency of carbonaceous materials.

These results are strictly dependent on the production and activation conditions of the material. In particular, the high conversion temperature of the feedstock (i.e., 850°C) enables the degradation of PAHs that were already present in the sludge and/or formed during pyrolysis at temperatures up to about 500°C (Castiglioni et al., 2022). The presence of significant percentages of SS in the feedstock subjected to co-pyrolysis also contributes to the lower production of PAHs. In fact, the bacterial biomass, which is made mainly of lipids and peptidoglycans, is less subjected to PAH formation than woody biomass, the latter consisting of well-known precursors of the formation of PAHs during pyrolysis (i.e., cellulose, hemicellulose, and lignin) (Bakari et al., 2024). The low release of ash and the elements monitored in accordance with EN 12915-1 is instead attributable to the treatment of the material with the BioDea® solution, whose high acidity (see **Table SM5-2**) contributes to the solubilisation of inorganic elements into the washing solution. It should also be noted that the mobility of the elements present in the material is

undoubtedly influenced by the high pyrolysis temperature used, which causes the decomposition of organic functional groups, partial pore collapse, and irreversible incorporation of inorganic species into the newly formed structure (Zhang et al., 2022). **Table SM5-3** also showed that the material has a high surface area (389 m^2/g), a pore size distribution predominantly oriented towards microporosity (341 m^2/g), and a high carbon content (65% on a weight basis).

Overall, these results support the potential implementation of this material in wastewater treatment and confirm that the applied technology is environmentally safe, despite SSBC derived from a hazardous waste. It is also noteworthy that the EN 12915-1 requirements, originally designed for materials used in drinking-water production, represent highly conservative thresholds compared to the objectives of the present study, which focuses on quaternary treatment of WWTP effluents rather than potable-water production.

3.2. Occurrence of pharmaceutical compounds in the VSSF influent

The full names of target analytes monitored in this study are listed in **Table IV-4**, where their abbreviations, detection frequency, and concentration ranges in the influent wastewater, and consumption in Italy are also reported.

Among the 35 PhCs and TPs investigated, 17 analytes were detected at least once in the VSSF influent during the eight-month period of the study (**Table IV-4**). More in detail, 11 analytes showed a 100% detection frequency, i.e., all 14 analysed samples had concentrations above the method detection limits reported in **Table SM5-6**, Section 6.1 of the *Supplementary material 5*. These compounds belonged to the therapeutic categories of non-steroidal anti-inflammatory drugs (NSAIDs, DIC), loop diuretics (FUR), antidepressants (VEN) and its O-desmethylated derivative O-DVEN), anticonvulsants (CBZ), angiotensin-converting-enzyme (ACE) inhibitors (RMP), antibiotics (SMX and LVF), antifungals (FLU), and β-blockers (ATE and BIS). Most of them were quantified in all inlet samples, showing concentrations ranging from tens to hundreds of ng/L. The only exception was ATE, which was detected in one of the 14 input samples analysed at concentrations below the MQL (approximately 7 ng/L versus 15 ng/L). A high detection rate was also observed for CLA, with 10 positive samples, five of which were above the MQL. Among antibiotics, TMP, which is commercially used in combination with SMX in a 1/5 ratio (w/w), was

present in about 35% of the investigated samples. ATO was also detected in six inlet samples, three of them showing concentrations higher than MQL. NSAIDs other than DIC and NSAID metabolites (i.e., KET, 2-HYIBU, and 4'-HYDIC) exhibited even lower detection frequencies.

The concentrations of PhCs determined in the inlet samples were between a few ng/L and hundreds of ng/L, depending on the analyte and the sample considered. These values should not be considered negligible as they refer to a WWTP effluent discharging into a surface water body and highlight the recalcitrance of PhCs to the treatments carried out in conventional WWTPs. Among the compounds detected in the WWTP secondary effluent, it is interesting to highlight the presence of hydroxylated metabolites, which represent an aspect of considerable concern, given that existing literature suggests that they possess a greater toxicity than their parent compounds (Rastogi et al., 2021; Świacka et al., 2022) and that for 2-HYIBU concentrations as high as several hundreds of ng/L were quantified (**Table IV-4**). These findings are consistent with recent studies on the occurrence of PhCs in wastewater, which have reported similar concentration ranges (Nguyen et al., 2024).

The occurrence of PhCs can be evaluated in the light of their use, as deduced by data contained in the report concerning the consumption of PhCs in Italy, published yearly by the Medicines Utilisation Monitoring Centre (OSMED) (The Medicines Utilisation Monitoring Centre, 2023). Interestingly, some drugs exhibiting among the highest detection frequencies were also the most consumed according to the OSMED report (e.g., RMP and FUR). However, some other drugs, which were characterized by lower levels of consumption, were equally ubiquitous, suggesting poor removal efficiency in WWTPs and indicating, therefore, a high persistence in the environment and a possible ecotoxicological risk disproportionate to human use patterns. This was, for example, the case of CBZ, VEN, and CLA, which are listed in the 2024/3019 European Directive on urban wastewater treatment as indicator micropollutants to be monitored in WWTP effluents (European Parliament and the Council, 2024). In contrast, other widely used drugs (e.g., TAM, ACE, and ASA) were not detected, likely due to their lower excretion rate as unchanged drug (Cham et al., 1982; Dunn et al., 2002; Forrest et al., 1982).

3.3. Cumulative removal of pharmaceutical compounds

Figure IV-4 shows the total mass of PhCs expressed as micromoles (µmol) determined in the inlet and outlet of the four different mesocosm configurations according to both the "mean" and the "integral" approaches (see Section 2.6). The polynomial regressions used for performing the integral calculations provided determination coefficients (R^2) for the influent masses of 0.79,

while for the effluents, R^2 was found in the range of 0.59-0.89 (**Figure SM5-2** of the *Supplementary material*). The estimations of the mass of PhCs made by the "integral" approach for SSBC-U and SSBC-P effluents were slightly higher than those performed using the "mean", being the difference equal to about 0.4 µmol, which corresponded to approximately 10%. In contrast, for the inlet and effluents from G-U and G-P, the integral approach led to lower estimates, with differences, however, contained in the range of 1.3-2.8 µmol, corresponding to 13%-17%.

Considering the "mean" approach, which allowed for evaluating the statistical significance of the variations observed between influent and effluent masses of PhCs, the effluents from all mesocosm configurations demonstrated a statistically significant reduction ($P<0.05$ and $P<0.01$ for G and SSBC systems, respectively), compared to the influent. However, the extent of removal varied considerably depending on the substrate type. The SSBC systems showed by far the best overall performance, achieving a removal efficiency of 66%-75% (SSBC-U) and 62%-71% (SSBC-P), depending on the calculation approach considered. The higher performance can be mainly attributed to the intrinsic adsorptive capacity of biochar, which is characterized by an extensive SSA (i.e., 389 m^2/g) and a porosity distribution (see **Table SM5-3**) compatible with the size of the target molecules, which is approximately in the range of 1-2 nm, as the maximum radius. As mentioned above, the planted systems (SSBC-P) behaved similarly to the unplanted one (SSBC-U), even though a slightly higher PhC emission was determined in the former. This was likely the consequence of two opposing phenomena, the latter being in this case more important: (i) on the one hand plants may positively contribute to the removal of PhCs through direct intake (Bianchi et al., 2020) and/or by acting as an adhesion support for the growth of bacteria potentially responsible for the degradation of organic compounds (Sacco et al., 2006); (ii) on the other hand, plants emit significant amounts of exudates (e.g., sugars, amino acids, and organic acids) from their roots (Koo et al., 2005) that can compete with PhCs for adsorption by biochar.

Interestingly, in systems filled with sand and gravel, the presence of plants seems to provide a positive, although slight contribution to the removal of PhCs, which was 27%-28% and 33%-36% in G-U and G-P mesocosms, respectively. This result can probably be attributed to the (i) mechanisms mentioned above, in agreement with the almost null adsorption capacity of materials commonly used as filling media in CWs (Ayadi et al., 2024).

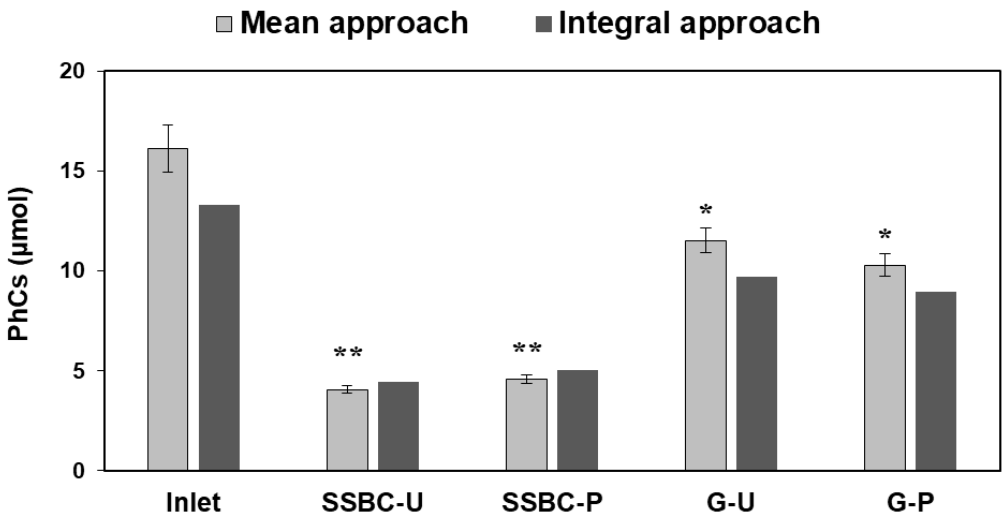

Figure IV-4: Total PhCs (µmol) in the inlet and outlet of mesocosms filled with biochar (SSBC) or gravel (G), planted (P) or unplanted (U), determined according to the "mean" (light grey) and "integral" (dark grey) approaches. Asterisks indicate statistically significant differences (* $P<0.05$; ** $P<0.01$) of the outlets compared to the inlet, according to the "mean approach", using the Games-Howell Test.

3.4. Behaviour of individual PhCs

3.4.1. Individual removals and temporal trends

It is interesting to evaluate the removal of individual pharmaceutical compounds in each mesocosm, in addition to the cumulative one, in order to discover any differences in their behaviour. **Figure IV-5** shows the distribution of mean removal percentages over the whole study period for the individual target analytes that were quantified in at least 25% of the analysed samples. SSBC-U mesocosms showed the most homogeneous behaviour, with mean removals ranging from 43% (RMP) to 95% (DIC), and 50% of the data included in the range 52%-70%. SSBC-P CWs provided removals similar, although slightly lower, than those observed in SSBC-U, with the only notable exception of CLA, which even showed negative removal, thus representing an outlier of the removal distribution. Mesocosms filled with gravel performed worse than those filled with biochar for all analytes investigated, confirming the data on cumulative removal. For mesocosms filled with gravel, the data obtained for individual analytes also confirm the higher removal of planted systems compared to those without plants, the latter exhibiting in four cases (i.e., FUR, FLU, RMP, and CLA) a negative mean removal.

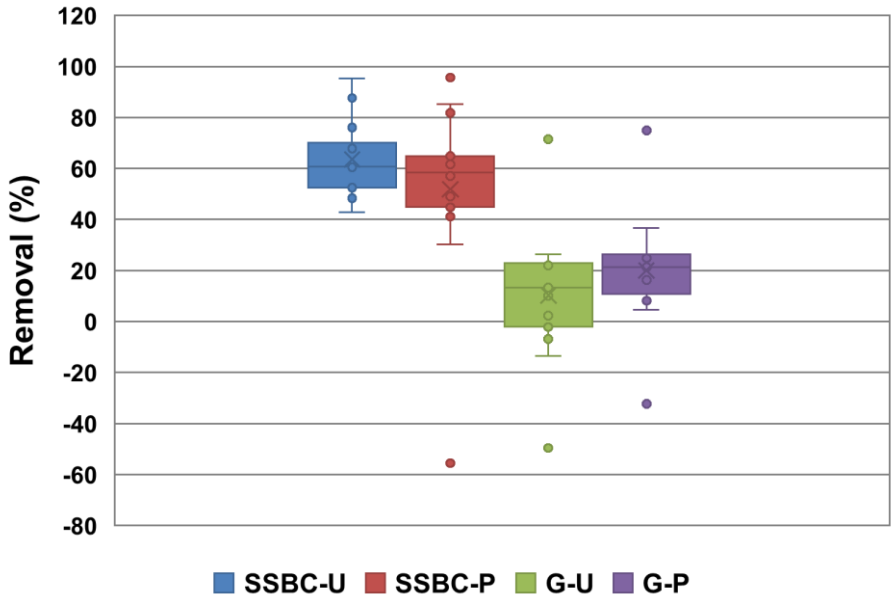

Figure IV-5: Boxplots of removal percentages determined in the four CW configurations for target analytes that were quantified in at least 25% of the analysed samples (i.e., ATE, ATO, BIS, CBZ, CLA, DIC, FLU, FUR, 2-HYIBU, LVF, O-DES, RMP, SMX, TMP, and VEN). Each box contains the values of the entire data series between the first and third quartiles. Line and cross inside the boxes indicate the median and mean of the entire data series, respectively. Upper and lower "whiskers" represent the values, respectively, obtained by increasing or decreasing the third and first quartile limits by 50%. Symbols outside the whiskers are the outliers.

Conclusions

This study describes for the first time the behaviour of a large panel of PhCs in CWs, both planted and unplanted, integrated with SSBC as a filling medium, comparing their removal performance with that achieved in conventional systems. Integration with biochar proved to be suitable for maintaining good removal rates of the target analytes (around 70% on average) immediately after the start-up of the CW and for a long period of time (around eight months). It should be underlined that the PhCs monitored in this study include many of those present in the various European Monitoring Watch Lists issued in the last ten years and in the recently promulgated European Directive on Urban Wastewater Treatment (European Parliament and the Council, 2024) for the evaluation of the efficiency of quaternary treatments. Specifically, substances such as CBZ, DIC, CLA, and VEN are explicitly listed as indicator micropollutants. Therefore, this study not only addresses current environmental concerns but also anticipates future regulatory requirements that will materialize with the transposition of the aforementioned directive for the advanced removal of organic micropollutants.

Reference

Ajibade, F.O., Yin, W.-X., Guadie, A., Ajibade, T.F., Liu, Y., Kumwimba, M.N., Liu, W.-Z., Han, J.-L., Wang, H.-C., Wang, A.-J., 2023. Impact of biochar amendment on antibiotic removal and ARGs accumulation in constructed wetlands for low C/N wastewater treatment. Chemical Engineering Journal 459, 141541.

Auvinen, H., Gebhardt, W., Linnemann, V., Du Laing, G., Rousseau, D.P., 2017. Laboratory-and full-scale studies on the removal of pharmaceuticals in an aerated constructed wetland: effects of aeration and hydraulic retention time on the removal efficiency and assessment of the aquatic risk. Water Science and Technology 76(6), 1457-1465.

Ayadi, M., Passaseo, D., Bonaccorso, G., Fichera, M., Renai, L., Venturini, L., Colzi, I., Fibbi, D., Del Bubba, M., 2024. Biochar from co-pyrolysis of biological sludge and sawdust in comparison with the conventional filling media of vertical-flow constructed wetlands for the treatment of domestic-textile wastewater. Water Science & Technology 89(5), 1252-1263.

Bakari, Z., Fichera, M., El Ghadraoui, A., Renai, L., Giurlani, W., Santianni, D., Fibbi, D., Bruzzoniti, M.C., Del Bubba, M., 2024. Biochar from co-pyrolysis of biological sludge and woody waste followed by chemical and thermal activation: end-of-waste procedure for sludge management and biochar sorption efficiency for anionic and cationic dyes. Environmental Science and Pollution Research 31(24), 35249-35265.

Bianchi, E., Biancalani, A., Berardi, C., Antal, A., Fibbi, D., Coppi, A., Lastrucci, L., Bussotti, N., Colzi, I., Renai, L., 2020. Improving the efficiency of wastewater treatment plants: Bio-removal of heavy-metals and pharmaceuticals by Azolla filiculoides and Lemna minuta. Science of the Total Environment 746, 141219.

Borsetto, C., Dykes, C., Kockiri, B., Song, L., Wellington, E.M., Abolfathi, S., 2025. Constructed wetlands as nature-based barriers: Mitigating antimicrobial resistance and pathogen dispersal in riverine systems. Journal of Hazardous Materials 495, 138855.

Castiglioni, M., Rivoira, L., Ingrando, I., Del Bubba, M., Bruzzoniti, M.C., 2021. Characterization techniques as supporting tools for the interpretation of biochar adsorption efficiency in water treatment: a critical review. Molecules 26(16), 5063.

Castiglioni, M., Rivoira, L., Ingrando, I., Meucci, L., Binetti, R., Fungi, M., El-Ghadraoui, A., Bakari, Z., Del Bubba, M., Bruzzoniti, M.C., 2022. Biochars intended for water filtration: A comparative study with activated carbons of their physicochemical properties and removal efficiency towards neutral and anionic organic pollutants. Chemosphere 288, 132538.

Cham, E.B., Dykman, J., Bochner, F., 1982. Urinary excretion of aspirin. British journal of clinical pharmacology 14(4), 562-564.

Cizmas, L., Sharma, V.K., Gray, C.M., McDonald, T.J., 2015. Pharmaceuticals and personal care products in waters: occurrence, toxicity, and risk. Environmental chemistry letters 13(4), 381-394.

Coppini, E., Palli, L., Antal, A., Del Bubba, M., Miceli, E., Fani, R., Fibbi, D., 2019. Design and start-up of a constructed wetland as tertiary treatment for landfill leachates. Water Science and Technology 79(1), 145-155.

Dai, Y., Zhang, N., Xing, C., Cui, Q., Sun, Q., 2019. The adsorption, regeneration and engineering applications of biochar for removal organic pollutants: a review. Chemosphere 223, 12-27.

Del Bubba, M., Anichini, B., Bakari, Z., Bruzzoniti, M.C., Camisa, R., Caprini, C., Checchini, L., Fibbi, D., El Ghadraoui, A., Liguori, F., 2020. Physicochemical properties and sorption capacities of sawdust-based biochars and commercial activated carbons towards ethoxylated alkylphenols and their phenolic metabolites in effluent wastewater from a textile district. Science of the Total Environment 708, 135217.

Delgado, N., Bermeo, L., Hoyos, D.A., Peñuela, G.A., Capparelli, A., Marino, D., Navarro, A., Casas-Zapata, J.C., 2020. Occurrence and removal of pharmaceutical and personal care products using subsurface horizontal flow constructed wetlands. Water Research 187, 116448.

Dunn, C.J., Matheson, A., Faulds, D.M., 2002. Tamsulosin: A Review of its Pharmacology and Therapeutic Efficacy in the Management of Lower Urinary Tract Symptoms. Drugs & Aging 19(2), 135-161. https://doi.org/10.2165/00002512-200219020-00004.

El Barkaoui, S., Mandi, L., Aziz, F., Del Bubba, M., Ouazzani, N., 2023. A critical review on using biochar as constructed wetland substrate: Characteristics, feedstock, design and pollutants removal mechanisms. Ecological Engineering 190, 106927.

El Ghadraoui, A., Ouazzani, N., Ahmali, A., El Mansour, T.E.H., Aziz, F., Hejjaj, A., Del Bubba, M., Mandi, L., 2020. Treatment of olive mill and municipal wastewater mixture by pilot scale vertical flow constructed wetland. Desalination and Water Treatment 198, 126-139. https://doi.org/https://doi.org/10.5004/dwt.2020.26009.

European Committee for Standardization, 2009. EN 12915:2009, Products used for the treatment of water intended for human consumption - Granular Activated Carbon.

European Parliament and the Council, 2024. Directive (EU) 2024/3019 of the European Parliament and of the

Council of 27 November 2024 concerning urban wastewater treatment. Official Journal of the European Union L series, 1-62.
Feng, L., Gao, Z., Hu, T., He, S., Liu, Y., Jiang, J., Zhao, Q., Wei, L., 2023. Performance and mechanisms of biochar-based materials additive in constructed wetlands for enhancing wastewater treatment efficiency: A review. Chemical Engineering Journal 471, 144772.
Forrest, J.A., Clements, J., Prescott, L., 1982. Clinical pharmacokinetics of paracetamol. Clinical pharmacokinetics 7(2), 93-107.
Gorito, A.M., Ribeiro, A.R., Almeida, C., Silva, A.M., 2017. A review on the application of constructed wetlands for the removal of priority substances and contaminants of emerging concern listed in recently launched EU legislation. Environmental pollution 227, 428-443.
Ilyas, H., Van Hullebusch, E.D., 2020. Performance comparison of different types of constructed wetlands for the removal of pharmaceuticals and their transformation products: a review. Environmental Science and Pollution Research 27(13), 14342-14364.
Kataki, S., Chatterjee, S., Vairale, M., Sharma, S., Dwivedi, S., Gupta, D., 2021. Constructed wetland, an eco-technology for wastewater treatment: A review on various aspects of microbial fuel cell integration, low temperature strategies and life cycle impact of the technology. Renewable and Sustainable Energy Reviews 148, 111261.
Koo, B.J., Adriano, D.C., Bolan, N.S., Barton, C.D., 2005. ROOT EXUDATES AND MICROORGANISMS, in: Hillel, D. (Ed.) Encyclopedia of Soils in the Environment. Elsevier, Oxford, pp. 421-428. https://doi.org/https://doi.org/10.1016/B0-12-348530-4/00461-6.
Krzyszczak, A., Dybowski, M.P., Czech, B., 2021. Formation of polycyclic aromatic hydrocarbons and their derivatives in biochars: The effect of feedstock and pyrolysis conditions. Journal of Analytical and Applied Pyrolysis 160, 105339.
Liu, H., Hu, Z., Zhang, J., Ngo, H.H., Guo, W., Liang, S., Fan, J., Lu, S., Wu, H., 2016. Optimizations on supply and distribution of dissolved oxygen in constructed wetlands: a review. Bioresource Technology 214, 797-805.
Nguyen, M.-K., Lin, C., Bui, X.-T., Rakib, M.R.J., Nguyen, H.-L., Truong, Q.-M., Hoang, H.-G., Tran, H.-T., Malafaia, G., Idris, A.M., 2024. Occurrence and fate of pharmaceutical pollutants in wastewater: Insights on ecotoxicity, health risk, and state–of–the-art removal. Chemosphere 354, 141678.
Pandey, D., Singh, S.V., Savio, N., Bhutto, J.K., Srivastava, R., Yadav, K.K., Sharma, R., Nandipamu, T.M.K., Sarkar, B., 2025. Biochar application in constructed wetlands for wastewater treatment: A critical review. Journal of Water Process Engineering 69, 106713.
Petrie, B., Rood, S., Smith, B.D., Proctor, K., Youdan, J., Barden, R., Kasprzyk-Hordern, B., 2018. Biotic phase micropollutant distribution in horizontal sub-surface flow constructed wetlands. Science of the total environment 630, 648-657.
Rastogi, A., Tiwari, M.K., Ghangrekar, M.M., 2021. A review on environmental occurrence, toxicity and microbial degradation of Non-Steroidal Anti-Inflammatory Drugs (NSAIDs). Journal of Environmental Management 300, 113694.
Ravichandran, M.K., Philip, L., 2022. Assessment of the contribution of various constructed wetland components for the removal of pharmaceutically active compounds. Journal of Environmental Chemical Engineering 10(3), 107835.
Renai, L., Scordo, C.V.A., El Ghadraoui, A., Santana-Viera, S., Rodriguez, J.J.S., Orlandini, S., Furlanetto, S., Fibbi, D., Lambropoulou, D., Del Bubba, M., 2021. Quality by design optimization of a liquid chromatographic-tandem mass spectrometric method for the simultaneous analysis of structurally heterogeneous pharmaceutical compounds and its application to the rapid screening in wastewater and surface water samples by large volume direct injection. Journal of Chromatography A 1649, 462225.
Sacco, C., Pizzo, A.M., Tiscione, E., Burrini, D., Messeri, L., Lepri, L., Bubba, M.D., 2006. Alkylphenol Polyethoxylate Removal in a Pilot-Scale Reed Bed and Phenotypic Characterization of the Aerobic Heterotrophic Community. Water environment research 78(7), 754-763.
Salah, M., Zheng, Y., Wang, Q., Li, C., Li, Y., Li, F., 2023. Insight into pharmaceutical and personal care products removal using constructed wetlands: A comprehensive review. Science of The Total Environment 885, 163721.
Su-qing, W., Jun-jun, C., Yanran, D., Zhen-bin, W., Wei, L., 2012. Purification efficiencies and microbial community structure of integrated vertical-flow constructed wetland for domestic wastewater treatment during acclimation period. Desalination and Water Treatment 48(1-3), 302-309.
Świacka, K., Maculewicz, J., Świeżak, J., Caban, M., Smolarz, K., 2022. A multi-biomarker approach to assess toxicity of diclofenac and 4-OH diclofenac in Mytilus trossulus mussels-First evidence of diclofenac metabolite impact on molluscs. Environmental Pollution 315, 120384.
The Medicines Utilisation Monitoring Centre, 2023. National Report on Medicines use in Italy: Year 2022. Italian Medicines Agency, Rome.

Tsihrintzis, V.A., 2017. The use of vertical flow constructed wetlands in wastewater treatment. Water Resources Management 31(10), 3245-3270.
Valipour, A., Ahn, Y.-H., 2016. Constructed wetlands as sustainable ecotechnologies in decentralization practices: a review. Environmental Science and Pollution Research 23(1), 180-197.
Vause, D., Heaney, N., Lin, C., 2018. Differential release of sewage sludge biochar-borne elements by common low-molecular-weight organic acids. Ecotoxicology and Environmental Safety 165, 219-223. https://doi.org/https://doi.org/10.1016/j.ecoenv.2018.09.005.
Venditti, S., Brunhoferova, H., Hansen, J., 2022. Behaviour of 27 selected emerging contaminants in vertical flow constructed wetlands as post-treatment for municipal wastewater. Science of the Total Environment 819, 153234.
Verlicchi, P., Zambello, E., 2014. How efficient are constructed wetlands in removing pharmaceuticals from untreated and treated urban wastewaters? A review. Science of the Total Environment 470, 1281-1306.
Vymazal, J., Zhao, Y., Mander, Ü., 2021. Recent research challenges in constructed wetlands for wastewater treatment: A review. Ecological Engineering 169, 106318.
Yao, J., Huang, J., Qian, X., Xu, J., Tang, M., 2025. Operational characteristics of constructed wetlands amended with reed and sludge granular biochar: Decontamination and metabolism of nitrogen. Chemical Engineering Journal, 167797.
Zhang, F., Shen, C., Zhao, Y., Kong, L., Ju, F., Ji, B., Man, Y.B., Shan, S., Li, Y., Zhang, J., 2025. Biofilm-enhanced PFAS removal in constructed wetlands: Sewage sludge biochar drives adsorption and microbial synergy. Chemical Engineering Journal, 167257.
Zhang, X., Zhao, B., Liu, H., Zhao, Y., Li, L., 2022. Effects of pyrolysis temperature on biochar's characteristics and speciation and environmental risks of heavy metals in sewage sludge biochars. Environmental Technology & Innovation 26, 102288.
Zhong, M., Zhang, Z., Zhang, J., Luo, Z., Chen, Y., Liu, M., Gong, B., Cui, H., Cui, L., 2025. Impact of sewage sludge biochar spheres as constructed wetland substrates on antibiotic removal and application. Journal of Environmental Management 380, 125186.
Zhuang, L.-L., Li, M., Li, Y., Zhang, L., Xu, X., Wu, H., Liang, S., Su, C., Zhang, J., 2022. The performance and mechanism of biochar-enhanced constructed wetland for wastewater treatment. Journal of Water Process Engineering 45, 102522.

General Conclusion and Research Future Directions

1. General Conclusion

In the context of increasing environmental concerns and the urgent need for sustainable water management solutions, biochar (BC) has emerged as a promising material for wastewater treatment. Produced from agricultural residues through pyrolysis, BC offers a low-cost, eco-friendly approach to pollutant removal while contributing to waste valorisation and circular economy strategies.

This thesis investigated the preparation, characterisation, and application of BC for treating domestic wastewater, including both conventional and emerging pollutants. The entire biochar value chain was covered, from optimising preparation conditions to integrating it into filtration systems and constructed wetlands, revealing its versatility and limitations. The findings showed that the physicochemical properties and adsorption capacity of BC are strongly affected by the type of biomass and the temperature of the pyrolysis process. High-temperature biochars exhibited enhanced carbon content, thermal stability, surface area, and adsorption capacities, particularly for organic pollutants like methylene blue. Among the tested biochars, those derived from olive waste (DOW) at 800°C exhibited the most promising performance for methylene blue removal, affirming the potential of optimized pyrolysis conditions in tailoring BC properties for specific environmental applications.

Beyond adsorption studies, the research extended to the integration of BC into various biofiltration systems, including constructed wetlands (CWs) and column filtration systems (CFS). In these contexts, BC amendments improved the removal of a broad spectrum of conventional pollutants such as nitrogen species (e.g., NH_4^+-N, TN: total nitrogen, TKN: total kjeldahl nitrogen), organic matter (e.g., COD), solids (e.g., TSS), and faecal indicators, particularly under low to moderate organic loading rates. The BC-enhanced systems supported microbial activity, notably nitrification, although challenges remained in removing phosphorus, sulphates, and hardness due to material and system limitations, suggesting the need for complementary materials or system adaptations. Furthermore, increasing the concentration of BC in the biofilter substrate did not significantly improve treatment performance. Additionally, the efficiency of the biofilters' treatment declined under higher organic loads, underlining the importance of optimised dosing and system configuration.

In the context of emerging contaminants, such as pharmaceutical compounds (PhCs), the VF-

CWs showed high removal efficiencies for several compounds. Yet, the integration of BC did not universally enhance PhCs removal, largely due to compound-specific behaviours and variability in BC properties. Persistent compounds like carbamazepine and fluoxetine were only marginally removed using biochar with relatively low specific surface area, underscoring the need for further system refinement. Actually, biochar from co-pyrolysis of sewage sludge and sawdust showed much better performances and proved to be effective in ensuring a higher and durable removal of PhCs compared to conventional CW substrates.

Overall, this work confirms the viability of BC as a low-cost, locally available, and environmentally friendly material for enhancing nature-based wastewater treatment systems. It contributes valuable insights into the optimization of BC production and application, while also highlighting the necessity for continued research into long-term system performance, microbial interactions, and the treatment of complex and emerging pollutants. The outcomes support the advancement of circular economy approaches through the valorisation of agricultural waste in sustainable environmental technologies.

2. Future Research Directions

Building on the outcomes of this work, future research should focus on the following areas:

a) Develop standardized production protocols and explore physical/chemical activation to enhance the adsorption of persistent contaminants.
b) Evaluate hydraulic stability, pollutant removal, and biochar aging under real operational conditions.
c) Test regeneration methods (thermal, chemical, biological) to extend biochar lifespan and reduce costs.
d) Study biochar effects on microbial communities, plant growth, and pollutant transformation in constructed wetlands.
e) Develop integrated models (hydrodynamics–sorption–biodegradation) to optimize system configuration and scale-up.
f) Monitor pharmaceutical degradation pathways and assess environmental risks of transformation products.
g) Conduct LCA and cost–benefit studies to evaluate economic and environmental viability.
h) Combine biochar-based treatment with advanced processes (e.g., disinfection, polishing steps) for persistent pollutants.
i) Quantify carbon sequestration, climate mitigation potential, and synergies with nutrient recovery.

Supplementary materials

Supplementary Materials 1 – Chapter II

1. Biochar characterization

1.1. TG-DTG analysis

The TG-DTG analysis was performed by using a Perkin Elmer (Waltham, MA, USA) TGA thermogravimetric analyzer under a nitrogen atmosphere in a temperature range from 50 °C to 950 °C and with a heating rate of 10 °C·min^{-1}.

1.2. Elemental analysis

C, H, N, and S contents were determined using a Euro EA-CHNSO Elemental Analyzer. The percentage oxygen content was estimated to be the difference between the other elements:

O (%) = 100 – (C% + H% + N% + S% + AC).

1.3. Proximate analysis

The volatile matter (VM) was determined by the closed furnace vent port, preheated to 950 °C, and placed in covered crucibles with preheated biochar at 105 °C (ASTM Standard D1762-84).

The ash content (AC) was determined following the official method (ASTM Standard D1762-84) by heating the biochar from ambient to 750 °C at a rate of 5 °C min^{-1}, holding 750 °C for 6 h, and then cooling to 105 °C. The material was weighed to a constant weight.

The fixed carbon (FC) is the carbon remaining after the removal of volatile matter, moisture, and ash content from the biofuel.

The biochar thermal stability (TS) was calculated as the ratio between FC and the sum of FC and VM. Values closer to one indicate a more stable biochar.

1.4. Physisorption analysis

The biochar sample was preliminarily degassed under nitrogen flow at 200 °C for 1 h, then evacuated under high vacuum (< 10–2 mbar), supplied by an oil-based vacuum pump coupled to a high vacuum system, for 0.50 h and finally activated in situ, by heating at 200 °C, at a rate of 5 °C min^{-1}, for 180 min. After treatment, the textural properties of the material were

determined by nitrogen adsorption and desorption experiments at -196 °C using a Micromeritics (Norcross, GA, USA) adsorption analyzer model 3Flex. The specific surface area (SSA) was calculated with the Brunauer-Emmet-Teller method (BET) in the relative pressure range (P/P°) 0.01–1.0, selecting a linear portion of the BET graph in compliance with the Rouquerol criteria. The mesopore size distribution was determined by the Barret-Joyner-Halenda (BJH) model applied to desorption data, while the assessment of microporosity was carried out by the t-plot model, using the Harkins-Jura model as a thickness curve equation. For the porosimetry of chars, a minimum equilibrium interval of 10 s and 20 s was used, respectively, in the relative pressure (P/P°) ranges of 0.01–0.1 and 0.1–1.0, with a maximum relative tolerance of 5% of the targeted pressure and an absolute tolerance of 5 mmHg.

1.5. Morphological and structural analysis

SEM-EDX is a method capable of generating high-resolution images of the sample surface and collecting element spectra in selected points of the material. In this study, the images and the spectra were carried out using a TESCAN (Brno, Czech Republic) SEM, model VEGA3.

FT-IR analysis was performed using a Perkin Elmer (FTIR spectrometer, model FT-IR 100); thus, the spectra were recorded on KBr pellets in the range of 400 - 4000 cm^{-1}, with a resolution of 4 cm^{-1} for each determination.

The crystal phases of the biomass samples were analyzed by XRD. The patterns were registered in the 2Θ range from 5 to 80 using a Bruker D8 Advance diffractometer, equipped with a Ni-filtered CuKa (1.5418 Å) radiation source (0.1 ° step, 1.00 s step time).

The composition of the inorganic elements was identified using the Bruker S2 PUMA X-ray fluorescence spectrometer (Bruker XRF instruments, Germany). About 1.0 g of the sample was mounted in a Spectra Membrane Ultra-Polyester Thin-Film with a diameter of 4 cm and a thickness of 1.5 µm. The XRF analysis was performed under an air atmosphere, and the data were analyzed by Spectra Elements software (AXS-34).

Table SM1-1: Experimental design and conditions and responses, and responses (Y1: Yield, Y2: SAA, and Y3: methylene blue adsorption capacity)

Run	Factors		Responses		
			Yield (%)	SAA (m^2/g)	MB adsorption (mg/g)
1	700	PAC	22.35	6.67	155.49
2	800	WAC	8.27	18.25	232.89
3	700	BAC	17.51	11.46	197.77
4	800	PAC	22.28	11.57	268.09
5	800	BAC	15.7	19.15	358.37
6	600	WAC	12.68	9.85	40.94
7	800	DOW	31.1	21.66	432.01
8	600	BAC	19.93	10.54	117.72
9	600	PAC	22.42	9.98	40.94
10	700	WAC	10.11	12.5	98.6
11	700	DOW	32.75	15.65	183.73
12	600	DOW	33.52	6.88	42.66

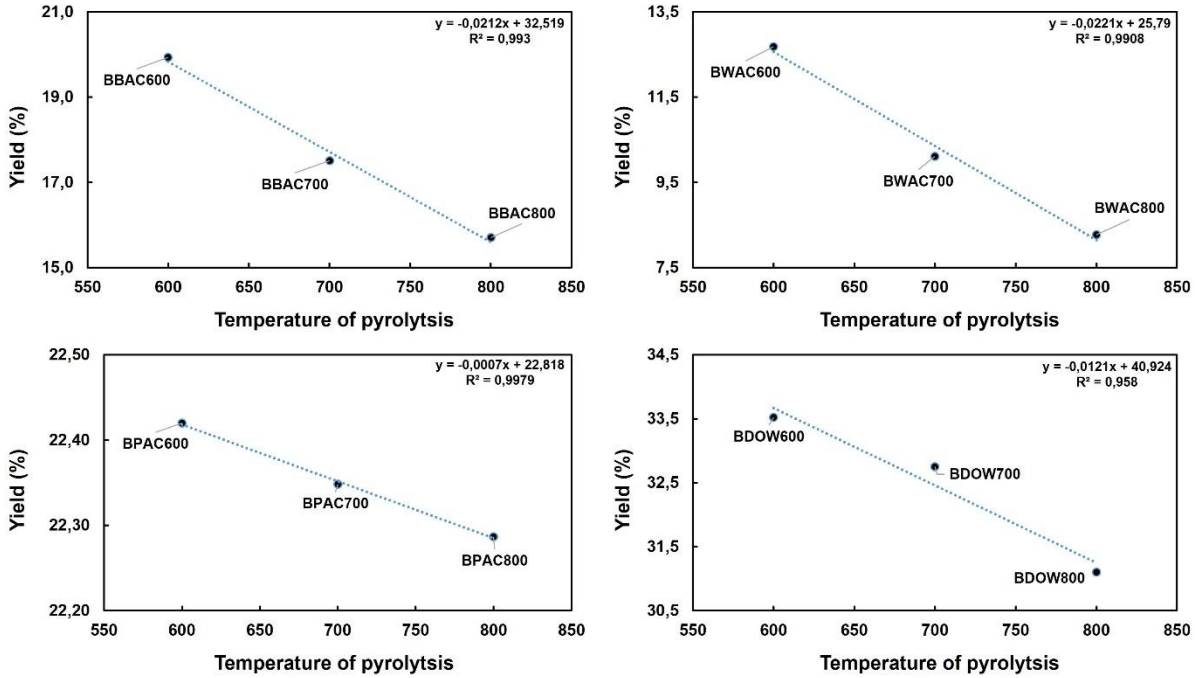

Figure SM1-1: Effect of pyrolysis temperature on the yield of biochars derived from DOW: de-oiled olive mill waste, BAC: black argan press cake, PAC: pellet argan cake, and WAC: white argan press cake.

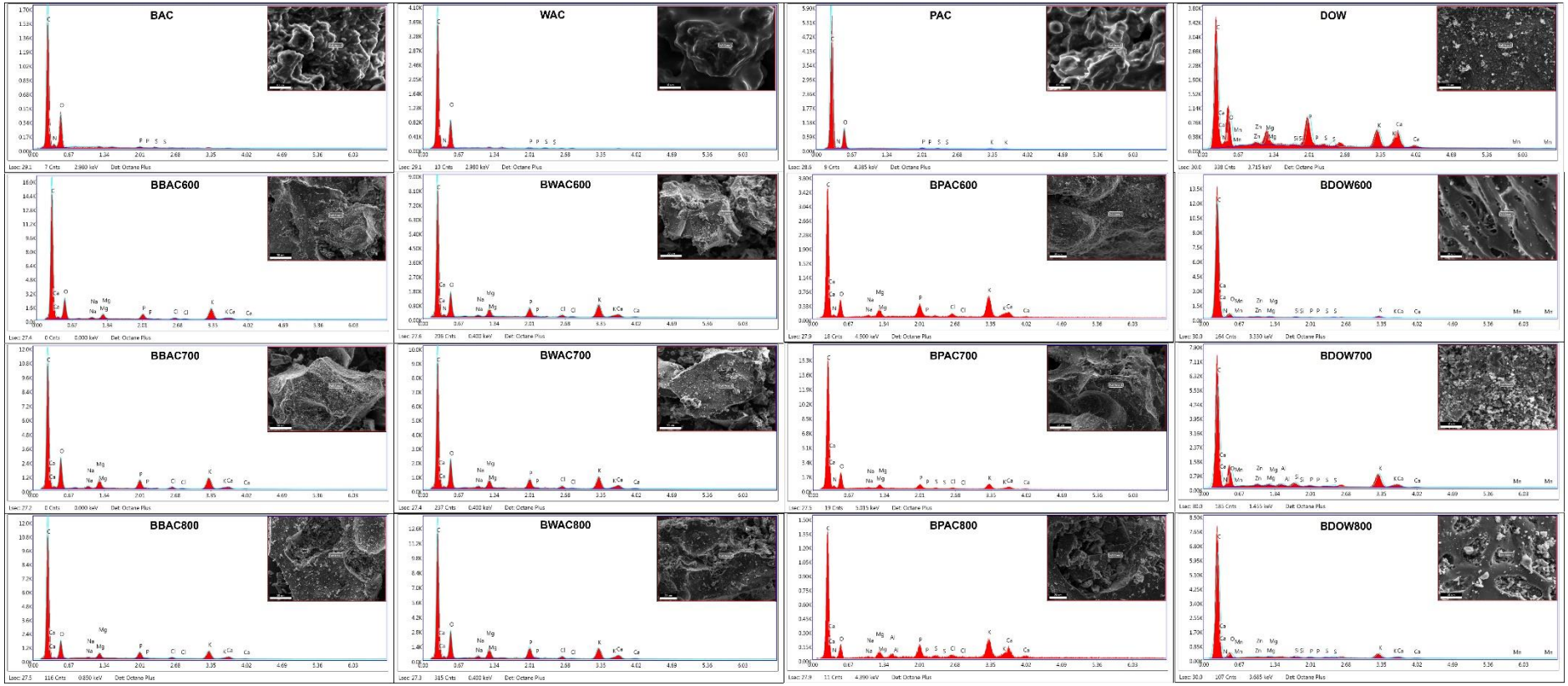

Figure SM1-2: EDX spectra quantification of the produced biochars derived from DOW: de-oiled olive mill waste, BAC: black argan press cake, PAC: pellet argan cake, and WAC: white argan press cake.

Table SM1-2: FT-IR Spectra band assignment of the samples

Wavelength (cm^{-1})	**Mode**	**Correspondence**
3000–3700	H–OH Stretching	Phenols, carboxylic groups
2856–2923	C–H Stretching	Aliphatic compounds
1745	C=O Stretching	Aldehyde
1650	C=C Stretching	Aromatic ring
1547	C=C Stretching	Aliphatic structures
1460	C–H Bending	Alkane
1384	C–O Vibrations	Carboxylate groups
1000–1250	C–O Stretching	Lignin and polysaccharides

Supplementary Materials 2 – Chapter III

1. Biochar characterization

1.1. Structural and morphological analysis

The morphology of the biochar was carefully examined using a field emission scanning electron microscope, in particular, the VEGA3 LMU model. FTIR spectra of the biochar were recorded in the 400-4000 cm^{-1} range using a Bruker VERTEX 70 FTIR spectrophotometer.

1.2. Elemental analysis

The determination of C, H, N, and S contents was performed using a Euro EA-CHNSO Elemental Analyzer. The percentage oxygen content was estimated as the difference with those of the other elements: O (%) = 100 – (C% + H% + N% + S%).

1.3. Proximate analysis

The volatile matter (VM) was determined by the closed furnace vent port and preheated to 950 °C, placed in covered crucibles with preheated biochar at 105 °C (ASTM Standard D1762-84).

The ash content (AC), determined in accordance with the official method (ASTM Standard D1762-84), by heating the biochar from ambient to 750 °C at a rate of 5 °C min^{-1}, holding 750 °C for 6 h, then cooling to 105 °C, was obtained by weighing the material to a constant weight.

While the fixed carbon (FC) is the carbon remaining after removing volatile matter, moisture, and ash content from the biofuel.

1.4. pH of the point of zero charge

The biochar sample, air-dried and crushed to a particle size < 3 mm, divided into 0.1 g aliquots, is placed in contact with 50 mL of 0.1 M NaCl solution previously adjusted to pH values of 2, 3, 4, 5, 6, 7, 8, 9, 10, and 11 by addition of HCl and NaOH (pH_i). The sealed flasks were shaken at 150 rpm for 32 h before recording the final pH value (pH_f) of the supernatant.

The difference between pHi and pH_f ($\Delta pH=pH_i-pH_f$) must be plotted as a function of pHi, and the point of intersection of the resulting curve with the pHi axis is the pH of the point of zero charge (pH_{PZC}).

1.5. Physisorption analysis

The biochar sample was preliminarily degassed under nitrogen flow at 200 °C for 1 h, then evacuated under high vacuum (< 10–2 mbar), supplied by an oil-based vacuum pump coupled to a high vacuum system, for 0.50 h and finally activated in situ, by heating at 200 °C, at a rate of 5 °C min-1, for 180 min. After treatment, the textural properties of the material were determined by nitrogen adsorption and desorption experiments at -196 °C using a Micromeritics (Norcross, GA, USA) adsorption analyser model 3Flex. The specific surface area (SSA) was calculated with the Brunauer-Emmet-Teller method (BET) in the relative pressure range (P/P°) 0.01–1.0, selecting a linear portion of the BET graph in compliance with the Rouquerol criteria. The mesopore size distribution was determined by the Barret-Joyner-Halenda (BJH) model applied to desorption data, while the assessment of microporosity was carried out by the t-plot model, using the Harkins-Jura model as the thickness curve equation. For the porosimetry of chars, a minimum equilibrium interval of 10 s and 20 s was used, respectively, in the relative pressure (P/P°) ranges of 0.01–0.1 and 0.1–1.0, with a maximum relative tolerance of 5% of the targeted pressure and an absolute tolerance of 5 mmHg.

Table SM2-1: Physicochemical characteristics of biochar from olive pomace

Parameters	**Biochar produced**
Ash contents (%)	4.92
VM (%)	12.93
Fixed carbon[a] (%)	82.15
C_{Org} (%)	90.11
C_{Ic} (%)	0.002
C_{Tc} (%)	90.12
N (%)	1.31
H (%)	2.0
S (%)	0
O[a] (%)	6.57
Atomic ratio O/C	0.054
Atomic ratio H/C	0.26
Atomic ratio (O + N)/C	0.067
BET surface area ($m^2 g^{-1}$)	106
Micropore surface area ($m^2 g^1$)	n.d.
Mesopore surface area ($m^2 g^1$)	113

[a] calculated by difference.

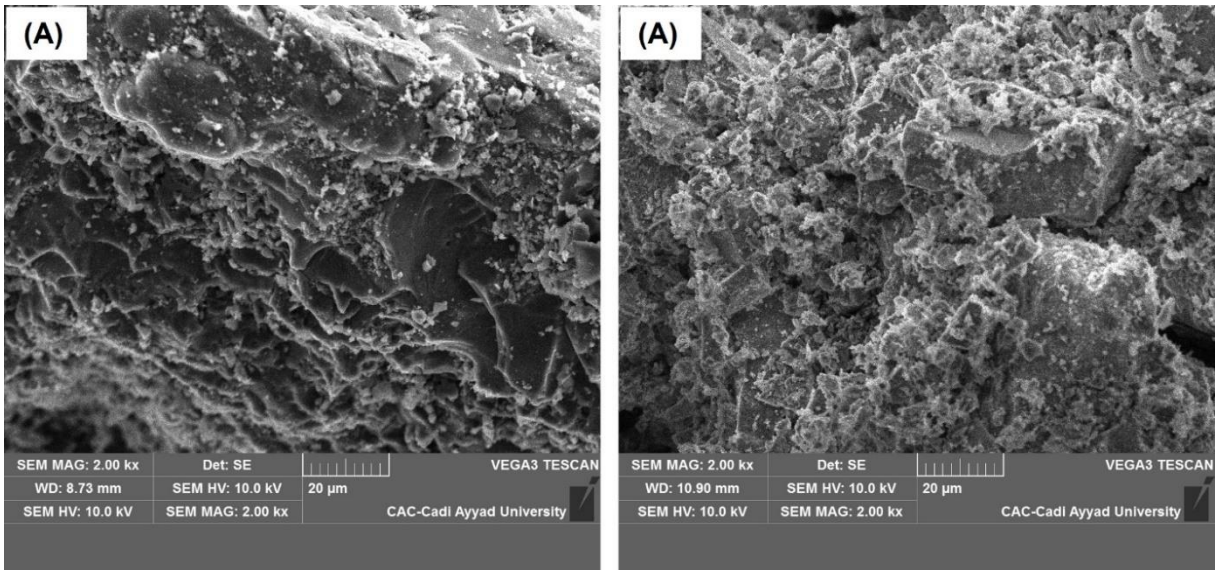

Figure SM2-1: SEM surface scan of biochar (A) and sand (B) used in CFS

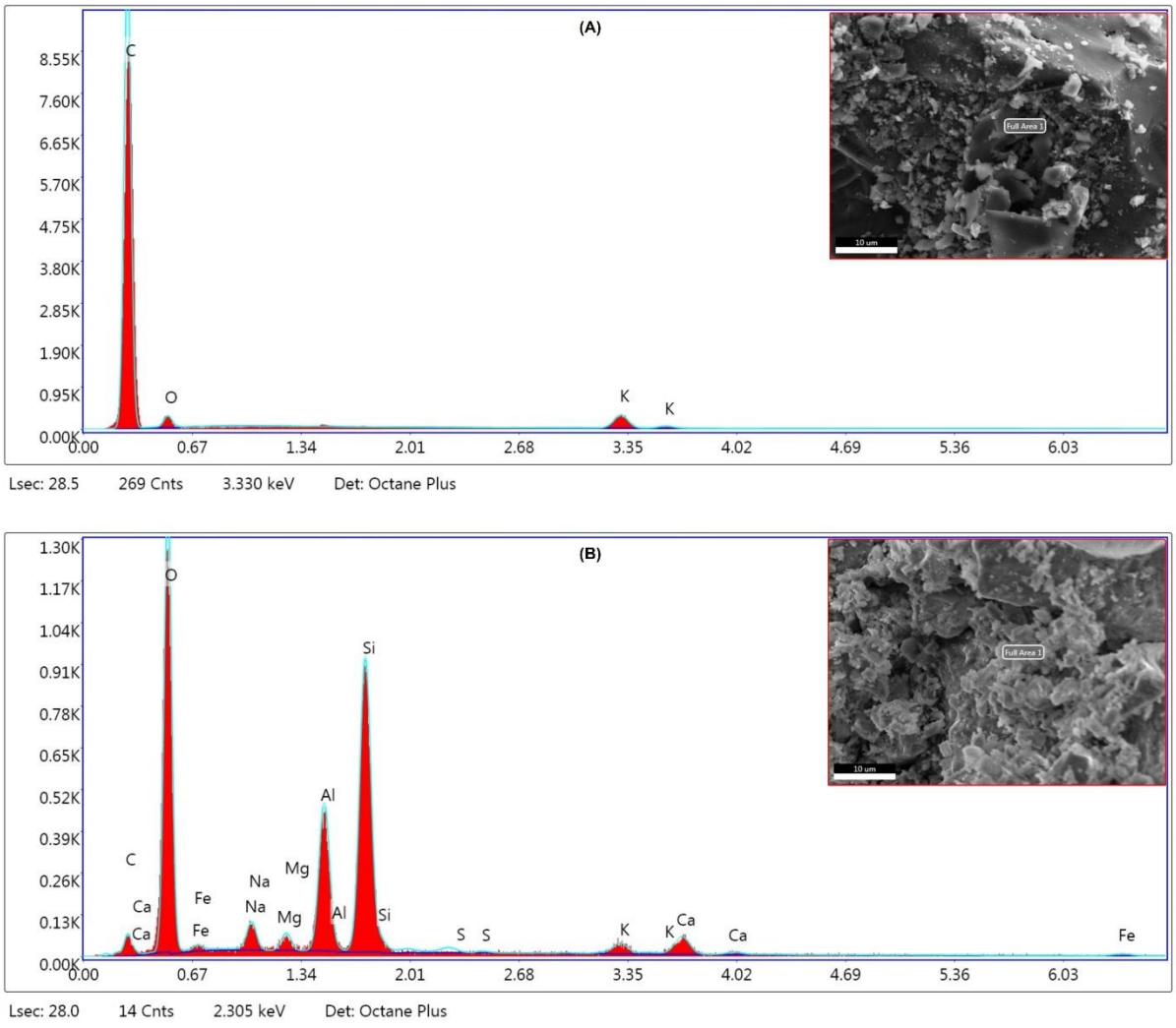

Figure SM2-2: EDX pics of biochar (A) and sand (B) used in CFS

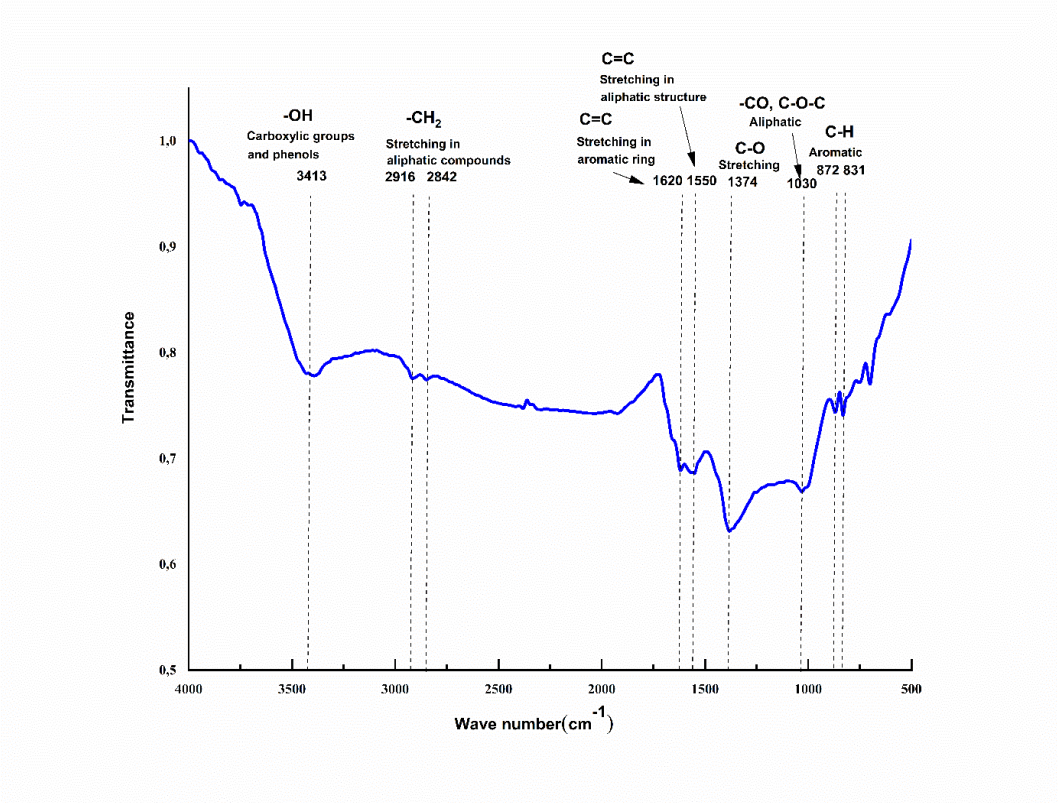

Figure SM2-3: FT-IR analysis of biochar produced

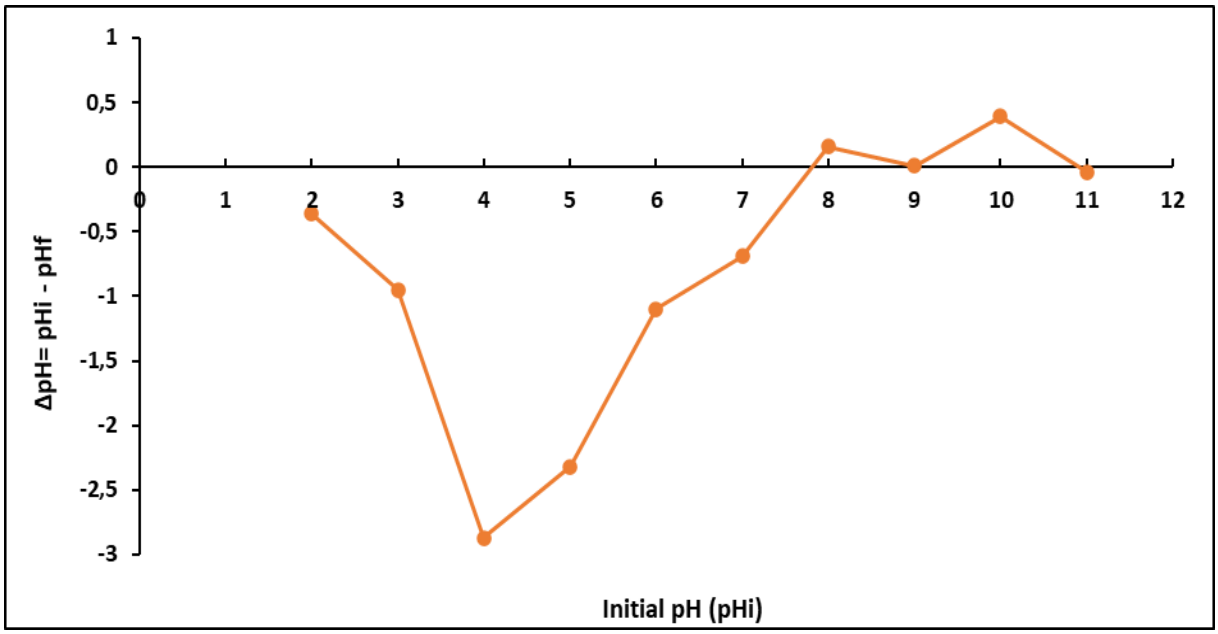

Figure SM2-4: Point of zero charge of biochar produced

Table SM2-2: Inorganic composition of biochar and sand realized by EDX

Element	Inorganic composition of biochar		Inorganic composition of sand	
	Weight %	**Atomic %**	**Weight %**	**Atomic %**
C	83.43	91.49	3.69	6.38
O	6.02	4.95	42.81	55.60
Fe	-	-	0.99	0.37
Na	-	-	2.25	2.03
Mg	-	-	1.21	1.03
Al	-	-	11.85	9.13
Si	-	-	27.63	20.45
S	-	-	0.06	0.04
K	10.55	3.56	2.84	1.51
Ca	-	-	6.68	3.46

Figure SM2-5: Picture of the sand and the biochar produced from olive pomace used in this study.

2. Treatment performance in different CFSs

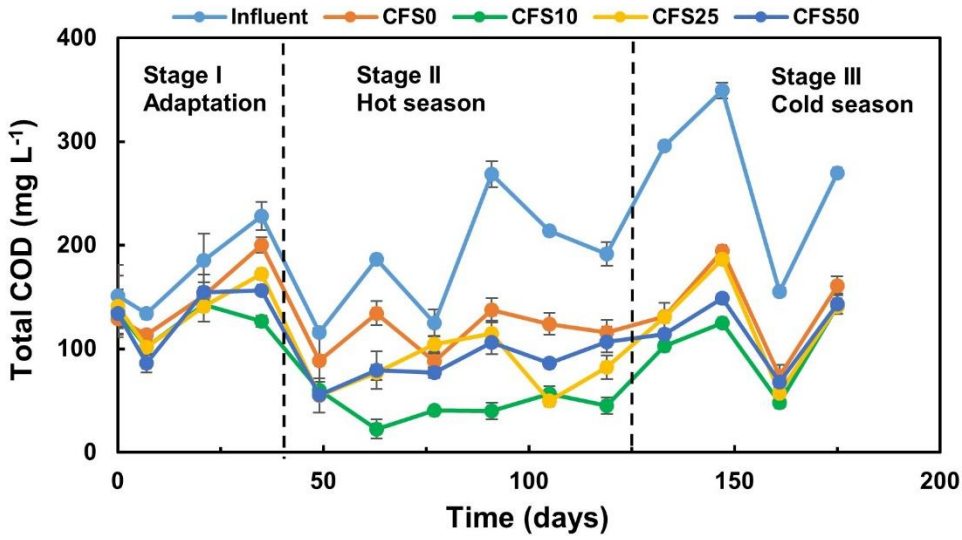

Figure SM2-6: Evolution of the total chemical oxygen demand concentration in the influent and effluent of column filtration systems filled with sand (CFS0), and sand-biochar mixtures with 10% (CFS10), 25% (CFS25), and 50% (CFS50) of biochar.

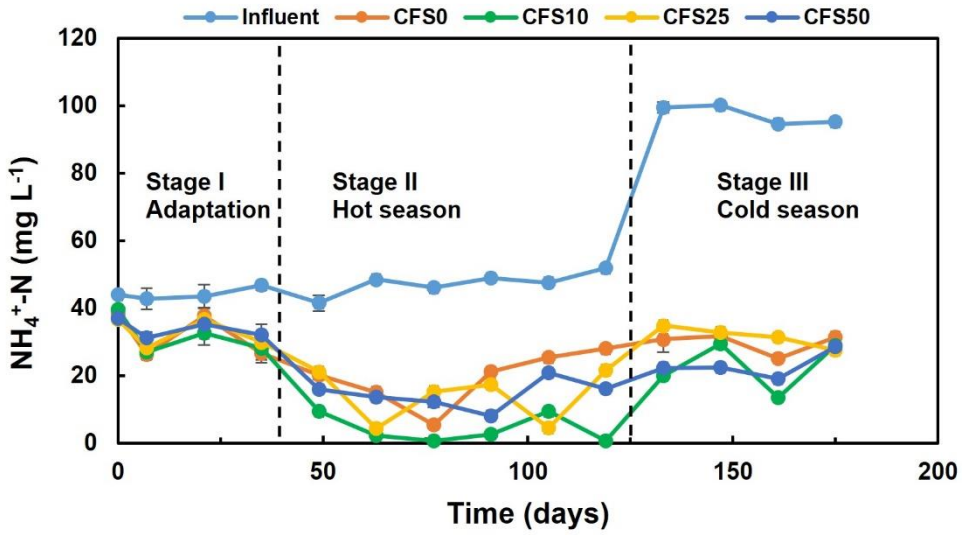

Figure SM2-7: Evolution of the ammonia concentration in the influent and effluent of column filtration systems filled with sand (CFS0), and sand-biochar mixtures with 10% (CFS10), 25% (CFS25), and 50% (CFS50) of biochar.

Supplementary Materials 3 – Chapter III

1. Biochar characterisation

1.1. Structural and morphological analysis

The morphology of the biochar, particularly the VEGA3 LMU model, was carefully examined using a field emission scanning electron microscope.

1.2. Elemental analysis

C, H, N, and S contents were determined using a Euro EA-CHNSO Elemental Analyser. The percentage oxygen content was estimated as the difference with those of the other elements: O (%) = 100 – (C% + H% + N% + S% + AC).

1.3. Proximate analysis

The volatile matter (VM) was determined by the closed furnace vent port and preheated to 950 °C, placed in covered crucibles with preheated biochar at 105 °C (ASTM Standard D1762-84).

The ash content (AC) was determined in accordance with the official method (ASTM Standard D1762-84) by heating the biochar from ambient to 750 °C at a rate of 5 °C min−1, holding 750 °C for 6 h, and then cooling to 105 °C. The material was weighed to a constant weight.

The fixed carbon (FC) is the carbon remaining after the removal of volatile matter, moisture, and ash content from the biofuel.

1.4. pH of the point of zero charge

The biochar sample, air-dried and crushed to a particle size < 3 mm, divided into 0.1 g aliquots, is placed in contact with 50 mL of 0.1 M NaCl solution previously adjusted to pH values of 2, 3, 4, 5, 6, 7, 8, 9, 10, and 11 by addition of HCl and NaOH (pHi). The sealed flasks were shaken at 150 rpm for 32 h before recording the final pH value (pHf) of the supernatant.

The difference between pHi and pHf (ΔpH=pHi-pHf) must be plotted as a function of pHi, and the point of intersection of the resulting curve with the pHi axis is the pH of the pH_{PZC}.

1.5. Physisorption analysis

The biochar sample was preliminarily degassed under nitrogen flow at 200 °C for 1 h, then

evacuated under high vacuum (< 10–2 mbar), supplied by an oil-based vacuum pump coupled to a high vacuum system, for 0.50 h and finally activated in situ, by heating at 200 °C, at a rate of 5 °C min-1, for 180 min. After treatment, the textural properties of the material were determined by nitrogen adsorption and desorption experiments at -196 °C using a Micromeritics (Norcross, GA, USA) adsorption analyser model 3Flex. The specific surface area (SSA) was calculated with the Brunauer-Emmet-Teller method (BET) in the relative pressure range (P/P°) 0.01–1.0, selecting a linear portion of the BET graph in compliance with the Rouquerol criteria. The mesopore size distribution was determined by the Barret-Joyner-Halenda (BJH) model applied to desorption data, while the assessment of microporosity was carried out by the t-plot model, using the Harkins-Jura model as the thickness curve equation. For the porosimetry of chars, a minimum equilibrium interval of 10 s and 20 s were used, respectively, in the relative pressure (P/P°) ranges of 0.01–0.1 and 0.1–1.0, with a maximum relative tolerance of 5% of the targeted pressure and an absolute tolerance of 5 mmHg.

Supplementary Materials 4 – Chapter IV

1. Biochar characterization

1.1. Structural and morphological analysis

The morphology of the biochar was carefully examined using a field emission scanning electron microscope, in particular, the VEGA3 LMU model. FTIR spectra of the biochar were recorded in the 400-4000 cm^{-1} range using a Bruker VERTEX 70 FTIR spectrophotometer.

1.2. Elemental analysis

The determination of C, H, N, and S contents was performed using a Euro EA-CHNSO Elemental Analyser. The percentage oxygen content was estimated as the difference with those of the other elements: O (%) = 100 – (C% + H% + N% + S% + Ash content).

1.3. Proximate analysis

The volatile matter (VM) was determined by the closed furnace vent port and preheated to 950 °C, placed in covered crucibles with preheated biochar at 105 °C (ASTM Standard D1762-84).

The ash content (AC), determined in accordance with the official method (ASTM Standard D1762-84), by heating the biochar from ambient to 750 °C at a rate of 5 °C min^{-1}, holding 750 °C for 6 h, then cooling to 105 °C, was obtained by weighing the material to a constant weight. While the fixed carbon (FC) is the carbon remaining after removal of volatile matter, moisture, and ash content from the biofuel.

1.4. pH of the point of zero charge

The biochar sample, air-dried and crushed to a particle size < 3 mm, divided into 0.1 g aliquots, is placed in contact with 50 mL of 0.1 M NaCl solution previously adjusted to pH values of 2, 3, 4, 5, 6, 7, 8, 9, 10, and 11 by addition of HCl and NaOH (pH_i). The sealed flasks were shaken at 150 rpm for 32 h before recording the final pH value (pH_f) of the supernatant.

The difference between pHi and pH_f ($\Delta pH=pH_i-pH_f$) must be plotted as a function of pHi, and the point of intersection of the resulting curve with the pHi axis is the pH of the point of zero charge (pH_{PZC}).

1.5. Physisorption analysis

The biochar sample was preliminarily degassed under nitrogen flow at 200 °C for 1 h, then evacuated under high vacuum (< 10–2 mbar), supplied by an oil-based vacuum pump coupled to a high vacuum system, for 0.50 h and finally activated in situ, by heating at 200 °C, at a rate of 5 °C min^{-1}, for 180 min. After treatment, the textural properties of the material were determined by nitrogen adsorption and desorption experiments at -196 °C using a Micromeritics (Norcross, GA, USA) adsorption analyser model 3Flex. The specific surface area (SSA) was calculated with the Brunauer-Emmet-Teller method (BET) in the relative pressure range (P/P°) 0.01–1.0, selecting a linear portion of the BET graph in compliance with the Rouquerol criteria. The mesopore size distribution was determined by the Barret-Joyner-Halenda (BJH) model applied to desorption data, while the assessment of microporosity was carried out by the t-plot model, using the Harkins-Jura model as the thickness curve equation. For the porosimetry of chars, a minimum equilibrium interval of 10 s and 20 s was used, respectively, in the relative pressure (P/P°) ranges of 0.01–0.1 and 0.1–1.0, with a maximum relative tolerance of 5% of the targeted pressure and an absolute tolerance of 5 mmHg.

Table SM4-1: Physicochemical characteristics of biochar from olive pomace

Parameters	**Biochar produced**
Ash contents (%)	4.92
VM (%)	12.93
Fixed carbon[a] (%)	82.15
C_{Org} (%)	90.11
C_{Ic} (%)	0.002
C_{Tc} (%)	90.12
N (%)	1.31
H (%)	2.0
S (%)	0
O[a] (%)	6.57
Atomic ratio O/C	0.054
Atomic ratio H/C	0.26
Atomic ratio (O + N)/C	0.067
BET surface area (m^2/g)	106
Micropore surface area (m^2/g)	n.d.
Mesopore surface area (m^2/g)	113

[a] calculated by difference.

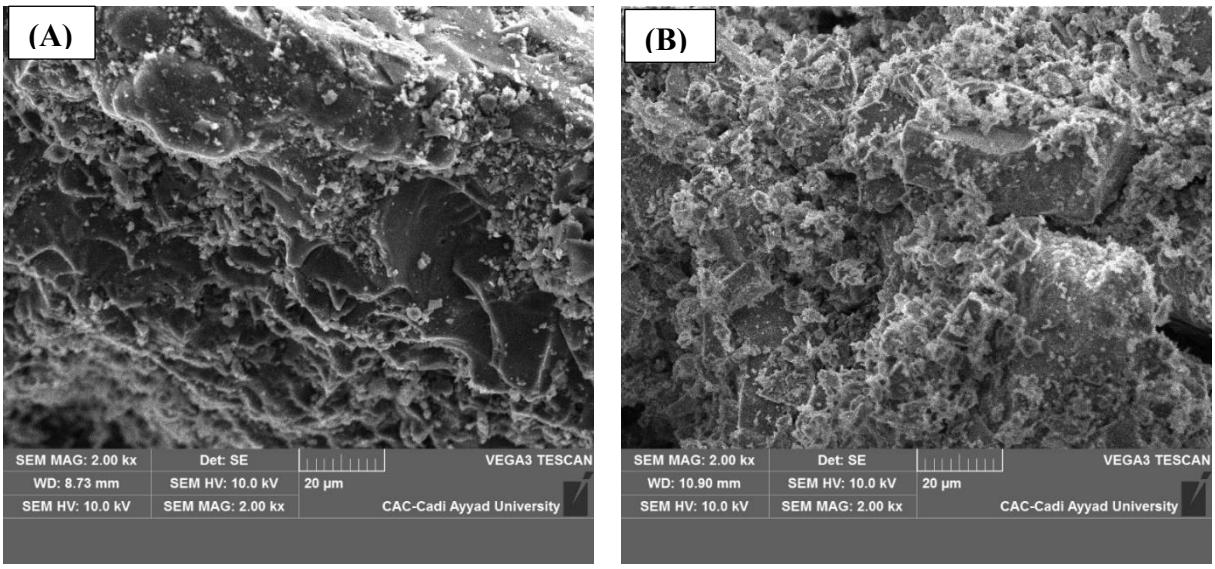

Figure SM4-1: SEM surface scan of biochar (A) and sand (B) used in VF-CWs

2. Analytical methodology

2.1. Conventional water quality parameters

Water quality parameters were determined using the standard methods of AFNOR (1997) and Rodier (2009). TSS were measured by filtering the samples through a 0.45 µm Millipore (Burlington, MA, USA) glass fibre filter, followed by drying at 105 °C until a constant weight was achieved (AFNOR-T90-105). COD was determined via dichromate digestion and colourimetry (AFNOR T90-101). TP was analysed using the molybdate–ascorbic acid method following potassium peroxydisulfate digestion (AFNOR T 90-023), while orthophosphate (PO_4^{3-}) was quantified using the same method (AFNOR T 90-022). TKN was measured via Kjeldahl mineralisation, ammonium distillation, and acidimetric titration. Ammoniacal nitrogen was determined using the indophenol method (AFNOR T 90-015), nitrite (NO_2^-–N) using the diazotation method (AFNOR T 90-013), and nitrate (NO_3^-–N) after reduction to nitrite via a copper–cadmium column (Rodier, 2009), while the TN is calculated as the sum of TKN, NO_2^-–N, and NO_3^-–N. Sulphates were measured nephelometrically, and total hardness, calcium and magnesium were determined simultaneously using the EDTA titrimetric method. Dissolved oxygen (DO), electrical conductivity (EC), and pH were measured in situ with a multi-parameter HI 9829 probe (HANNA, Woonsocket, RI, USA). The absorbance of the influent and effluent samples was measured at 254 and 420 nm. The pathogen indicators of faecal pollutants (e.g., FS,

FC, TC) were quantified following AFNOR standard methods (AFNOR 1997). TC and FC were grown on TTC Tergitol medium and incubated at 37 °C and 44.5 °C, respectively, for 24 h before colony counting. FS were enumerated on BEA medium at 44.5 °C for 24 h. The bacterial removal efficiency was expressed by the following equation:

$$\log_{10} \text{removal} = \log (\text{influent/effluent})$$

2.2. QuEChERS extraction of particulate samples

The procedure was adapted from a methodology developed for the extraction of pharmaceutical compounds in sewage sludge samples. One gram of freeze-dried sludge was weighed into a 50 mL centrifuge tube, and 5 mL of ultrapure water was added. The mixture was hand-shaken for 15 s and vortex-mixed for 1 min, and 10 mL of CH_3CN was added. After a further step of hand-shaking (15 s) and vortex mixing (1 min), 2 g of NaCl and 2 g of $MgSO_4$ were added, and the obtained mixture underwent additional hand-shaking and vortex-mixing processes. The tube was centrifuged at 1200 g for 4 min, and 1 mL of the CH_3CN supernatant phase was made up to 10 mL with acidic water. Finally, the diluted extracts were analysed by LC-MS/MS.

2.3. Apparent recovery

The apparent recovery percentage of the method was assessed, following the IUPAC indications, by spiking in triplicate 1 g f.d. aliquots with mass-labeled compounds (5 ng g^{-1} for Diclofenac-D4, Venlafaxine-D6, Carbamazepine-D10). In order to evaluate the QuEChERS extraction efficiency, three 1 g freeze-dried aliquots of the particulate samples were fortified with mass-labeled compounds (5 ng g^{-1} for Diclofenac-D4, Venlafaxine-D6, Carbamazepine-D10). It should be noted that these compounds cover the entire range of physicochemical properties of the investigated molecules (e.g., log K_{OW} 2,77-0,74) and are therefore representative of the whole set of target analytes. The spiking procedure was performed by adding 500 mL of the CH_3CN standard solution to 1 g of dried sludge, then the solvent was evaporated at room temperature for 24h.

Pharmaceutical concentrations in the spiked samples, after the QuEChERS extraction, were then quantified (C_{found}) using a standard calibration curve prepared in the matrix-free procedural blank and AR% calculated according to the following equation.

$$AR\% = \frac{Cfound}{Cspiked} * 100$$

Based on the procedure described above, the apparent recovery percentage takes into account the combined effect of both matrix effects and reduced recovery during partition stages (e.g., between water and acetonitrile) due to the presence of matrix components. The QuEChERS extraction efficiency of mass-labeled analytes was found in the range of 72-121% and resulted in therefore suitable method for the extraction of selected PhCs and their transformation products (TPs) from sewage sludge.

Table SM4-2: List of the investigated pharmaceutical compounds and related transformation products, their abbreviations and selected physicochemical properties: molecular weight (MW, Da), CAS number, Log K_{OW}[a] (pH=7), pK_a [a] (most acidic/most basic, T=25 °C).

Category	Compound	Abbreviation	MW	CAS	Log Kow	pK_a
Non-steroidal anti-inflammatory drugs and related transformation products	Diclofenac	DIC	296.15	15307-86-5	1.38	4.01/-1.08
	Diclofenac-D4 [b]	DIC-D4	300.15	153466-65-0	1.38	4.01/-1.08
	4'-Hydroxydiclofenac [c]	4'-HYDIC	312.15	64118-84-9	0.89	3.77/0.41
	Ibuprofen	IBU	206.28	15687-27-1	1.71	4.85/n.a.
	1-Hydroxyibuprofen [c]	1-HYIBU	222.28	53949-53-4	0.29	4.57/n.a.
	2-Hydroxyibuprofen [c]	2-HYIBU	222.28	51146-55-5	0.03	4.63/n.a.
	3-Hydroxyibuprofen [c]	3-HYIBU	222.28	53949-54-5	0.09	4.57/n.a.
	Ketoprofen	KET	254.28	22071-15-4	0.72	4.00/n.a.
	Flurbiprofen	FLU	244.26	5104-49-4	2.07	5.12/n.a.
	Fenbufen	FEN	254.28	36330-85-5	0.29	4.22/n.a.
	Naproxen	NAP	230.26	22204-53-1	0.29	4.24/n.a.
	O-Desmethylnaproxen [c]	O-DMNAP	216.23	52079-10-4	-0.30	4.35/n.a.
β-Blockers	Atenolol	ATE	266.34	29122-68-7	-1.80	14.08/9.27
	Bisoprolol	BIS	325.4 4	66722-44-9	-0.03	14.09/9.27
Antibiotics	Ciprofloxacin [d, e]	CIP	331.34	85721-33-1	-0.77	5.96/8.69
	Erythromycin [d]	ERY	733.93	114-07-8	0.60	12.45/9.00
	Azithromycin [d]	AZI	748.98	83905-01-5	-3.05	12.46/11.56
	Clarithromycin [d]	CLA	747.95	81103-11-9	1.24	12.46/9.00
	Sulphamethoxazole [e, f]	SMZ	253.28	723-46-6	0.03	5.86/1.97
	Trimethoprim [e, f]	TMP	290.32	738-70-5	0.92	n.a./7.16
Antifungals	Clotrimazole [e, f]	CLT	344.84	23593-75-1	5.79	n.a./6.26
	Miconazole [e]	MIC	416.12	22916-47-8	5.87	n.a./6.48
	Fluconazole [e, f]	FLC	306.28	86386-73-4	0.56	12.68/2.3
Psychiatric drugs	Carbamazepine	CBZ	236.27	298-46-4	1.90	13.94/n.a.
	Carbamazepine-D10 [b]	CBZ-D10	236.27	298-46-4	1.90	13.94/n.a.
	Diazepam	DZP	284.74	439-14-5	3.08	13.04/2.92
	Venlafaxine [e, f]	VEN	277.41	93413-69-5	0.74	14.42/9.01
	Venlafaxine-D6 [b,	VEN-D6	324.93	1216539-56-8	0.74	14.42/9.01
	O-Desmethylvenlafaxine [c, e, f]	O-VEN	263.38	93413-62-8	0.59	9.8/8.9
Diuretics	Furosemide	FUR	330.74	54-31-9	-1.50	3.5/-0.72
Statins	Atorvastatin	ATO	558.64	134523-00-5	0.91	4.31/n.a.
Analgesics	Acetaminophen	ACE	151.16	103-90-2	0.47	9.46/n.a.
Antihypertensive	Ramipril	RAM	415.51	87333-19-5	0.04	3.66/5.27
Urinary α-Blockers	Tamsulosin	TAM	408.51	106133-20-4	0.64	9.78/8.84
Gastric Protector	Pantoprazole	PAN	383.37	102625-70-7	2.17	9.54/3.55
	Ranitidine	RNT	314.40	66357-35-5	-0.32	n.a./8.35

[a] Calculated by Chemicalize online platform (ChemAxon, Budapest, HU) [b] Internal standards. [c] Major metabolites. [d] Pharmaceutical compounds included in the Watch List 2018/840/EU. [e] Pharmaceutical compounds included in the Watch List 2020/1161/EU. [f] Pharmaceutical compounds included in the Watch List 2022/1307/EU.

Supplementary Materials 5 – Chapter IV

1. Target analytes

The list of target analytes and internal standards, as well as their physicochemical properties, are reported in Table SM5-1.

Table SM5-1: List of the investigated pharmaceutical compounds and related transformation products. their abbreviations and selected physicochemical properties: molecular weight (MW, Da); CAS number; Log KOWa (pH=7); pKa a (most acidic/most basic. T=25 °C).

Category	Compound	Abbreviation	MW	CAS	Log Kow	pK_a
Non-steroidal anti-inflammatory drugs and related transformation products	Diclofenac	DIC	296.15	15307-86-5	1.38	4.01/-1.08
	Diclofenac-D4 [b]	DIC-D4	300.15	153466-65-0	1.38	4.01/-1.08
	4'-Hydroxydiclofenac [c]	4'-HYDIC	312.15	64118-84-9	0.89	3.77/0.41
	Ibuprofen	IBU	206.28	15687-27-1	1.71	4.85/n.a.
	1-Hydroxyibuprofen [c]	1-HYIBU	222.28	53949-53-4	0.29	4.57/n.a.
	2-Hydroxyibuprofen [c]	2-HYIBU	222.28	51146-55-5	0.03	4.63/n.a.
	3-Hydroxyibuprofen [c]	3-HYIBU	222.28	53949-54-5	0.09	4.57/n.a.
	Ketoprofen	KET	254.28	22071-15-4	0.72	4.00/n.a.
	Flurbiprofen	FLU	244.26	5104-49-4	2.07	5.12/n.a.
	Fenbufen	FEN	254.28	36330-85-5	0.29	4.22/n.a.
	Naproxen	NAP	230.26	22204-53-1	0.29	4.24/n.a.
	O-Desmethylnaproxen [c]	O-DMNAP	216.23	52079-10-4	-0.30	4.35/n.a.
	Acetylsalicylic acid	ASA	180.16	50-78-2	-2.02	3.41/n.a.
β-Blockers	Atenolol	ATE	266.34	29122-68-7	-1.80	14.08/9.27
	Bisoprolol	BIS	325.4 4	66722-44-9	-0.03	14.09/9.27
Antibiotics	Levofloxacin	LVF	361.37	100986-85-4	-0.80	5.77/8.31
	Ciprofloxacin [d. e]	CIP	331.34	85721-33-1	-0.77	5.96/8.69
	Erythromycin [d]	ERY	733.93	114-07-8	0.60	12.45/9.00
	Azithromycin [d]	AZI	748.98	83905-01-5	-3.05	12.46/11.56
	Clarithromycin [d]	CLA	747.95	81103-11-9	1.24	12.46/9.00
	Sulphamethoxazole [e. f]	SMZ	253.28	723-46-6	0.03	5.86/1.97
	Trimethoprim [e. f]	TMP	290.32	738-70-5	0.92	n.a./7.16
Antifungals	Clotrimazole [e. f]	CLT	344.84	23593-75-1	5.79	n.a./6.26
	Miconazole [e]	MIC	416.12	22916-47-8	5.87	n.a./6.48
	Fluconazole [e. f]	FLC	306.28	86386-73-4	0.56	12.68/2.3
Psychiatric drugs	Carbamazepine	CBZ	236.27	298-46-4	1.90	13.94/n.a.
	Carbamazepine-D10 [b]	CBZ-D10	236.27	298-46-4	1.90	13.94/n.a.
	Diazepam	DZP	284.74	439-14-5	3.08	13.04/2.92
	Venlafaxine [e. f]	VEN	277.41	93413-69-5	0.74	14.42/9.01
	Venlafaxine-D6 [b.]	VEN-D6	324.93	1216539-56-8	0.74	14.42/9.01
	O-Desmethylvenlafaxine [c. e. f]	O-VEN	263.38	93413-62-8	0.59	9.8/8.9
Diuretics	Furosemide	FUR	330.74	54-31-9	-1.50	3.5/-0.72
Statins	Atorvastatin	ATO	558.64	134523-00-5	0.91	4.31/n.a.
Analgesics	Acetaminophen	ACE	151.16	103-90-2	0.47	9.46/n.a.
Antihypertensive	Ramipril	RMP	415.51	87333-19-5	0.04	3.66/5.27
Urinary α-Blockers	Tamsulosin	TAM	408.51	106133-20-4	0.64	9.78/8.84
Gastric Protector	Pantoprazole	PAN	383.37	102625-70-7	2.17	9.54/3.55
	Ranitidine	RNT	314.40	66357-35-5	-0.32	n.a./8.35

[a] Calculated by Chemicalize online platform (ChemAxon. Budapest. HU) [b] Internal standards. [c] Major metabolites. [d] Pharmaceutical compounds included in the Watch List 2018/840/EU. [e] Pharmaceutical compounds included in the Watch List 2020/1161/EU. [f] Pharmaceutical compounds included in the Watch List 2022/1307/EU.

2. Characteristics of the Baciacavallo WWTP

The total influent flow to the Baciacavallo WWTP (Prato, Italy) consists of about 49% of industrial wastewater from textile production processes, 50% of domestic wastewater, and a small percentage (0.07%) of sewage from septic tanks. The treatment process involves (i) initial

filtration with bar screens, (ii) primary sedimentation, (iii) biological oxidation, and (iv) clariflocculation. A further treatment with ozone is operating as a final refining system for the removal of residual dyeing agents and organic micropollutants recalcitrant to biological oxidation. The effluent from the ozonation stage is finally released into the Ombrone River.

3. Lab-scale microcosms

Figure SM5-1 illustrates the 12 microcosms located in the outdoor Natural Wastewater Treatment Laboratory (NatLab) of the Department of Chemistry, University of Florence. Table SM5-2 reports the detailed chrono program of the sampling campaign.

Figure SM5-1: Picture of the laboratory scale vertical flow systems at the NatLab laboratory.

4. Biochar production and characterization

Biochar was washed with the BioDea® solution, whose characteristics are shown in Table SM5-2.

Table SM5-2: Characteristics of the BioDea® solution used in this study for the chemical activation of biochars, presented as mean (n = 3) and standard deviation (in bracket).

	Unit	Value
pH	-	4.0 (0.5)
Acetic acid	% v/v	2.2 (0.2)
Phenols	gr kg^{-1}	2.96 (0.08)
Polyphenols	gr kg^{-1}	24 (2)
As	µg L^{-1}	1.16 (0.07)
Cd	µg L^{-1}	5.5 (0.4)
Cr	µg L^{-1}	1.64 (0.05)
Hg	µg L^{-1}	0.29 (0.03)
Ni	µg L^{-1}	14.9 (0.7)
Pb	µg L^{-1}	61 (3)
Sb	µg L^{-1}	3.1 (0.2)
Se	µg L^{-1}	7.3 (0.8)

The elements and polycyclic aromatic hydrocarbons (PAHs) determined according to the EN 12915-1 in the material leachate are shown in Table SM5-3.

Table SM5-3: Water leachable elements (As, Cd, Cr, Hg, Ni, Pb, Sb, and Se, expressed as µg/L) and sum of selected water leachable polycyclic aromatic hydrocarbons (PAHs, ng/L), ash content (%), pH of the point of zero charge (pH_{PZC}), total specific surface area (SSA, m^2/g), micropore SSA (m^2/g), mesopore SSA (m^2/g). and elemental composition (C, H, N, S, and O relative percentage).

Parameter	Value	EN 12915-1 limit
Ash	10.5	15
Sum of PAHs[(b)]	12	20
As	<0.1[(a)]	10
Cd	<0.1[(a)]	0.5
Cr	1.4	5
Hg	<0.1[(a)]	0.3
Ni	1.8	15
Pb	1.1	5
Sb	<0.1	3
Se	<0.1[(a)]	3
pH_{PZC}	7.1	-
SSA	389	-
Micropore SSA	341	-
Mesopore SSA	36	-
C	65.0	-
H	1.0	-
N	0.8	-
S	<0.05[(a)]	-
O	22.1	-

[(a)] Limits of quantification. [(b)] PAHs regulated by the EN 12915-1: fluoranthene. benzo(b)fluoranthene. benzo(k)fluoranthene. benzo(a)pyrene. indeno(1.2.3-c.d)pyrene. and benzo(g.h.i)perylene

5. Sample collection and analysis

Sample collection occurred between July 2022 and March 2023, covering a study period of approximately 8 months. The timeline of the collection of samples for the analysis of PhCs is shown in Table SM5-4.

Table SM5-4: Chrono program of the sampling campaign

ID	Date (dd/mm/yy)	Days after start-up	Weeks after start-up
1	26/07/2022	2	0.29
2	28/07/2022	4	0.57
3	01/08/2022	8	1.14
4	18/08/2022	25	3.57
5	06/09/2022	44	6.29
6	19/09/2022	57	8.14
7	03/10/2022	71	10.14
8	18/10/2022	86	12.29
9	27/10/2022	95	13.57
10	29/11/2022	128	18.29
11	13/12/2022	142	20.29
12	25/01/2023	185	26.43
13	07/02/2022	198	28.29
14	08/03/2023	227	32.43

5. Analysis of conventional water quality parameters

Full information on the protocols followed for the determination of Chemical oxygen demand, the inorganic forms of nitrogen, and phosphorus are described below, whereas the obtained data are reported in Table SM5-4.

5.1. Chemical oxygen demand

Chemical oxygen demand was determined using the reagent kits "TNT for COD, 0-40 mg/L O_2" and "TNT for COD, 0-150 mg/L O_2", according to the USEPA approved HACH method 8000, which is based on the classical sample digestion at 150°C for 2 h with $K_2Cr_2O_7$ as oxidation reagent in a 50% sulphuric acid medium, in the presence of Ag_2SO_4 (oxidation catalyst) and $HgSO_4$ (complexing agent). Oxidizable organic compounds react, reducing the dichromate ion to the green Cr(III), and the remaining Cr(VI) is determined at 420 nm.

5.2. Total nitrogen

Total nitrogen was determined by the HACH method 10071, which is based on the alkaline

persulfate sample digestion at 105°C that converts all forms of nitrogen to nitrate. Sodium metabisulfite is then added to eliminate halide interferences, and nitrates are reacted with chromotropic acid under strongly acidic conditions to form a yellow complex with an absorbance maximum at 410 nm.

5.3. Ammonia

Ammonia was determined by the "ammonia nitrogen TNT, 0.02-2.5 mg/L NH_3-N" and "ammonia nitrogen TNT 0.4-50 mg/L NH3-N" kits, according to the HACH method 10031, which consists of the reaction of ammonia with chlorine to form monochloramine. Then, monochloramine is reacted with salicylate to form 5-aminosalicylate, which is in turn oxidized in the presence of a sodium nitroprusside catalyst to form a blue coloured compound. The blue colour is masked by the yellow colour from the excess reagent present to give a green solution, which is analysed at 655 nm.

5.4. Nitrite

Nitrites were analyzed by the USEPA-approved HACH method 8507, using the "NitriVer 3 nitrite reagent, 0.02-0.30 mg/L NO_2^--N" reagent kit. The method consists of the reaction of nitrites with sulfanilic acid to form an intermediate diazonium salt, which couples with chromotropic acid to produce a pink coloured complex measured at 507 nm.

5.5. Nitrate

Nitrates were determined according to the USEPA-approved HACH method 8000 ("NitraVer 5 Nitrate reagent, 0.3-30 mg/L NO_3^--N"), based on the reaction between nitrates and chromotropic acid under strongly acidic conditions to yield a yellow product with a maximum absorbance at 410 nm.

5.6. Total phosphorus

Total phosphorus was determined by the USEPA-approved HACH method 8190, using the "PhosVer 3 with acid persulfate digestion, 0.00–1.10 mg/L" kit, which is based on the reaction of orthophosphate with molybdate to obtain a phosphomolybdate complex in an acid environment. Ascorbic acid then reduces the complex, giving an intense molybdenum blue colour.

5.7. Orthophosphate

Orthophosphates were determined by the USEPA approved HACH method 8048, using the "PhosVer 3 reagent, 0.02 - 2.50 mg/L PO_4^{3-}" kit, which is based on the reduction of phosphates by ascorbic acid. The solution to be analysed is acidified and treated with ammonium molybdate $(NH4)_2MoO_4$ and potassium antimonyl tartrate ($C_8H_4K_2O_{12}Sb_2 \cdot 3H_2O$). The presence of a reducing agent such as ascorbic acid leads to the formation of a complex called molybdate blue that gives the solution a typical blue colour, revealing the presence of phosphate ions in the sample.

Table SM5-4: Mean values and standard deviation (in bracket) of pH, electrical conductivity (EC, µS/cm), dissolved oxygen (DO, mg/L), total suspended solids (TSS, mg/L), chemical oxygen demand (COD), total nitrogen (T-N), ammonia nitrogen (NH_4^+-N), nitrite nitrogen (NO_2^--N), nitrate nitrogen (NO_3^--N), orthophosphate (PO_4^{3-}), total phosphorus (T-P) in the inlet and outlet of microcosms filled with biochar (SSBC) or gravel (G), planted (P), or unplanted (U).

Parameter	Inlet	SSBC-P	SSBC-U	G-P	G-U
pH	7.6 (0.4)[a]	7.7 (0.5)[a]	7.7 (0.4)[a]	7.5 (0.5)[a]	7.6 (0.3)[a]
EC	3038 (828)[a]	2940 (804)[a]	2920 (833)[a]	2991 (846)[a]	2955 (774)[a]
DO	1.0 (0.6)	1.6 (0.4)[a]	1.5 (0.3)[a]	1.3 (0.3)[a]	1.2 (0.4)[a]
TSS	8 (9)[a]	5 (4)[a]	5 (5)[a]	6 (3)[a]	7 (7)[a]
COD	34 (5)[a]	22 (8)[b]	21 (10)[b]	29 (10)[ab]	29 (9)[ab]
T-N	18 (4)[a]	11 (4)[b]	12 (4)[b]	14 (4)[ab]	14 (4)[ab]
NH_4^+-N	14 (3)[a]	5 (2)[b]	5 (2)[b]	9 (3)[c]	10 (3)[c]
NO_2^--N	0.6 (0.6)[a]	0.6 (0.7)[a]	0.5 (0.6)[a]	0.8 (1.0)[a]	0.7 (1.0)[a]
NO_3^--N	4 (2)[a]	9 (4)[b]	10 (5)[b]	6 (3)[c]	7 (3)[c]
PO_4^{3-}	1.6 (1)[a]	1.0 (0.8)[b]	1.4 (1.0)[ab]	1.3 (0.9)[ab]	1.3 (0.9)[ab]
T-P	1.8 (0.8)[a]	1.3 (0.9)[a]	1.6 (0.6)[a]	1.5 (0.7)[a]	1.5 (0.8)[a]

Within the same parameter. values with different letters are statistically different according to the Games–Howell test for comparison of mean values ($P < 0.05$).

6. Analysis of PhCs in wastewater and particulate samples

6.1. Occurrence in wastewater samples

Determination of PhCs was carried out through QuEChERS extraction of solid samples followed by LC-MS/MS analysis. Full details of the developed is here described. Concentrations of target analytes found in particulate samples are reported in Table SM5-6.

Table SM5-6: Mean values (n=3) and standard deviation (in brackets) of selected pharmaceutical compounds detected in particulate matter (PM). Total mass adsorbed by PM accumulated throughout the entire period of treatment (213 days) is also reported. See Table 2 for acronyms meaning.

Compound	Concentration (ng g^{-1})	Total mass (ng)
KET	28.62 (24)	2194.769
4'-HYDIC	10.00 (0)	766.522
DIC	6.81(3)	522.202
AZI	3.08 (.5)	235.880
VEN	1.7083 (0.6)	130.993
CAR	1.69 (0.19)	129.506
CLA	1.30 (0.7)	99.568
CLT	1.23 (0.03)	94.222
FUR	0.77 (0.94)	59.101
MCL	0.50 (0)	38.614
PAN	0.47 (0.06)	36.324
DZP	0.29 (0.15)	22.110
BIS	0.26 (0.39)	20.170
TMP	0.14 (0.06)	10.570
TAM	0.05 (0.06)	3.597

The removal percentages of the investigated PhCs observed in microcosms throughout the entire sampling campaign are reported in Table SM5-7. Furthermore, a comparative study was conducted on the performance of constructed wetlands in removing PhCs (Table SM5-8). considering their most common configurations: horizontal subsurface flow (HSSF). vertical subsurface flow (VSSF). and hybrid constructed wetland (HB) systems.

Table SM5-7: Mean values and standard deviation (in bracket) for removal (%) of the detected analytes in the inlet and outlet of microcosms filled with biochar (SSBC) or gravel (G), planted (P), or unplanted (U).

	SSBC-P	**SSBC-U**	**G-P**	**G-U**
DIC	92 (6)	93 (6)	73 (7)	70 (7)
FUR	50 (40)	58 (30)	-10 (81)	-23 (85)
O-VEN	60 (28)	62 (28)	17 (17)	9 (19)
CBZ	55 (30)	63 (25)	24 (17)	21 (12)
RMP	40 (35	53 (35)	15 (30)	0.1 (21.8)
SMX	41 (33)	46 (28)	16 (26)	2 (30)
VEN	57 (30)	62 (27)	24 (22)	22 (24)
FLU	45 (36)	57 (30)	-39 (29)	-57 (33)
ATE	62 (30)	67 (24)	19 (26)	16 (25)
CLA	-74 (247)	48 (54)	-28 (116)	-62 (260)
BIS	45 (29)	50 (26)	21 (11)	15 (15)
LVF	57 (20)	55 (21)	23 (28)	22 (29)
PAN	86 (60)	130 (53)	-49 (88)	-11 (47)
ATO	98 (70)	119 (96)	37 (57)	45 (177)
TMP	85 (23)	78 (32)	19 (12)	8 (18)
2-HYIBU	85 (13)	87 (14)	49 (44)	26 (64)
4'-HYDIC	<MQL	<MQL	<MQL	<MQL
KET	<MQL	<MQL	<MQL	<MQL
ERY	<MQL	<MQL	<MQL	<MQL

6.2. Occurrence in wastewater samples

The trend of total mass of PhCs determined in the influent and effluents of the investigated mesocosms are reported in Figure SM5-2, where the sixth-degree polynomial regression is also reported.

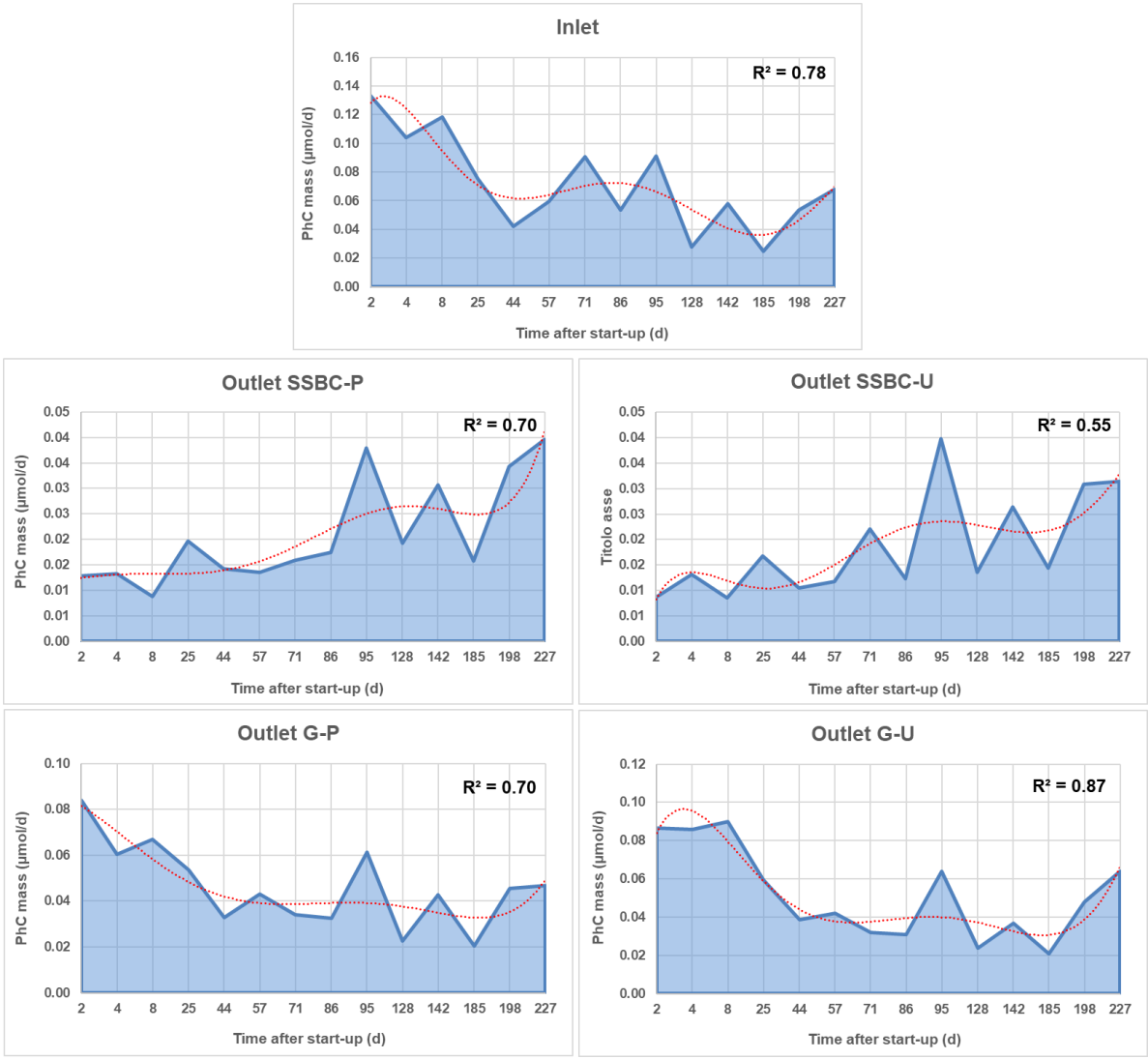

Figure SM5-2: Trend of the total mass of PhCs in the influent and effluents of the mesocosms investigated. The determination coefficients (R^2) of the sixth-degree polynomial regression are also reported.

6.3. QuEChERS extraction

The procedure was adapted from a methodology developed for the extraction of pharmaceutical compounds in sewage sludge samples (Rossini et al. Analytica Chimica Acta 935 (2016) 269-281). One gram of freeze-dried sludge was weighed into a 50 mL centrifuge tube. and 5 mL of ultrapure water was added. The mixture was hand-shaken for 15 s and vortex-mixed for 1 min. and 10 mL of CH_3CN was added. After a further step of handshaking (15 s) and vortex mixing (1 min), 2 g of NaCl and 2 g of $MgSO_4$ were added, and the obtained mixture underwent additional handshaking and vortex-mixing processes. The tube was centrifuged at 1200 g for 4 min., and 1 mL of the CH3CN supernatant phase was made up to 10 mL with acidic water. Finally. The diluted extracts were analyzed by LC-MS/MS as for the wastewater samples.

6.4. Apparent recovery

The apparent recovery percentage of the method was assessed. Following the IUPAC indications, by spiking in triplicate 1 g f.d. aliquots with mass-labelled compounds (5 ng g^{-1} for Diclofenac-D4, Venlafaxine-D6, Carbamazepine-D10). In order to evaluate the QuEChERS extraction efficiency. Three 1 g freeze-dried aliquots of the particulate samples were fortified with mass-labelled compounds (5 ng g^{-1} for Diclofenac-D4, Venlafaxine-D6, and Carbamazepine-D10). It should be noted that these compounds cover the entire range of physicochemical properties of the investigated molecules (e.g., log K_{OW} 2.77-0.74) and are therefore representative of the whole set of target analytes. The spiking procedure was performed by adding 500 mL of the CH_3CN standard solution to 1 g of dried sludge, then the solvent was evaporated at room temperature for 24h.

Pharmaceutical concentrations in the spiked samples. after the QuEChERS extraction. were then quantified (C_{found}) using a standard calibration curve prepared in the matrix-free procedural blank, and AR% calculated according to the following equation.

$$AR\% = \frac{Cfound}{Cspiked} * 100$$

Based on the procedure described above, the apparent recovery percentage takes into account the combined effect of both matrix effects and reduced recovery during partition stages (e.g, between water and acetonitrile) due to the presence of matrix components. The QuEChERS extraction efficiency of mass-labelled analytes was found in the range of 72-121% and resulted therefore suitable for the extraction of selected PhCs and their transformation products (TPs) from sewage sludge.

Table SM5-7: Removal percentages of pharmaceutical compounds (PhCs) in constructed wetlands (CWs) treating real wastewater. HLR=hydraulic loading rate (L m^{-2} d^{-1}) HRT=hydraulic retention time (d); T=temperature (°C); R%=removal percentage; Design: HSSF=horizontal subsurface flow; VSSF=vertical subsurface flow. HB=Hybrid Constructed Wetland.

PhCs[a]	R(%)	Plant	CW design	HLR/HRT	Substrate	T	Reference
CBZ	28	Unplanted	HSSF	34/4	Gravel	23-32	Zhang. 2011
DIC	41						
IBU	60						
NAP	52						
CBZ	27	*Typha angustifolia*					
DIC	55						
IBU	80						
NAP	91						
ACE	99	*Phragmites australis*	HSSF	n.a./11	Gravel. Sand	n.r.	Vymazal. 2017 (A)
FUR	81						
HCT	54						
CLA	66						
TRM	69						
IBU	75						
IBU	28	*Phragmites australis*	HSSF	34.5/5.5	Gravel	7-18	Nivala, 2019
NAP	32						
DIC	25						
CBZ	13						
IBU	31	*Phragmites australis*	HSSF	561/0.6	Gravel	n.r.	Petrie, 2018[§]
NAP	32						
ATE	77						
PRO	30						
CBZ	0						
VEN	2						
DIC	-5						
SMX	30						
CLA	46						
ATO	66						
DIC	72	*Phragmites australis*	VSSF	300/0.25	Gravel	4-27	Our study
FUR	-10						
O-DES	17						
CBZ	24						
RMP	15						
SMX	16						
VEN	24						
FLU	-39						
ATE	19						
CLA	-28						
BIS	21						
LVF	23						
PAN	-49						
ATO	37						
DIC	92	*Phragmites australis*			Biochar		
FUR	50						
O-DES	60						
CBZ	55						
RMP	40						
SMX	41						
VEN	57						
FLU	45						
ATE	62						

PhCs[a]	R(%)	Plant	CW design	HLR/HRT	Substrate	T	Reference
CLA	-74						
BIS	45						
LVF	56						
PAN	86						
ATO	98						
CIP	-28	*Phragmites australis*	VSSF	133/~3	Gravel	21-25	Ávila, 2021
OFL	-200						
AZI	-17						
CLA	58						
CLI	-200						
SMX	98						
TMP	93						
METRO	82						
PIP	80						
AMP	55						
IBU	95	*Phragmites australis*	VSSF	93/6	Gravel	7-21	Kahl, 2017
NAP	89						
DIC	53						
ACE	-2						
CBZ	-8						
TRM	-6	*Phragmites australis*	VSSF	200/n.r.	Sand	n.r.	Tadić, 2024
CBZ	17						
DIC	78						
VEN	-5						
CLA	40						
PRO	77						
SMX	34						
FLU	-23						
SMZ	100	Canna x generalis	HB: HSSF + VSSF	135.4/1	Gravel. sand	18-25	Sakurai, 2021
CIP	95						
NOR	100						
SDZ	100						
TMP	100						
OFL	100						
SMER	100						
SMX	89	*Canna indica, Cyperus alternifolius. Arundo donax*	HB: VF + HF	500/1	Gravel	10-21	Dan, 2020
Others	51-91						
CIP	92	*Typha Angustifolia*	HB**:** VF + HSSF	1920/1	Sand (VF). Zeolite (HSSF)	0.5-32	Al-Mashaqbeh, 2024
OFL	93						
ERI	61						
ENRO	97						
FLUM	45						
LINC	50						
CBZ	<8						
DIC	<8						

[a] Abbreviations of PhCs: ACE=acetaminophen; AMP=ampicillin ; ATE=atenolol; ATO=atorvastatin; AZI=azithromycin; CBZ=carbamazepine; CIP=ciprofloxacin; CLA=clarithromycin; CLI=clindamycin; DIC=diclofenac; ENRO=enrofloxacin; ERI=erythromycin; FLC= fluconazole; FLUM=flumequine; FUR=furosemide; HCT=hydrochlorothiazide; IBU=ibuprofen; LINC=lincomycin; IOM=iomeprol; IRB=irbesartan; KET=ketoprofen; NAP=naproxen; NOR=norgestrel; OFL=ofloxacin; PIP=piperacillin; PRO=propranolol; SDZ=sulfadiazine; SMER; SMX=Sulfamethoxazole; SMZ=; TMP=trimethoprim; TRM=tramadol; VEN= venlafaxine.

§ This study includes 52 pharmaceutical compounds.